Università degli studi di Trieste

Department of physics

Master Degree in Physics

Quality evaluation of different Atmospheric Boundary Layer parameterizations implemented in the meteorological WRF model. An annual focus study over Friuli Venezia Giulia.

Candidate:
Pierluigi Masai

Supervisor:
Prof. Dario Giaiotti

Assistant Supervisor:
Dott.ssa Anna Chiara Goglio

Academic year 2016-2017

Università degli studi di Trieste

Dipartimento di fisica

Laurea magistrale in fisica

Valutazione della qualità di diverse parametrizzazioni dello Strato Limite Atmosferico implementate nel modello WRF. Un caso studio annuale sul Friuli Venezia Giulia.

Candidato:
Pierluigi Masai

Relatore:
Prof. Dario Giaiotti

Correlatore:
Dott.ssa Anna Chiara Goglio

Anno accademico 2016-2017

Abstract

The dynamics of the Atmospheric Boundary Layer is of great importance for many activities. Many reasons drive the interest in studying the Atmospheric Boundary Layer (ABL), mainly the fact that life takes place in it and many anthropogenic activities have a direct impact on it and are influenced by it. Many studies are available in literature that test the performance of different ABL parameterizations but they usually focus on the capacity of the models to reproduce vertical profiles. It is instead the aim of this work to investigate how well surface fields are reproduced. The evaluation of surface physical quantities with high space-time resolution is fundamental to initialize other models, e.g. oceanographic models and pollutant dispersion models. Seven different simulations with the Weather Research and Forecasting (WRF) model differing in atmospheric boundary layer (ABL) schemes were realized. Each simulation was performed at a $2\,km$ horizontal resolution reproducing an entire year (2016) over Friuli Venezia Giulia. Simulated data were validated against measurements taken at different places over the region. The physical fields which were considered for the analysis are the temperature at $2\,m$, the wind speed at $10\,m$, the downward shortwave radiation and hourly precipitations.

Abstract

La dinamica dello Strato Limite Atmosferico (ABL da 'Atmospheric Boundary Layer') è di grande importanza per molte attività. Diverse ragioni spingono allo studio dell'ABL, principalmente il fatto che la vita vi ha luogo e molte attività antropiche ne sono condizionate oltre ad avervi un impatto diretto. Molti studi che valutano la qualità di diverse parametrizzazioni dell'ABL si possono trovare in letteratura ma generalmente si incentrano sulla capacità dei modelli di riprodurre i profili verticali. È invece obiettivo di questo lavoro valutare quanto i campi di superficie siano ben simulati. La valutazione di campi fisici di superficie con alta risoluzione spazio-temporale è fondamentale per inizializzare altri modelli, ad esempio quelli utilizzati per studi oceanografici e di dispersione degli inquinanti. Sono state realizzate sette diverse simulazioni con il modello WRF (Weather Research and Forecasting model), differenti fra loro per lo schema di parametrizzazione dell'ABL. Ogni simulazione è stata eseguita con una risoluzione orizzontale di $2\,km$, riproducendo un intero anno (2016) di tempo atmosferico sopra la regione Friuli Venezia Giulia. I dati simulati sono stati poi validati con delle misure prese presso varie località nella regione. Le quantità fisiche considerate per l'analisi sono state la temperatura a $2\,m$ di altezza dal suolo, la velocità del vento a $10\,m$ dalla superficie, la radiazione a onda corta incidente al terreno e le precipitazioni orarie.

Acknowledgements

I would like to express my gratitude to:

- My supervisor and my assistant supervisor, who patiently guided me in this work always willing to advise and help me.

- The whole CRMA team who were very kind to me and enabled me to accomplish this thesis.

- ARPA FVG for letting me work at their agency.

- My fellow students. I shared many moments of both difficulty and joy with them and the path to this thesis would not have been the same without them.

- My family and friends, who always stood by me. I know I can always count on them.

Without the help of all these people, this work would have never been done.

"Der bestirnte Himmel über mir
und das moralische Gesetz in mir"

Immanuel Kant

"We do not inherit the earth from our ancestors,
we borrow it from our children"

Wendell Berry

Contents

Introduction

The Atmospheric Boundary Layer (ABL), also known as Planetary Boundary Layer (PBL), is at the center of many studies. Human life and anthropogenic activities occur in the ABL and are influenced by its evolution. Therefore, to properly describe the physical phenomena that take place in it and possibly to forecast them is a matter of vital interest. Many theories have been developed over the years to portray the ABL evolution but much work is yet to be done. In fact, numerical models are still unable to include all physical phenomena at once. There are many limits to simulations, e.g. the resolution, both in time and space, and the accuracy of the measurements needed to input the models. Furthermore, models need to run the faster it is possible in order to provide information useful to take proper decisions in time. Many parameterizations of the ABL have been developed over the years and they have been implemented in different numerical models. Parameterizations may vary for the way some equations are approximated or for different ways of portraying a given physical phenomenon. Some parameterizations have been specifically developed to describe peculiar situations. The aim of this work was to provide an evaluation of the performances of ABL parameterizations implemented in the Weather Research and Forecasting (WRF) Model. Many studies had already been made that compare the performances of different parameterizations of the ABL with the WRF model (e.g. Hu et al., 2010). However, such studies usually focus on the capacity of the parameterizations to well portray the vertical profiles in the ABL (e.g. Coniglio et al., 2013) or energetic quantities when dealing with peculiar events (e.g. Cohen et al., 2015). This thesis, on the other hand, focuses on the evaluation of surface fields, which characterize the ABL in the first few meters. The evaluation of such quantities is extremely important for oceanographic and air quality studies because they can serve as an input for new numerical models dealing with such topics. The impact different parameterizations might have can be considerable (see Banks and Baldasano, 2016 and Boadh et al., 2016). This work considered an area with a great diversity in morphological and climatological characteristics, i.e. the Friuli Venezia Giulia region in north-eastern Italy, and realized simulations with a high horizontal resolution in space ($2\,km$) making it comparable with the study of Banks et al., 2016. Anyhow, unlike all the studies found in literature, this work considers an entire year of simulations validated against measurements while, usually, just a couple of days are considered. Such facts made it possible to evaluate the performances of the various parameterizations in different periods of the year and at different places comprising the open sea, the coastal region,

central plains and the mountainous region.

Chapter 1 provides information about the physics underlying the dynamics of the ABL. The main equations of fluid dynamics are presented and the problems arising in their solution are discussed. The topics of turbulence and closure techniques are depicted. Chapter 2 describes the WRF model, presenting its computational chain and some precautions which need to be taken into account when running it. Chapter 3 and 4 respectively report information about the simulations and the measurements. Chapter 5 is dedicated to the data analysis. Chapter 6 presents the conclusions. In appendix A the Kolmogorov-Smirnov test and the Taylor diagrams are presented. In appendix B statistical values of both the measurements and the simulated data are reported in many tables. In Appendix C an example of a namelist needed to run the WRF model is presented. At the end there are a glossary with the acronyms used in this thesis and the bibliography.

This work was carried out at the Regional Environment Protection Agency of Friuli Venezia Giulia (ARPA FVG), with the support of the Regional Center of Environmental Modeling (CRMA).

Chapter 1

The Atmospheric Boundary Layer

1.1 Introduction

The atmospheric boundary layer is that part of the lower atmosphere directly influenced by the presence of the Earth surface, which acts as a confining element. The dynamics of the ABL is ruled by the balances of three quantities: energy, mass and momentum. The physics of the ABL relies on two main fields of study: fluid dynamics and thermodynamics. ABL properties are sensitive to many elements, both geographical and temporal; for example the latitude and the period of the year define the inclination of incoming solar radiation affecting the energy balance. Consequently, the height of the ABL varies with time and space. It is important to underline that, given the continuous evolution of the ABL between different states (see section 1.7) and the different scale dimensions which characterize the motion, ABL dynamics can be separated from the dynamics of the upper free atmosphere which instead supplies boundary conditions to the evolution of the ABL. This does not mean that the ABL and the free atmosphere do not influence each other but different phenomena drive their evolution. ABL evolution has a great impact on the upper atmosphere at climatic and global scales, so even though over a few hours or over a few days the free atmosphere seems to be scarcely influenced by the ABL, feedback processes have to be parameterized.

In the free atmosphere the wind is usually in agreement with the geostrophic balance and the flow is laminar without turbulence (e.g. Holton, 1979). Instead the air in the ABL is

conditioned by the drag of the surface and turbulence is a key characteristic of the dynamics.

In order to understand ABL evolution, the underlying physics has to be studied. Sections 1.2 to 1.5 present a recap of fluid dynamics and thermodynamics, outlining the main aspects needed to describe atmospheric processes. Section 1.6 deals with the topic of the closure problem which is the starting point for the study of ABL parameterizations at the core of this thesis. Section 1.7 briefly summarizes phenomenological features of the ABL evolution while section 1.8 introduces the concept of ABL parameterizations.

1.2 Elements of fluid dynamics

The atmosphere is a fluid made up of gases, mainly Nitrogen (about 78%), Oxygen (about 21%) and Argon (about 1%). In addition to gases, the atmosphere is also made up of vapors, whose treatment requires some care (see section 1.5). Since the study of the atmosphere, at least in the layers closer to the surface, deals with large masses of air, it is reasonable to rely on continuum mechanics. In reality materials are made up of discrete atoms, separated by space, while a continuum is a body that can be divided in infinitesimal parts that can still be described in terms of continuous functions. In fluid mechanics a good criterion to evaluate the validity of the continuum assumption is given by the Knudsen number, which is defined as the ratio of the molecular mean free path length of the fluid λ and a characteristic physical length scale L of the flow under study:

$$Kn = \frac{\lambda}{L}$$

The smaller the value of the Knudsen number the more appropriate it is to rely on the continuum assumption. Typically the distinction between a molecular flow and a continuum flow is made for a value of the Knudsen number of 10. In conditions of small Knudsen number, and so within the framework of continuum mechanics, an important concept can be introduced: the fluid parcel. A fluid parcel is a small amount of fluid whose dynamical evolution can be completely described and which preserves the properties of a continuum, i.e. density, temperature, velocity and all the other physical fields have defined values. The mass of a fluid parcel is well defined and does not change with time whereas its volume may change (compressible flow) or not

(isochoric flow). Parcels are not to be confused with particles: parcels describe properties of fluid particles (atoms and molecules) averaged over a length scale which is large when compared with the molecular mean free path but small when compared with the typical length scales of the motion under consideration. Therefore, parcels dimension can vary from centimeters in the case of a flow in a pipe to hundreds of meters in the case of convective motions in the atmosphere. It has to be underlined that, in real fluids, parcels do not always consist of the same particles because as time goes by molecular diffusion changes the parcel properties; nonetheless it is reasonable to attain to the mathematical definition of a parcel for time scales of the motion shorter than those of molecular diffusion.

In continuum mechanics the properties and the related dynamics of a medium are described through the use of tensors, such as the strain tensor and the stress tensor, and of functions considered continuous in time and space for or all physical fields both scalar, e.g. density and temperature, and vector, e.g. velocity. More specifically, for a fluid the relationship between the stress tensor and the velocity gradient tensor is determined by the properties of the fluid itself. It is usual to consider at first a fluid which is isotropic and to look for a linear proportionality between the two tensors (for more details see Batchelor 2000).

At the core of continuum mechanics there is the need to describe the evolution of some physical fields which characterize the medium. In fluid mechanics the main interest is on the velocity field and there are two different approaches in building the equations: the Eulerian point of view and the Lagrangian point of view, which are equivalent and lead to the same results anyway (see figure 1.1). The Eulerian description represents a field as a continuous function of time and space and can be interpreted as the point of view of an observer at rest who watches the flow as it passes by and modifies the properties of the medium at any point. On the other hand, the Lagrangian description considers single fluid parcels, each one virtually labeled and distinguished from the others, and follows their motion through time specifying their positions. The Eulerian velocity field $\vec{u}$ is related to the Lagrangian position field by the 'material derivative' (also known as 'Lagrangian derivative'):

$$\frac{\mathrm{D}}{\mathrm{D}t} = \frac{\partial}{\partial t} + (\vec{u} \bullet \nabla)$$

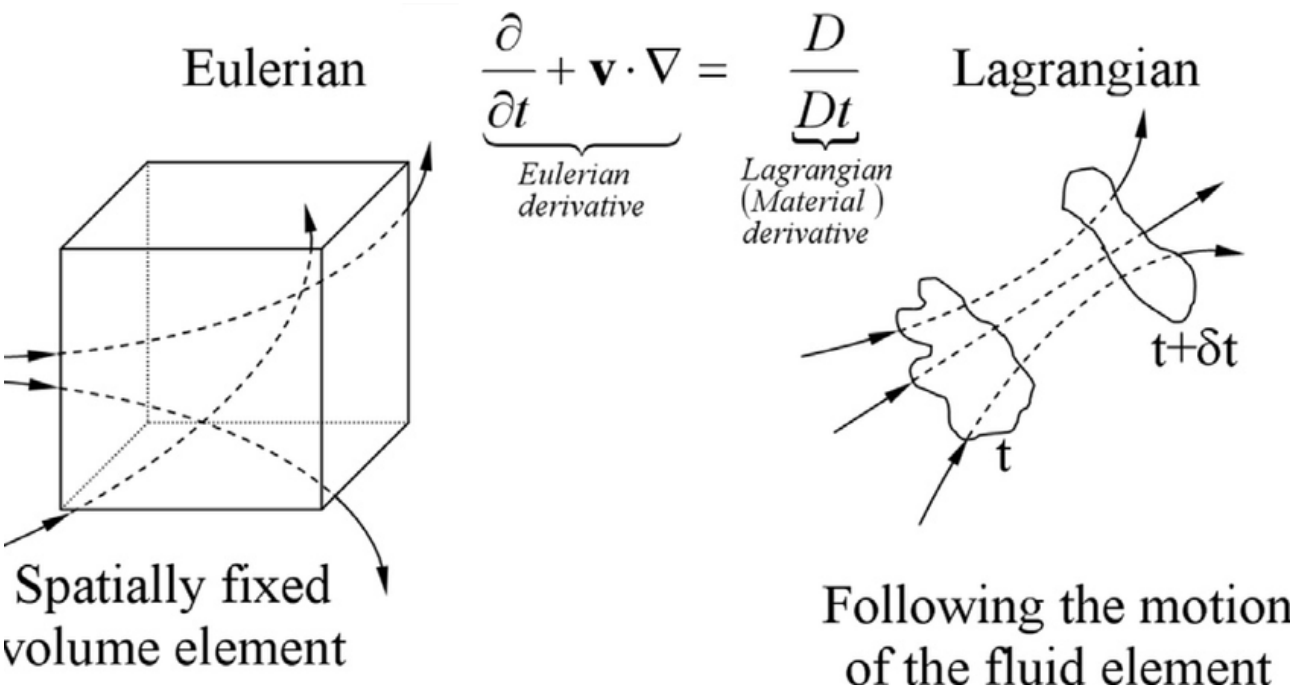

Figure 1.1: A representation of the Eulerian description and the Lagrangian description

For a fluid the motion of a parcel is described by the Navier-Stokes equations which in vectorial form are:

$$\rho \frac{\mathrm{D}\vec{u}}{\mathrm{D}t} = -\nabla P + \mu \triangle \vec{u} + \vec{F}_{body} \tag{1.1}$$

where $\vec{u}$ is the velocity field, P is the pressure, μ is the dynamic viscosity, $\triangle$ is the Laplace operator and $\vec{F}_{body}$ is the resultant of the body forces.

The study of the atmosphere and of the oceans have to consider the rotation of the Earth and the NSE are usually rewritten in the rotating coordinate frame so that they take the form:

$$\frac{\mathrm{D}\vec{u}}{\mathrm{D}t} = -2\vec{\Omega} \times \vec{u} - \frac{1}{\rho}\nabla P + \nu \triangle \vec{u} + \vec{g} \tag{1.2}$$

where $\vec{\Omega} = (0, \Omega\cos\phi, \Omega\sin\phi) = (0, \Omega_y, \Omega_z)$ is the angular velocity vector of the Earth rotation, ν is the kinematic viscosity (also called “momentum diffusivity") and $\vec{g}$ already includes the corrections for the centrifugal effects. It is useful for further studies to introduce the latitude ϕ and define the Coriolis parameters $f \equiv 2\Omega\sin\phi$ and $\tilde{f} \equiv 2\Omega\cos\phi$ which lead to the Coriolis vector $\vec{f} = (0, -\tilde{f}, f)$. The variation of the Coriolis parameters indicates the local importance of the Earth's rotation and is a key element in some studies which simplify the equations recurring to the f-plane approximation or to the β-plane approximation. It is important to

underline that equations 1.2 are in vectorial form and apply to a general frame of reference. Once the coordinate system is set it is possible to make further assumptions and simplify the equations, e.g. the aforementioned f-plane and β-plane approximations (see for example Cavallini and Crisciani, 2012).

The focus of this thesis is on the dynamics of the ABL which in its local evolution does not interest wide areas, so in the next sections a reference frame following the shape of the Earth, i.e. with two directions parallel two the surface (the meridional component in the direction South-North and the zonal component in the direction West-East) and a third direction always perpendicular to the ground, is considered. Thus, NSE can be newly rewritten and, using Einstein's notation (which implies summation over repeated indexes), they become:

$$\frac{\mathrm{D}u_i}{\mathrm{D}t} = -g\delta_{i3} + \epsilon_{ijk}v_j f_k - \frac{1}{\rho}\frac{\partial P}{\partial x_i} + \nu\frac{\partial}{\partial x_j}(\frac{\partial v_i}{\partial x_j}) \tag{1.3}$$

where δ_{i3} is the Kronecker delta with the second index specified for the vertical direction and ϵ_{ijk} is the Levi-Civita tensor. It has to be stressed that NSE, in the way they are presented here, apply to a fluid considered to be isotropic, homogeneous, incompressible and that satisfies the Stokes hypothesis regarding certain parameters. These can be strong approximations but for geophysical studies they are reasonable. NSE alone cannot provide all the information needed to know the motion of the fluid because there are more variables than equations. Aside from NSE which expresses the conservation of momentum, fluid dynamics relies on other equations which express the conservation of energy (see section 1.5) and the conservation of mass. The conservation of mass is described by the continuity equation:

$$\frac{1}{\rho}\frac{\mathrm{D}\rho}{\mathrm{D}t} + \nabla \bullet \vec{u} = 0 \tag{1.4}$$

NSE are a non-linear set of equations and to this day no explicit solution is still known (except for trivial or specific cases). Such a fact shows from the start how the evolution of the atmosphere cannot be simply evaluated. NSE need approximations and experimental corrections to be studied. There is not an official proper way to proceed in such studies but there are many fundamental elements which can guide the decisions. The key idea is to underline the properties

of the flow separating them form the properties of the fluid. In fact, different systems which share similar conditions at different scales have similar dynamics. In order to quantify such observations NSE have to be non-dimensionalized. This is a very important step in the analysis of the equations and a few examples are needed. First of all it has to be observed that any physical variable can be expressed as the product of a dimensionless variable and a dimensional value, e.g. $t = \mathrm{t} \cdot \mathrm{T}$ where t is the variable time ($[t] = s$), t is a dimensionless variable and T is a dimensional value ($[\mathrm{T}] = s$). The dimensionless variable t keeps the functional properties of t and varies along with it. On the other hand T can be seen as representative of the modulus of t and acts as a constant with respect to functional actions such as derivation or integration. The value T can be used to characterize the scale, i.e. an approximative quantification of the range of variation for the phenomena under consideration; this concept can be associated to the more accurate concept of order of magnitude. Such a representation applies to any physical variable, both scalar and vectorial, and can be extended to operators such as derivatives too. Here a few examples:

$$u_i = \mathrm{u}_i \cdot \mathrm{U} \qquad x_i = \mathrm{x}_i \cdot \mathrm{L} \qquad \frac{\partial}{\partial x_i} = \frac{\partial}{\partial \mathrm{x}_i} \cdot \frac{\mathrm{dx}_i}{\mathrm{d}x_i} = \frac{1}{L} \cdot \frac{\partial}{\partial \mathrm{x}_i} \qquad \frac{\partial}{\partial t} = \frac{\partial}{\partial \mathrm{t}} \cdot \frac{\mathrm{dt}}{\mathrm{d}t} = \frac{U}{L} \cdot \frac{\partial}{\partial \mathrm{t}}$$

It is a little bit harder to deal with pressure and density since for the study of the ABL it is more important to pay attention to the little variations (oscillations) of these quantities rather than to their magnitude; usually, a characteristic value P_0 of pressure is considered to define the dimensionless variable $\mathrm{P} = \frac{P - P_0}{\rho \mathrm{U}^2}$. Also, in the study of the atmosphere it is common to consider the Boussinesq approximation, according to which density variations are important only in relation with the gravity term whereas when they multiply the inertia term they can be neglected. A particular scale of motion can then be identified specifying the values of the scale quantities. Many definitions of the atmospheric scales of motion, based on the different phenomena that can take place, have been proposed over the years, perhaps the most important are the ones from Orlanski (Orlanski, 1975) and Fujita (Fujita, 1981). For example, the so-called 'synoptic scale' of motion is defined approximately by $\mathrm{U} = 30m \cdot s^{-1}$ and $\mathrm{L} = 1 \cdot 10^6 m$.

Expressing all the variables as described, NSE can be non-dimensionalized and take the form:

$$\frac{\mathrm{U}}{\mathrm{L}}\frac{\partial(\mathrm{u}_i\mathrm{U})}{\partial \mathrm{t}} + \mathrm{U}^2\mathrm{u}_j\frac{1}{\mathrm{L}}\frac{\partial \mathrm{u}_i}{\partial \mathrm{x}_j} = -g\delta_{i3} + \epsilon_{ijk}\mathrm{U}\mathrm{u}_j\mathrm{f}_k\mathrm{f} - \frac{1}{\mathrm{L}}\frac{1}{\rho}\rho\mathrm{U}^2\frac{\partial \mathrm{P}}{\partial \mathrm{x}_i} + \nu\frac{1}{\mathrm{L}^2}\frac{\partial}{\partial \mathrm{x}_j}\frac{\partial(\mathrm{u}_i\mathrm{U})}{\partial \mathrm{x}_j} \tag{1.5}$$

Multiplying 1.5 by L/U^2 and considering the operator $\frac{\mathrm{D}}{\mathrm{Dt}} = \frac{\partial}{\partial \mathrm{t}} + \mathrm{u}_i\frac{\partial}{\partial x_i} \neq \frac{\mathrm{D}}{\mathrm{D}t}$ we obtain:

$$\frac{\mathrm{Du}_i}{\mathrm{Dt}} = -\frac{1}{Rf}\delta_{i3} + \frac{1}{Ro}\epsilon_{ijk}\mathrm{u}_j\mathrm{f}_k - \frac{\partial \mathrm{P}}{\partial \mathrm{x}_i} + \frac{1}{Re}\frac{\partial}{\partial \mathrm{x}_j}\frac{\partial(\mathrm{u}_i\mathrm{U})}{\partial \mathrm{x}_j} \tag{1.6}$$

In 1.6 some important dimensionless quantities, analogous the previously described Knudsen number, are introduced:

- the Froude number $Rf = \frac{\mathrm{U}^2}{g\mathrm{L}}$
- the Rossby number $Ro = \frac{\mathrm{U}}{\mathrm{fL}}$
- the Reynolds number $Re = \frac{\mathrm{UL}}{\nu} = \frac{\mathrm{UL}\rho}{\mu}$

These dimensionless parameters define the flow which means that they characterize a particular configuration of the motion of the fluid regardless of the physical extension of the flow. It is now immediate to understand that in case these quantities maintain the same values the functional form of the solutions of the NSE does not change. It is then possible to say that the motion of a parcel in a river can be the same, from a mathematical point of view, of that of a parcel of air in the upper atmosphere or of a parcel of oil in a pipe, provided that the values of the aforementioned dimensionless quantities are the same. Moreover, from a physical point of view the actual values of Rf, Ro and Re provide peculiar information on the flow:

- Ro quantifies the importance of the Coriolis force. A large value of Ro indicates that the rotation is not important.
- Rf quantifies the importance of gravity. A large value of Rf indicates the presence of stratification in the fluid.
- Re quantifies the importance of friction. A large value of Re indicates that the friction is not important for the flow.

Another quantity which can be useful to describe the properties of the flow is the Mach number $Rm = \frac{\mathrm{U}}{c}$ where c is the speed of sound.

1.3 Laminar and turbulent flows

Among the parameters discussed at the end of section 1.2, the most important to characterize the flow of a fluid is certainly the Reynolds number. In the atmosphere many configuration are to be considered, namely:

- Synoptic scale: $Re \sim 2 * 10^{12}$
- Daytime ABL: $Re \sim 1 * 10^{7}$
- Nighttime ABL: $Re \sim 1 * 10^{-1}$

It is so clear that in the study of the atmosphere the action of friction is important but not at every scale. Re is also a great tool to distinguish two different kinds of flow: the laminar flow and the turbulent flow. Laminar flows are characterized by the motion of the fluid in parallel layers with no disruption in between. There are no eddies or swirls of fluid and, close to a solid surface, particles move orderly in straight lines parallel to the surface itself. Laminar flows are associated with a low Reynolds number. On the other hand, turbulent flows are characterized by chaotic motions in which unsteady vortices of different dimensions form and influence the dynamics. A vortex is a closed, or almost closed, circular trajectory and in general vortices can be seen as zones of the fluid which periodically exhibit the same conditions with some fluctuations. Turbulent flows are associated with a large Reynolds number. The transition between laminar and turbulent flows is not universally defined and depends strongly on the geometry of the physical system (see figure 1.2). In order for turbulence to develop the flow has to interact with a confining element, i.e. a rigid surface which confines the fluid or the interface between two fluids where a strong gradient of a property (e.g. density) is present. In the presence of a confining element, as Re increases, small perturbations form which can lead to the growth of secondary circulations or to the detachment of small vortices which then grow away from the confining element itself. A typical example is the transition of the flow around

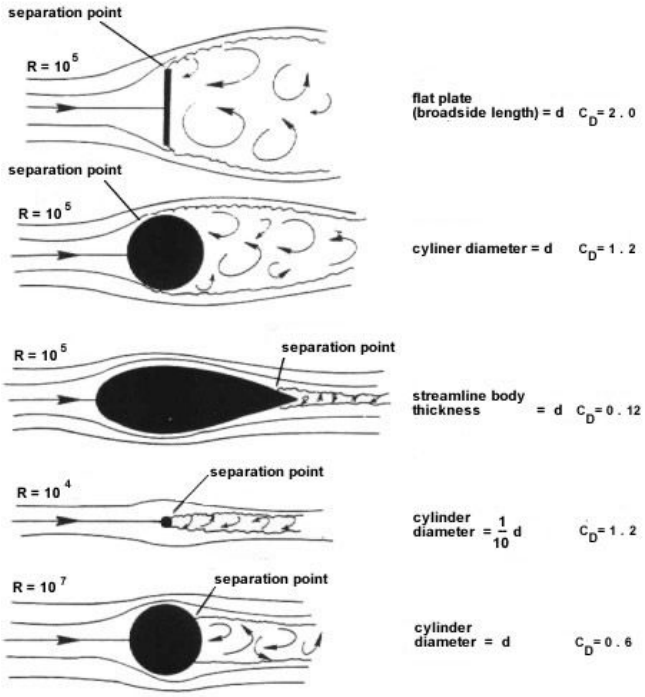

Figure 1.2: With different geometries turbulence does not develop in the same way. Flow separation may occur for different values of the Reynolds number. Drag coefficients depend on the dimensions of the obstacles. Five situations are shown. The first three depict different geometries while the last two show what happens if the same geometric structure as in the second situation faces a different Re or different dimensions. For more details see Kundu and Cohen, 2010

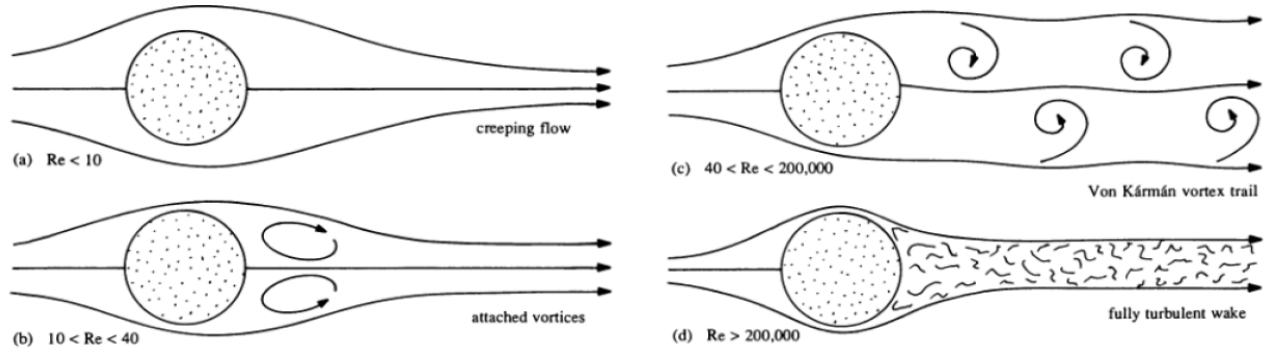

Figure 1.3: The behaviour of the flux around a cylindrical object. As Re increases the so-called Von Karman vortices form and turbulence develops.

a cylindrical object with the formation of the so-called Von Karman vortices (see Figure 1.3). The dependence of turbulence formation on the geometry can be seen in Figure 1.2 and it is a very important subject in engineering studies. To summarize, from the dynamical point of view turbulence can develop in two ways: if there is instability in the fluid because of the presence of a gradient for some quantities, such as temperature, which leads to the formation of convective motions causing mixing and transfer, than it is regarded as 'convective turbulence', whereas if there is a velocity shear which causes the formation of circular turbulent motions, than it is regarded as 'mechanical turbulence'.

It is important to stress that to associate turbulence with chaos can be misleading because turbulence actually has some organized aspects. In fact, turbulence is a mixture of coherent

structures distributed in space and time which evolve in a random way. The coherent structures are essentially what we introduced as vortices which show such a coherence at least over the region of their extent, namely a size l. From the experimental point of view, eulerian measures (i.e. performed at a fixed point in space) show time series with fluctuations that appear to be random. In fact, the fluid evolution is deterministic, but chaotic. In case new measures were to be made, the new time series would be different but the average values would be the same, provided that the conditions which determine the system were the same. Such a feature is the consequence of an ergodic behavior, i.e. the time average of the process is the same as its spatial average and as its ensemble average, which is the average over the probability space. We can therefore quantify average values and compare the measurements with the theory. It is important to keep in mind that the instruments partially filter the signals and could give wrong data if the inertia of the instruments themselves was not overcome.

1.3.1 Taylor's hypothesis and Kolmogorov's theory

It is very important, especially from an experimental point of view, to find a way to link spatial and temporal dimensions of a vortex. To do so, it is possible to rely on Taylor's hypothesis, named after sir Geoffrey Ingram Taylor who first introduced it. Taylor's hypothesis introduces the concept of 'frozen turbulence' which refers to systems in which the advection of a vortex past a fixed point occurs in an amount of time significantly shorter than the time scale of existence of the vortex itself, so that the advection can be taken to be entirely due to the mean flow (see figure 1.4). Taylor's hypothesis actually implies that on certain time scales the properties of a vortex are conserved in the motion. This fact can be expressed saying that the lagrangian derivative of a property ξ of the vortex is null:

$$\frac{\partial \xi}{\partial t} = -u\frac{\partial \xi}{\partial x} - v\frac{\partial \xi}{\partial y} - w\frac{\partial \xi}{\partial z} \;\Rightarrow\; \frac{\mathrm{D}\xi}{\mathrm{D}t} = 0 \tag{1.7}$$

which furnishes the link between spatial and temporal dimensions of a vortex from an eulerian point of view. A flow in which vortices move according to Taylor's hypothesis generates, in eulerian measurements, signals at fixed frequencies of the order of the various times of existence

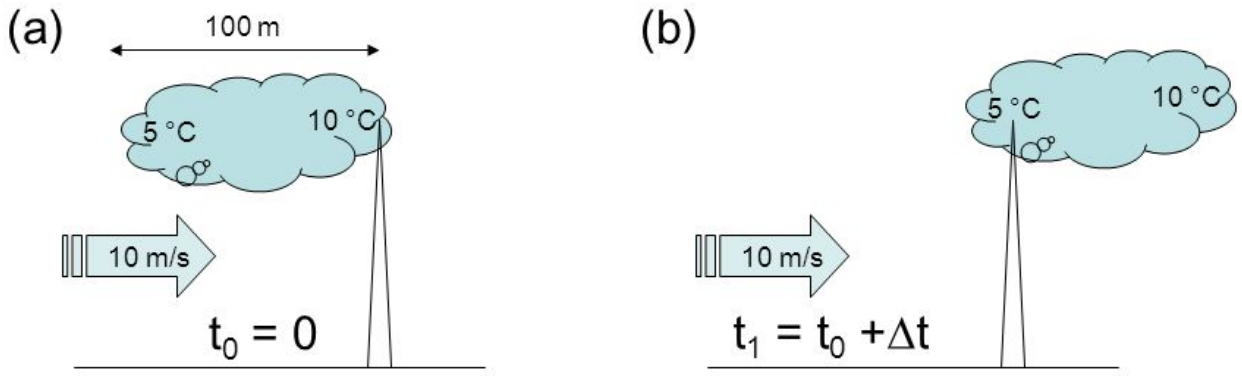

Figure 1.4: A depiction of Taylor hypothesis. An idealized eddy moves rapidly enough not to change noticeably for the sensor: it appears to be frozen. Adapted from Stull, 1988

of a vortex that can be detected if the sample rate is significantly inferior to those time scales.

In order to stress many of the aforementioned features of turbulence it is convenient to produce a power spectrum of an eulerian measure of velocity. Figure 1.5 shows the wind power spectral density of some measures performed at Brookhaven by Van der Hoven (see der Hoven, 1957). Some peaks are evident testifying the contribute of different phenomena to the energy balance. Thanks to Taylor's hypothesis we can interpret a determinate frequency as a representative time scale for the existence of a vortex and associate to that vortex a length to estimate its dimensions according to equation 1.7. It is then possible to recognize the action of large scale phenomena, such as cyclones, and distinguish them from turbulent phenomena. A striking fact which can be observed in the power spectrum is the presence of an energy gap between the turbulent phenomena scale and the daily phenomena scale. It is possible to deduce that turbulent motions evolve on time scales which range from milliseconds to minutes. Always thanks to Taylor's hypothesis it is possible to switch from a temporal power spectrum (frequency spectrum) to a spatial power spectrum (wavenumber spectrum) like the one shown in Figure 1.6. To better understand all the features expressed by such graph it is important to recall Richardson's concept of energy cascade and Kolmogorov's theory which later formalized it. Lewis E. Richardson first expressed in the 1920s the key idea that there is a continuous transfer of energy in a fluid between different scales of motion, in particular vortices form at all scales but energy is injected by the mean flow just at the large scales whereas it is dissipated at the small molecular scales. On the other hand at the intermediate scales no dissipation or injection of energy take place but a non-linear and non-viscous behaviour enables a continuous

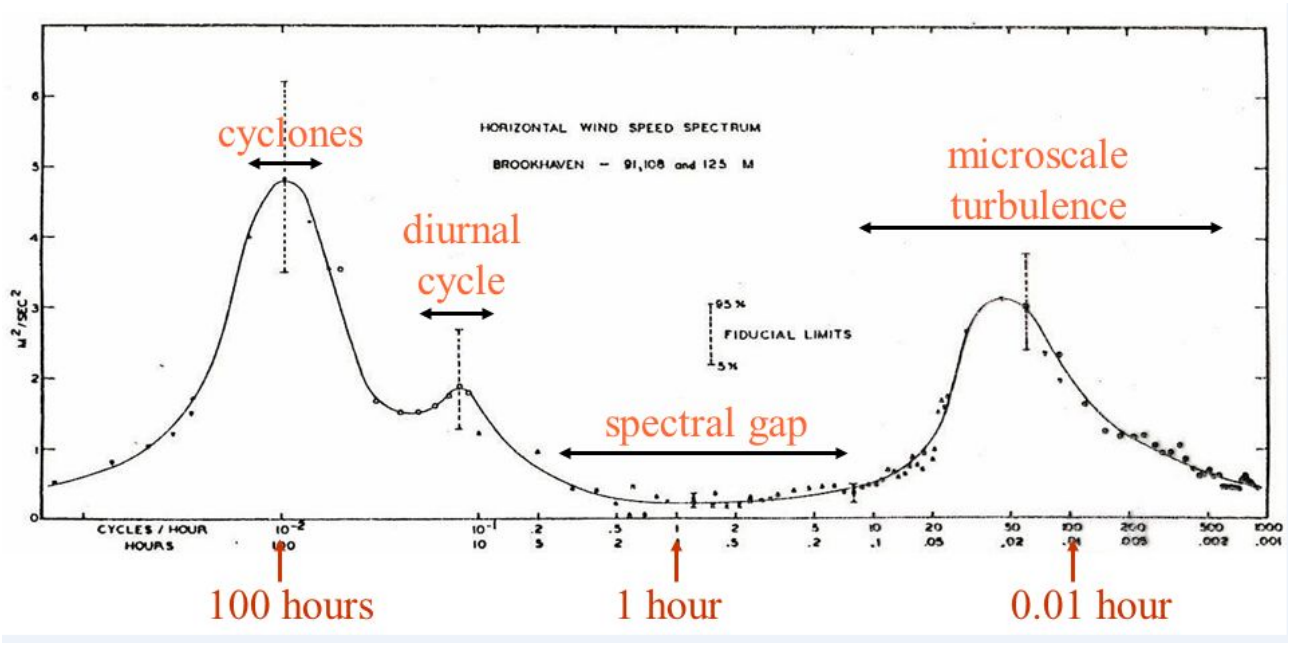

Figure 1.5: The power spectrum of the time series of the wind intensity in the ABL measured at Brookhaven. Adapted from der Hoven, 1957.

transfer of energy from higher to smaller scales like a cascade. To quote Richardson himself ("Weather Prediction by Numerical Process." Cambridge University Press, 1922):

"Big whorls have little whorls
Which feed on their velocity;
And little whorls have lesser whorls,
And so on to viscosity
in the molecular sense."

The key idea introduced in section 1.3 to consider non-dimensionalized equations in order to point out general behaviours of fluid motion can be further taken and leads to the similarity theory. The aim of similarity theory is to empirically find universal relationships between non-dimensionalized variables of fluids. Similarity theory strongly relies on Buckingham π theorem which is a formalization of Rayleigh's method of dimensional analysis (see Barenblatt, 2003). Buckingham theorem states that, given an equation involving n physical variables but just k physical dimensions, it is possible to rewrite such an equation in terms of a set of p=n-k dimensionless parameters built upon the original variables. Once the equation is rewritten the additional information needed to specify the parameters can be obtained with experimental measurements which will specify the equation for the physical system under consideration. It is very important to stress from the start that the results obtained through the use of similarity theory and dimensional analysis are general but when they are applied to a determined system

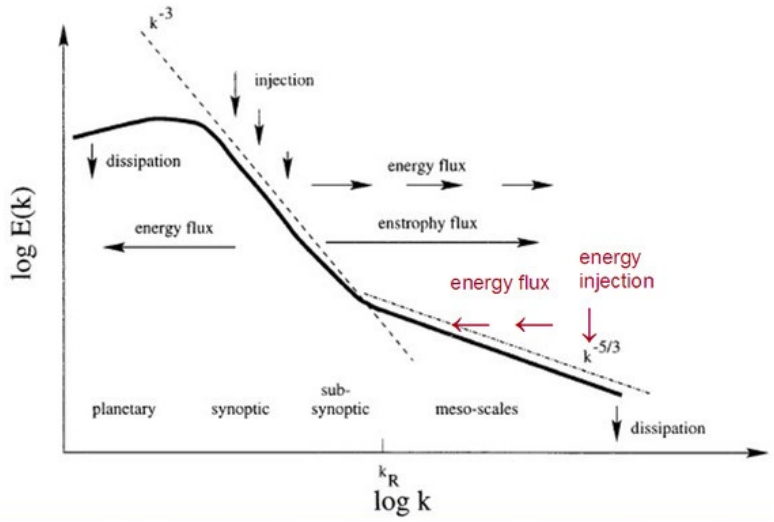

Figure 1.6: A power spectrum of the wind speed in terms of the wavenumber. The various scales of motion are identified and different phenomena are evidenced. In particular two almost linear, in the logarithmic scale, regimes are outlined.

their validity is restricted to systems with the same configuration, i.e. the same dimensionless parameters. In the 1940s Andrey N. Kolmogorov used similarity theory and was able to quantify Richardson's intuition. As previously told, turbulence can be thought to consist of eddies of different sizes and an eddy can be conceived to be a turbulent motion which shows some coherence over the region of its extent. It is possible to associate to each eddy a scale length l which represents its extension. Eddies of size l belonging to the same flow will have a velocity $u = u(l)$ and a timescale $\tau(l) = l/u(l)$ which represent their motion. As a consequence each scale of motion can be identified with a different Reynolds number $Re = lu(l)/\nu$. A particular Reynolds number can also be associated with the mean flow at the largest scale, namely Re_M. Kolmogorov characterized three different turbulent scales: the integral scale, the inertial scale (also known as the Taylor scale) and the dissipative scale (also known as the Kolmogorov scale). The integral scale is associated with a large Reynolds number, therefore eddies are formed directly from the mean flow, the motion is extremely turbulent and friction is negligible, so that no dissipation take place. On the other hand the Kolmogorov scale is associated with a small Reynolds number, namely $Re_\eta = O(1)$, therefore eddies have small extensions, friction is more important than advection and energy is dissipated into heat. The Taylor scale is associated with Reynolds numbers in between those of the other scales. At the Taylor scale eddies form from bigger eddies and create smaller eddies in a way analogous to Richardson's idea.

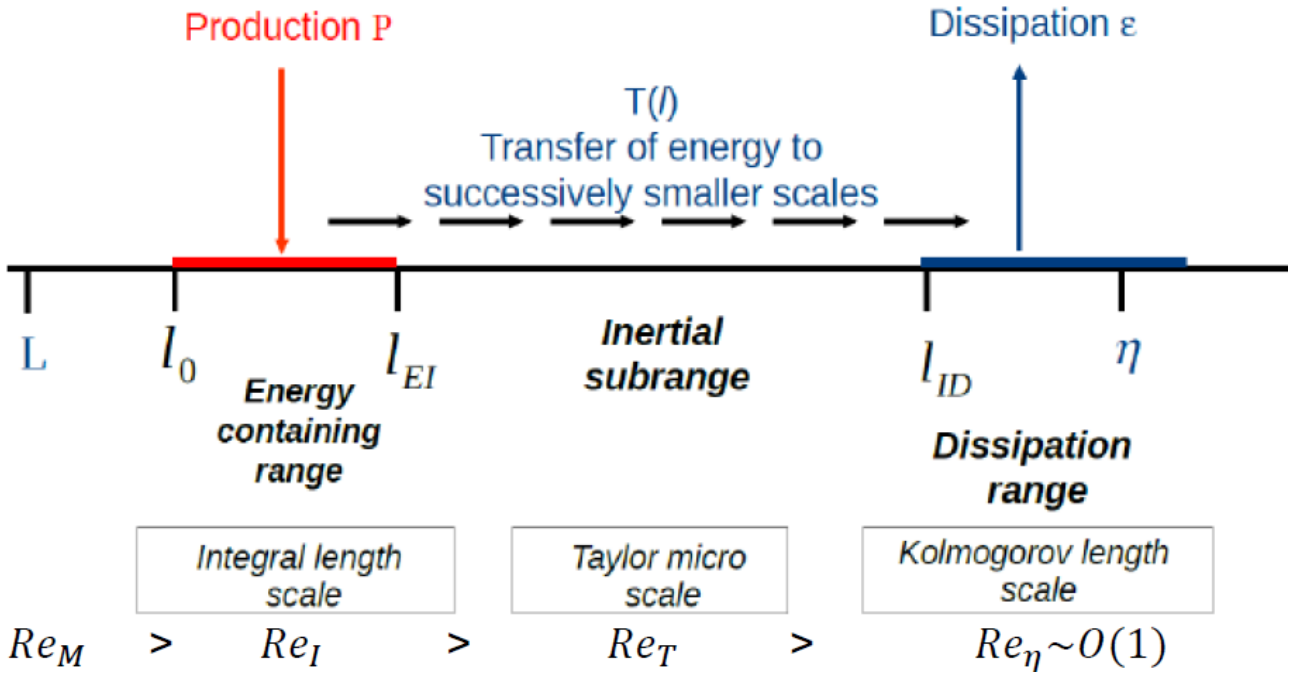

Figure 1.7: A schematic representation of the energy cascade. Energy is injected at the integral scale and dissipated at the Kolmogorov scale. A different Reynolds number is associated with each scale. Adapted from Pope, 2000.

To develop his theory Kolmogorov made three hypothesis which can be simply summarized as:

1. If the Reynolds number of the mean flow Re_M is sufficiently high, the small scales turbulent motions are statistically isotropic.

2. In every turbulent flow, if the Reynolds number of the mean flow Re_M is sufficiently high, the statistics of the small scale motion (the Kolmogorov scale) have a universal form that depends only on the dissipation rate ϵ and the kinematic viscosity ν.

3. In every turbulent flow, if the Reynolds number of the mean flow Re_M is sufficiently high, the statistics of the motion of the inertial scale have a universal form that depends only on the dissipation rate ϵ and is independent of the kinematic viscosity ν.

The first two hypothesis rely on the idea that in the process of the cascade formation of the eddies, information about the directionality and the geometry of the mean flow gets lost (the mean flow can still be anisotropic). Such idea makes sense because new small vortices form chaotically. As a consequence the smallest eddies will show analogous properties regardless of the mean flow and it is possible to assume that their statistical behaviour is universal. The

third hypothesis is based on the observation that Re is still relatively large at the Taylor scale and the advection term should be much more important than the viscous term. On the basis of his hypothesis and through dimensional analysis, Kolmogorov was able to describe the scale lengths of each scale and, more importantly, to determine the distribution of the turbulent energy spectrum among the eddies of different sizes. A very important and striking result, known as Kolmogorov $-5/3$ power law, is an equation for $E(k)$ in the inertial scale:

$$E(k) = C \cdot \epsilon^{2/3} \cdot k^{-5/3}$$

where C is the universal Kolmogorov constant, which was experimentally determined to be $C = 1.5$. Through the years many equations to describe even the dissipation range and the production range have been developed. Without going any further it can just be said that in general the full spectrum can be expressed with the introduction of two more parameters as:

$$E(k) = C \cdot \epsilon^{2/3} \cdot k^{-5/3} \cdot f_L \cdot f_\eta$$

Furthermore, it has been shown that the more the Reynolds number of the mean flow increases, the more the integral scale gets separated from the Kolmogorov scale while the Taylor scale grows (see figure 1.8). Actually this phenomena is studied in function of the Reynolds number of the Taylor scale which is smaller than the Reynolds number of the mean flow but varies accordingly to it. Anyhow, it has to be remembered that Kolmogorov's theory is an asymptotic theory and experiments have shown it to work well in the limit of very high Reynolds number. Also, Kolmogorov's theory assumes the energy cascade to take place in only one way: from larger eddies to smaller eddies. From the experimental point of view, even energy transfers from smaller scales to larger scales have been observed to take place (again, see figure 1.6 for the atmospheric case). Such a phenomena is known as 'backscatter'. However, the main energy transfer takes obviously place from larger to smaller scales. For the sake of completeness, we introduce the kinetic energy per unit mass of the mean flow and the turbulent kinetic energy, i.e. associated with turbulent motion, per unit mass:

$$E = \frac{MKE}{m} = \frac{1}{2}(\overline{u}^2 + \overline{v}^2 + \overline{w}^2) \qquad \overline{e} = \frac{TKE}{m} = \frac{1}{2}(\overline{u'^2} + \overline{v'^2} + \overline{w'^2})$$

where the bars denote an averaging operation and the apices denote the term to be a variation;

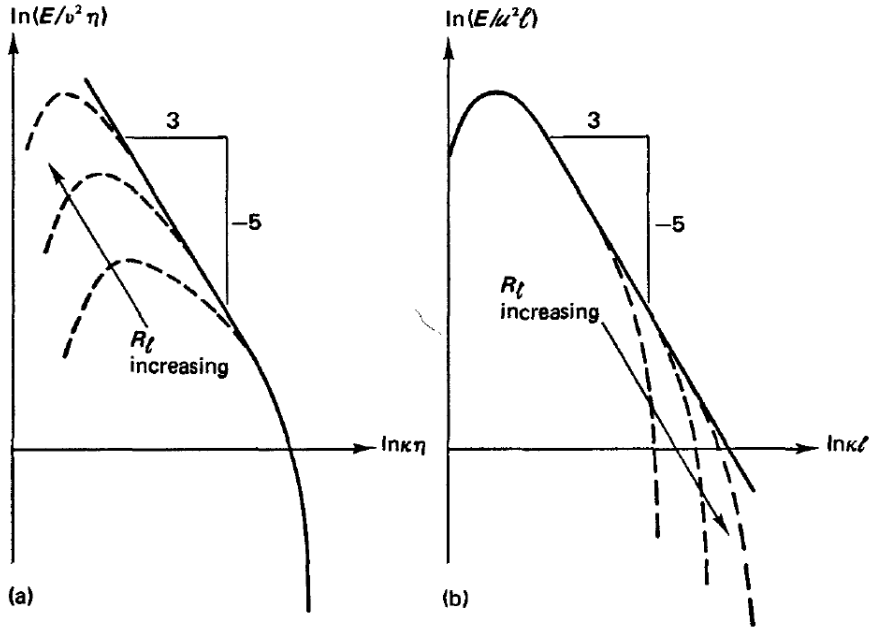

Figure 1.8: The variation of the energy spectrum in the wavenumber domain with respect to the Reynolds number of the Taylor scale. The spectrum can be normalized with the parameters of the Kolmogorov scale (a) or the integral scale (b). Adapted from Tennekes et al. 1972.

these aspects will be given meaning in section 1.4. It is now important to take a look at the equations for the time variation of E and $\overline{e}$.

$$\frac{\partial E}{\partial t} + \overline{u_i}\frac{\partial E}{\partial x_i} = -g\overline{w} - \frac{\overline{u_i}}{\overline{\rho}}\frac{\partial \overline{P}}{\partial x_i} + \nu\overline{u_i}\frac{\partial^2 u_i}{\partial x_j^2} + \overline{u_i' u_j'}\frac{\partial \overline{u_i}}{\partial x_j} - \frac{\partial \overline{u_i' u_j'}\,\overline{u_i}}{\partial x_j} \tag{1.8}$$

$$\frac{\partial \overline{e}}{\partial t} + \overline{u_i}\frac{\partial \overline{e}}{\partial x_i} = \delta_{i3} g\frac{\overline{u_i'\theta_V'}}{\overline{\theta_V}} - \overline{u_i' u_j'}\frac{\partial \overline{u_i}}{\partial x_j} - \frac{\partial \overline{u_i' e}}{\partial x_i} - \frac{1}{\overline{\rho}}\frac{\partial \overline{u_i' P'}}{\partial x_i} - \epsilon \tag{1.9}$$

These two equations will not be discussed in detail (for further studies see Stull, 1988), but they provide an immediate and important result which testifies the observations of this chapter. In fact, the two equations share a term: the fourth on the right side of the equation 1.8 is the same as the second on the right side of equation 1.9. These two terms are indeed the same but they figure with opposite signs in the two equations. These terms involve the so-called Reynolds stresses (see section 1.4) and represent the energy mechanically produce by the action of turbulence. Therefore, these equations testify that the energy injected in the turbulent motions comes from the energy of the mean flow.

1.4 Reynolds decomposition

So far it has been shown that fluid dynamics relies on non-linear equations and flows can exhibit chaotic behaviour. Nonetheless, some coherent features of turbulence have been outlined. It has been said that turbulence is a mixture of coherent structures distributed in space and time which evolve in a random way but it has also been introduced the concept of ergodic behaviour. In the study of the atmosphere, and in particular of the ABL, it is reasonable to consider turbulence to be homogeneous and stationary, i.e. statistically not changing over time. Therefore, it is possible to accept the ergodic condition and so to consider that space, time and ensemble averages coincide for different measurements taken over similar systems, i.e. systems with the same physical conditions. These considerations suggest to rely on statistics in order to study the evolution of the physical fields. The goal would be to have a set of prognostic equations, i.e. which predict the time evolution, for all the physical variables. Reynolds developed a powerful method to do so. The basic idea is to express every physical field as the sum of its expectation value and a deviation which represents the action of turbulence. For example, for the temperature T we would have:

$$T = \overline{T} + T' \qquad \text{with} \qquad \overline{T} = E[T] \qquad \text{and} \qquad E[T'] = 0$$

$E[T]$ is the expectation value of T and for real measurements has to be computed with a statistical estimator such as the average (the notation $\overline{T}$ denotes a generic average). It is important to say that the expectation values are taken for physical fields that are functions of time and space and so they also depend on time and space. Once every variable is decomposed according to Reynolds' idea, new equations can be found. It has to be underlined that the expectation values are intended to provide information about the mean flow and so, from the experimental point of view, an appropriate physical system has to be under study, i.e. these ideas apply to flows large enough to consider the turbulent contributions as random variations so that the expectation value of these variations can be regarded as null. It is therefore important to take an appropriate interval of time or space when averages are taken with experimental measurements otherwise turbulent phenomena would not be outlined. Obviously, these consideration can be related to the spectra discussed in the previous sections (see figure 1.5 and 1.6). Now, in order to proceed in finding the new equations, Reynolds' method can be schematically summarized in the following five steps:

1. identify the fundamental equations and simplify them through the use of scale analysis to adapt them to the system under study
2. expand every variable in their average and perturbation components
3. compute the expectation value of the entire equations obtaining prognostic equations for the mean variable
4. use the continuity equation to express the results in the form of a flux
5. subtract the averaged equations from the initial ones to get prognostic equations for the perturbations

Following these rules every equation can be rewritten and lead to new equations. An important property playing a role in the process is the fact that averages are linear operations and so, when the expectation value of an equation is taken (step 3) the perturbation terms cancel out unless two or more of them multiply each other. In fact, the expectation value of a quantity like $u' \cdot v'$ is not necessarily null since it actually is the covariance of the two quantities:

$$E[u'] \cdot E[v'] = E[u - E[u]] \cdot E[v - E[v]] = E[uv] - E[u]E[v] = cov[uv]$$

It is immediate to understand that the new equations will have many of this correlation terms which express the action of turbulence. To make an example consider the equation for the mass conservation of a general tracer of concentration (mass per volume) C:

$$\frac{\partial C}{\partial t} + u_i \frac{\partial C}{\partial x_i} = -K_C \frac{\partial^2 C}{\partial x_i^2} + \frac{S_C}{\rho_{air}}$$

where K_C is a diffusivity constant and S_C is a source term. Following Reynolds method this equation leads to:

$$\frac{\partial \overline{C}}{\partial t} + \overline{u_i} \frac{\partial \overline{C}}{\partial x_i} = -K_C \frac{\partial^2 \overline{C}}{\partial x_i^2} + \frac{S_C}{\rho_{air}} - \frac{\partial}{\partial x_i} E[C' u_i']$$

The evolution of the correlation terms arising in the equations is not known at first. If the fifth step of the aforementioned sequence is performed, prognostic equations for the correlation terms are obtained but they always contain correlation terms of higher order, e.g. $E[u'v'w']$ or $E[u'v'^2]$. The procedure could be further taken to obtain prognostic equations for second order correlations, which would contain third order correlations requiring new equations containing fourth order correlations and so on. It seems therefore that there is no end to such calculations

and the system cannot be closed. In order to overcome these difficulties many solutions to the so-called 'closure problem' have been proposed (see section 1.6). Now, terms which involve the product of a component of the velocity and a generic quantity α express the flux, i.e. transport, of that quantity in the direction of the velocity, which is to say that, for example, a term like UT expresses the transport of temperature in the x direction through an advective process. Reynolds decomposition makes it possible to distinguish between two different kind of fluxes: kinematic fluxes which are driven by the mean flow and are represented by terms like $\overline{U} \cdot \overline{\alpha}$, and eddy fluxes which are driven by turbulent motions and are represented by terms like $\overline{u'\alpha'}$. Among eddy fluxes it is interesting to focus on the turbulent momentum fluxes which act formally like stresses and are called Reynold stresses. It is in fact possible to define the Reynolds stress tensor $\tau'_{ij} = \rho\left(\overline{u'_i u'_j}\right)$. It can be shown that τ'_{ij} is symmetric. It is important to underline that Reynolds stresses are not real stresses but they are called so just because they act like ones.

1.5 The thermodynamics of the atmosphere

As previously said, the atmosphere is made up of gases and vapors, mainly water vapor. The difference between a gas and a vapor is fundamental: a vapor is a substance in the gas phase but at a temperature lower than its critical temperature. Therefore, if compressed, i.e. if pressure increases, vapors can change phase and condensation or sublimation processes, as long as their opposites, can take place. Although there can be some deviations, the behavior of atmospheric gases can be well approximated with that of an ideal gas and so the ideal gas law is considered to apply to the dynamics:

$$P = \rho R T \tag{1.10}$$

where R is not the universal gas constant $R* = 8.31\, J \cdot mol^{-1} \cdot K^{-1}$ but the ratio between the product of the Avogadro number and the Boltzmann constant, and the molar mass of the atmosphere. Equation 1.10 applies to water vapor as well but water vapor is usually treated separately from the other gases present in the atmosphere since its variation can be very rapid and takes part in many important processes, e.g. the formation of clouds. Water vapor partial pressure is usually denoted with the letter e.

1.5.1 Water condensation

It is now clear that a way to quantify the presence of water in the atmosphere is needed. Many quantities can be introduced but the main two are the mixing ratio r and the specific humidity q, given by the following equations:

$$r = \frac{\rho_v}{\rho_d} \qquad q = \frac{\rho_v}{\rho} \tag{1.11}$$

where the vapor density ρ_v, the air density ρ and the dry air density $\rho_d = \rho - \rho_v$ have been introduced. These two quantities are simply related by:

$$r = \frac{q}{1-q} \qquad q = \frac{r}{1+r} \tag{1.12}$$

Usually r and q are small quantities and in the atmosphere $r \approx q$ but from the experimental point of view r has a greater importance to evaluate the vapor pressure. In fact we can now rewrite equation 1.10 to apply it to the water vapor and the dry air:

$$e \equiv P_v = \rho_v R_v T \qquad P_d = \rho_d R_d T \tag{1.13}$$

Equations 1.12 and 1.13 can be combined to find:

$$r = \frac{R_d}{R_v}\frac{e}{P_d} = \epsilon\frac{e}{P_d} = 0.622\frac{e}{P-e} \tag{1.14}$$

The vapor pressure e is a fundamental quantity in atmospheric studies and is given the special name of saturation vapor pressure, or equilibrium vapor pressure, when the concentration of the water vapor is equal to the equilibrium value (at the temperature of the air), and is represented with the symbol e_s. Saturation can be a misleading concept (see Bohren and Albrecht, 1998). The idea to be kept in mind is that a vapor when compressed or cooled varies its properties so that pressure e can equal the equilibrium value e_s and when this happens, condensation occurs. It is therefore important to measure the “distance" of a vapor from its equilibrium configuration and this can be done introducing a new quantity: the relative humidity. There are two main definitions of the relative humidity: the classical one which considers the ratio between the vapor pressure e and the saturation vapor pressure e_s, and the one proposed by the World Meteorological Organization (WMO) which considers the ratio between the mixing

ratio r and the saturation mixing ratio r_s:

$$RH = \frac{e}{e_s} \qquad RH_{WMO} = \frac{r}{r_s} \tag{1.15}$$

The relative humidity is usually expressed as a percent (RH×100). The two definitions agree in their extremes: they both equal 0% when there is no vapor and 100% when the equilibrium is reached (actually RH can exceed 100% and in such cases air is said to be supersaturated). The following connection can be derived:

$$\frac{r}{r_s} = \frac{e}{e_s}\left(\frac{P - e_s}{P - e}\right) \tag{1.16}$$

Equation 1.16 shows that the two definitions of RH are slightly different since in the air $e << P$. The equilibrium vapor pressure changes its value with temperature and this dependence can be described with the Clausius-Clapeyron equation (see Bohren and Albrecht, 1998):

$$\frac{\mathrm{d}e_s}{\mathrm{d}T} = \frac{1}{T}\frac{l_v}{\alpha_v - \alpha_w} \tag{1.17}$$

where l_v is the enthalpy of vaporization per unit mass and α is the specific volume, respectively for vapor and liquid water. Equation 1.17 can be integrated to obtain:

$$e_s\,(t) = 0.611 \cdot exp\left(\frac{17.3t}{t + 237.3}\right) \tag{1.18}$$

where some parameters are experimentally evaluated and the temperature t is in °C. Studies can be further taken to find many relations capable to evaluate the variations of the saturation vapor pressure of pure water both on a liquid and a solid surface (see Bohren and Albrecht 1998). Such aspects are fundamental in the formation of water droplets. Vapor needs a non-gaseous surface in order to condensate, otherwise water would immediately evaporate again. In the atmosphere a great variety of particles, whose dimensions may vary from $1\mu m$ to 1/100 of a mm, can fit for that and they are generally referred to as cloud condensation nuclei (CCN). Vapor in the atmosphere can reach very low temperature (down to −13°C) without condensing and water vapor is said to be supercooled. It is also possible that vapor directly forms ice crystals when deposited on certain particles known as ice nuclei (IC). Water droplets can exist at the liquid state for temperatures down to −37°C (in such cases water is said to be supercooled). The fact that the saturation vapor pressure at a given temperature is lower on a

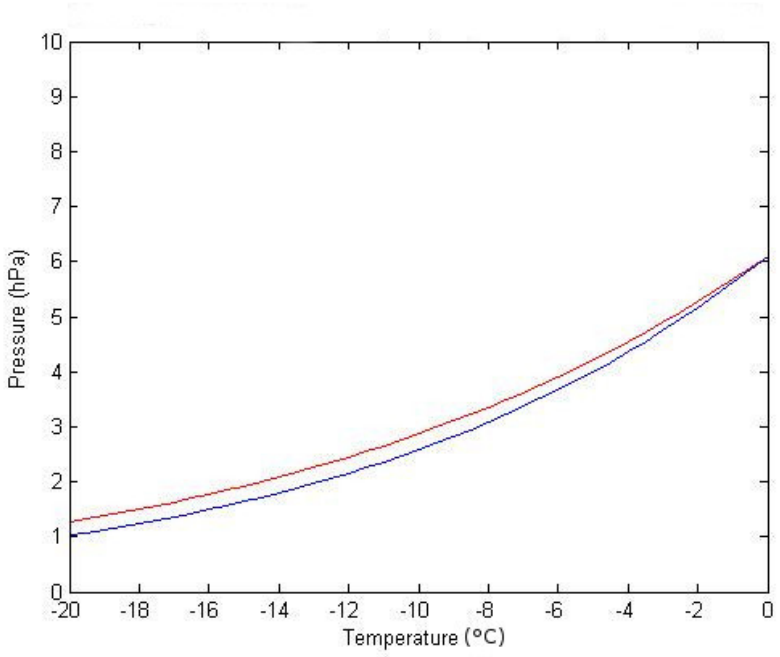

Figure 1.9: Saturation vapor pressure over liquid (red) and ice (blue). The red line is above the blue one testifying that at a given temperature it is easier for ice crystal to grow than it is for liquid droplets.

solid ice surface than it is on a liquid supercooled water surface (see image 1.9), implies that it is easier for ice crystals to grow rather than it is for water droplets. This has strong implications on the formation of rain, graupel and hazel. In order to reach the ground, a rain droplet needs to be big enough not to evaporate during the fall. There are many theories about the growth of droplets and the development of rain but the main processes are certainly coalescence (e.g. Rogers and Yau, 1989) and the Wegener-Bergeron-Findeisen process (e.g. Wallace and Hobbs 2006).

1.5.2 The energy balance

For an isolated system, energy is conserved according to the first law of thermodynamics. The atmosphere is obviously not an isolated system since it exchanges energy with the solid earth, the ocean, the Sun and the outer space. The energy balance at the planetary surface can be expressed through an equation derived from the first law of thermodynamics and the ideal gas law. Without being too specific, the variation of temperature in a given volume of air in time is related to the heat flux through the same volume in time. Many processes contribute to the net heat flux: solar radiation, earth radiation, turbulence, advection, friction, plant transpiration, evaporation and others. Considering the diurnal evolution of the ABL, which is the main topic of section 1.7, the radiation contributes are the most important. Usually the

net radiation term is split into four components. According to Stull (Stull, 1988):

$$Q* = K\uparrow + K\downarrow + I\uparrow + I\downarrow$$

where the single components represent respectively:

- $K\uparrow$ = upwelling reflected short wave (solar) radiation
- $K\downarrow$ = downwelling shortwave radiation transmitted through the air
- $I\uparrow$ = longwave (infrared, IR) radiation emitted up
- $I\downarrow$ = longwave diffusive IR radiation down

The distinction between shortwave (approximately from $300\,nm$ to $800\,nm$) and longwave radiation (essentially from $4\,\mu m$ to $100\,\mu m$), so that only two wavelength bands are considered, is possible because the solar spectrum has a peak at the normal visible light wavelengths and the earth/atmosphere system emits infrared radiation characteristic of its absolute temperature (the usual range varies approximately from 280K at the surface to 245K at the top of the atmosphere). Furthermore, since there are no other bodies near the earth which could contribute in a significant way, it is possible to consider just those two bands.

1.5.3 Vertical stability

In the study of the ABL the vertical direction exhibits different features because of the action of gravity. Vertical motions are usually treated separately from horizontal motion. Even from the point of view of scale analysis vertical motions are different from horizontal ones: typical vertical velocities are of the order of $1\,m \cdot s^{-1}$ while horizontal velocities are of the order of $10\,m \cdot s^{-1}$. Anyhow, the presence of wind shear in relation to the height and the radiative processes which heat or cool the air near the surface can generate convective turbulent motions, i.e. advective motions which tend to mix the fluid. From now on, 'stability' has to be intended in relation to vertical motions. It is so important to introduce some parameters or variables to quantify the degree of the stability of a fluid both for theoretical and experimental reasons, especially in the study of the ABL. The main quantities which are usually considered are potential temperature, the Brunt-V*äisälä* frequency and the Richardson number. These quantities are meant to provide information about the state and the evolution of a column of

fluid, therefore it is more important their variation in different parts of the fluid rather than their value at a specified point.

Potential temperature is introduced to take into consideration the pressure variations of the environment in which a parcel of air moves adiabatically. It would be intuitive to say that warmer air raises up while colder air sinks down but this is not true in general because if pressure diminishes while the height increases there can be stratification with warmer air beneath colder air (think for example that temperatures are lower at the top of a mountain than they are at the base). Potential temperature is defined as:

$$\theta = T\left(\frac{P_0}{P}\right)^{\frac{R}{c_P}}$$

where P_0 is a reference pressure (usually $1000\,hPa$). The variation of the potential temperature with height provides an excellent tool to evaluate vertical stability (see figure 1.10). It is important to say that θ does not take into consideration the presence of water vapor in the air but that cannot be neglected in practical studies because processes like condensation and evaporation contribute significantly to the energy balance other than being obviously fundamental in the formation of clouds and precipitations. In order to describe more appropriately the dynamics of the atmosphere new quantities can be introduced, namely the virtual potential temperature θ_V which is associated to the potential temperature in an analogous way to that in which the virtual temperature T_V, which is the temperature that dry air must have to equal the density of moist air at the same pressure, is associated to the absolute temperature T:

$$T_V = T \cdot (1 + 0.61 \cdot r) \qquad \theta_V = \theta \cdot (1 + 0.61 \cdot r)$$

where r is the mixing ratio, i.e. the ratio in a given volume of air between the mass of water vapor and dry air. For saturated (cloudy) air '$0.61 \cdot r$' has to be replaced by '$0.61 \cdot r_{sat} - r_L$' where r_{sat} is the water-vapor saturation mixing ratio and r_L is the liquid-water mixing ratio.

The Brunt-Väisälä frequency N, also known as the buoyancy frequency, is the frequency of oscillation of a parcel displaced vertically in a stratified environment. In fact, the study of the motion of a parcel of density ρ_0 in an environment with a density $\rho(z)$ varying with height leads to the equation for the vertical displacement z' (e.g. Holton, 1972):

$$\frac{\mathrm{D}^2 z'}{\mathrm{D}t^2} - \frac{g}{\rho_0}\frac{\partial \rho(z)}{\partial z} z' = \frac{\mathrm{D}^2 z'}{\mathrm{D}t^2} + N^2 z' = 0 \tag{1.19}$$

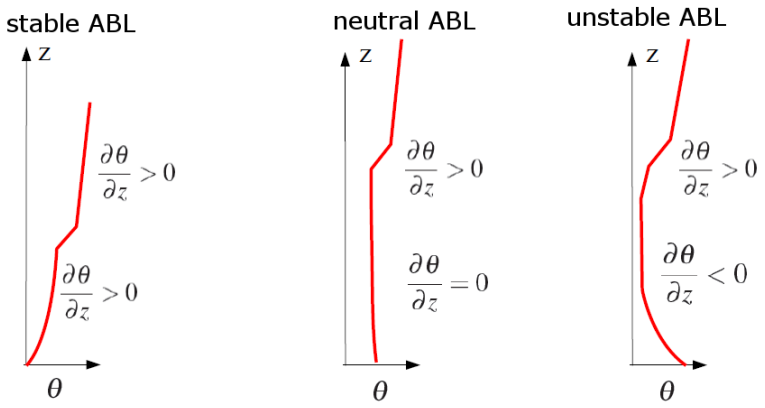

Figure 1.10: The vertical profile of the potential temperature as a criterion for vertical stability. In each case the upper part is stable to testify the presence of the free atmosphere, which is seldom unstable, above the ABL.

Equation 1.19 has the mathematical structure of the equation of an harmonic oscillator and so N can effectively be interpreted as a frequency. If $N^2 > 0$, then a parcel vertically displaced oscillates back towards its starting position, therefore the stratification is stable. Otherwise, if $N^2 < 0$, equation 1.19 has exponential solutions and a parcel displaced vertically is accelerated away from its initial position, therefore there is instability and convective motions can form. N is differently specified in the atmosphere (where it is function of the potential temperature θ profile) and in the ocean (where it is function of the potential density ρ_θ profile):

$$N = \left(\frac{g}{\theta}\frac{\partial\theta}{\partial z}\right)^{\frac{1}{2}} \qquad \text{or} \qquad N = \left(-\frac{g}{\rho_\theta}\frac{\partial\rho_\theta}{\partial z}\right)^{\frac{1}{2}}$$

This new expression for the Brunt-Väisälä frequency connects with the potential temperature and validates the criterion shown in figure 1.10.

In a stable environment, vertical turbulent motions act against gravity. In fact, gravity tends to stratify a fluid while turbulence tends to mix a fluid and homogenize its properties. Therefore the strength of gravity with respect to the strength of turbulence is an indicator of stability. To quantify these observation the Richardson number Rf has been introduced. Recalling equation 1.9, the Richardson number is defined as the ratio of the first and the second terms on the right side and is usually simplified assuming horizontal homogeneity and neglecting subsidence (in this case Rf is usually referred to as Richardson flux number). From its definition, Rf is a dimensionless quantity like Re and provides information about the properties of the flow rather than local properties of the fluid. Moreover, relying on the K-closure (see section 1.6) Rf can be further simplified to get the so-called gradient Richardson number Ri which can be related

to the Brunt-Väisälä frequency:

$$Rf = \frac{\frac{g}{\overline{\theta_V}}\left(\overline{w'\theta'_V}\right)}{\left(\overline{u'_i v'_j}\right)\frac{\partial \overline{u_i}}{\partial x_j}} \cong \frac{\frac{g}{\overline{\theta_V}}\left(\overline{w'\theta'_V}\right)}{\left(\overline{u'w'}\right)\frac{\partial \overline{u}}{\partial z} + \left(\overline{v'w'}\right)\frac{\partial \overline{v}}{\partial z}} \qquad Ri = \frac{\frac{g}{\overline{\theta_V}}\frac{\partial \overline{\theta_V}}{\partial z}}{\left(\frac{\partial \overline{u}}{\partial z}\right)^2 + \left(\frac{\partial \overline{v}}{\partial z}\right)^2} = \frac{N^2}{\left(\frac{\partial \overline{u}}{\partial z}\right)^2 + \left(\frac{\partial \overline{v}}{\partial z}\right)^2}$$

Ri is introduced because Rf cannot be easily evaluated from measurements in non-turbulent fluxes due to the correlation terms. Anyhow, for practical calculations Ri needs to be discretized and in the end it is the so-called bulk Richardson number R_B to be used. If $Ri >> 1$ gravity dominates and the kinetic energy is not enough to homogenize the fluid that gets stratified. On the other hand, if $Ri < 0$ then N^2 is negative as well, the fluid is unstable and the flow is turbulent. So, high positive values of Ri are associated with laminar flows while negative values of Ri are associated with turbulent flows. Small positive values of Ri characterize a flow that is potentially unstable, i.e. turbulence has not fully developed but some eddies are forming from the mean flow. Experimentally a critical value $R_c = 0.25$ has been identified: when Ri becomes smaller than R_c laminar flows get unstable and in flows that were previously stratified Kelvin-Helmholtz waves are observed to form. In order for the flow to become laminar again, Ri has to grow and get larger than a new value $R_t > R_c$. These experimental observations suggest that hysteresis phenomena take place and they also testify that turbulence needs two conditions to develop: flow instability and an ignition mechanism.

1.6 The closure problem

At the end of section 1.4, it has been concluded that the system of equations needed to describe the dynamics of turbulent fluids is not closed and the correlation terms which appear after the Reynolds method has been applied need to be parameterized. This is the basis of the so-called closure problem which is at the core of fluid dynamics studies and many approaches to solve it have been developed. First of all some distinctions have to be made. The order of an equation is defined as the sum of the powers to which the expectation values in the highest order term of the equation are raised to; for example an equation containing a term like $E[(x - E[x])^2 (y - E[y]) (z - E[z])]$ is said to be of the fourth order. A fundamental aspect that has to be underlined is that higher order terms are not necessarily small refinements of lower order terms like for Taylor series: a higher order moment can have a value way larger than a lower order moment. Usually, when the system is desired to be closed at the nth order, (n+1)th

order moments are parameterized through experimental measures. The highest order equation kept in the system determines the order of the closure. There are two major approaches to the closure problem: local closure and non-local closure.

1.6.1 Local closure

The local closure approach parameterizes the turbulent variations at every point of the space as functions of the mean quantities or their gradients at the same points. Turbulence is so described in an analogous way to molecular diffusion: turbulent fluxes are seen as counter-gradient fluxes, e.g.:

$$\overline{u_i' u_j'}\left(\vec{x},t\right) = \alpha \overline{u_i}\left(\vec{x},t\right) \overline{u_j}\left(\vec{x},t\right) \tag{1.20a}$$

$$\overline{u_j' s'} = -K_s \frac{\partial \overline{s}}{\partial x_j} \tag{1.20b}$$

Local closure has been well studied for many orders but the higher the order the more intensive are the calculations needed. Typically, models avoid considering closures of an order higher than 2. Some models consider particular subsets of equations and are regarded to as half order models. Next some brief information about the main schemes of local closure in the ABL studies.

Zero order closure techniques do not consider prognostic equations, not even for mean values. Every variable is directly parameterized as a function of time and space. Turbulence is not taken into consideration.

Half order techniques analyze a selected subset of the equation of the first order. These techniques are not used anymore.

First order closure is also known as K-closure. The prognostic equations for the mean values of variables such as the wind speed, temperature and humidity of the 0-order are to be solved. Usually the geostrophic wind is assumed to be known and taken as a boundary condition. Second order moments have to be parameterized and the usual way is to describe the fluxes as analogous to diffusive phenomena with the introduction of a proper eddy diffusivity constant K_α for the generic α variable (see equations 1.20). K-closure has been shown to hold efficient as long as vortices do not have too large dimensions with respect to the ABL height. Therefore, K-closure is well suited for a stable or neutrally stratified ABL but does not work with a highly unstable and convective ABL. The K_α constants introduced are properties of the flow and some

generalized models do not consider them constants but functions of temperature and pressure. This description has one important limit: the fluxes are considered to act down-gradient and so the K_α constants are required to be positive but turbulent motions in convective ABL can generate counter-gradient fluxes. K_α constants have to be either experimentally evaluated or parameterized with similarity theory arguments. An important example of parameterization is Prandtl's mixing length theory (e.g. Stull, 1988). First order closure is not able to treat strong turbulent layers but can describe a variety of phenomena such as the Ekman spiral both in the atmosphere and in the ocean.

One-and-a-half order closure retains the prognostic equation for mean variables at 0-order and adds two equations to the system: a prognostic equation for the turbulent kinetic energy, i.e. equation 1.9, and a prognostic equation for the variance of the potential temperature $\overline{\theta'^2}$. The information provided by these new two equations is used to study the variation of the parameterizations of the first order closure $K_\alpha\left(\overline{e}, \overline{\theta'^2}\right)$.

Second order closure aims to develop prognostic equations for the second order moments, therefore correlation terms such as $\overline{u'v'w'}$, $\overline{w'e}$ or $\overline{w'\theta'^2}$ have to be parameterized. Typically, parameterizations try to express a down-gradient behavior of the third order moments towards the second order moments. It is rare in numerical models to implement higher orders of closure than this.

1.6.2 Non-local closure

Non-local closure schemes consider the equations in integral form and are numerically intensive. While local closure schemes describe the unknown fields as functions of the variables in the neighborhood of the point in space under consideration, non-local closure schemes try to consider the influence of an extended volume. Typically, the reciprocal influence of different regions of the layer is considered to be significant only in the vertical direction. An example of these method can be given considering a column of air divided into N boxed regions one on top of each other. If $\overline{\xi_i}$ is the concentration of a generic passive tracer ξ in box i, its evolution in time can be expressed as:

$$\overline{\xi_i}\left(t+\Delta t\right) = \sum_{j=1}^{\mathrm{N}} c_{ij}\left(t, \Delta t\right) \overline{\xi_j}\left(t\right) \tag{1.21}$$

Equation 1.21 applies to every variable of interest. The terms c_{ij} form the transilient matrix; they express the general influence of box j on box i and must satisfy a condition for the mass conservation: $sum_{j=1}^{\mathrm{N}} c_{ij} = 1$. This method can be also implemented in a continuous form.

An alternative approach to non-local closure is provided by the spectral diffusivity theory. This idea takes the equations of the K-closure and expresses the K_α parameters as dependent on the wavenumber k of a given vortex. Then an integration over all the wavenumbers is taken and spectral analyses are performed. For example, for a generic variable ξ the following equation can be introduced:

$$\frac{\partial \overline{\xi}\,(k)}{\partial t} = K\,(k)\,\frac{\partial^2 \overline{\xi}\,(k)}{\partial z^2} \tag{1.22}$$

Nonlocal transport should better portray phenomena such as surface-layer cooling, mixed-layer heating, and entrainment.

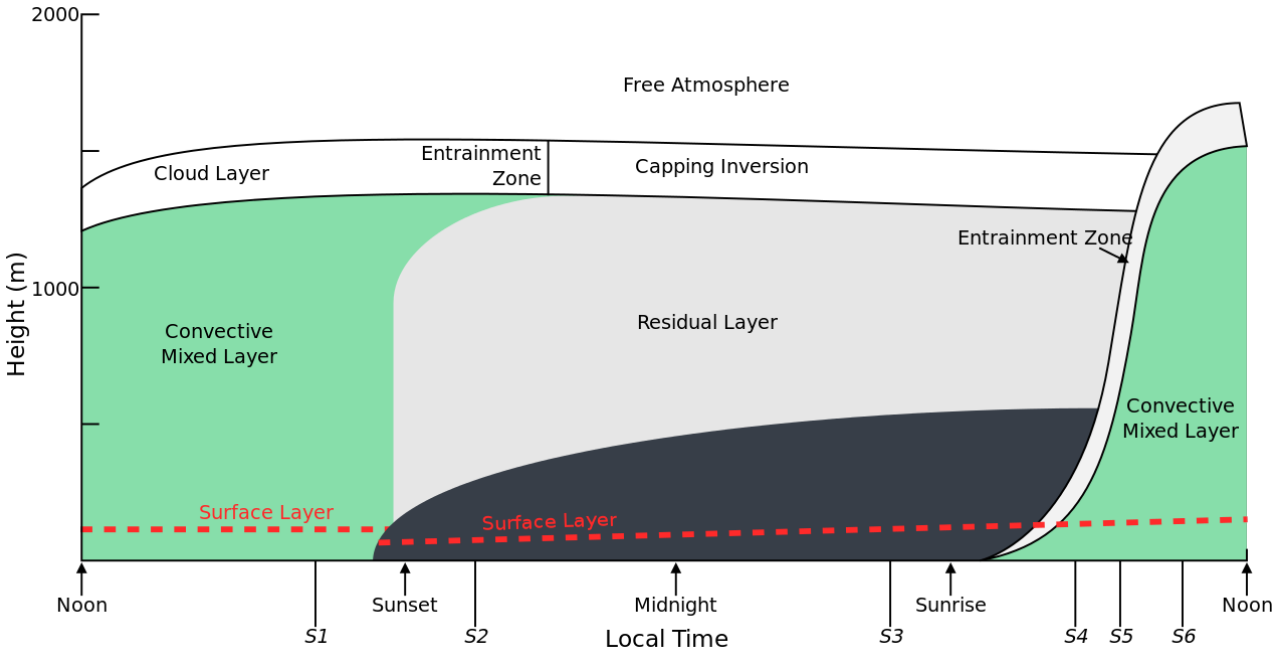

Figure 1.11: A schematic representation of the typical evolution of the ABL. Adapted from Stull, 1988.

1.7 The diurnal evolution of the atmospheric boundary layer

The dynamics of the ABL is quite complicate since the system itself is chaotic and characterized by the presence of many non-linear phenomena. Anyhow, from the phenomenological point of view some periodical aspects can be highlighted. Given the alternation of night and day, without considering the polar regions, a diurnal cycle takes place (see figure 1.11). From sunrise until sundown the Sun radiates energy which heats the air. The balance of incoming and outgoing radiation implies the formation of warmer (colder) air parcels near the surface during daytime (night time). As a consequence during the day parcels tend to float form the surface towards the sky and convective motion take place mixing the air vertically whereas during the night parcels tend to sink and air in the ABL gets stratified.

1.7.1 Daytime evolution

During the day, the heating effect of solar incoming radiation drives the dynamics. Regardless of the presence of clouds, after dawn the air near the ground gets heated so that it gets

lighter and starts to rise. The air which takes the place of the rising parcels will then be heated as well and the process continues giving birth to convection. The formation of convective motions keeps moving air along the vertical direction mixing all the properties of the fluid, i.e. because of this motion the fluid gets homogenized and a column of fluid will tend to exhibit an approximately constant value of the concentration of tracers (e.g. the mixing ratio). This is a behaviour typical of turbulent flows. Schematically, in its daily configuration the ABL can be divided into three parts: the surface layer (SL), the mixed layer (ML) and the entrainment zone (EZ). The SL is the closest part to the surface which includes all those morphological elements which strongly influence the air due to friction and exchanges of properties, e.g. vegetation and urban structures. The SL tends to exhibit a super-adiabatic profile, i.e. temperature diminishes strongly with the height (and so does potential temperature), more than a parcel adiabatically raised would do; this is a feature of instability. Friction at the earth surface usually causes the SL to develop a strong wind shear (see figure 1.12); it has to be kept in mind that ideally the no-slip condition at the surface should hold. The mixed layer, sometimes referred to as the convective layer (CL), is the body of the ABL where the larger convective motions take place. The mixed layer is also the part of the ABL in which the properties are more homogenized, in particular potential temperature and humidity are nearly constant with height (see figure 1.12). The more the surface is heated and energy is given to the air, the more the mixed layer will grow in height. The entrainment zone separates the ML from the free atmosphere (FA). The EZ is characterized by the presence of parcels which sink from the FA and parcels which end their ascent from the ML. In the EZ exchanges of properties between the FA and the ML take place and clouds may form. The geostrophic wind $\vec{u}_g$, which characterizes the FA, is usually taken as a boundary condition at the top of the ABL and both models and observations show the wind to develop a sub-geostrophic profile in the ABL (see figure 1.12). The fact that the wind cannot exceed the geostrophic value in the ABL is mainly due to the strong friction at the surface: during the day, turbulent fluxes are large, and the wind will reach a steady state (i.e. no acceleration of the wind) and the mean terms of the zonal and meridional components can be parameterized as:

$$\overline{u}_{day} = u_g - \frac{1}{f}\frac{\partial \overline{v'w'}}{\partial z} \qquad \overline{v}_{day} = \frac{1}{f}\frac{\partial \overline{u'w'}}{\partial z}$$

The height of the ABL, which can be defined in many ways, e.g. the point at which the Richardson number changes sign or the base of the entrainment zone, can reach values up to

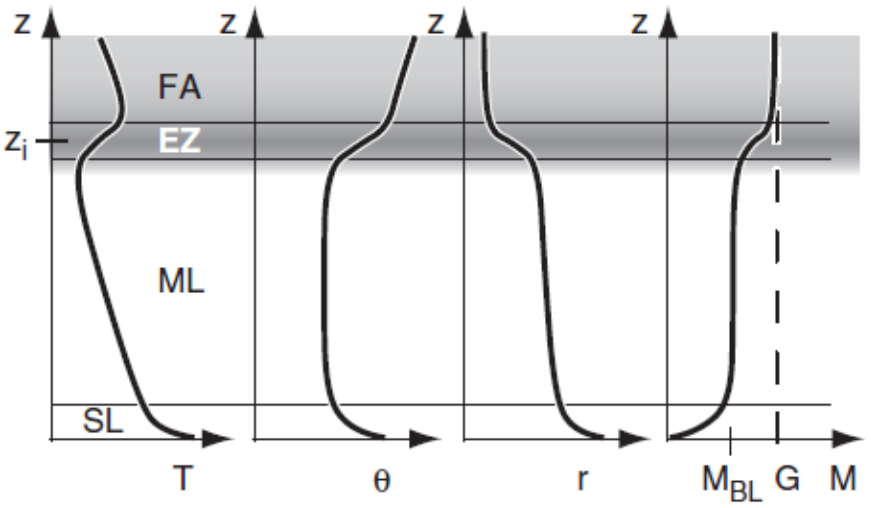

Figure 1.12: The vertical profiles of some physical quantities in the daytime ABL. The shading delineates statically unstable (white) to very stable (black) layers. The G values indicates the geostrophic wind in the FA. The θ profile testifies a super-adiabatic profile in the SL. Adapted from Stull, 1988.

$4000\,m$ on a desert during summertime while the usual value at the mid latitudes oscillates around $2000\,m$. Convective motions start diminishing their intensity in the afternoon and even before twilight they tend to cease because the net flux of energy in the ABL gets negative and the energy lost by radiative transmission is more than that gained from solar radiation. Therefore, as time passes by the daily ABL leaves room to the nocturnal ABL.

1.7.2 Night-time evolution

After sunset, the SL rapidly cools and parcels near the surface, which are less dense than the above ones, are prevented from rising up. Turbulence ceases to form in about an hour (recalling figure 1.5, the lifetime of the largest vortices is about half an hour). Consequently, without considering exceptional cases, e.g. nights with strong winds, air tends to stratify and the nocturnal boundary layer (NL) forms. The NL starts forming from the ground "infiltrating" under the daily ABL but cannot reach the heights of the daily ABL so that a well mixed residual layer (RL) remains above the NL, disconnected from the surface (see figure 1.11). The RL is separated at the top from the FA by the so-called capping inversion (CI) which is characterized by a strong inversion and prevents air from the ABL to raise into the FA. The NL is characterized by thermal inversions, i.e. the temperature profile increases with the height near the surface so that cooler air is below warmer air and a stable configuration holds. Typically the NL reaches heights of $200\,m$ to $400\,m$; over sea during winter time it can get down to $80\,m$. Turbulence hardly develops, if not for strong wind shears associated with particular synoptic conditions, e.g. the passage of a front, and consequently surface winds at night are much lower and less

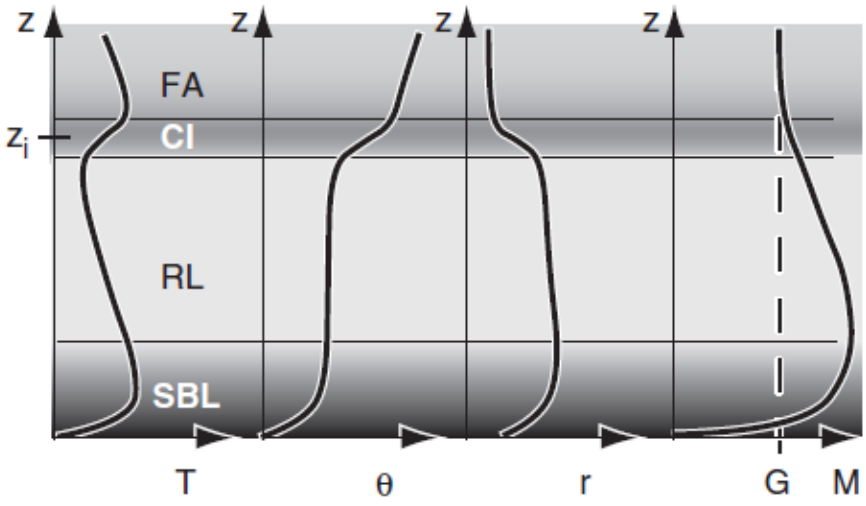

Figure 1.13: The vertical profiles of some physical quantities in the night time ABL. The shading delineates statically unstable (white) to very stable (black) layers. The G value indicates the geostrophic wind in the FA. The M profile testifies the presence of LLJ. Adapted from Stull, 1988.

gusty than during the day. On the other hand, low-level jets (LLJ), known as nocturnal jets, usually located 100 to 300 m above the ground, may form. LLJ are essentially fast moving masses of air, whose wind speed can reach values up to $20\,m \cdot s^{-1}$ (on rare occasions LLJ with wind speed up to $30\,m \cdot s^{-1}$ have also been observed). LLJ generally form overland under clear sky conditions, can extend for hundreds of kilometers in length and are super-geostrophic, i.e. the wind speed exceeds the geostrophic wind one (see figure 1.13). Many factors can contribute to the formation of LLJ, among which it is interesting to mention inertial oscillations (for further studies see Stull, 1988 or Garratt 1992). Turbulent mixing terms can be removed from the equations but the acceleration terms have to be considered so that an oscillatory equation for the mean zonal wind can be derived:

$$\frac{\partial^2 \overline{u}}{\partial t^2} = -f^2 \left(\overline{u} - u_g\right) \tag{1.23}$$

Equation 1.23 is the equation of a simple harmonic motion and leads to the following expression for the mean zonal and meridional wind:

$$\overline{u}_{night} = u_g + \overline{v}_{day} sin\left(ft\right) + \left(\overline{u}_{day} - u_g\right) cos\left(ft\right)$$

$$\overline{v}_{night} = \overline{v}_{day} cos\left(ft\right) - \left(\overline{u}_{day} - u_g\right) sin\left(ft\right)$$

It is easy to see that the ageostrophic component of the wind in such expressions performs a clockwise rotation about the geostrophic wind and that the geostrophic value of the wind can be exceeded.

1.8 ABL parameterizations

In section 1.7 a phenomenological description of the main features of ABL dynamics was proposed but, in order to make quantitative evaluations regarding the evolution of the ABL, specific parameterizations have to be developed. Sections 1.4 and 1.6 underlined the difficulties in solving the equations upon which fluid dynamics is based. In particular section 1.6 dealt with the closure problem and the necessity to rely on experimental evaluations in order to close the system of equations. In section 1.3 it was discussed how Kolmogorov and others have made use of dimensional-analysis to describe turbulence. It was also mentioned that the Buckingham Pi theorem provides a theoretical basis for such dimensional studies which can be formalized in a similarity theory. It has to be stressed that the expression “similarity theory" does not refer to a specific theory but rather to a set of theories which at the core use dimensional analysis aiming to find relationships between different quantities in non-dimensional form and revealing underlying scaling laws (see Garratt, 1992). There are, therefore, many similarity theories. In order to develop a similarity theory a general procedure is provided by the so-called Buckingham Pi theory which improves Rayleigh's method of dimensional analysis, first developed by Lord Rayleigh (see Stull, 1988). The procedure involves the formation of dimensionless groups of variables starting from the physical variables which characterize the system under study. Given the physical variables, the dimensionless groups that can be formed are not unique and different choices lead to different similarity theories. In this context different similarity theories are referred to as different classes of similarity scale. The selection of the key variables, also referred to as scaling variables for a particular class of similarity, is a fundamental step in the development of a theory. Through the years, many studies have been made and long lists of scaling variables can be found (e.g. Stull, 1988). It is interesting to note that no time scale is usually picked since it can be derived form a combination of the length and velocity scales. Different classes of similarity, i.e. different ways to parameterize the equations, are related to different physical conditions: a convective layer will be better described with different parameterizations than those suitable for a stable layer. The purpose of this thesis is to compare the performances of different parameterization schemes of the ABL implemented in the WRF model. Such schemes will be better described in chapter 3 and they all rely on similarity theories.

A few scaling quantities are now introduced to give some examples:

- the friction velocity $u_*^2 = \left(\overline{u'w'_s}^2 + \overline{v'w'_s}^2\right)^{1/2} = \left(\tau'_{xz}{}^2 + \tau'_{yz}{}^2\right)^{1/2} / \overline{\rho}$
- the Obukhov length $L = \frac{-\overline{\theta_v} u_*^3}{kg\left(\overline{w'\theta'_v}\right)_s}$
- the Deardorff velocity $w_* = \left(\frac{gz_i}{\overline{\theta_v}} \left(\overline{w'\theta'_v}\right)_s\right)^{1/3}$

The friction velocity u_*, also known as shear velocity, is proportional to the magnitude of Reynolds' stress at the surface and is very important to describe the velocity profile when turbulence is generated by wind shear. The Obukhov length L is introduced by manipulating equation1.9 with the friction velocityu_* and the von Karman constant k and can be used to identify the height above the surface at which buoyancy overcomes the mechanical production of turbulence. Under convective conditions, buoyant and shear production terms become equal at about $z = -0.5\,L$. Typically, L is negative during the day and positive during the night. The Deardorff velocity w_*, also known as free convection scaling velocity or convective velocity, is a scaling quantity suitable for mixed layers with strong convection depending on the buoyancy flux and on the height of the mixed layer z_i. It is important to underline that the determination of the boundary layer height h is most critical to the representation of nonlocal mixing.

Chapter 2

The WRF model

2.1 Introduction

The Weather Research and Forecasting (WRF) model is a numerical model developed and improved in the last two decades for purposes of both research and operational forecasting use. WRF is a limited area model designed to work on many different computing platforms (it is particularly suited for parallel computing environments) and is available via free download. The model simulates many physical processes and can resolve a wide range of scales both in time and space. Each run requires initial and boundary conditions that are usually supplied by global simulations. Users have the possibility of defining the domain and many physical parameterizations. All these properties make the WRF model very flexible. WRF is constantly updated and new versions are released every year. For this work version 3.9 was used (see Skamarock et al., 2008).

WRF considers the atmosphere as a fully compressible and non-hydrostatic fluid. Equations are integrated applying Runge-Kutta methods. A terrain-following mass vertical coordinate is adopted to write the equations (see figure 2.1). Such coordinate, named η, is defined by:

$$\eta = \frac{P_h - P_{ht}}{P_{hs} - P_{ht}}$$

where P_h is the hydrostatic component of the pressure whereas P_{hs} and P_{ht} are respectively the hydrostatic pressure along the surface and at top boundaries. An Arakawa-C grid system is used (see figure 2.2). On such a grid scalar quantities are evaluated at the center of a cell while vector quantities are evaluated in the middle of the cell boundaries. Scalar quantities at the

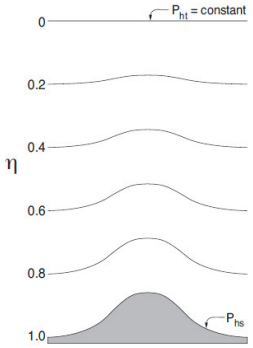

Figure 2.1: A depiction of the terrain-following hydrostatic-pressure vertical coordinate η.

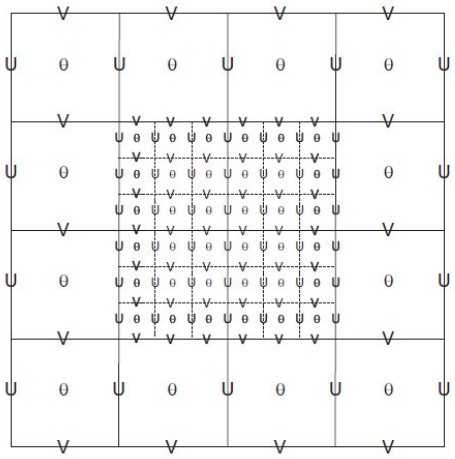

Figure 2.2: A depiction of the Arakawa-C grid staggering. The solid lines represent coarse grid cell boundaries; the dashed lines represent the boundaries for each fine grid cell. The horizontal components of velocity (U and V) and the potential temperature θ are shown as representative of vector and scalar quantities.

center of a cell represent a mean value over the cell while vector quantities at the boundaries represent an average across each cell face.

2.2 WRF computational chain

There are three main steps in the WRF computational chain: the pre-processing activities, the run and the post-processing activities. These three different kinds of activities basically consist in: definition of the domain and interpolation of initial and boundary conditions on it, integration of the physical equations, manipulation and visualization of the results.

2.2.1 Pre-processing: WPS

The pre-processing activities are handled by the WRF Pre-processing System (WPS) which executes a sequence of programs in order to prepare the input for the dynamics solver (see figure 2.3). WPS is available for download along WRF and new versions are released as well. For this work version 3.9.1 of WPS was used. To run WPS, files containing meteorological and static fields are required, namely the values in space of physical quantities that will be used to initialize and drive the WRF model. This work used input files provided by the European

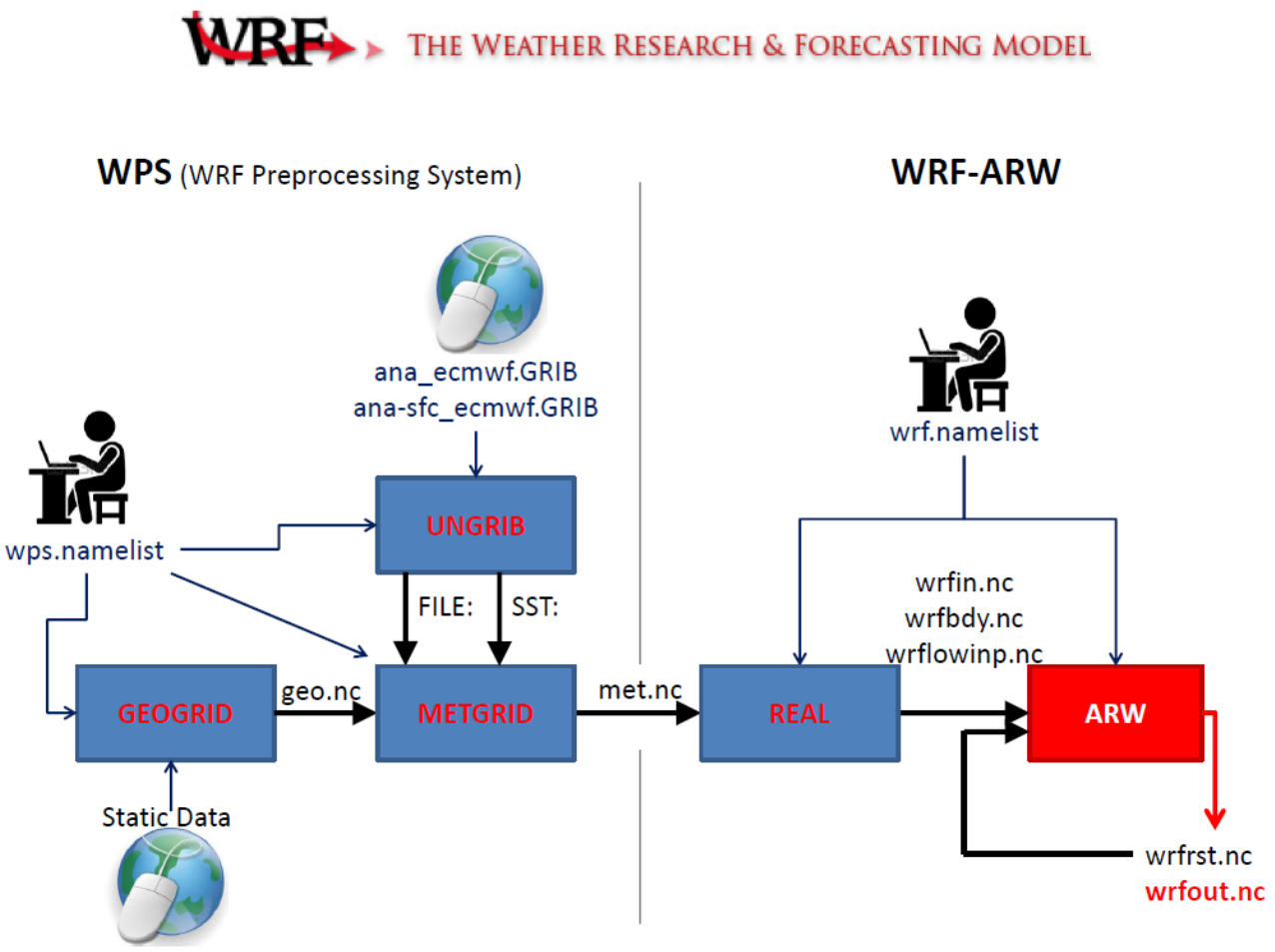

Figure 2.3: The computational chain of the WRF model.

Center for Medium-Range Weather Forecasts (ECMWF). Furthermore users have to edit a namelist specifying options that tell the WPS which files to select and how to handle them. WPS consists of three different programs: *ungrib.exe*, *geogrid.exe* and *metgrid.exe*.

Ungrib.exe

Ungrib.exe extracts information about the values of the different meteorological fields from GRIB files. In case sea surface temperature (SST field) assimilation has to be done, users have to run *ungrib.exe* twice, changing the source files if the SST field is archived in a different set of files with respect to the ones containing the boundary conditions. For the SST run, the namelist has to be modified. This program generates files in an intermediate format.

Geogrid.exe

Geogrid.exe defines the grid of the virtual space in which equations are to be solved from the WRF model. *Geogrid.exe* is independent from *ungrib.exe*, meaning these two programs can be

run separately. *Geogrid.exe* needs a file named 'GEOGRID.TBL' in which there are specifics for all the fields such as:

==========

name = VAR

priority = 1

dest_type = continuous

masked=water

fill_missing=0.

interp_option = default:average_4pt

interp_option = 10m:average_4pt

interp_option = 20m:average_4pt

interp_option = 30m:average_4pt

interp_option = 1deg:average_4pt

interp_option = 2deg:average_4pt

rel_path = default:orogwd_10m/var/

rel_path = 10m:orogwd_10m/var/

rel_path = 20m:orogwd_20m/var/

rel_path = 30m:orogwd_30m/var/

rel_path = 1deg:orogwd_1deg/var/

rel_path = 2deg:orogwd_2deg/var/

==========

In the end some netcdf files named 'geod<domain>.nc' are generated.

Metgrid.exe

Metgrid.exe has the function to interpolate the meteorological fields, arranged by *ungrib.exe*, on the model grid defined by *geogrid.exe*. These new files are the input files for WRF. In order to be run, *metgrid.exe* needs a file named 'METGRID.TBL' in which there are, for all physical fields, many specifications which tell how to perform the interpolations of the values on the grid. For example, the settings of two important fields are next shown:

```
   ==========================================
name=SKINTEMP mpas_name=skintemp
interp_option=sixteen_pt+four_pt+wt_average_4pt+wt_average_16pt+search
masked=water
interp_water_mask = LANDSEA(0)
fill_missing=0.
==========================================
==========================================
name=SST
interp_option=sixteen_pt+four_pt+wt_average_4pt+wt_average_16pt+search
masked=land
interp_land_mask=LANDSEA(1)
fill_missing=0.
missing_value=-1.E30
flag_in_output=FLAG_SST
==========================================
```

SST assimilation

WRF does not describes the evolution the sea surface temperature, which is taken as a boundary condition. Therefore, if long runs have to be made (longer than a couple of days), it is fundamental to update the SST every day. SST assimilation is performed during the pre-processing activities. At the beginning of this work, while setting the model, two kinds of surface boundary conditions were tested, namely those provided by '*ana*' files, having a $50\,km$ horizontal resolution, and those provided by '*ana-sfc*' files, having a $15\,km$ horizontal resolution. The latter ones were used in the simulations. Updates can be done with the frequency chosen by the user but the SST values actually change just once a day. This of course is inappropriate for a proper description of oceanographic phenomena but, since the SST updates influence significantly just runs longer than a few days, it is acceptable. In order to appreciate the higher resolution provided by the '*ana-sfc*' files, it is vital to properly 'mask' the domain. WRF distinguishes land from sea surface thanks to some fields named 'LANDMASK' and 'LANDSEA'. These fields define some masks over the terrain as-

suming different values on land and on water. The LANDSEA mask was found to be better than the LANDMASK mask in terms of resolution. Their usage must be specified for every physical field which requires it in the METGRID.TBL file cited when discussing *metgrid.exe*. Two lines have to be specified: 'masked=land' ('masked=water') indicates that the field has to be interpolated only over water (land) and 'interp_land_mask=LANDSEA(1)' ('interp_water_mask = LANDSEA(0)') specifies that water (land) is defined by those points where the LANDSEA field is not equal to 1 (0) but is equal to 0 (1). In fact, LANDSEA equals 0 over land and 1 over sea (on the contrary of LANDMASK which equals 1 over land and 0 over water). The specifics of the SST and the SKINTEMP fields were provided previously in this section (2.2.1). It can be seen that masks are specified in order to interpolate the SST fields over sea and the SKINTEMP field over land (see figure 2.4b and 2.4c). The specific 'interp_option=sixteen_pt+four_pt+wt_average_4pt+wt_average_16pt+search' is very important as well: it tells the program to interpolate the points at the highest possible resolutions. The chain of specifics, connected with the '+' sign, lets the program start with the finest resolution when possible and then use the lower ones when not possible (compare figure 2.4a and 2.4b). Figure 2.4d shows the SKINTEMP field over a domain comprising both land and water. The values over water are defined by the assimilation of the SST field.

2.2.2 The run: WRF

Once WPS activities have ended and the input files are ready, WRF can run. WRF can actually realize simulations both for ideal and real cases. Ideal cases are not of interest for this work. To simulate real events, an initialization program has to be run first: *real.exe*. After *real.exe*, a numerical integration program (*wrf.exe*) is run. The WRF system contains two dynamical solvers, referred to as the ARW (Advanced Research WRF) core and the NMM (Nonhydrostatic Mesoscale Model) core. ARW was utilized in this work. The WRF model is also provided with other programs such as *tc.exe* which is used to study tropical cyclones, but they were not considered for this work. Before starting the processing activities, all the physical options desired and the domain specifics have to be defined in a file (*namelist.input*). The period of integration and the eventual generation of restart files must be set as well. Among the options there is one which specifies the ABL parameterization. Such option influences the equations to be integrated. Prognostic equations are solved for every grid point (actually some

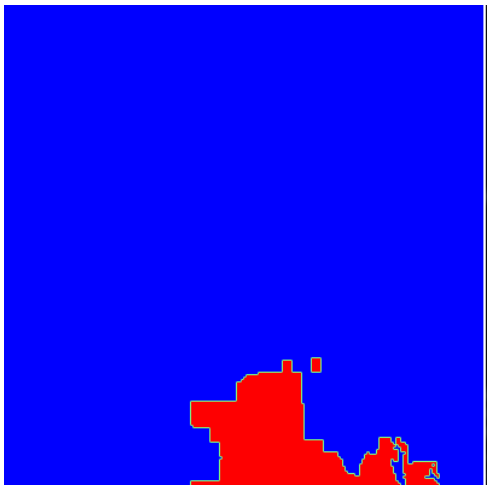

(a) SST mask over water with low definition interpolation.

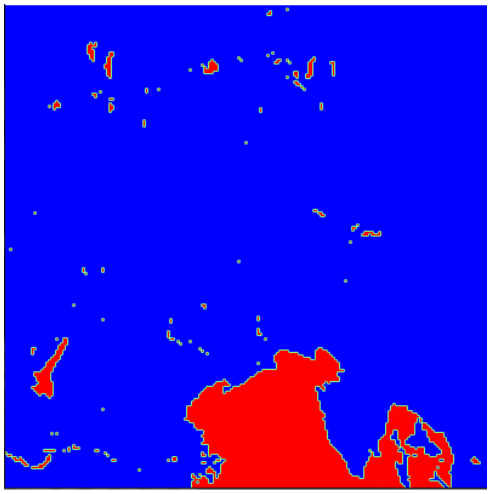

(b) SST mask over water with high definition interpolation.

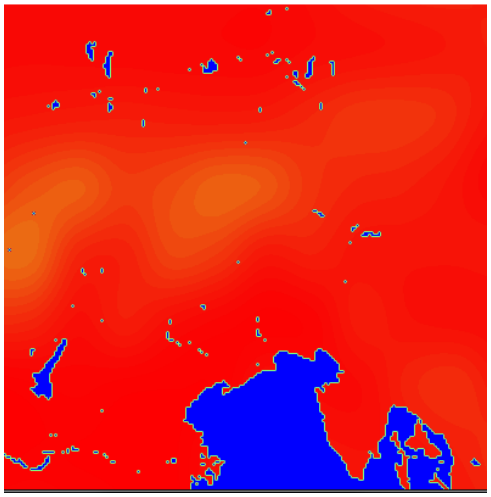

(c) SKINTEMP field mask over land.

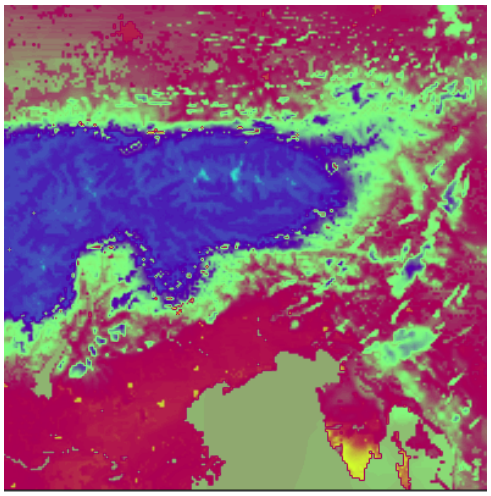

(d) SKINTEMP field over all the domain.

Figure 2.4: An example of the action of the masks over a domain and the importance of interpolation.

fields are staggered: remember the Arakawa-C grid depicted in figure 2.2) on the considered levels. The number of levels can also be set in the options but a larger number of levels does not guarantee better performances. For this work 30 levels plus the ground level were considered. The first level height is about a hundred meters but varies from point to point (remember the terrain-following mass vertical coordinate η shown in figure 2.1). At every time step the fields within the surface layer (SL), at points between the ground and the first level, are evaluated with diagnostic equations defined by the particular ABL parameterization considered and so by the way the equations are closed relying on a given similarity class (see sections 1.6 and 1.8).

2.2.3 Post-processing

WRF models outputs files in netCDF format, which is a standard in the atmospheric sciences. After the simulations have ended, netCDF files may be analyzed and manipulated according to the needs. The main supporting post-processing utilities are: NCL, RIP4, ARWpost, UPP, and VAPOR.

These activities are those most time consuming and require a lot of computational and programming work. During this thesis a lot of time was dedicated to the post-processing that led to the results.

Chapter 3

Simulations

Calculations were submitted to a computer cluster using four computational nodes consisting of 40 cores each.Each simulation took about 24000 (160x150) core x computational hours. In this chapter the specifics adopted for the realization of the simulations are shown and explained. One section is dedicated to summarize some characteristics of the parameterizations.

3.1 Domain settings

Simulations were performed considering three nested domains (see figure 3.1). Such domains were chosen to include respectively most of Europe down to north Africa (domain d01), Italy (domain d02) and the Friuli Venezia Giulia region (domain d03). Domains d01 and d03 are square, domain d02 is rectangular. The specifics are reported in table 3.1. The number of points in the grid along the west-east and the north-south directions are respectively specified by 'e_we' and 'e_sn'. The number of vertical levels, included the ground, is defined by 'e_vert'. The time and space resolutions and the values that define the nesting point are reported as well.

At the beginning of the simulations initial and boundary conditions were defined specifying the

domain	time step	resolution	grid	parent_id	i-start	j-start	e_we	e_sn	e_vert
d_01	$200\,s$	$50\,km$	1	0	1	1	96	96	31
d_02	$40\,s$	$10\,km$	2	1	36	27	136	156	31
d_03	$8\,s$	$2\,km$	3	2	68	112	91	91	31

Table 3.1: Summary of the settings for the three considered domains.

values of every variable at each point of the domain. Then, every six hours boundary conditions

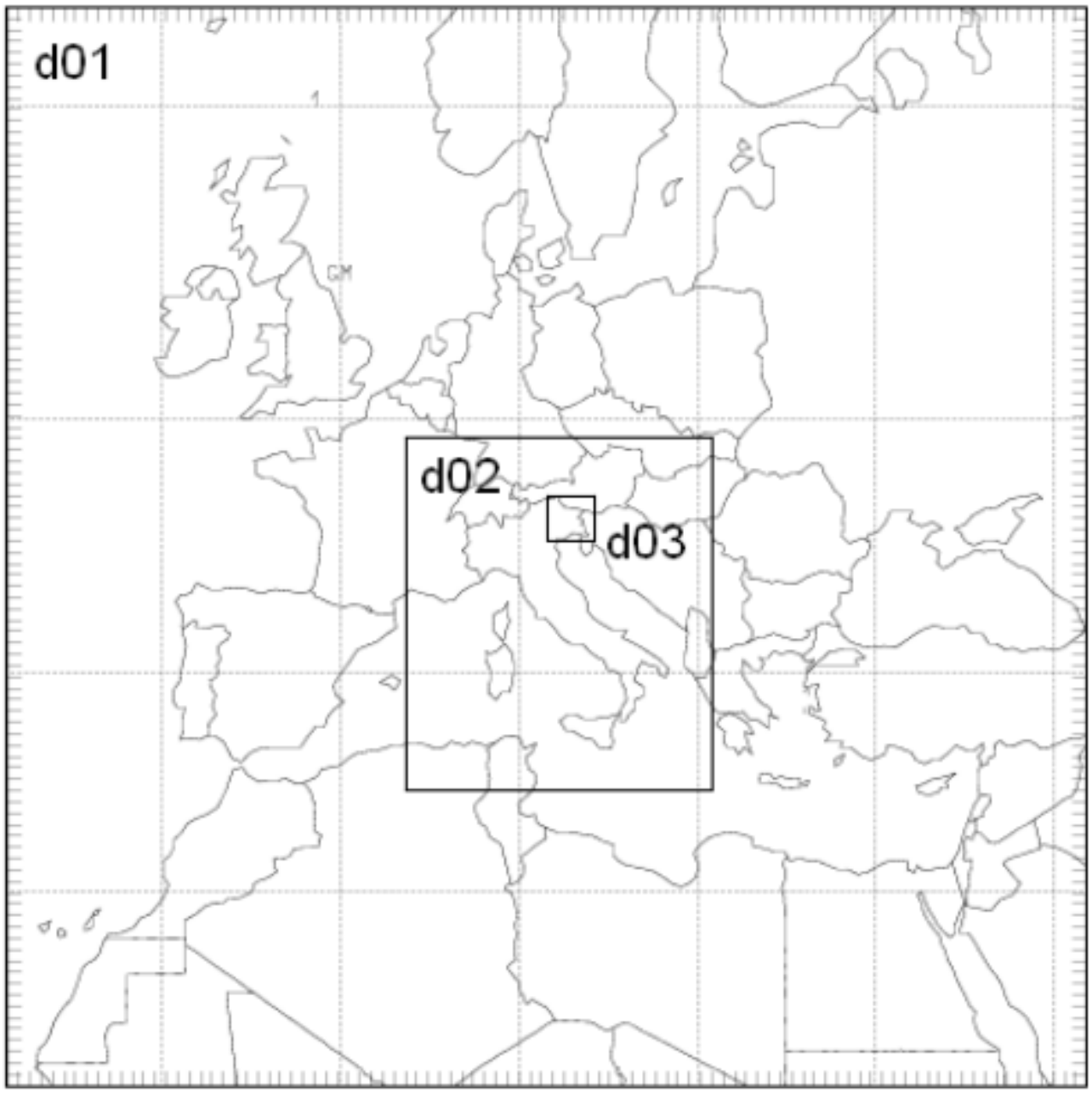

Figure 3.1: The three nested domains considered in the simulations.

were uploaded on the borders of the three domains so that simulations were guided all the year long. A drift of the simulation in their evolution is excluded because of such a continuous change of the dynamical boundary conditions and because the static boundary conditions, i.e. the model of soil (see section 3.2), are very good. Spin-up phenomena at the beginning of the simulations can be neglected since the model settles in the first few hours and they are not noticeable when looking at the entire simulated year.

3.2 PBL parameterizations

In the next subsections, brief presentations of the main characteristics of the parameterizations considered in this work are reported. No aim of completeness is intended: the purpose is just to underline general aspects of their behaviors necessary for the data analysis. Table 3.2 shows a brief summary of the closure order and the type of scheme of the various parameterizations. Also the values of the physical options which have to be specified in the WRF namelist are reported. Option 'bl_pbl' defines the scheme of the ABL. Option 'sf_sfclay_physics' defines the surface layer: 0 for no surface layer, 1 for the Monin-Obukhov Similarity scheme, 2 for the Monin-Obukhov Janjic Eta Similarity scheme, 7 for the Pleim-XU scheme. Option 'sf_surface_physics' is the land-surface option: 0 for no surface temperature prediction, 1 for the thermal diffusion scheme with five layers, 2 for the Noah Land-Surface Model (unified NCEP/NCAR/AFWA scheme with soil temperature and moisture in four layers, fractional snow cover and frozen soil physics), 7 for the Pleim-Xu scheme.

ABL scheme	code	local	order of closure	bl_pbl	sf_sfclay_physics	sf_surface_physics
improved asymmetric convective model	ACM2	hybrid	1	7	7	7
BouLac	BLC	yes	1.5	8	2	2
Grenier-Bretherton-McCaa	GBM	yes	1.5	12	1	2
MYJ	MYJ	yes	1.5	2	2	2
MYNN3	MN3	yes	2	6	2	2
Shin-Hong	SHG	hybrid	1.5	11	1	2
YSU	YSU	no	1	1	1	2

Table 3.2: Summary of ABL parameterizations specifics.

3.2.1 ACM2

ACM2 is an hybrid model which tries to improve the original asymmetric convective model ACM. ACM was originally developed to describe large-scale turbulence characterized by large transport driven by convective plumes. ACM is a non-local scheme and its weakness is the inability to portray small-scale subgrid turbulent mixing which is usually described by eddy diffusion schemes, which on the other hand assume all turbulence is subgird and cannot describe deep convection. ACM2 was designed to overcome these problems combining the non-locality of ACM with an eddy diffusion scheme. Therefore, ACM should well describe both supergrid and subgrid scale components of turbulent phenomena in convective boundary layers (see Pleim, 2007a and Pleim 2007b). ACM2 is reported to perform better than simple eddy diffusion

models which include a nonlocal term in the form of a gradient adjustment. Without going into much detail, nonlocal and local equations are both implemented. They run separately and are combined in the evaluation of the fluxes at the top of the various levels so that total quantities are conserved. Also, a coefficient, f_{conv}, which ranges from 0 to 1, is introduced to evaluate the degree of importance of local evaluations against nonlocal evaluations. When $f_{conv} = 0$, ACM2 behaves as an eddy diffusion scheme; when $f_{conv} = 1$, ACM2 behaves like ACM. ACM2 is reported to well represent ABL heights, temperature profiles, and surface heat fluxes.

3.2.2 BLC

At the surface level, the vertical turbulent fluxes are calculated with bulk transfer formulae which combine quantities at the surface and at the first level (see Bougeault and Lacarrere, 1989). For the higher levels, the vertical turbulent fluxes are computed using vertical diffusion coefficients which depend on the TKE. This scheme is a so-called one-and-a-half order closure scheme (there is a prognostic equation for the TKE). This model is reported to well represent clear-air turbulence in regions where the flow passes over steep orography.

3.2.3 GBM

This scheme was developed to give a realistic description of stratocumulus capped boundary layers (SCBLs), especially over tropical and sub-tropical oceans. It is based on a one-and-a-half order turbulent closure model and includes an entrainment closure at the top of a convective boundary layer, where an infinitely thin inversion is assumed to exist (see Grenier and Bretherton 2001). Eddy diffusivity and eddy viscosity are related to the TKE. Entrainment treatment is based on Turner-Deardoff closure (see Turner, 1973), which relates the entrainment rate to the TKE of the BL and also to an eddy length scale and to the strength of the inversion. Inversion can be treated with three different approaches: prognostic inversion, reconstructed inversion, and flux-level-restricted inversion (for more details see Grenier and Bretherton 2001). Entrainment closure is not used in stable boundary layers and in such cases GBM reduces to a standard 1.5 turbulent closure model. Vertical TKE transport has been artificially increased, so that the profiles would better match those of the large eddy simulations (LES). Some studies were

made to test this model capabilities (see Bretherton et al., 2004 and McCaa and Bretherton, 2004).

3.2.4 MYJ

Turbulence is described relying on the level 2.5 closure in the Mellor Yamada hierarchy (see Mellor and Yamada, 1974) in the FA and in the ABL whereas the level 2 closure in the Mellor Yamada hierarchy is considered for the SL (see Janjić, 1990). The heat flux from the surface into the ground is proportional to the net flux at the surface. The temperature of the deep ground is base on a dependence of the temperature at 2.5 m under the surface on the latitude and the terrain height. The snow height is prognostically evaluated. 4th order nonlinear diffusion schemes are used for lateral diffusion; the diffusion coefficients depend on the TKE. The Betts and Miller scheme for deep and shallow convection is adopted (Betts, 1986 and Betts and Miller, 1986) but some additional options are added, e.g. the precipitating water is allowed to evaporate in unsaturated underlying layers. It is reported that MYJ is a good model to forecast severe storms but some problems were found with excessive precipitations and the treatment of convective forcing. Over the years some improvements have been made (e.g. Janjić 1994).

3.2.5 MN3

The MYNN model is an improvement of the Mellor-Yamada model developed by Nakanishi and Niino (see Nakanishi and Niino 2004). MYNN is available in two versions: the level-2.5 version MYNN2, which is a 1.5 order closure scheme, and the level-3 version, which is a second order closure scheme; the latter is the one used in this study (MN3 for brevity). MYNN2 is of course computationally less expensive than MYNN3. Several restrictions are imposed on turbulent quantities, such as temperature variance, in order to avoid numerical instability (higher order closure models can behave pathologically). MYNN can reproduce the occurrence of Kelvin-Helmholtz instability and periodic oscillations. MYNN is reported to well represent the horizontal distribution of advection fogs and the vertical profiles of mean quantities such as temperature (see Nakanishi and Niino 2006).

3.2.6 SHG

SHG is an hybrid model. One of the main goals in the development of this scheme was to better portray the subgrid-scale (SGS) turbulent transport in CBLs. Local and nonlocal transport are separately calculated and then combined with multiplications with a gridsize dependency function (see Shin and Hong 2015). SHG was developed to overcome the difficulties in treating the so-called 'gray-zone', also known as 'terra incognita' (see Wyngaard, 2004). The gray-zone is characterized by the fact that the scale Δ of the spatial filter is comparable with the scale l of the energy- and flux-containing turbulence. In the gray-zone, the vertical transports of quantities such as heat and moisture can vary strongly as a function of resolution. Local and nonlocal equations are separately parameterized according to their different scale dependencies. The gray-zone grid size is shown to increase with the ratio between the surface friction velocity u_* and the convective velocity scale w_*; this ratio is used as a parameter to define different regimes. Eddy-diffusivity techniques are used to describe the local heat transport. To define the diffusivity parameters, explicit grid-size-dependent functions are considered. SHG has been tested against YSU and shown to perform better (see Shin and Hong 2015). The model has also been shown to have spinup problems and to be limited to dry CBLs.

3.2.7 YSU

YSU scheme relies on K-theory. An important feature of YSU is the presence of an explicit treatment of entrainment processes at the top of the ABL (see Hong et al., 2006). ABL mixing is increased in the thermally induced free convection regime and decreased in the mechanically induced forced convection regime. Turbulent mixing is treated with nonlocal closure techniques.

3.3 Extraction of the simulated values

After the simulations had been completed, the physical fields were prepared for the comparison with the measurements. Four fields were considered: temperature at $2\,m$, wind speed at $10\,m$, hourly precipitations and short wave radiation. Time series for these fields were extracted from the netCDF files generated by the simulations through the use of the Climate Data Operators CDOs (see Schulzweida, 2006). In order to optimize the work, it is appropriate

to first 'merge' more files into one and only then perform the extractions so that the number of times CDOs are called is reduced and much computational time is spared. Since netCDF files can be very large (some hundreds of GB), it is also important not to merge too many files together. To create monthly files was found to be a good choice (the merging process together with the following extraction would require less than 4 hours utilizing one core). The 'remapnn' command was used for the extractions. Such command identifies a particular point whose coordinates must be defined and, in case the point falls within a cell of the grid rather than on a grid point, it returns a value which is a weighted average of the values at the grid points which define the aforementioned cell. This could be a limit at zones with complex orography because neighbouring grid points might be placed at significantly different heights and the resulting averaged values would be distorted. Analogous problems could happen at coastal regions if neighbouring points are one on water and one on land.

Chapter 4

Measures

4.1 Introduction

The simulations realized with the WRF model for this work have been tested against measurements over the domain available to ARPA FVG, the Regional Environment Protection Agency of Friuli Venezia Giulia. ARPA FVG constantly monitors the region with several measurement stations placed all over the territory (see figure 4.1). Measurements are taken respecting the World Meteorological Organization (WMO) indications (see Organization, 2007). Therefore, for every station the time series for the fields of temperature at $2\,m$, wind speed and direction at $10\,m$, relative humidity at $2\,m$, pressure, precipitation and solar radiation, with the resolution of an hour, are available. Table 4.1 shows the accuracy of the measurements for the various quantities.

variable	temperature	hourly precipitation	relative humidity	wind speed	pressure	hourly solar radiation
unit	$°C$	mm/h	%	m/s	hPa	kJ/m^2
accuracy	0.5	0.2	5	0.2	0.5	10

Table 4.1: Accuracy of field measurements.

4.2 The region

Friuli Venezia Giulia is a region in north-eastern Italy. It borders Slovenia to the east, Austria to the north and the Veneto Italian region to the west. To the south it faces the Adriatic Sea. The region has a temperate climate but its morphology is quite heterogeneous and it varies considerably from one area to the other. In the north there is the ending section of the Alps

whose heights can reach values larger than $2,800\,m$. In the mountainous area many lakes are present. The central plains are characterized by poor, arid and permeable soil. Therefore, FVG is an ideal region for ABL studies since it is possible to analyze the dynamics in many different conditions. For the study, FVG has been ideally divided into four regions which can be thought as homogeneous from the micrometeorological point of view, i.e. the thermal and pluviometric properties are comparable between places belonging to the same region. These regions are: the mountainous region, the central plains, the coastal region and the open sea. To study these regions some localities have been chosen as representatives, namely Udine, Fagagna and Cividale del Friuli for the central plains, Fossalon di Grado for the coastal region, the Paloma buoy for the open sea and Enemonzo for the mountainous region. The choice of the Paloma buoy was forced since it was the only station available in the open sea. Unlike the other stations the Paloma buoy station does not provide measurements of the precipitations and all fields are measured at the same height as the winds, i.e. $10\,m$. The choice of Enemonzo was not immediate. Many localities were under consideration to characterize the mountainous region but it is hard for the model to well portray them since the complicated orography can easily force the grid points to be at heights very different from the real ones. Enemonzo is in a valley and locally slopes are not too steep. Table 4.2 shows the real heights versus the model heights (above mean sea level) of the locations together with their coordinates.

station	real height (m)	model height (m)	latitude (deg N)	longitude (deg E)
Udine	91	82	46.036	13.228
Fagagna	147	147	46.102	13.084
Cividale del Friuli	127	116	46.081	13.421
Fossalon di Grado	0	2.5	45.716	13.460
Paloma buoy	0	0	45.617	13.567
Enemonzo	438	420	46.408	12.867

Table 4.2: Heights above mean sea level and coordinates of the stations.

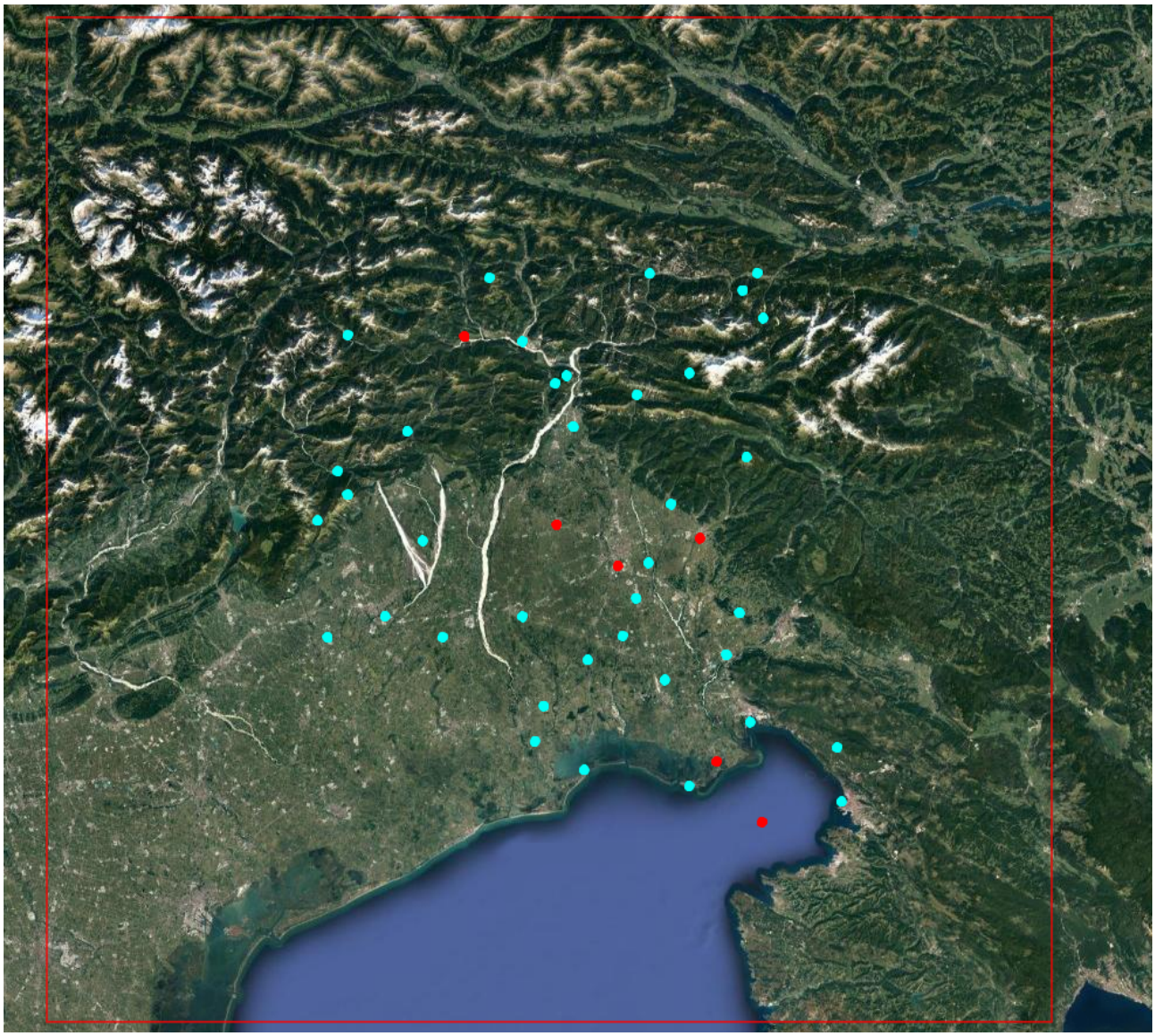

Figure 4.1: The position of the measurements stations over Friuli Venezia Giulia. Cyan dots represent all the stations originally considered for the analysis. Red dots represent the stations actually utilized for the analysis: the one at north is Enemonzo; the three in the middle are, from left to right, Fagagna, Udine and Cividale del Friuli; the one at the coast is Fossalon di Grado; the one in the sea represents the Paloma buoy. The red line delimits domain d03.

Chapter 5

Data analysis

"It doesn't matter how beautiful your theory is,
it doesn't matter how smart you are.
If it doesn't agree with experiment,
it's wrong."

Richard Phillips Feynman

This chapter shows the analysis conducted. The time series of the measurements over Friuli Venezia Giulia were confronted with the simulated data. time series graphs which show the behavior of all the simulations against the measurements were produced. To quantitatively evaluate the efficiency of the parameterizations, many statistical tools were used, namely the Kolmogorov-Smirnov test, the Taylor diagram and the usual calculation of statistical indicators such as mean values and percentiles. The tables with the main statistic values are presented in Appendix B.

5.1 Introduction

The realized simulations provide a lot of information and the main problem in the analysis was to decide which tests to conduct. time series of many variables were available. Since different behaviors take place during the year due to seasonal changes, it seemed appropriate to define different periods of time to be studied. At first groups of three months representing the four seasons were thought as the best option but simulations started in January and ended in December so two different half-winters were to be considered. It was then decided to realize annual and monthly evaluations. It is important to stress from the start that the time window

strongly influences the statistical evaluations because different phenomena dominate at different time scales. For example, considering the entire year and focusing on temperatures, the annual oscillation with large values during the Summer and low values during the winter is the main phenomena and diurnal oscillations are perceived almost as noise. On the other hand, considering a time window of a few days, the alternation between day and night drives the time series, hourly variations can be seen as small perturbations and synoptic phenomena such as the passage of a front modulate the signal.
The purpose of the analysis was to point out the strengths and weaknesses of the various parameterizations. In particular, an answer to the following guide questions was sought:

- Which ABL parameterization reproduces real data the best?
- Which are the main differences between the various ABL parameterizations?
- Are there any kind of limits in the simulations? (extrema not reproduced, physical principles not respected, etc.)

It has been noted that the results are sensibly different from those obtained by previous evaluations realized at ARPA FVG which considered a greater domain for the simulations. Such a fact testifies that equations are very sensible to boundary conditions (see figure 5.1).
Four different types of area were studied: central plains, coastal region, open sea and valley floor. To characterize the central plains the locations of Udine, Fagagna and Cividale del Friuli were chosen. Fossalon di Grado was picked to represent the coastal region while Enemonzo for the valley floor. The open sea area was studied with the data measured at the Paloma buoy. The choice of these locations is explained in chapter 4.

5.2 Temperatures

The annual oscillation is well portrayed by every model at every location with very small differences (e.g, figure 5.3). Taylor diagrams realized considering the entire year show covariances shifting between 0.9 and 0.95 (e.g., figure 5.2). Standard deviations are comparable between simulated data and measurements. It can then be argued that, over the year, all models reproduce the variability of the measurements.

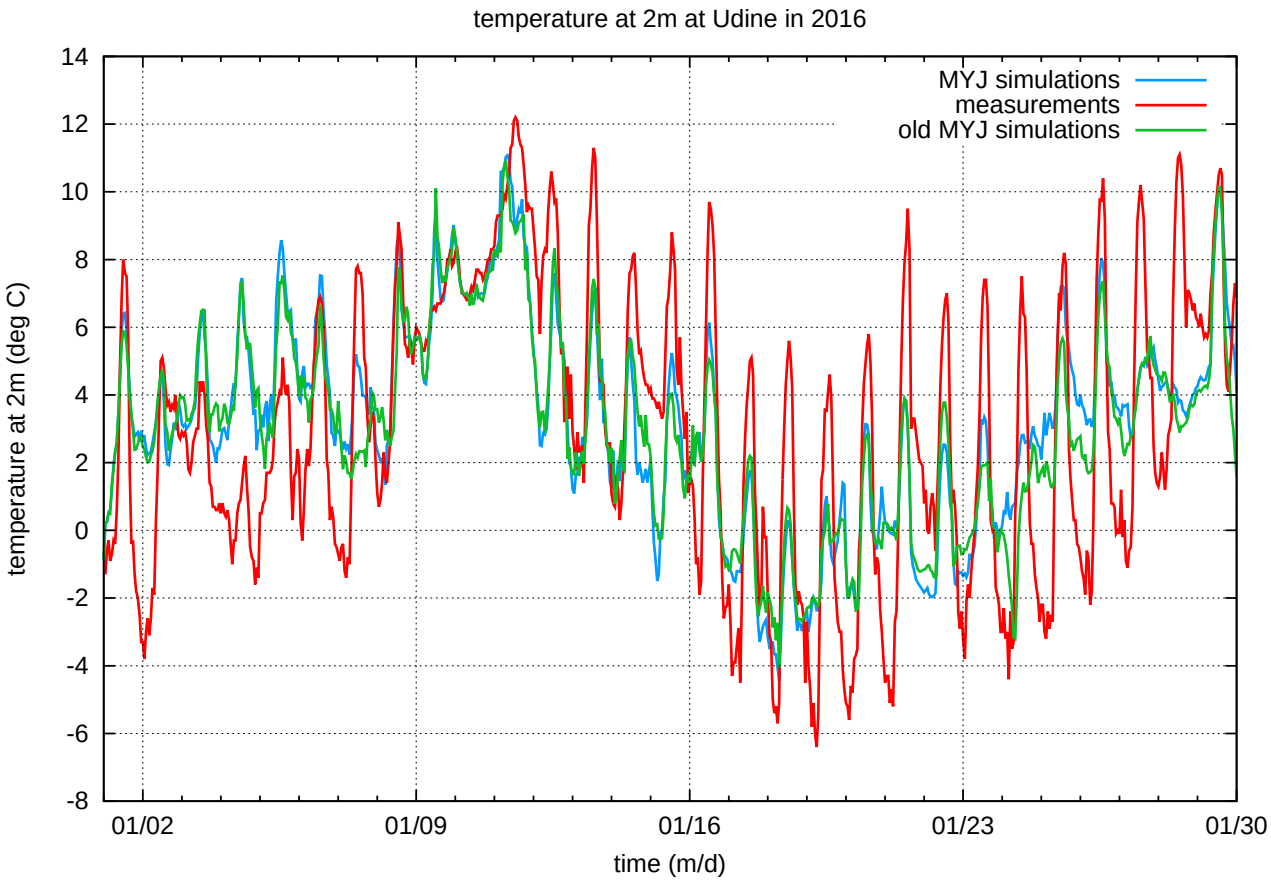

Figure 5.1: A confrontation between the time series of temperature for simulations realized with different small domains. Measurements are in red, old simulations with broader domain in green, new simulations with smaller domain are in cyan.

Central plains

For this analysis some measurements are missing in January at Fagagna. Therefore, the relative set of values could not be considered for the analysis. There are no particular differences between the three locations considered to characterize the central plains. The first thing that strikes is the incapability of all the parameterizations to reach the extrema in certain periods of the year, namely the minima during the winter and the maxima during the summer. The values shown in Appendix B evidence that minima are not reached by any scheme in December as can also be seen in figure 5.4. During the summer, so in June, July and August, minima are systematically overestimated as can be seen looking at the first and 25th percentiles in the tables. In June, maxima are underestimated at Udine as testified by the fact that the 99th percentile of the measurements is higher than that of any simulation. Most models keep underestimating the maxima in July but in August large values are mostly overestimated. The only model which does not overestimate large values in August and which distinguishes itself

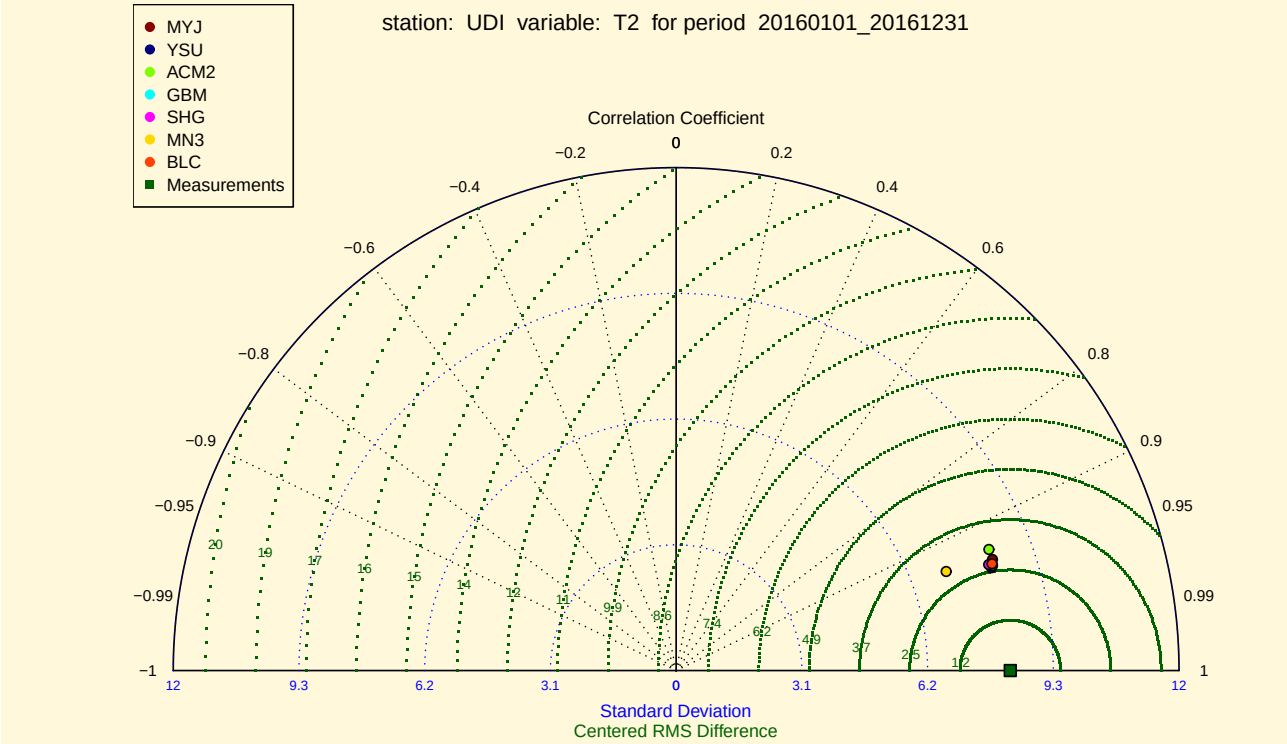

Figure 5.2: Taylor diagram for the temperatures at Udine in 2016.

from the others in an evident way is MN3. MN3 definitely underestimates the measurements in a systematic way: looking at the annual tables, the 99th percentile and maxima are about 5°C smaller. It can be stated that MN3 describes an ABL that is colder than normal.

It is also observed that in June, ACM2 produces temperatures systematically colder than the measurements. This is probably due to the fact that ACM2 intensifies turbulent mixing. The best model during the summer seems to be SHG.

Coastal region

In this transition area between the land and the sea, the presence of water definitely influences thermal balances. The sea has a large heat capacity and this causes all the parameterizations to overestimate minima during the winter and underestimate maxima during the summer. The WRF model portrays the grid point nearest to the coordinates of Fossalon di Grado to be on land but there are many points depicted on water around it. It is interesting to see the effect that this has on the Kolmogorov-Smirnov test when it is extended to more than one grid point. During the summer temperatures are lowered by the presence of the sea whereas during the fall, the winter and the spring temperatures are increased. Looking at the statistical values in Appendix B, all parameterizations produce similar results but MN3 which stands out for its

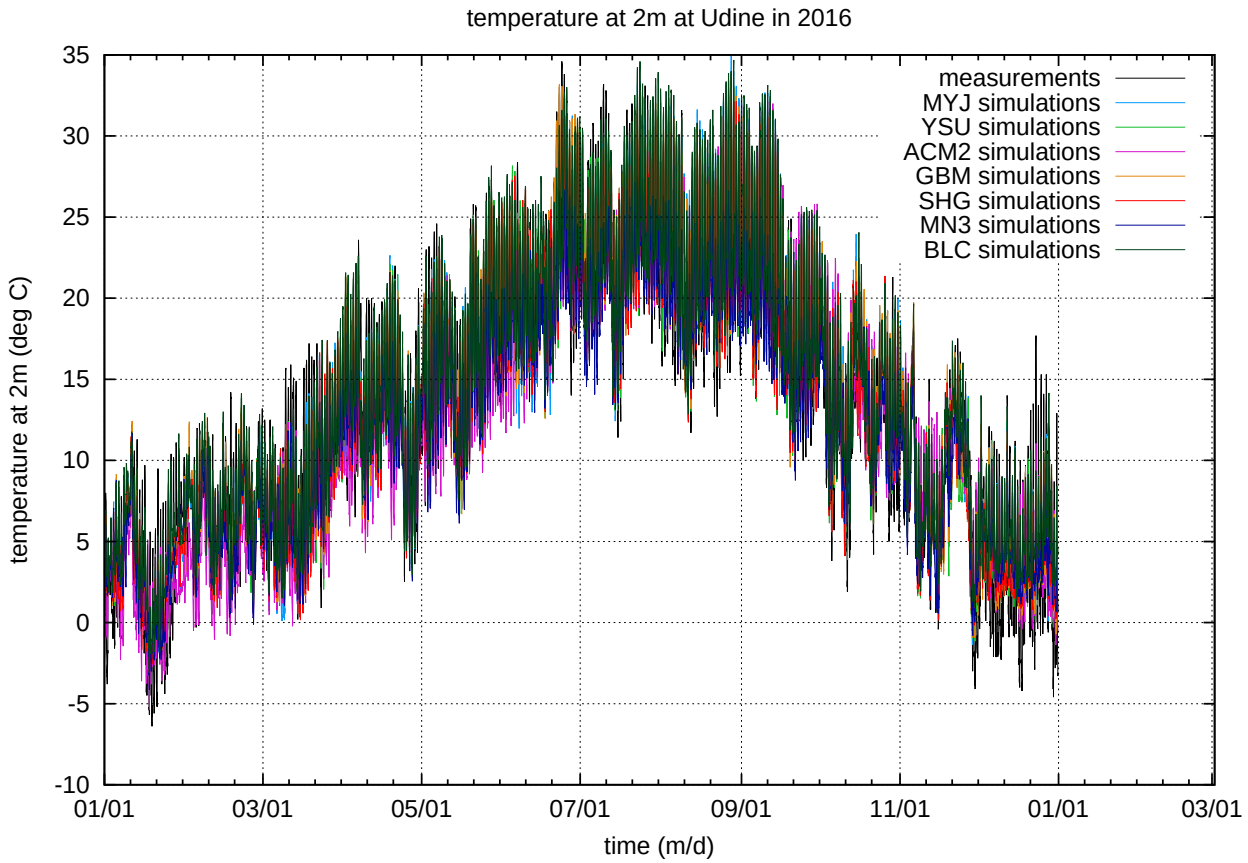

Figure 5.3: time series for the temperatures at Udine in 2016.

bad performances: it systematically underestimates large values; the 99th percentile is always significantly lower than those of the other parameterizations.

Open sea

Unfortunately measurements are missing for many days in January, November and December. Therefore, those moths could not be considered for the analysis. The first effect of being in the open sea is that the time series do not present the large oscillations typical of the land. Looking at the 75th and 99th percentiles shown in the tables, it can be seen that in September and October large values are systematically overestimated by all parameterization, whereas systematical underestimations of large values are evident in February, March, April, June and July. On the other hand, the 1st and 25th percentiles testify that minima are systematically overestimated in June, July, August and October (except in July by MN3). The parameterizations do not distinguish much from one another; the only parameterization which stands out is MN3 whose performance is certainly the worst. Anyhow, the Kolmogorov-Smirnov test and the statistical values can be misleading if we look at the time series. In fact the time series

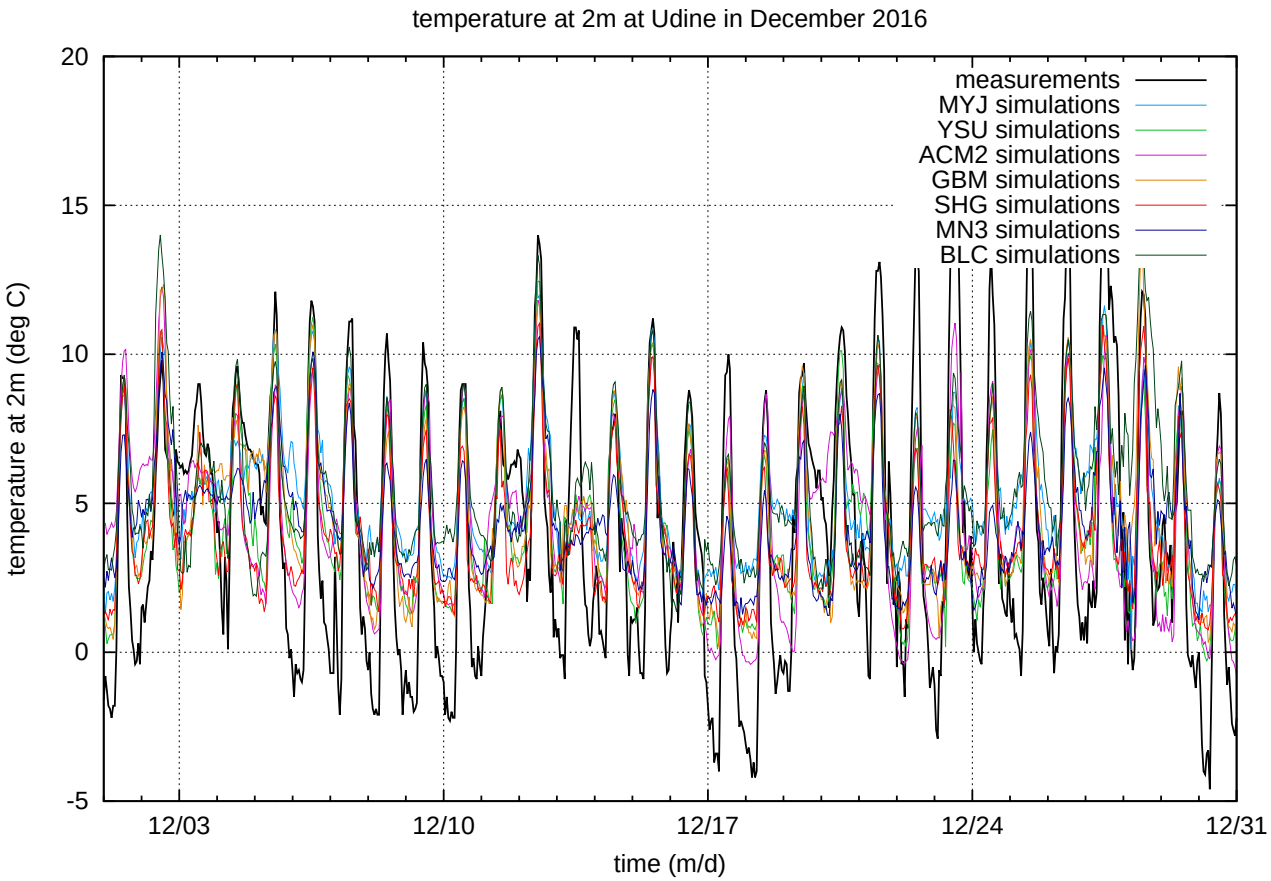

Figure 5.4: time series of the temperatures at Udine in December 2016.

show that periods of several days with systematic underestimations are alternated to periods of several days with overestimations. One thing which becomes evident from the time series is that every model is able to well portray conditions of mechanical turbulence when the ABL is completely mixed. A good example can be seen in figure 5.5. Between 07/13 and 07/15 a major event takes place: temperatures decrease rapidly (less than 24 hours) of almost 10°C. Many analogous events are observed during the year. These phenomena are due to strong winds such as the bora, a strong north-eastern katabatic wind which blows from Slovenia towards the Adriatic sea. Figure 5.5 also shows two periods of progressive heating, before and after the event on 07/13, which were characterized by light wind and clear weather. During such periods, every model shows difficulties in reproducing the diurnal variations but synoptic forcings are well portrayed.

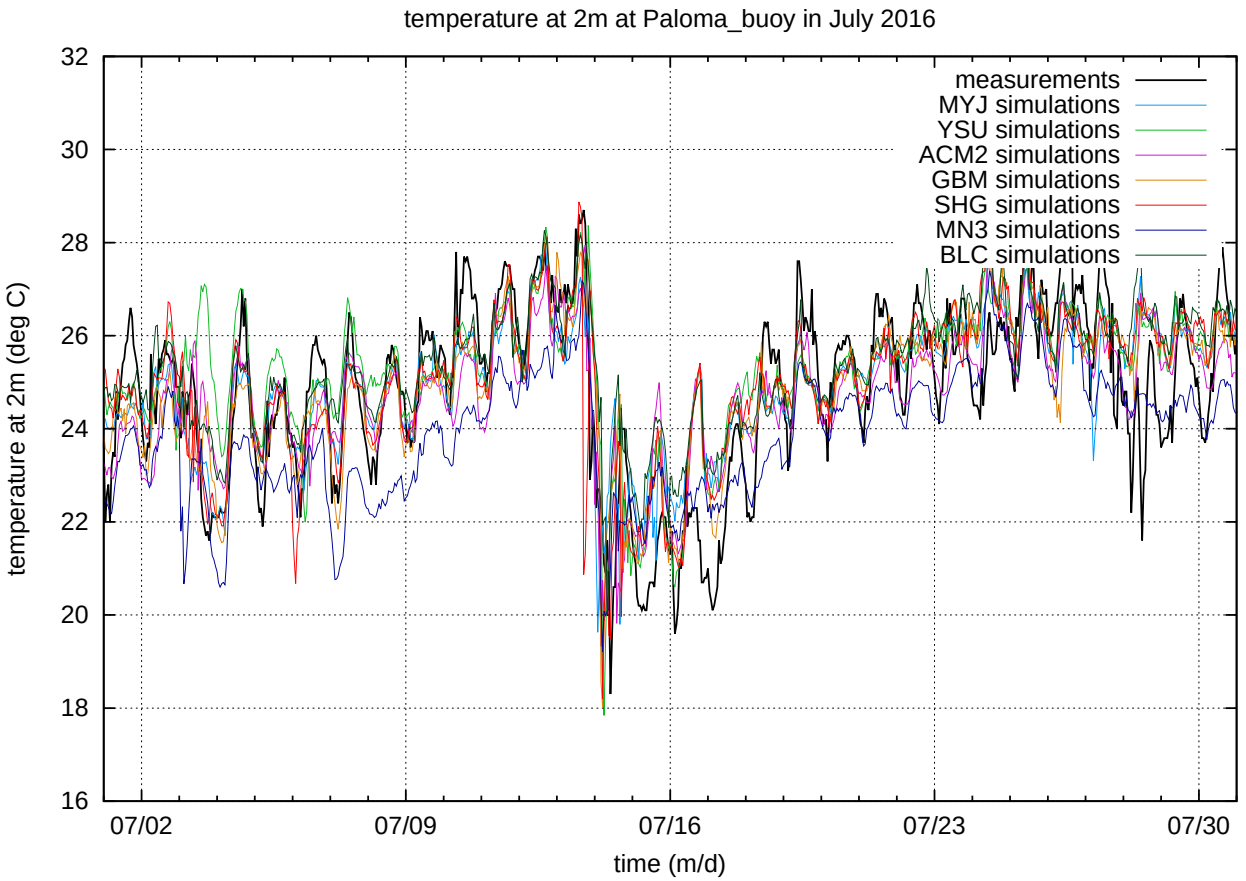

Figure 5.5: time series of the temperatures at the Paloma buoy in July 2016.

Valley floor

Unfortunately measurements are missing for many days in July, August, September and October. Therefore, those moths could not be considered for the analysis. The values of the 1st and 25th percentiles shown in the tables evidence that minima are always systematically overestimated but from ACM2. ACM2 underestimates minima in February and March; in the other months ACM2 overestimates minima but its performance is radically different from those of the other parameterizations. The time series of December show such a feature (see figure 5.6). It is evident that ACM2 perfectly portrays an initial radiative cooling after sunset in line with the σT^4-profile which characterizes the Stefan-Boltzmann law. On some days (12/13, 12/16 and 12/21) the series look perfect but on the other days large rapid hourly variations are evident. Over an hour, ACM2 temperature can vary of more than 8°C. This testifies that ACM2 exaggerates turbulent mixing moving parcels of air along the vertical direction very rapidly. It is also interesting to observe that, unlike ACM2, the other models probably better portray the physical phenomena typical of the SL. In fact, ACM2 profile looks quite smooth while both

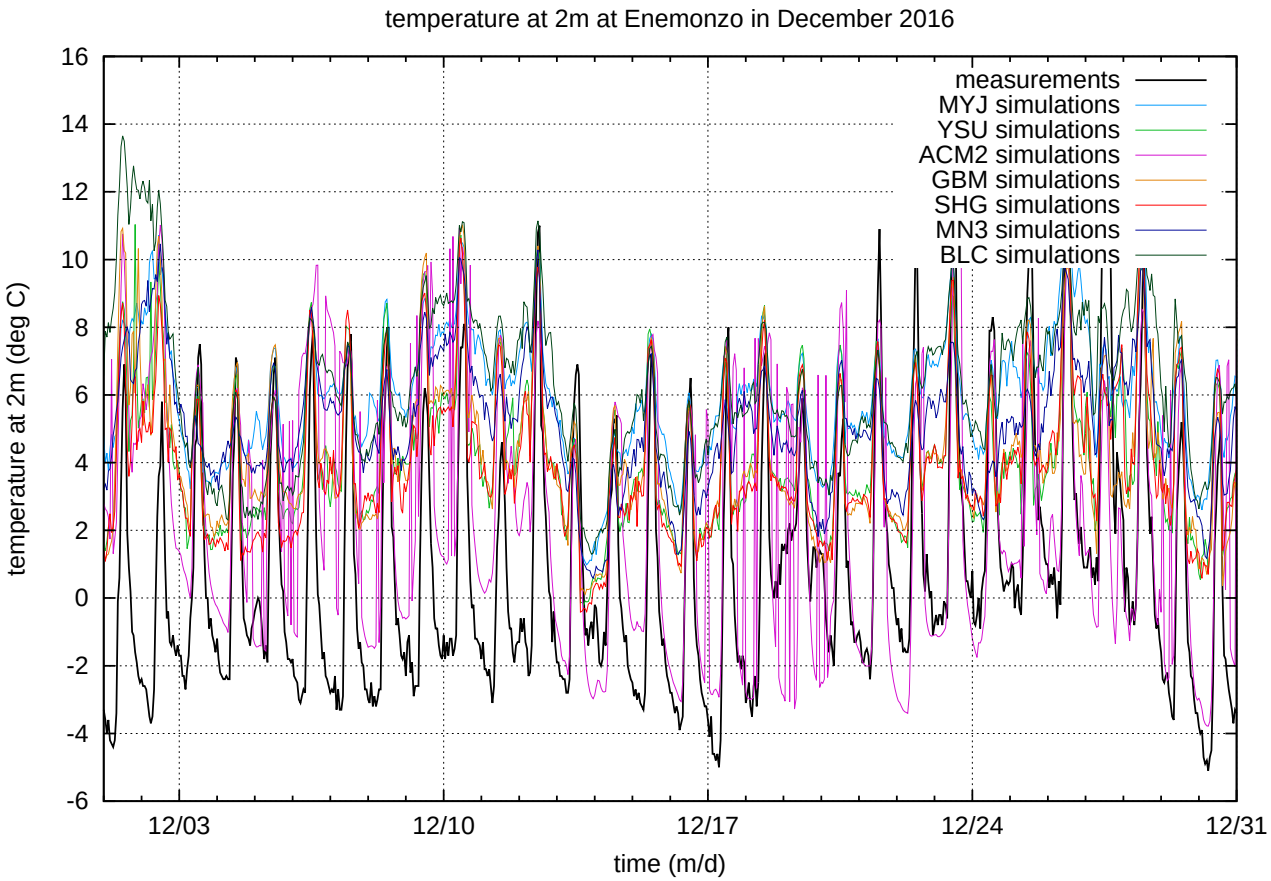

Figure 5.6: time series of the temperatures at Enemonzo in December 2016.

the measurements and the other models have a rough profile. The better portrayal of lower temperatures by ACM2 implies that ACM2 also better describes relative humidity. As can be deduced by the values shown in the tables, on the average, maxima are better represented by every parameterizations but from MN3 and ACM2. In fact MN3 and ACM2 systematically underestimate large values. It has to be noted that the major difficulties are in March as can be seen in figure 5.7. Probably, there is too much mixing and the lower layers cannot be kept warm.

5.3 Winds

The WRF model calculates the zonal and meridional components of the wind. Using the components, the magnitude of the wind was computed in order to confront it with the measurements. The direction of the wind was left out because we are mainly interested in the wind speed. Furthermore, it is periodic with period 2π and such a fact makes it difficult to discuss the behavior around the north direction.

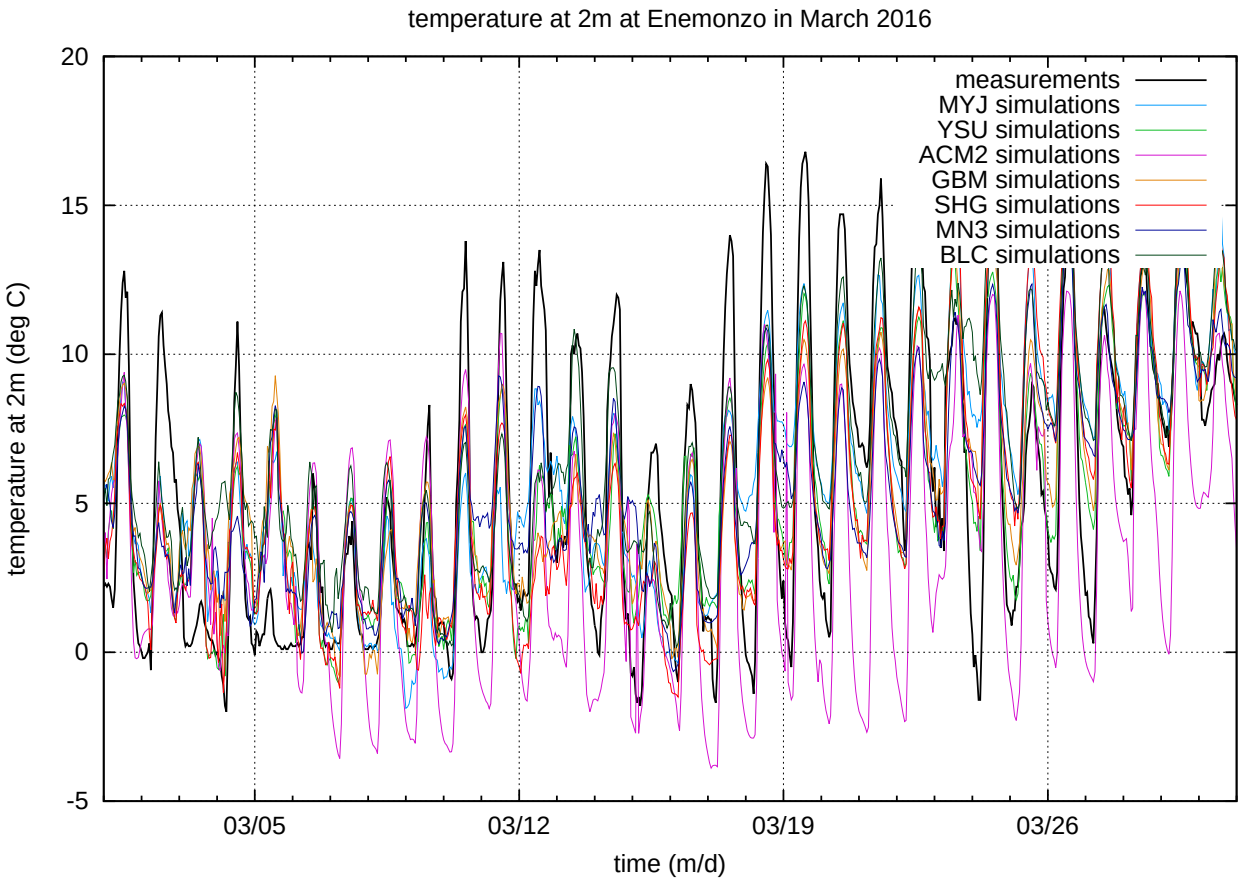

Figure 5.7: time series of the temperatures at Enemonzo in March 2016.

Taylor diagrams are generally very bad, i.e. the correlation between the measurements and the simulated data is always lower than 0.2 and sometimes it is also negative. This does not signify that the simulations were made in a wrong way but testifies the nature of wind. In fact, wind speed can change very rapidly at the surface, since turbulent motions develop over some minutes. The measurements are available once an hour but, since many sub-hourly phenomena contribute to the wind speed, it is reasonable that the correlation with the simulated data is very low. What is possible to investigate is whether the largest values are well reproduced and whether, on the average, there are systematical biases.

Central plains

In January the anemometer at Udine broke in conjunction with a blast and for the following days measurements are missing. All the models depict strong winds in those days so there probably was a mesoscale perturbation.

The simulations exhibit peculiar differences between the area near Udine and the areas near

Cividale del Friuli and Fagagna. It has to be kept in mind that Udine is placed at the center of Friuli and is not significantly influenced by orographic effects whereas both Cividale del Friuli and Fagagna are placed at the embouchure of a valley: Cividale del Friuli is at the embouchure of the Natisone valley while Fagagna is at the embouchure of the Tagliamento valley. Therefore, Cividale del Friuli and Fagagna are windier than Udine because of many local breezes. Generally winds are overestimated by the parameterizations. Looking at the statistical values shown in the tables it is clear that at Udine both light and strong winds are systematically overestimated. On the other hand, at Cividale del Friuli and Fagagna, light winds are mostly underestimated (pay attention to the 1st and 25th percentiles). At Cividale del Friuli and Fagagna, strong wind are generally overestimated like at Udine but in certain months some parameterizations may underestimate them and it is peculiar the case of December at Fagagna: both maxima and minima are systematically underestimated (see figure 5.8).

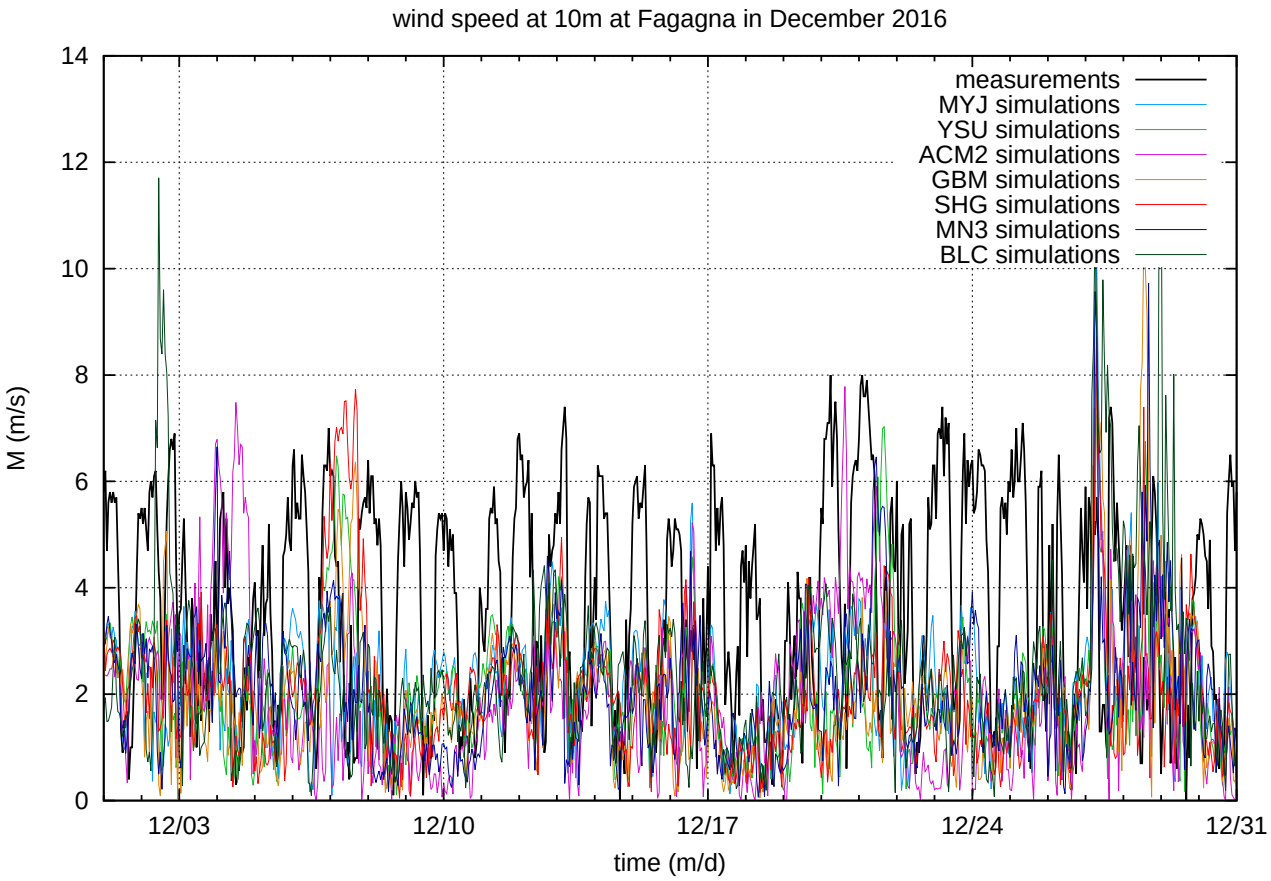

Figure 5.8: time series of the wind speed at Fagagna in December 2016.

During the summer, the time series show the presence of large values (more than $10\,m/s$) reached for just one hour. Such gusts of wind are typical of convective phenomena which take

place at the mesoscale. It is interesting to observe that synoptic events, such as the coming of a front, which cause strong winds, are foreseen by the parameterizations by many hours (e.g. in February).
It is interesting to compare a Kolmogorov-Smirnov test at Udine with one at Fagagna or Cividale del Friuli (the behavior at Fagagna is analogous to the behavior at Cividale del Friuli). The distribution of the measurements at Fagagna is almost flat signifying that there is an equal probability to have any value of the wind speed in the range from $1\,m/s$ to $6\,m/s$, which is in agreement with the observation that the area near Fagagna is windy. On the other hand, the distribution of the measurements at Udine shows two contributes: one by the local effects of the area and one by the synoptic phenomena.
Generally strong winds vary very rapidly in the simulations, i.e. no periods longer than a couple of hours are characterized by sustained winds are seen. There are only a few exceptions over the year and they are simulated by ACM2 and SHG which are the only hybrid models.

Coastal region

The first noticeable thing which emerges from the values shown in the tables is that the area near Fossalon di Grado is windier than the central plains. This is reasonable because the coasts are characterized by breezes and winds driven by the thermal gradient between the land and the sea. The measurements testify that the windiest months are in the transition seasons: March, April and November. Such a fact is probably due to the fact that in such periods the temperature gradient between the land and the sea is stronger than during the other periods of the year. A systematical overestimation of both large and low values characterizes the simulations all year long. The only parameterizations which has a slightly different behavior is ACM2 that in July tends to underestimate large values but well portrays mean values. GBM, SHG and YSU slightly underestimate large values in April.

Open sea

Unfortunately some measurements are missing in January, November and December. Therefore, those months could not be considered in the analysis. The values shown in the tables show very clearly that winds are stronger over the sea than they are over the land and the coastal areas. This is correct because winds blow faster over the sea since there is less friction than there is over the land. A systematical overestimation of large values is evident. The only month

when large values seem to be underestimated is April. That is due to the fact that a major event that took place on 04/28 and lasted several hours was not reproduced by the simulations. A strong event is seen to take place on 07/13. That is one of many gusts of the bora. The bora is well reproduce by the models all the year long. Such a feature is understandable since the boundary conditions which constantly drive the simulations certainly provide the right inputs to describe this mesoscale phenomenon. Another striking feature which emerges from the time series is that very rapid variations characterize the wind speed and there is no clear separation between day and night.

Valley floor

Unfortunately some measurements are missing in March. Therefore, that month could not be considered in the analysis. The representation of the winds in a region with complex orography is quite difficult and it cannot be expected to match properly the measurements. This is the case of this work since the resolution of the orography is not high. As can be deduced by the values shown in the tables, all parameterizations but ACM2 systematically overestimate the wind speed (values up to $16\,m/s$ are simulated while measurements never exceed $6.8\,m/s$). ACM2 exhibits a different behavior as it did for the temperatures. ACM2 often underestimates low values and overestimates large values not as much as the other parameterizations do. It is remarkable that the time series show an evident alternation between day and night from April to October with stronger winds during the day-time and lighter winds during the night-time. On the other hand, in the coldest months winds are lighter and an evident distinction between night and day is not obvious.

5.4 Radiation

The aim was to compare the shortwave downward radiation (SWDR) simulated by the WRF model with the radiation measured by the solarimeters. Shortwave radiation comprises visible and surrounding wavelengths that make up the solar spectrum. For the simulations, the Dudhia scheme was considered (option 'ra_sw_physics = 1'). Such a scheme (based on Dudhia, 1989) integrates the downward solar flux, accounting for clear-air scattering, water vapor absorption and cloud albedo. WRF simulations evaluate the radiative flux (sometimes called irradiance), i.e. the amount of power radiated through a surface per unit area (measured in W/m^2); the field is named "SWDOWN". On the other hand solarimeters integrate the flux over time and the values that are registered every hour can be seen as the energy per unit area per hour (measured in $J/(m^2 \cdot h)$) or as the average radiant exposure (measured in J/m^2), i.e. the radiant energy received by a surface per unit area. For the analysis, simulated data, available every hour, were considered as representative of an average value of the flux for the preceding hour and multiplied by 3600 to obtain an evaluation of the hourly integral and compare it with the measurements. This has some implications which appear evident when looking at the time series (e.g. figure 5.9). It is possible that the simulated data are computed at a particular moment, e.g. when the sky is partially covered by a cloud, so they are not representative of the whole hour. As a consequence, the time series of the simulations frequently exhibit rapid variations from hour to hour while measurements have a smoother profile. Such features are evident in figure 5.9, which shows the SWDR during the first days of July at Udine. Anyhow, for daily evaluations it is still possible to have a good estimate of the total energy. After sundown and before dawn, the SWDR is zero and this implies that a large number of values both in measurements and simulated data are equal to zero. Such a fact has a strong impact on the analysis. Since most values are equal to zero, Kolmogorov-Smirnov tests and statistical quantities such as the percentiles are systematically altered so that they cannot provide much information. Taylor diagrams are altered as well: they show a strong correlation (always larger than 0.8, even 0.9) because of the many hours when both measurements and simulated data are null. Since KS tests do not need temporal information, they were realized removing every null value from the time series. The resulting distributions appeared to be still altered because measurements had a large number of low non-zero values, many more than the simulated data. Such a feature testifies that many times during the year the simulations portrayed night-time, setting SWDR to zero, while the solarimeters could measure weak signals (integrated over the

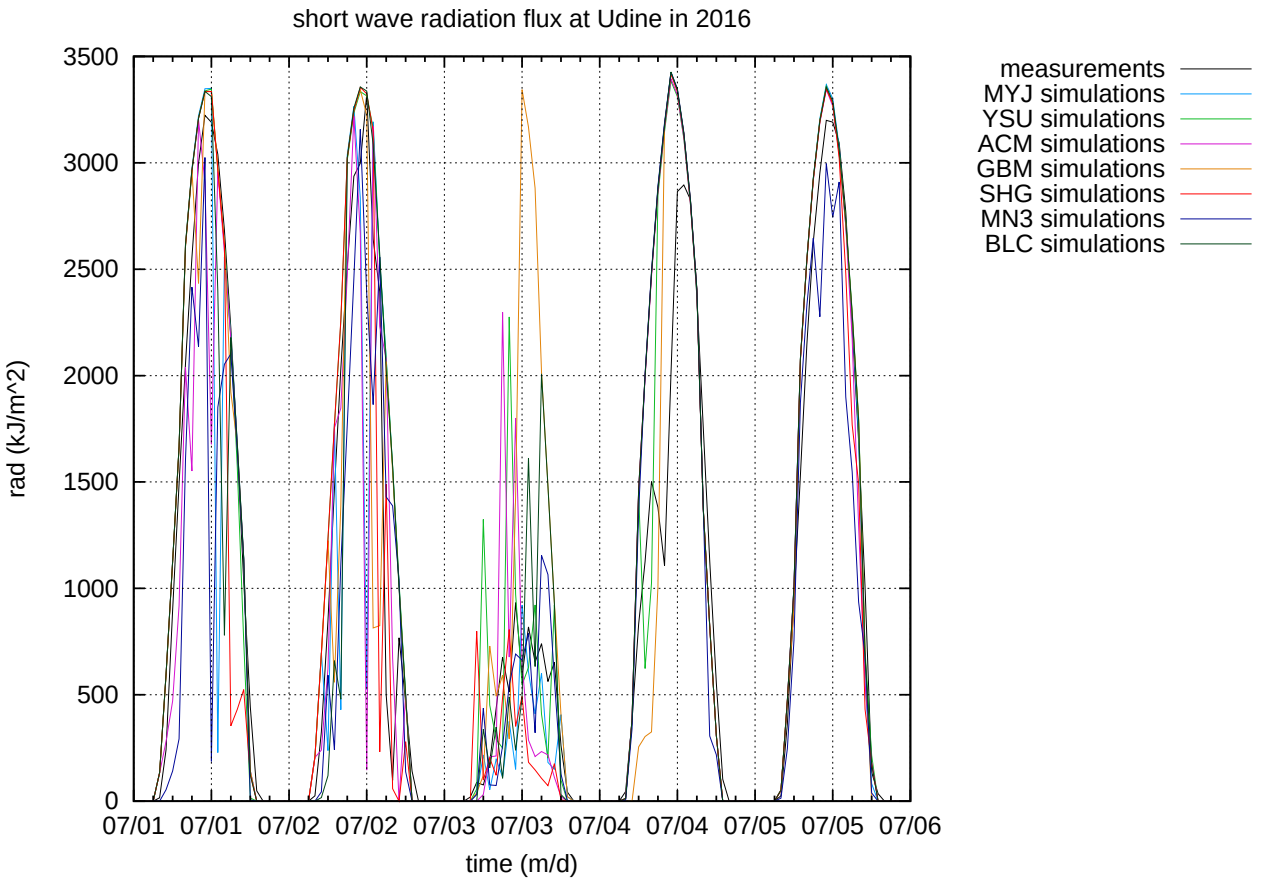

Figure 5.9: time series of the shortwave solar radiation at Udine during the first days of July 2016.

hours), perhaps some radiation reflected by the surrounding environment (terrain, buildings,..). It is interesting to notice that the number of times when measurements are almost zero while simulated data are zero is larger during the winter. This fact suggests that solarimeters actually measure some reflected radiation. During the winter, the sun is lower in the sky and it has to be kept in mind that WRF simulations evaluate radiation contribute integrating only along columns with no exchange in the horizontal directions. Regardless of these inconveniences, linear regressions should show whether simulations are able to reproduce the measurements or whether there are some systematic deviations. Looking at both the time series and the linear regressions, no systematical difference has been noted between the parameterizations. Aside from some peculiar events (a cloudy or rainy day), all parameterizations seem to well portray solar radiation. Most of the slopes evaluated by the linear regressions are in agreement with the value 1. The only month when the slope is systematically incompatible with 1 at every location and for every simulation is January. Figure 5.10 shows how many null simulated data are in correspondence with non-null measurements. This is the reason why the slope is so low.

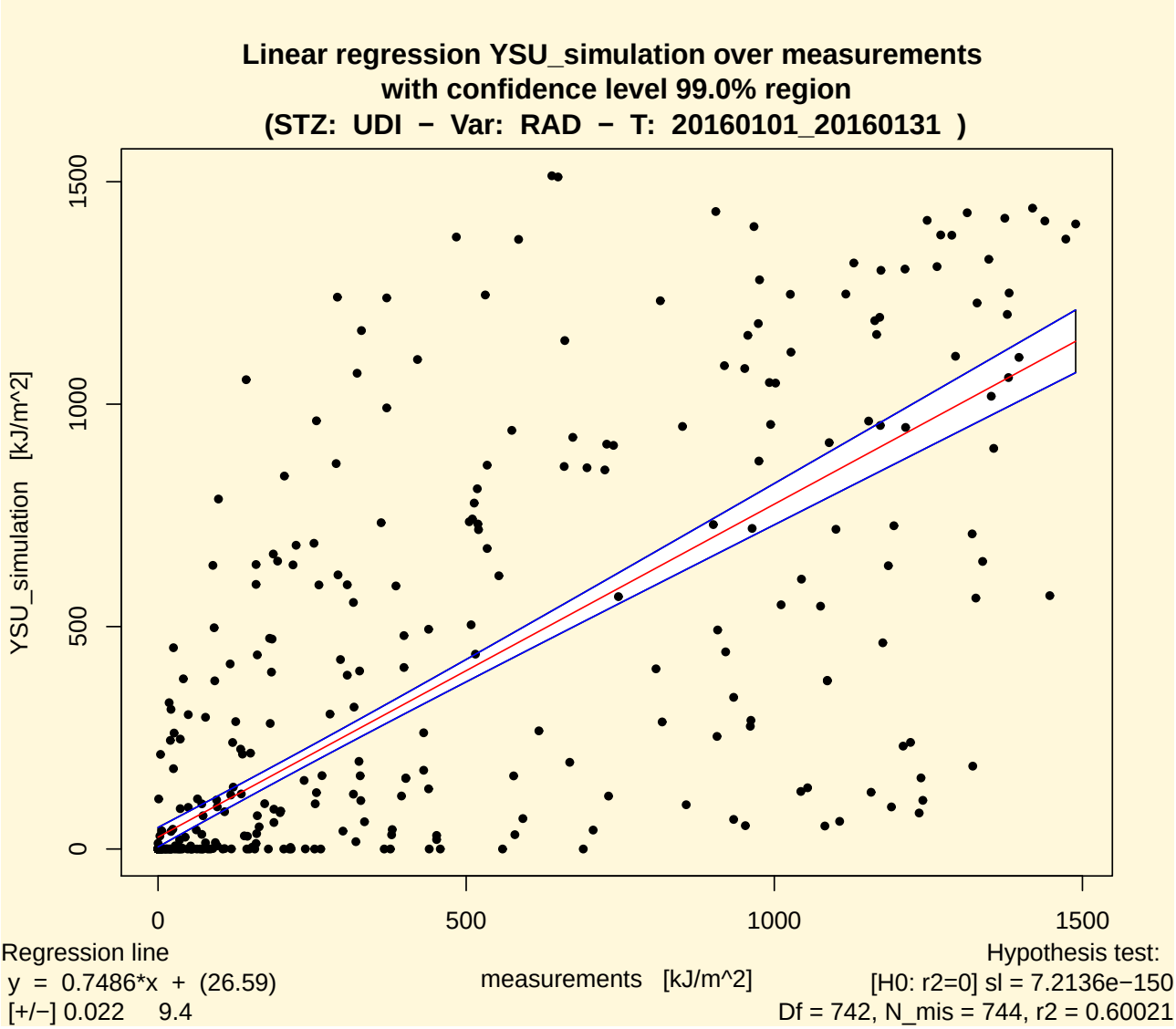

Figure 5.10: Linear regression for the downward shortwave solar radiation at Udine in January 2016 for the YSU scheme.

From October to February the presence of all such couples of values forces the linear regression to underestimate the slope which is always lower than 1. On the other hand, from March to September the estimated slopes can be larger than 1. There is no significant difference between the various locations in the central plains and the other regions exhibit an analogous behavior. Anyhow, it is interesting to see that during the warmest months the population of the areas above and below the regression lines are different. In particular the area above the regression lines shows more points with high simulated values and low measurements than the points with low simulated values and large measurements that populate the area below the regression lines (see figure 5.11). Such a feature is probably due to the fact that during the summer many convective motion take place and it is easier for clouds to form. Many clouds can develop rapidly

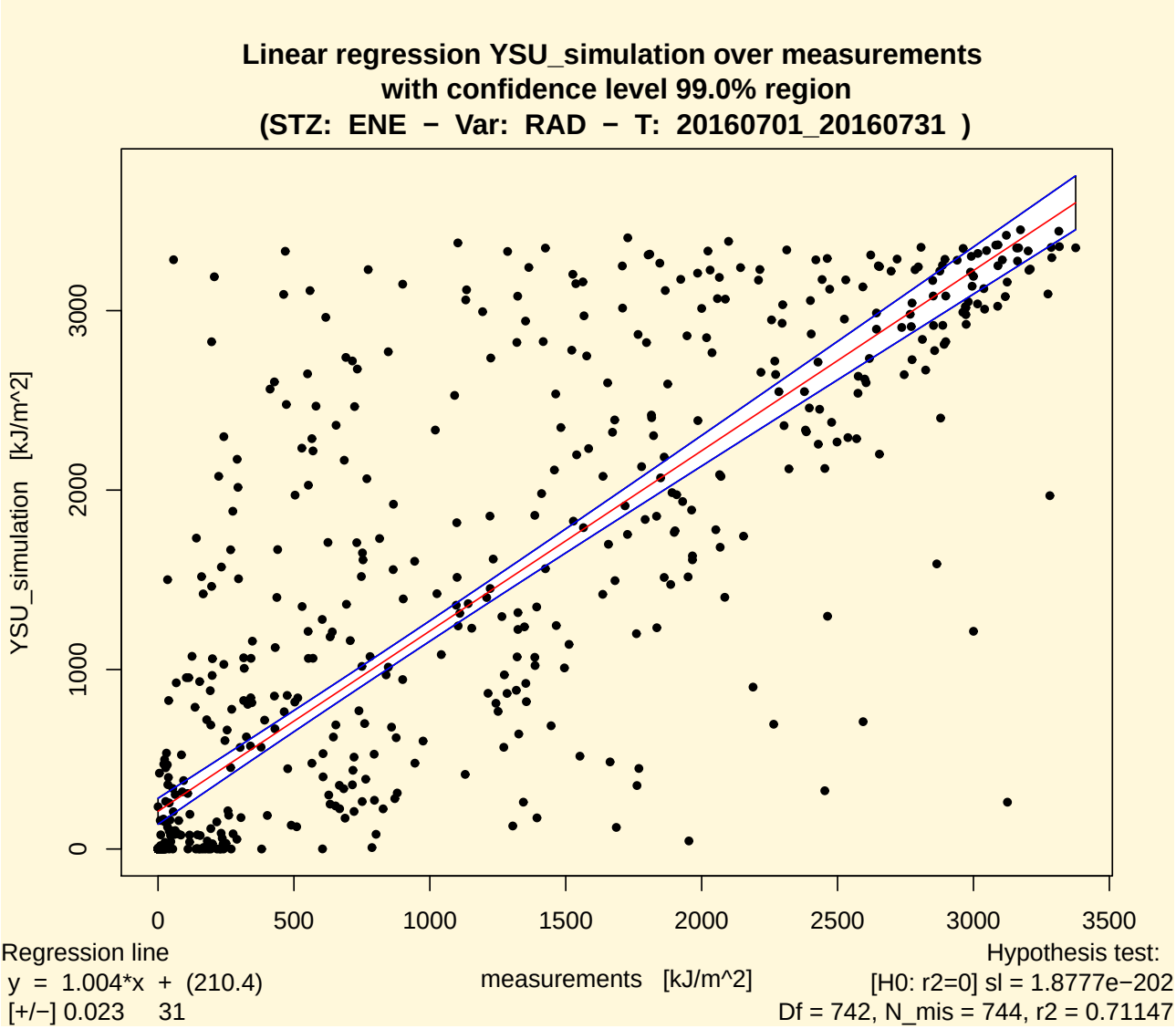

Figure 5.11: Linear regression for the downward shortwave solar radiation at Enemonzo in July 2016 for the YSU scheme.

and then move away. If the simulations register the radiative flux in a moment when there is no cloud, measurements will be easy overestimated since the integrated flux over the hour is influenced by the many clouds which pass by and shadow the solarimeters. This phenomena is enhanced at Enemonzo rather than at the sea testifying that the models have more difficulties to portray cloud formation over complex orography.

To overcome the problems due to the heterogeneity in the distributions of low values between measurements and simulations, KS test were then realized discarding values under $50\,kJ/m^2$. The resulting distribution are still a good tool to establish whether the various schemes properly portray reality since large values do not share the problems of the low values. Most models systematically overestimate low and central values all year long at every place. Large values seem

to be well portrayed: the tails of the simulations are in agreement with those of the measurements. The only exception is the month of December: every parameterizations underestimates the largest values (see figure 5.12). Furthermore, in December a hunch is visible around the

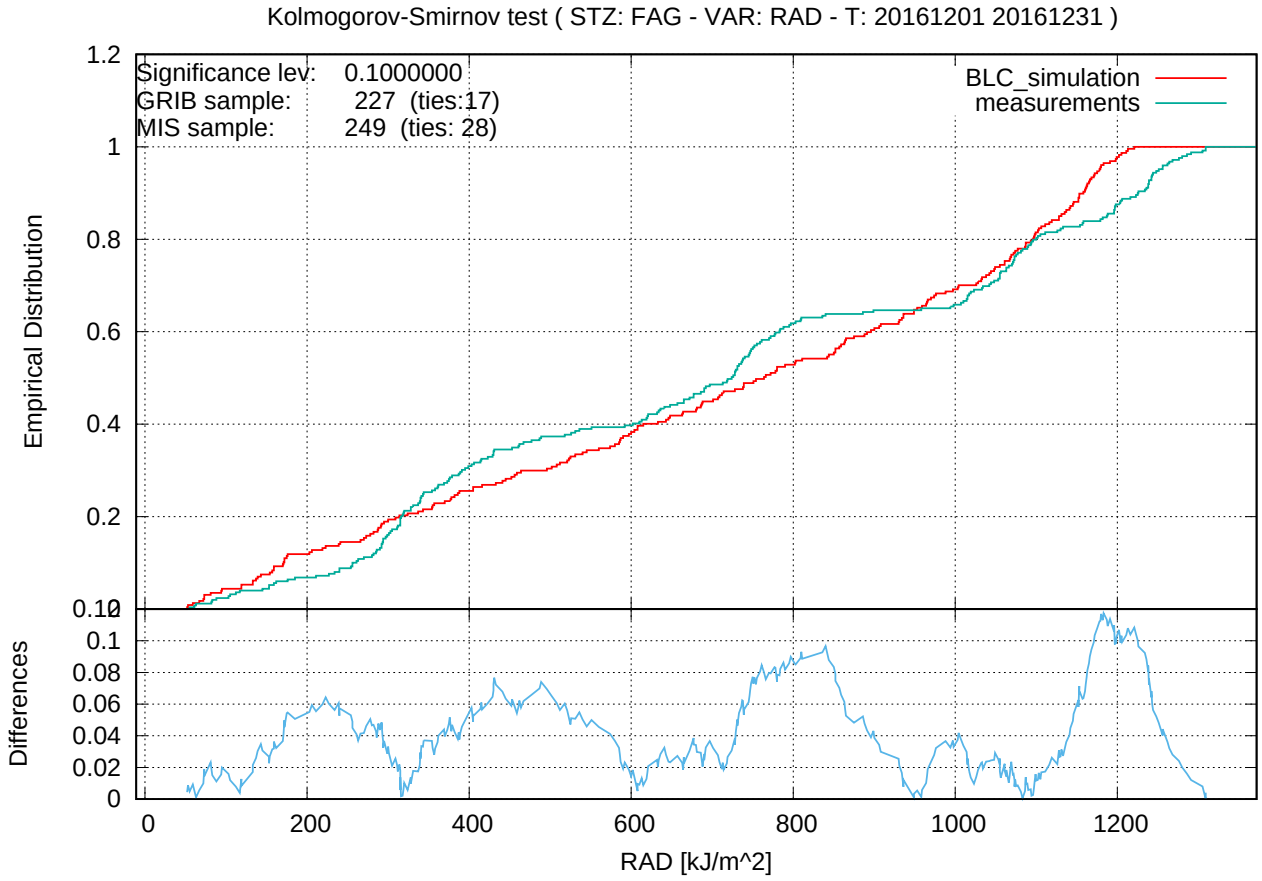

Figure 5.12: Kolmogorov-Smirnov test for the SWDR at Fagagna in December for the BLC scheme. Values less than $50\,kJ/m^2$ were discarded.

middle values. This is probably due to a couple of days whose evolution was not well described by the simulations: since there are few values left in this evaluation once all the low values are removed, if one or two days are not properly described, a tenth if not more of the values will be very different between measurements and simulations and such hunches will form. Comparing all the KS tests, MN3 stands out as the closest to the measurements by far (see for example figure 5.13).

It is very interesting to perform a spectral analysis of the time series of the radiation, for the fundamental frequency and some harmonics of a periodic signal can be highlighted. All parameterizations reproduce the alternation of night and day and the astronomical constraints are imposed to the model with great precision. Power spectra all look alike regardless of the parameterization or the location. Figure 5.14 shows the power spectrum of the SWDR at

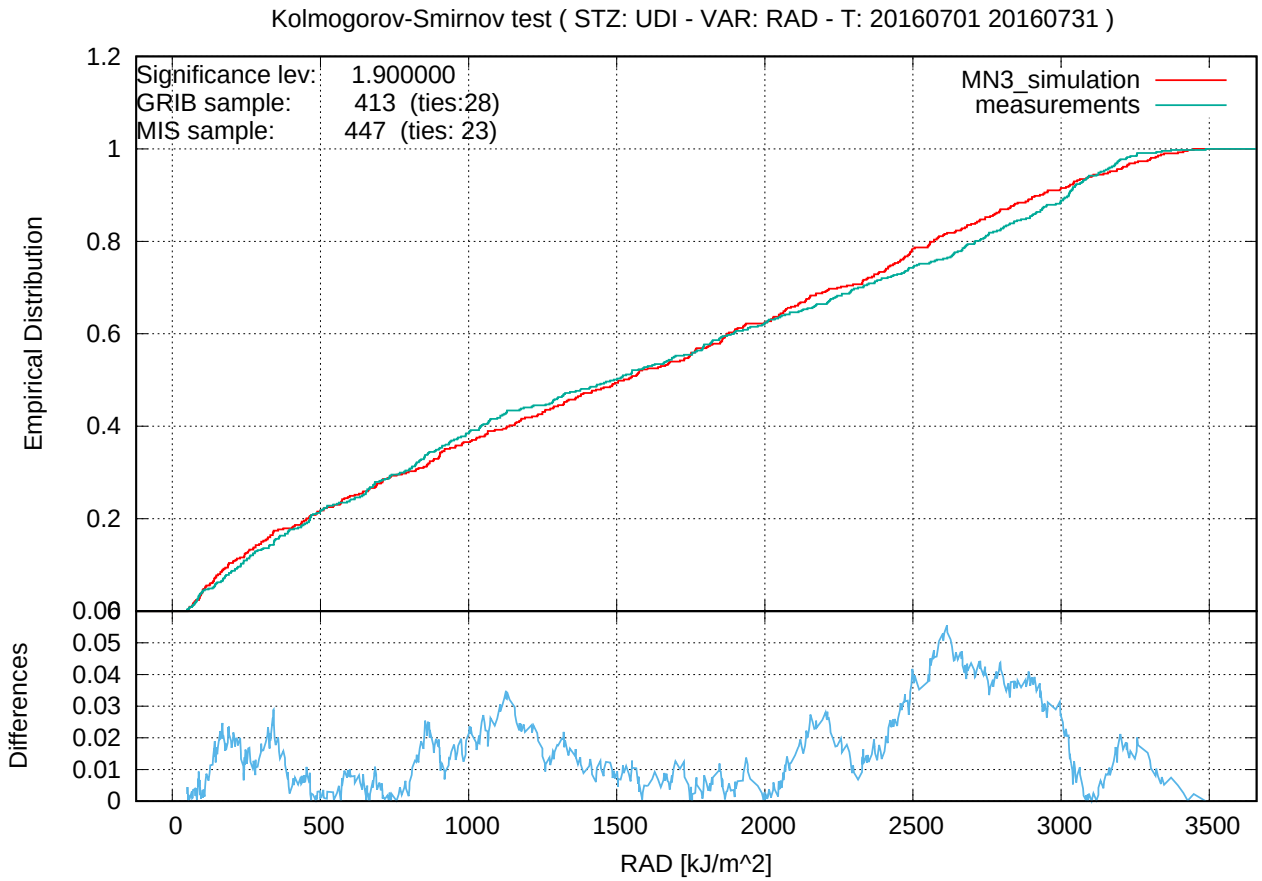

Figure 5.13: Kolmogorov-Smirnov test for the SWDR at Udine in July for the MN3 scheme. Values less than $50\,kJ/m^2$ were discarded.

Udine. Both measurements and simulated data exhibit well defined peaks which coincide. The first peak represents the seasonal periodicity due to the revolution of the Earth around the Sun. The second peak represents the diurnal variations and is placed at 24h. The following peaks are the higher harmonics of the diurnal variations. In fact, the signal is null at night (see figure 5.9) and resembles a square wave in that it is a non-sinusoidal periodic signal in which the amplitude varies with a fixed frequency between zero and a peak diurnal value which is modulated along the year.

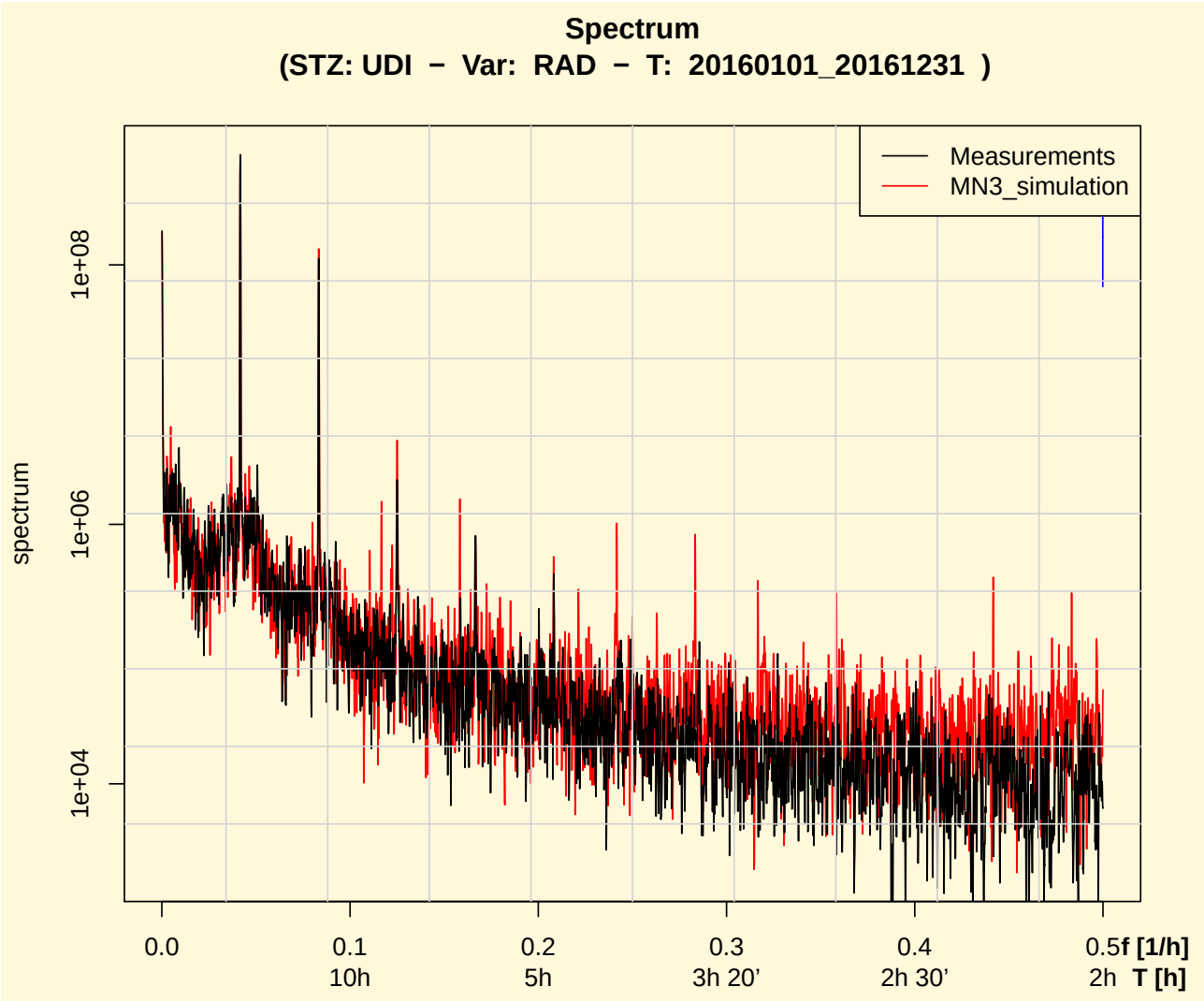

Figure 5.14: Annual power spectrum of the SWDR at Udine for the MN3 scheme.

5.5 Precipitation

The study of precipitations is more difficult than that of the other variables. Rain is a sporadic event, therefore the analysis of the time series is not straightforward. Most of the measurements and the simulated data are null. Some events may not be predicted by the simulations while others may be predicted but not have happened in reality. Furthermore, when models correctly predict rain they may anticipate it or delay it by a few hours. Because of these aspects, Taylor diagrams cannot be a useful tool in the analysis. KS tests are not an appropriate tool as well. When evaluating precipitations two main aspects are desirable: that simulations forecast the events when they actually take place and that the values of at least strong precipitations are well reproduced. To assess the skills of a set of forecasts many techniques have been developed (see Wilks, 2011). For example, contingency tables are a great tool to check whether a simulation well portrays the occurrence of precipitations in conjunction with reality. However, the main purpose of this work was to establish whether the various schemes are able to reproduces the largest measured values or not. To do such evaluations, all zeros were removed from the time series and statistical quantities, such as the percentiles, were computed with the remaining values and then reported in Appendix B. Distributions are limited from below and tails are long.

Measurements are not available at the Paloma buoy because there are no instruments to measure the precipitations there. The three remaining areas exhibit different behaviors. The various schemes do not exhibit a systematic tendency to generate strong or low precipitations. Their performances vary significantly with the period of the year though, which is reasonable. MN3 appears to be the rainiest in the central plains and in the coastal region where the number of recorded events is significantly larger than that of the other parameterizations if the entire year is considered (in a given month this is not necessarily true). Also MN3 recorded events are more than the measured ones whereas all the other parameterizations underestimate the number of events. The situation is quite different at Enemonzo where measured events are many more than the simulated ones. This suggests that WRF is perhaps unable to properly portray orographic precipitations, i.e. precipitations which form because of orographic effects such as the Stau effect. The majority of both the measured and simulated events are weak precipitations. This is well testified by the values in the tables: medians rarely exceed $1\,mm/h$ and the 75th percentiles are always lower than $5\,mm/h$. Anyhow, to check whether the parameterizations are able to reproduce strong precipitations, only the 99th percentiles and the

maxima are needed. YSU produces the strongest precipitations in the central plains with values larger than $40\,mm/h$ because of an isolated event in July. On the other hand, the 99th percentiles show YSU to produce weaker precipitations than the other schemes. Considering all the year, MN3 always has the largest 99th percentile at every place. It is interesting to note that, with a few exceptions, the parameterizations are unable to reproduce large precipitations at Enemonzo. This is evident when looking at the 99th percentiles. From June to September no scheme can reach the measurements. The scheme which gets the closest is YSU. The climate of Friuli Venezia Giulia is characterized by deep convective motions in the period from April to September while January, February and December are dry months. These aspects can be seen in the values shown in the tables. In particular, MN3 produces more precipitations in the central plains and at the coast exactly in the period from April to September. We can therefore deduce that MN3 tends to develop strong convective motions. January and February exhibit very weak precipitations: neither the measurements nor the simulations reach $10\,mm/h$. In December very weak precipitations (less than $1\,mm/h$) were recorded and simulated by some schemes at Cividale del Friuli and at Fossalon di Grado but at the other places it did not rain at all. Aside from MN3 the other schemes do not exhibit a definite behavior or systematic tendencies. Sometimes their predictions are comparable with the measurements, sometimes not at all. Some peculiar events can be identified but their analysis goes beyond the purposes of this work.

Chapter 6

Conclusion

6.1 Summary of Achievements

Seven annual simulations were performed and validated against measurements at specific points, chosen to highlight the capacity of the WRF model to portray the ABL evolution over different areas, ranging from the open sea to the mountains. Annual time series of the main surface fields show a high correlation with the measurements: seasonal variations are well reproduced by every parameterization so that they are all suitable for climatic studies. On the other hand, for some fields, monthly, weekly and daily time series show a weak correlation with the measurements. The four regions considered in this thesis exhibit different behaviours generally well portrayed by the model.

Temperatures are generally well reproduced by every scheme with the exception of MN3, which is bound by internal constraints. ACM2 was shown to better represent the minima at the valley floor.

Wind speed is generally overestimated by every parameterization but different behaviours were observed at different areas. Orography definitely has a strong impact on the wind which is not well reproduced by the model. A possible explanation for this effect is the low resolution of the orography in comparison to the micrometeorological phenomena.

Some difficulties were encountered when dealing with the radiation because the measurements are partially influenced by reflected radiation. Anyhow MN3 was shown to be the best scheme to evaluate the SWDR.

Concerning the precipitations the focus was on the capacity of the schemes to reproduce the largest observed values. MN3 is the rainiest among the parameterizations and also the best at

portraying the largest values. Some schemes, e.g. YSU, can develop heavy rain overestimating the reality.

Considering all the schemes, MN3 and ACM2 are far from the average trend. MN3 was the only second order closure scheme studied and resulted in being the best at portraying the SWDR. On the other hand MN3 was shown to be the worst when dealing with the temperatures; it is colder than the other parameterizations. ACM2 is an hybrid parameterization, which was shown to develop vertical mixing much more than the other schemes. ACM2 better simulates the minima of the temperature at the mountains but underestimates the average measurements more than the other schemes.

This thesis proved that it is possible to make a comparison between many ABL parameterizations in an atmospherically limited area model in a acceptable amount of time. This is possible thanks to the high performance computing (HPC) techniques.

6.2 Future Work

The simulations carried out in this work generated three dimensional fields that can be further analyzed in many ways. Other fields than those considered in this work could be under study, e.g. the mixing ratio. As suggested in chapter 5, precipitations should be studied through the use of contingency tables and extended areas should be considered since it is likely that a single grid point is not representative of real precipitations. Further measurements could be included in the validation process and used to establish whether there is a limit to the spatial resolution. Of course, all the classical vertical analysis of the model profiles could be conducted. The set of simulations could be enriched with new runs involving a new improvement recently developed for the WRF model that should better represent topographic effects and their influence on the wind speed, especially over the mountains and hills (see Jiménez and Dudhia, 2012).

These simulations have become part of the ARPA FVG databases and they will be subject of detailed studies in next years at ARPA FVG. In fact, according to the Fourth Paradigm concept (see Hey et al., 2009), a lot of information is stored in the databases just waiting to be analyzed. Many dynamical phenomena which characterize the ABL, e.g. breezes and orographic winds, will be at the center of such studies. Another topic that will be analyzed is the capability of the WRF model to portray the dynamical effects of the land-sea transition.

Appendices

Appendix A

Statistical tests

A.1 The Kolmogorov-Smirnov test

The Kolmogorov-Smirnov test is a test for non-parametric or distribution-free models (see Ledermann and Lloyd, 1984 or Siegel, 1956). Many statistical evaluations are based on the assumption that the distribution of the observations of interest belongs to a particular known parametric family of distributions (e.g. Normal distribution or Poisson distribution). In such cases the form of distribution is known and the parameters which characterize that distribution are to be evaluated. Non-parametric models are less restrictive because they do not depend on a particular underlying parametric family of distributions. In most cases it has only to be assumed that the underlying variables are continuous. The Kolmogorov-Smirnov test is based on the introduction of the empirical distribution function. Given a random sample $x_1, x_2, ..., x_n$, the empirical distribution function $F_n(x)$ is defined as:

$$F_n(x) = \begin{cases} 0 & x < x_{(1)} \\ k/n & x_{(k)} \leq x \leq x_{(k+1)} \qquad k = 1, 2, ..., n-1 \\ 1 & x \geq x_{(n)} \end{cases} \tag{A.1}$$

It is immediate to recognize A.1 as a step function (see figure A.1). Given one random sample $x_1, x_2, ..., x_n$, its empirical distribution function can be used to evaluate whether a specified distribution function $F_0(x)$ is the distribution function from which the random sample arose (one-sample Kolmogorov-Smirnov test). Given two independent random samples, their empirical distribution functions can be used to study whether the two samples come from the same distribution (two-samples Kolmogorov-Smirnov case). In both cases the key idea is to

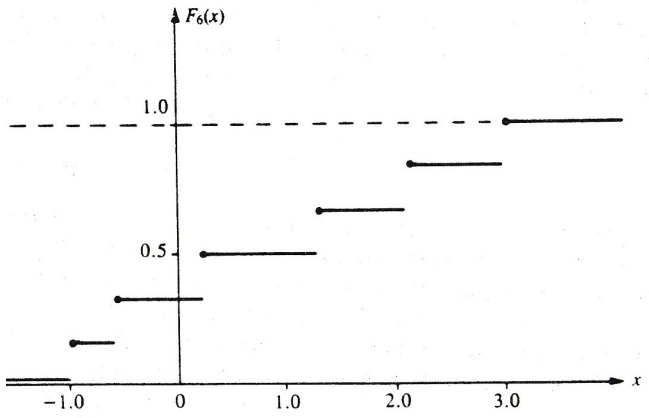

Figure A.1: An example of an empirical distribution function for a random sample of size $n = 6$. Adapted from Ledermann and Lloyd, 1984.

consider the differences between the distributions. The two-samples case is more important for this work and will now be described. Consider a random sample $x_1, x_2, ..., x_n$ from a population with continuous distribution function $F(x)$ and an independent random sample $y_1, y_2, ..., y_n$ from a population with continuous distribution function $G(x)$. Without specifying the form of $F(x)$ and $G(x)$ we wish to test whether they are the same distribution function. Therefore we have the null hypothesis:

$$H_1 : F(z) = G(z) \qquad \text{for every } z$$

against

$$H_2 : F(z) \neq G(z) \qquad \text{for some } z$$

Introducing the two empirical distribution functions $F_{n_1}(x)$ and $G_{n_2}(y)$, based on the two samples, the Kolmogorov-Smirnov two samples test considers the following quantity:

$$D_{n_1,n_2}(\mathbf{x}, \mathbf{y}) = \sup_{-\infty<z<+\infty} |F_{n_1}(z) - G_{n_2}(z)|$$

which is the largest difference between the two empirical distributions functions (see figure A.2) and can be seen as the value of a random variable $D_{n_1,n_2}(\mathbf{X}, \mathbf{Y})$. The exact sampling distribution of $D_{n_1,n_2}(\mathbf{X}, \mathbf{Y})$ is tabulated (see Siegel, 1956) and so practical evaluations can be done. In particular a critical region can be defined for the H_2 hypothesis:

$$A_2 = \text{observations:} D_{n_1,n_2}(\mathbf{x}, \mathbf{y}) > c_\alpha$$

where c_α is a constant defined by $P(A_2|H_1) = \alpha$. Anyhow, the Kolmogorov-Smirnov test provides important information just from a graphical point of view (see figure A.3). When the

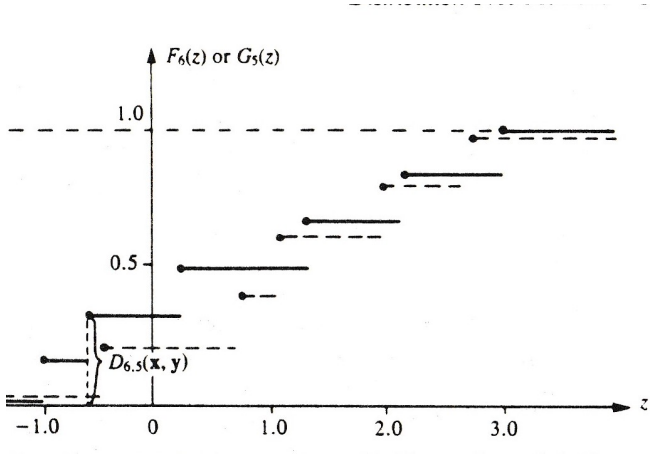

Figure A.2: An example of two empirical distribution functions for independent random samples and their differences. Adapted from Ledermann and Lloyd, 1984.

two empirical distribution functions are far apart, it is an indication that the two samples are not in agreement with each other. Another interesting aspect is that flat regions denote sets of values never assumed by the sample.

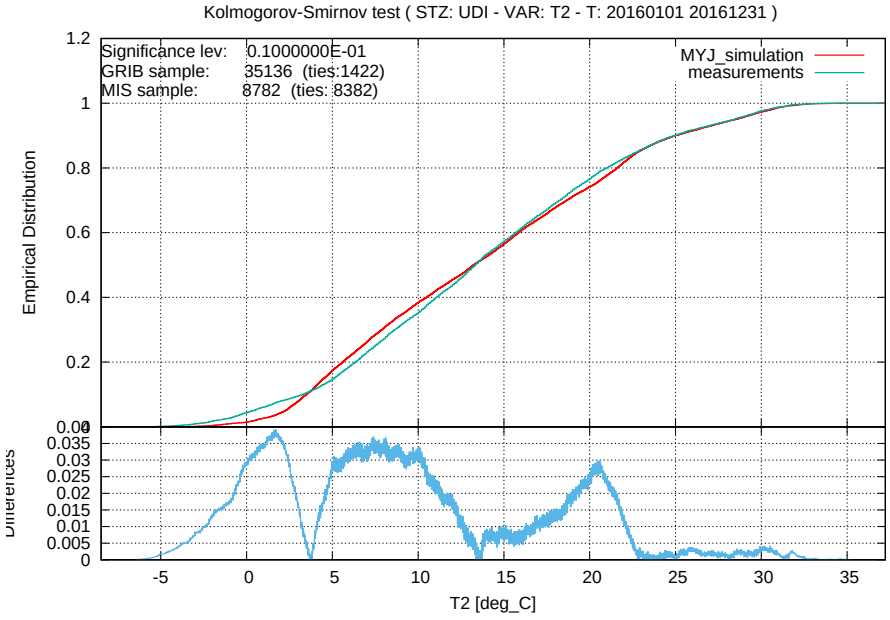

Figure A.3: An example of the K-S test for our analysis. The horizontal axis shows the range of values of the considered variable. The upper plot shows the empirical distribution functions of the measurements and the simulated values. The lower plot show the difference between the two empirical distribution functions.

A.2 Taylor diagram

Taylor diagrams are mathematical diagrams invented by Karl E. Taylor (see Taylor, 2001) to provide a useful tool to compare different models. These diagrams quantify the degree of correspondence between the measurements and the simulated data of different models regarding a particular variable using three different statistical quantities: the standard deviation σ, the Pearson correlation coefficient R and the centered pattern root-mean-square error E'. These

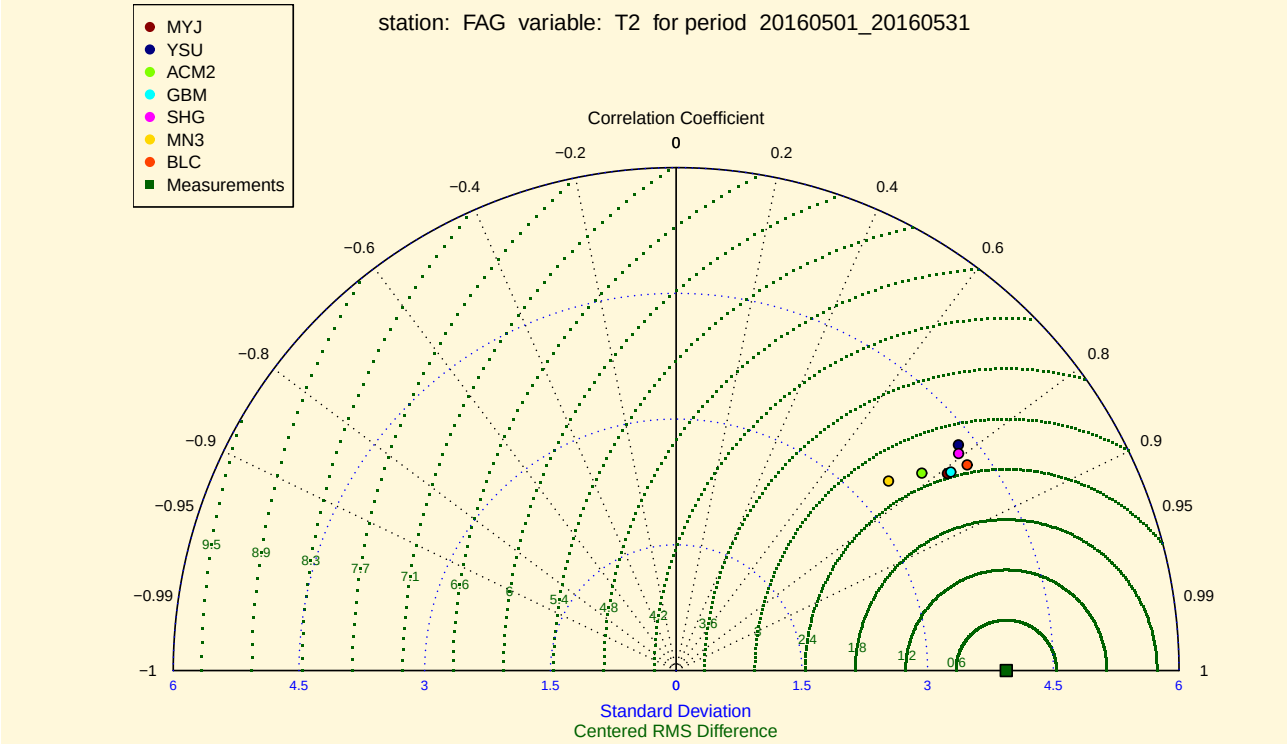

Figure A.4: An example of a Taylor diagram.

statistics are related by the following formula:

$$E'^2 = \sigma_f^2 + \sigma_r^2 - 2\sigma_f\sigma_r R$$

where σ_f and σ_r are the standard deviation of the test and reference fields respectively. Figure A.4 shows a Taylor diagram. The diagram has the form of a semi-circumference. The reference field standard deviation is indicated on the horizontal diameter; that point represents the measurements. The various models are represented with a point whose position of the diagram is defined by its standard deviation, measured along the radius, and the correlation coefficient measured along the circumference. The centered RMS difference can be read on the semi-circumferences centered on the point representing the observed values. It is immediate to understand that Taylor diagrams are a great tool to determine which model among those considered performs best. Usually cases with negative correlation coefficients are not considered and only the positive correlation coefficient half of the diagram is shown.

Appendix B

Statistical values

Next are presented some tables with the main statistical quantities evaluated for all the variables considered in this work analysis. Tables show the number of values, the minimum, the 1st percentile, the 25th percentile, the median, the 75th percentile, the 99th percentile, the maximum, the mean value and the standard deviation for the measurements (mea) and all the parameterizations. There is one section for every variable. For every variable, tables are ordered to present the locations in the following sequence: Udine, Cividale del Friuli, Fagagna, Fossalon di Grado, the Paloma buoy and Enemonzo. For every location there are a table which considers all the year and twelve monthly tables. In case a significant number of values are missing for a given month, the corresponding table is not shown and the annual one is removed as well.

B.1 Temperatures

All values are expressed in °C.

Temperatures in 2016 at Udine										
	# samples	min	1st perc	25th perc	median	75th perc	99th perc	max	mean	STD
mea	8782	-6.4	-2.8	7.5	13.3	19.5	31.3	34.6	13.7	8.2
ACM	8782	-5.4	-1.7	6.0	12.0	19.5	30.3	33.0	12.8	8.2
BLC	8782	-3.1	0.6	7.4	13.8	20.7	32.3	34.7	14.4	8.2
GBM	8782	-3.8	-0.7	6.9	13.7	20.0	31.2	33.7	13.9	8.2
MN3	8782	-4.1	-0.9	6.2	12.2	18.2	26.1	29.1	12.4	7.1
MYJ	8782	-4.4	-0.9	6.8	13.3	20.3	31.5	35.0	13.8	8.2
SHG	8782	-3.7	-0.7	6.5	13.2	19.6	30.4	32.1	13.4	8.1
YSU	8782	-4.2	-0.8	6.7	13.1	19.8	30.4	33.4	13.5	8.1

Temperatures in January 2016 at Udine										
	# samples	min	1st perc	25th perc	median	75th perc	99th perc	max	mean	STD
mea	744	-6.4	-5.2	0.2	3.5	6.8	11.3	12.2	3.3	4.2
ACM	744	-5.4	-3.7	-0.0	2.0	3.9	7.8	8.5	2.0	2.8
BLC	744	-3.1	-1.9	2.3	4.3	6.1	11.1	11.8	4.3	3.0
GBM	744	-3.8	-2.4	1.4	3.2	5.5	10.7	12.4	3.4	3.0
MN3	744	-4.1	-3.0	1.2	3.1	5.3	10.0	11.7	3.1	3.0
MYJ	744	-4.4	-3.3	1.6	3.5	5.1	10.1	11.1	3.3	3.0
SHG	744	-3.7	-2.7	1.2	3.3	5.0	9.7	11.5	3.2	2.9
YSU	744	-4.2	-2.9	1.4	3.5	5.0	9.4	11.4	3.2	2.9

Temperatures in February 2016 at Udine										
	# samples	min	1st perc	25th perc	median	75th perc	99th perc	max	mean	STD
mea	696	-0.3	0.5	5.4	7.1	8.9	12.4	14.2	7.1	2.6
ACM	696	-1.0	-0.6	2.6	4.3	6.5	10.1	10.5	4.6	2.7
BLC	696	1.3	1.7	5.4	7.4	9.2	13.0	14.1	7.3	2.7
GBM	696	0.9	1.5	5.0	7.1	8.8	12.2	13.2	6.9	2.7
MN3	696	-0.1	0.3	4.4	6.5	8.2	10.7	11.2	6.2	2.5
MYJ	696	-0.0	0.6	4.8	6.8	8.2	10.9	12.1	6.5	2.4
SHG	696	0.8	1.0	4.7	6.8	8.4	11.9	12.9	6.6	2.6
YSU	696	0.6	1.0	4.7	6.8	8.4	12.0	13.0	6.6	2.7

Temperatures in March 2016 at Udine										
	# samples	min	1st perc	25th perc	median	75th perc	99th perc	max	mean	STD
mea	744	0.2	1.6	6.2	8.8	12.3	17.2	17.7	9.3	3.8
ACM	744	-0.2	0.8	3.6	6.5	9.1	13.6	14.3	6.5	3.3
BLC	744	1.5	2.0	5.8	8.4	11.1	17.4	18.8	8.6	3.7
GBM	744	0.7	1.3	5.5	7.8	10.1	16.7	17.5	8.0	3.5
MN3	744	1.0	1.3	4.9	7.3	10.2	14.5	14.9	7.4	3.3
MYJ	744	0.1	0.4	4.8	7.7	10.7	16.4	17.2	7.8	4.0
SHG	744	0.1	0.8	5.1	7.7	10.6	16.5	17.4	7.9	3.8
YSU	744	1.4	1.8	5.1	7.7	10.2	15.9	17.0	7.8	3.4

Temperatures in April 2016 at Udine										
	# samples	min	1st perc	25th perc	median	75th perc	99th perc	max	mean	STD
mea	719	2.5	4.6	10.9	13.4	17.0	21.9	23.6	13.7	4.1
ACM	719	3.7	4.7	8.9	10.7	13.2	18.3	19.4	10.9	3.2
BLC	719	2.9	4.4	11.3	13.5	16.7	21.6	22.6	13.7	4.2
GBM	719	3.4	5.7	11.4	13.5	16.3	21.5	22.1	13.7	3.8
MN3	719	2.6	4.3	10.4	12.1	14.4	18.9	19.9	12.1	3.2
MYJ	719	4.0	4.6	10.9	13.1	15.9	21.7	22.6	13.3	3.8
SHG	719	3.1	4.3	10.9	13.1	15.8	20.7	21.6	13.1	3.8
YSU	719	3.6	4.5	11.0	13.4	16.1	21.5	22.1	13.5	3.9

Temperatures in May 2016 at Udine										
	# samples	min	1st perc	25th perc	median	75th perc	99th perc	max	mean	STD
mea	744	7.0	9.2	13.3	15.5	19.2	26.5	27.3	16.4	4.2
ACM	744	7.0	7.3	11.2	14.1	17.4	22.7	23.4	14.4	3.9
BLC	744	7.6	8.7	14.0	16.8	20.0	26.7	28.2	17.1	4.4
GBM	744	6.7	8.0	13.9	16.7	19.8	25.7	26.4	17.0	4.1
MN3	744	6.1	7.0	12.4	14.7	17.6	21.5	22.2	14.8	3.5
MYJ	744	7.3	8.4	13.3	15.8	19.5	25.5	26.4	16.4	4.2
SHG	744	6.8	8.2	13.1	16.1	19.6	25.5	26.4	16.5	4.3
YSU	744	6.7	7.9	13.1	16.2	19.6	25.9	26.6	16.5	4.4

Temperatures in June 2016 at Udine										
	# samples	min	1st perc	25th perc	median	75th perc	99th perc	max	mean	STD
mea	719	12.5	13.6	17.6	20.4	24.0	33.6	34.6	21.2	4.6
ACM	719	11.7	12.4	16.1	20.0	22.8	28.4	28.9	19.9	4.2
BLC	719	13.7	15.4	18.6	22.1	25.1	32.2	33.0	22.2	4.3
GBM	719	12.6	14.4	17.8	21.7	24.5	32.7	33.2	21.8	4.6
MN3	719	12.9	13.9	17.3	19.4	21.7	26.4	28.0	19.6	3.1
MYJ	719	12.0	13.3	17.4	21.6	23.8	31.0	31.6	21.2	4.5
SHG	719	13.0	14.4	18.2	21.4	24.4	31.0	31.4	21.6	4.1
YSU	719	12.6	14.8	18.5	21.5	24.4	30.8	31.3	21.6	4.0

Temperatures in July 2016 at Udine										
	# samples	min	1st perc	25th perc	median	75th perc	99th perc	max	mean	STD
mea	744	11.4	13.4	20.9	23.6	28.4	32.6	33.2	24.3	4.5
ACM	744	13.9	15.3	19.7	22.6	26.1	29.6	30.1	22.9	3.7
BLC	744	13.9	15.5	21.4	24.0	28.1	33.9	34.6	24.7	4.4
GBM	744	13.7	15.2	20.7	23.2	27.0	32.1	33.0	23.7	4.1
MN3	744	13.1	14.0	19.6	21.5	23.8	27.6	29.1	21.4	3.2
MYJ	744	12.4	13.9	21.0	23.6	27.2	32.5	33.3	23.9	4.3
SHG	744	13.5	14.5	20.3	23.1	26.8	31.2	32.1	23.4	4.1
YSU	744	13.1	14.1	20.8	23.8	27.5	31.1	32.0	23.9	4.0

Temperatures in August 2016 at Udine										
	# samples	min	1st perc	25th perc	median	75th perc	99th perc	max	mean	STD
mea	744	11.7	13.6	18.3	21.7	26.7	31.2	31.9	22.4	4.9
ACM	744	14.6	15.9	20.0	22.9	26.9	31.7	33.0	23.5	4.0
BLC	744	12.9	14.4	20.6	23.1	28.6	33.6	34.7	24.2	4.9
GBM	744	13.2	14.3	19.5	22.5	27.4	32.6	33.7	23.4	4.7
MN3	744	14.0	15.1	18.8	20.6	23.2	26.6	28.2	20.9	2.9
MYJ	744	14.6	15.7	20.5	23.1	28.1	33.4	35.0	24.1	4.6
SHG	744	12.3	13.9	19.4	22.3	26.8	31.7	32.1	22.8	4.4
YSU	744	12.5	13.9	19.1	22.4	26.9	32.4	33.4	22.8	4.6

Temperatures in September 2016 at Udine										
	# samples	min	1st perc	25th perc	median	75th perc	99th perc	max	mean	STD
mea	720	10.0	11.4	16.8	19.9	23.8	31.5	31.8	20.6	5.0
ACM	720	12.8	13.5	17.7	20.9	24.8	32.0	32.3	21.6	4.8
BLC	720	11.3	12.5	17.1	20.9	24.9	32.5	33.2	21.5	5.2
GBM	720	9.5	11.8	16.4	20.1	23.8	31.3	32.4	20.6	5.1
MN3	720	8.8	11.1	15.3	17.7	20.0	25.6	26.2	17.9	3.6
MYJ	720	10.7	11.9	17.0	20.6	24.1	32.3	32.7	21.0	5.2
SHG	720	9.4	10.8	15.9	19.4	23.3	30.8	31.3	20.1	5.0
YSU	720	9.4	11.0	15.9	19.5	23.6	31.2	31.6	20.2	5.2

Temperatures in October 2016 at Udine										
	# samples	min	1st perc	25th perc	median	75th perc	99th perc	max	mean	STD
mea	744	1.9	4.0	10.4	13.2	15.7	22.2	23.4	13.0	4.2
ACM	744	7.5	8.0	10.8	13.5	16.5	22.0	22.6	13.8	3.6
BLC	744	6.1	7.4	11.6	14.3	17.2	22.7	24.4	14.4	3.7
GBM	744	4.3	6.0	11.8	14.8	17.8	21.6	23.5	14.6	3.8
MN3	744	5.2	6.6	10.5	13.1	15.5	19.9	21.4	13.0	3.3
MYJ	744	6.2	7.0	11.4	14.4	17.1	22.8	24.0	14.3	3.7
SHG	744	4.1	5.5	10.9	13.7	16.5	21.3	22.8	13.7	3.8
YSU	744	3.9	6.1	10.4	13.3	16.3	21.5	22.4	13.4	3.7

Temperatures in November 2016 at Udine										
	# samples	min	1st perc	25th perc	median	75th perc	99th perc	max	mean	STD
mea	720	-4.1	-3.0	6.5	9.7	12.3	16.1	17.5	9.0	4.2
ACM	720	0.4	1.6	7.3	9.6	12.0	16.5	18.1	9.6	3.4
BLC	720	1.0	1.6	5.8	9.2	12.5	18.2	19.7	9.3	4.1
GBM	720	-0.9	-0.7	5.4	8.4	11.5	17.3	19.7	8.5	4.2
MN3	720	-0.8	0.2	4.8	7.9	10.7	15.1	17.6	7.7	3.8
MYJ	720	-1.4	0.1	5.3	8.7	11.7	17.1	18.7	8.5	4.1
SHG	720	-0.8	-0.1	5.1	8.1	11.6	16.5	18.4	8.3	4.2
YSU	720	-1.2	-0.9	5.4	8.2	11.4	16.3	17.9	8.2	4.1

Temperatures in December 2016 at Udine										
	# samples	min	1st perc	25th perc	median	75th perc	99th perc	max	mean	STD
mea	744	-4.6	-3.7	0.2	3.2	7.2	14.7	17.7	4.0	4.5
ACM	744	-1.4	-0.7	2.1	4.2	6.3	10.8	12.3	4.3	2.9
BLC	744	1.4	1.9	3.7	4.8	7.0	12.9	14.2	5.5	2.5
GBM	744	-0.7	0.3	2.3	4.0	6.4	11.7	13.8	4.5	2.7
MN3	744	0.6	1.1	2.8	4.0	5.3	9.7	10.6	4.3	2.0
MYJ	744	0.1	1.4	3.5	4.8	6.6	10.8	12.4	5.2	2.2
SHG	744	0.2	0.8	2.4	3.3	5.3	10.3	11.0	4.0	2.3
YSU	744	-0.5	-0.2	2.3	3.5	5.7	10.7	12.4	4.2	2.6

Temperatures in 2016 at Cividale del Friuli										
	# samples	min	1st perc	25th perc	median	75th perc	99th perc	max	mean	STD
mea	8784	-4.3	-0.9	7.5	13.1	19.4	31.1	34.7	13.7	7.8
ACM	8784	-3.9	-0.9	6.4	12.2	19.7	30.0	33.1	13.1	7.9
BLC	8784	-2.9	0.6	7.6	13.8	21.0	32.0	34.6	14.6	8.0
GBM	8784	-3.3	-0.5	7.0	13.7	20.2	31.1	34.1	14.0	8.1
MN3	8784	-4.3	-0.8	6.3	12.3	18.3	25.7	28.9	12.4	6.9
MYJ	8784	-4.3	-0.5	7.0	13.5	20.5	31.4	34.5	14.0	8.1
SHG	8784	-3.4	-0.4	6.6	13.2	20.0	30.4	32.5	13.6	8.0
YSU	8784	-3.6	-0.6	6.8	13.1	20.2	30.2	33.5	13.7	8.0

Temperatures in January 2016 at Cividale del Friuli										
	# samples	min	1st perc	25th perc	median	75th perc	99th perc	max	mean	STD
mea	744	-4.3	-3.4	1.0	3.6	6.9	10.9	12.0	3.8	3.7
ACM	744	-3.9	-2.9	0.8	2.6	4.3	9.1	9.8	2.6	2.7
BLC	744	-2.9	-2.0	2.7	4.8	6.6	11.3	12.4	4.7	3.1
GBM	744	-3.3	-2.4	1.8	3.7	5.8	11.2	12.3	3.7	3.1
MN3	744	-4.3	-2.8	1.5	3.7	5.6	10.5	11.4	3.5	3.0
MYJ	744	-4.3	-3.2	2.0	4.0	5.6	10.5	11.2	3.8	3.0
SHG	744	-3.4	-2.8	1.8	3.6	5.6	10.2	11.6	3.6	3.0
YSU	744	-3.6	-2.9	1.8	3.7	5.5	10.5	11.7	3.6	3.1

Temperatures in February 2016 at Cividale del Friuli										
	# samples	min	1st perc	25th perc	median	75th perc	99th perc	max	mean	STD
mea	696	0.8	1.4	5.3	7.1	8.7	11.9	13.9	7.0	2.4
ACM	696	-0.5	0.6	3.4	4.9	6.8	10.2	11.1	5.1	2.3
BLC	696	1.4	2.0	5.5	7.4	9.2	12.9	14.0	7.4	2.5
GBM	696	0.9	1.5	5.1	7.0	9.0	12.5	13.9	7.0	2.6
MN3	696	0.0	0.4	4.3	6.3	8.4	10.6	11.8	6.3	2.5
MYJ	696	0.5	0.9	4.9	6.7	8.3	10.6	11.4	6.6	2.3
SHG	696	1.0	1.3	4.8	6.6	8.4	11.1	12.9	6.6	2.5
YSU	696	0.9	1.2	4.8	6.9	8.7	11.8	13.1	6.7	2.6

Temperatures in March 2016 at Cividale del Friuli										
	# samples	min	1st perc	25th perc	median	75th perc	99th perc	max	mean	STD
mea	744	1.9	2.8	6.5	8.5	11.5	16.5	17.5	9.1	3.4
ACM	744	1.0	1.8	4.1	6.8	9.2	13.8	15.5	6.8	3.0
BLC	744	1.6	2.0	5.8	8.3	11.1	17.2	18.5	8.6	3.6
GBM	744	0.5	1.8	5.4	7.6	10.0	16.5	17.4	7.9	3.4
MN3	744	1.2	1.5	4.9	7.1	9.7	14.4	14.9	7.3	3.1
MYJ	744	-0.4	0.6	4.7	7.5	10.6	16.2	16.9	7.7	3.9
SHG	744	1.3	1.5	5.0	7.7	10.4	16.3	17.2	8.0	3.7
YSU	744	1.6	2.3	5.2	7.5	10.2	15.4	16.2	7.8	3.2

Temperatures in April 2016 at Cividale del Friuli										
	# samples	min	1st perc	25th perc	median	75th perc	99th perc	max	mean	STD
mea	720	3.7	4.2	10.9	12.9	16.3	21.3	22.6	13.2	4.0
ACM	720	4.6	5.4	9.3	11.1	13.2	18.4	19.5	11.3	3.0
BLC	720	3.1	4.9	11.6	13.9	16.7	21.5	22.4	13.9	4.0
GBM	720	3.9	5.3	11.4	13.6	16.2	21.2	22.1	13.7	3.8
MN3	720	3.6	4.4	10.4	12.1	14.0	18.9	19.6	12.0	3.1
MYJ	720	4.5	5.2	11.3	13.3	15.7	21.2	22.0	13.4	3.6
SHG	720	3.6	4.4	11.3	13.2	15.7	20.5	21.2	13.2	3.7
YSU	720	3.6	4.6	11.3	13.4	15.9	21.2	21.7	13.5	3.8

Temperatures in May 2016 at Cividale del Friuli										
	# samples	min	1st perc	25th perc	median	75th perc	99th perc	max	mean	STD
mea	744	7.5	8.9	12.6	14.7	18.3	25.7	27.1	15.8	4.1
ACM	744	6.8	8.0	11.8	14.4	17.4	22.6	23.6	14.7	3.7
BLC	744	7.7	8.8	14.0	16.9	19.7	26.3	27.8	17.0	4.1
GBM	744	6.6	7.5	14.0	16.3	19.4	25.9	26.7	16.7	4.0
MN3	744	6.6	7.5	12.5	14.6	17.2	20.9	21.6	14.7	3.2
MYJ	744	7.0	8.3	13.3	16.0	19.2	25.4	26.6	16.4	3.9
SHG	744	5.2	6.8	13.2	15.9	19.3	25.6	26.6	16.3	4.3
YSU	744	5.9	7.5	13.0	16.0	19.3	25.8	26.8	16.3	4.3

Temperatures in June 2016 at Cividale del Friuli										
	# samples	min	1st perc	25th perc	median	75th perc	99th perc	max	mean	STD
mea	720	12.7	13.2	16.8	19.9	23.1	32.9	34.5	20.6	4.6
ACM	720	12.5	12.9	16.5	20.1	22.4	28.1	28.7	20.0	3.9
BLC	720	15.0	15.4	18.8	21.9	24.5	31.8	32.4	22.1	4.0
GBM	720	13.1	14.0	17.8	21.6	24.4	32.1	32.8	21.7	4.5
MN3	720	12.9	14.2	17.2	19.2	21.3	26.1	27.4	19.5	2.9
MYJ	720	12.5	14.0	17.6	21.3	23.5	30.6	31.0	21.2	4.3
SHG	720	13.1	14.3	18.3	21.3	24.0	30.7	31.2	21.5	3.9
YSU	720	13.0	14.7	18.5	21.6	24.1	30.5	31.1	21.6	3.8

Temperatures in July 2016 at Cividale del Friuli										
	# samples	min	1st perc	25th perc	median	75th perc	99th perc	max	mean	STD
mea	744	12.4	14.1	21.2	23.6	28.3	33.7	34.7	24.5	4.5
ACM	744	13.8	15.6	20.0	22.5	25.7	28.8	29.5	22.8	3.3
BLC	744	14.1	16.2	22.1	24.5	28.0	33.9	34.6	24.9	4.1
GBM	744	14.9	15.5	21.0	23.6	26.8	32.0	33.1	23.8	3.9
MN3	744	13.2	14.5	19.9	21.5	23.4	27.6	28.9	21.4	3.0
MYJ	744	12.9	14.8	21.8	23.9	27.0	32.5	33.4	24.1	4.0
SHG	744	12.4	13.6	20.8	23.5	26.7	31.4	32.2	23.6	4.0
YSU	744	12.9	14.2	21.2	23.7	27.4	30.9	32.1	24.0	3.8

Temperatures in August 2016 at Cividale del Friuli										
	# samples	min	1st perc	25th perc	median	75th perc	99th perc	max	mean	STD
mea	744	13.1	14.0	19.1	21.7	26.5	31.0	32.0	22.6	4.4
ACM	744	15.3	17.2	20.5	22.7	26.6	32.1	33.1	23.5	3.7
BLC	744	13.7	14.8	21.4	23.9	28.3	33.3	34.1	24.5	4.4
GBM	744	14.7	15.9	20.6	23.1	27.4	32.7	34.1	23.9	4.2
MN3	744	14.5	15.3	19.2	20.6	22.9	26.2	27.7	21.0	2.6
MYJ	744	15.2	17.0	21.5	24.0	28.3	33.5	34.5	24.7	4.2
SHG	744	13.5	15.1	20.3	22.7	27.0	31.8	32.5	23.4	4.1
YSU	744	14.2	15.0	20.0	22.7	26.9	32.3	33.5	23.2	4.1

Temperatures in September 2016 at Cividale del Friuli										
	# samples	min	1st perc	25th perc	median	75th perc	99th perc	max	mean	STD
mea	720	11.3	12.7	16.8	19.9	22.8	30.6	31.3	20.3	4.5
ACM	720	13.5	14.1	18.2	21.4	24.5	31.7	32.0	21.9	4.5
BLC	720	11.5	13.1	17.8	21.5	24.6	32.1	32.9	21.8	4.9
GBM	720	11.0	12.7	16.9	20.7	24.0	31.2	32.4	21.0	4.8
MN3	720	8.5	10.1	15.6	18.0	19.8	25.1	25.9	17.9	3.3
MYJ	720	11.2	11.8	17.5	21.2	24.1	32.3	33.2	21.4	4.9
SHG	720	9.8	12.0	16.4	20.2	23.6	30.8	31.7	20.6	4.9
YSU	720	10.4	12.4	16.3	20.2	23.6	31.0	31.3	20.6	4.8

Temperatures in October 2016 at Cividale del Friuli										
	# samples	min	1st perc	25th perc	median	75th perc	99th perc	max	mean	STD
mea	744	3.9	5.4	10.4	12.9	15.3	21.9	23.4	13.0	3.7
ACM	744	8.1	8.7	11.3	13.6	16.3	21.4	22.5	14.0	3.2
BLC	744	6.5	8.0	11.9	14.3	16.9	22.1	24.0	14.4	3.4
GBM	744	5.0	6.8	11.8	14.6	17.2	21.6	23.0	14.5	3.4
MN3	744	6.6	7.2	10.7	13.2	15.4	19.3	20.6	13.1	3.0
MYJ	744	6.9	7.6	11.9	14.4	16.9	21.9	24.2	14.4	3.3
SHG	744	4.6	6.4	11.1	13.5	16.3	21.1	23.0	13.7	3.5
YSU	744	3.9	6.3	10.9	13.3	16.0	20.7	21.5	13.4	3.4

Temperatures in November 2016 at Cividale del Friuli										
	# samples	min	1st perc	25th perc	median	75th perc	99th perc	max	mean	STD
mea	720	-1.7	-0.5	6.6	10.0	12.6	16.0	16.6	9.3	3.9
ACM	720	1.4	1.8	7.6	10.1	11.9	16.2	17.6	9.7	3.2
BLC	720	1.3	1.8	5.7	9.5	12.6	17.4	18.9	9.3	4.0
GBM	720	-1.1	0.2	5.7	8.7	11.5	16.9	18.3	8.7	4.0
MN3	720	0.6	1.2	5.0	8.1	10.7	15.1	17.1	7.9	3.6
MYJ	720	-2.0	0.5	5.5	8.8	12.1	17.1	18.3	8.7	4.0
SHG	720	-0.5	0.4	4.9	8.0	11.9	16.0	18.2	8.3	4.2
YSU	720	-1.3	0.1	5.4	8.4	11.7	16.1	17.9	8.4	4.0

Temperatures in December 2016 at Cividale del Friuli										
	# samples	min	1st perc	25th perc	median	75th perc	99th perc	max	mean	STD
mea	744	-0.9	-0.2	3.2	4.9	7.1	14.1	15.3	5.3	3.1
ACM	744	0.5	0.9	3.4	4.8	6.5	10.7	11.9	5.0	2.2
BLC	744	2.0	2.5	4.6	5.8	7.5	12.2	13.6	6.2	2.1
GBM	744	1.3	1.5	3.3	4.5	6.5	11.4	13.2	5.1	2.3
MN3	744	1.2	1.7	3.6	4.5	5.8	9.9	10.8	4.8	1.8
MYJ	744	2.1	2.6	4.5	5.6	7.1	10.8	12.3	5.9	2.0
SHG	744	1.4	1.8	3.3	4.1	5.9	10.5	12.0	4.7	2.1
YSU	744	0.9	1.5	3.4	4.5	6.2	11.1	12.0	5.0	2.2

Temperatures in February 2016 at Fagagna										
	# samples	min	1st perc	25th perc	median	75th perc	99th perc	max	mean	STD
mea	693	0.6	1.5	5.2	6.5	8.1	12.1	14.6	6.6	2.3
ACM	693	-0.4	-0.1	2.7	4.2	6.2	9.3	10.4	4.4	2.3
BLC	693	1.4	1.7	5.1	6.9	8.6	12.5	13.8	6.9	2.5
GBM	693	1.3	1.5	4.7	6.6	8.4	11.9	13.2	6.6	2.5
MN3	693	-0.2	0.3	4.0	6.0	7.8	10.3	10.9	5.8	2.4
MYJ	693	0.4	0.8	4.4	6.3	7.6	10.1	10.7	6.0	2.3
SHG	693	0.4	1.1	4.4	6.3	7.8	11.1	12.6	6.1	2.5
YSU	693	0.7	1.0	4.3	6.3	7.8	11.7	12.7	6.2	2.5

Temperatures in March 2016 at Fagagna										
	# samples	min	1st perc	25th perc	median	75th perc	99th perc	max	mean	STD
mea	744	1.4	2.6	6.5	8.8	12.0	16.4	17.4	9.2	3.4
ACM	744	0.5	0.8	3.4	6.2	8.7	13.1	13.8	6.2	3.2
BLC	744	0.9	1.3	5.2	7.7	10.7	16.7	17.9	8.1	3.7
GBM	744	0.5	1.1	5.1	7.1	9.8	16.2	17.3	7.5	3.5
MN3	744	0.5	1.1	4.8	6.8	9.5	13.7	14.7	7.1	3.1
MYJ	744	0.1	0.5	4.7	7.5	10.2	15.8	16.3	7.5	3.8
SHG	744	0.4	0.7	4.8	7.2	10.3	16.1	16.8	7.6	3.7
YSU	744	1.3	1.9	5.0	7.3	10.0	14.9	15.9	7.5	3.2

Temperatures in April 2016 at Fagagna										
	# samples	min	1st perc	25th perc	median	75th perc	99th perc	max	mean	STD
mea	720	2.7	4.4	11.3	13.3	16.5	21.5	22.2	13.5	3.8
ACM	720	4.1	4.8	8.6	10.4	12.8	17.8	18.8	10.6	3.0
BLC	720	3.0	4.2	11.1	13.4	16.3	20.8	21.9	13.4	3.9
GBM	720	3.2	5.4	10.9	13.2	16.0	20.8	21.4	13.3	3.7
MN3	720	2.9	3.4	10.0	11.8	13.6	18.2	19.0	11.6	3.1
MYJ	720	4.0	4.5	10.8	12.7	15.4	20.9	22.0	13.0	3.7
SHG	720	2.7	4.1	10.8	12.9	15.4	20.1	20.9	12.8	3.7
YSU	720	3.4	4.8	10.9	13.1	15.7	20.9	21.6	13.2	3.7

Temperatures in May 2016 at Fagagna										
	# samples	min	1st perc	25th perc	median	75th perc	99th perc	max	mean	STD
mea	744	8.7	9.7	13.3	15.5	18.8	26.1	27.3	16.3	3.9
ACM	744	6.5	7.9	11.4	14.0	17.2	22.6	23.5	14.4	3.7
BLC	744	8.0	8.9	13.7	16.6	19.4	26.1	27.6	16.8	4.2
GBM	744	6.6	7.9	13.8	16.3	19.4	25.3	25.8	16.6	4.0
MN3	744	5.8	6.9	12.1	14.4	16.9	20.9	21.5	14.4	3.4
MYJ	744	6.3	7.6	13.2	15.6	18.8	24.8	25.8	16.1	4.0
SHG	744	6.2	7.4	12.9	15.7	19.2	25.4	25.8	16.1	4.2
YSU	744	6.3	8.0	12.9	15.8	19.1	25.6	26.4	16.1	4.3

Temperatures in June 2016 at Fagagna										
	# samples	min	1st perc	25th perc	median	75th perc	99th perc	max	mean	STD
mea	720	12.6	13.2	17.4	19.9	23.5	33.7	34.9	20.8	4.5
ACM	720	12.1	12.6	16.1	19.8	22.4	28.0	28.3	19.7	4.1
BLC	720	12.4	15.1	18.3	21.5	24.4	31.3	32.4	21.7	4.0
GBM	720	12.4	14.5	17.6	21.2	24.2	31.9	32.4	21.4	4.5
MN3	720	12.6	13.5	16.8	19.1	21.2	25.7	26.8	19.2	2.9
MYJ	720	12.4	13.6	16.9	21.0	23.4	30.2	30.8	20.8	4.3
SHG	720	12.4	13.8	18.0	20.9	24.0	30.3	30.6	21.2	3.9
YSU	720	12.2	14.5	18.0	21.1	24.0	30.0	30.6	21.2	3.9

Temperatures in July 2016 at Fagagna										
	# samples	min	1st perc	25th perc	median	75th perc	99th perc	max	mean	STD
mea	744	13.7	16.0	20.9	23.3	27.5	31.9	32.6	24.0	4.0
ACM	744	13.8	15.2	19.8	22.3	25.4	28.8	29.3	22.5	3.5
BLC	744	14.1	15.4	21.4	23.8	27.3	32.6	33.3	24.3	4.0
GBM	744	13.1	13.9	20.5	23.0	26.3	31.2	31.8	23.2	4.0
MN3	744	12.5	13.5	19.4	21.3	23.3	27.1	28.4	21.1	3.0
MYJ	744	13.2	14.1	21.2	23.2	26.5	31.1	32.0	23.5	3.9
SHG	744	12.8	13.7	20.2	22.8	26.1	30.7	31.3	23.0	3.9
YSU	744	13.0	13.8	20.6	23.0	27.0	30.5	31.4	23.5	3.8

Temperatures in August 2016 at Fagagna										
	# samples	min	1st perc	25th perc	median	75th perc	99th perc	max	mean	STD
mea	744	12.1	14.5	19.0	21.3	25.7	30.6	31.9	22.2	4.2
ACM	744	14.7	16.0	19.8	22.4	26.0	31.0	31.7	22.9	3.8
BLC	744	13.4	14.9	20.5	23.0	27.4	32.4	33.7	23.7	4.4
GBM	744	13.9	14.7	19.7	22.3	26.6	32.1	33.0	23.1	4.3
MN3	744	14.4	15.0	19.0	20.5	22.6	25.6	26.8	20.7	2.5
MYJ	744	13.7	15.8	20.6	22.9	26.7	32.0	33.2	23.6	3.9
SHG	744	12.8	14.4	19.4	21.9	26.0	30.8	31.3	22.5	4.1
YSU	744	12.6	14.1	19.1	22.2	26.3	32.2	33.2	22.6	4.3

Temperatures in September 2016 at Fagagna										
	# samples	min	1st perc	25th perc	median	75th perc	99th perc	max	mean	STD
mea	720	11.7	12.7	16.8	19.9	22.9	30.5	31.1	20.4	4.6
ACM	720	12.5	13.7	17.8	21.1	24.4	31.3	31.6	21.4	4.6
BLC	720	11.3	13.2	17.3	20.9	24.3	31.8	32.6	21.3	4.8
GBM	720	9.5	11.2	16.5	20.0	23.6	31.0	31.9	20.5	4.9
MN3	720	8.1	10.9	15.1	17.8	19.8	24.9	25.7	17.7	3.4
MYJ	720	11.0	12.3	17.0	20.5	23.6	31.5	32.0	20.8	4.9
SHG	720	9.1	11.5	15.7	19.5	23.0	29.8	30.4	19.8	4.8
YSU	720	9.3	10.8	16.1	19.5	23.2	30.7	31.2	20.1	5.0

Temperatures in October 2016 at Fagagna										
	# samples	min	1st perc	25th perc	median	75th perc	99th perc	max	mean	STD
mea	744	4.1	4.9	10.0	12.6	15.0	21.5	23.0	12.7	3.6
ACM	744	7.1	7.7	10.9	13.4	16.0	21.8	22.4	13.6	3.4
BLC	744	6.7	7.6	11.6	14.1	16.5	22.4	24.4	14.1	3.5
GBM	744	4.6	5.9	11.6	14.4	17.0	20.4	21.2	14.1	3.5
MN3	744	5.7	6.7	10.6	12.8	15.1	19.1	20.3	12.8	3.0
MYJ	744	6.2	6.8	11.6	14.1	16.4	21.2	23.1	13.9	3.3
SHG	744	4.0	5.2	10.7	13.4	15.9	20.7	22.9	13.3	3.6
YSU	744	4.3	5.4	10.4	12.9	15.7	21.2	22.0	13.0	3.5

Temperatures in November 2016 at Fagagna										
	# samples	min	1st perc	25th perc	median	75th perc	99th perc	max	mean	STD
mea	720	-2.3	-1.3	6.2	9.4	11.8	14.9	15.5	8.6	3.8
ACM	720	1.1	1.7	7.1	9.6	11.4	15.5	17.5	9.3	3.1
BLC	720	0.4	1.1	5.4	9.0	12.1	17.3	18.9	8.7	3.9
GBM	720	-0.5	-0.1	5.2	7.9	11.0	16.3	18.1	8.0	4.0
MN3	720	0.1	0.7	4.8	7.4	10.3	14.2	16.5	7.4	3.6
MYJ	720	-0.9	0.4	5.1	8.0	11.3	16.1	18.0	8.1	3.9
SHG	720	-0.7	0.1	4.6	7.6	10.7	15.3	17.1	7.7	3.9
YSU	720	-0.5	-0.2	4.9	7.8	10.8	15.2	16.2	7.7	3.7

Temperatures in December 2016 at Fagagna										
	# samples	min	1st perc	25th perc	median	75th perc	99th perc	max	mean	STD
mea	744	-1.7	-1.0	2.2	4.6	6.7	13.8	15.9	4.8	3.4
ACM	744	-0.4	-0.3	2.6	3.9	5.9	10.1	11.4	4.3	2.4
BLC	744	1.4	2.8	4.5	5.6	7.0	11.9	12.9	5.9	1.9
GBM	744	0.4	1.1	2.7	4.0	5.8	11.0	12.9	4.5	2.3
MN3	744	1.1	1.5	3.3	4.2	5.4	9.7	10.8	4.5	1.8
MYJ	744	1.3	1.5	4.2	5.3	6.8	10.2	11.0	5.5	1.9
SHG	744	-0.0	0.7	2.4	3.4	5.0	9.4	11.8	3.9	2.1
YSU	744	-0.1	0.5	2.4	3.6	5.2	10.4	11.3	4.1	2.2

Temperatures in 2016 at Fossalon di Grado										
	# samples	min	1st perc	25th perc	median	75th perc	99th perc	max	mean	STD
mea	8784	-4.5	-1.4	8.5	14.2	20.6	31.4	33.8	14.7	8.0
ACM	8784	-1.8	1.0	7.9	13.4	20.7	29.7	32.7	14.3	7.6
BLC	8784	-2.1	1.8	8.7	14.7	21.5	30.7	34.9	15.2	7.5
GBM	8784	-2.2	0.5	8.0	14.5	20.9	29.2	32.9	14.6	7.5
MN3	8784	-1.5	0.1	7.9	13.4	19.6	26.6	31.0	13.7	6.9
MYJ	8784	-2.6	0.3	8.1	14.2	21.0	29.6	33.9	14.6	7.6
SHG	8784	-2.2	0.7	7.8	14.0	20.7	28.9	32.9	14.3	7.5
YSU	8784	-2.2	0.4	7.9	13.9	20.7	28.7	31.7	14.4	7.5

Temperatures in January 2016 at Fossalon di Grado										
	# samples	min	1st perc	25th perc	median	75th perc	99th perc	max	mean	STD
mea	744	-4.5	-3.1	1.3	4.2	7.2	13.5	14.8	4.2	3.9
ACM	744	-1.8	-0.9	2.4	3.9	5.8	12.6	13.0	4.4	3.0
BLC	744	-2.1	-1.1	3.7	6.2	8.0	13.1	14.4	5.9	3.2
GBM	744	-2.2	-1.5	2.3	5.0	7.3	13.4	14.4	5.0	3.4
MN3	744	-1.5	-1.1	2.5	5.0	7.0	12.8	13.3	4.8	3.2
MYJ	744	-2.6	-1.8	2.5	5.0	6.9	12.7	13.2	4.8	3.2
SHG	744	-2.2	-1.5	2.4	5.1	7.0	13.6	14.3	5.0	3.3
YSU	744	-2.2	-1.6	2.7	5.1	7.0	13.6	14.3	5.0	3.3

Temperatures in February 2016 at Fossalon di Grado										
	# samples	min	1st perc	25th perc	median	75th perc	99th perc	max	mean	STD
mea	696	-0.2	0.5	6.3	7.7	9.6	12.7	13.7	7.8	2.5
ACM	696	-0.4	1.8	5.2	6.6	8.6	11.4	11.6	6.9	2.3
BLC	696	0.9	3.5	6.7	8.3	10.0	13.2	14.5	8.3	2.3
GBM	696	1.9	2.8	6.2	8.0	9.8	12.7	13.4	7.9	2.4
MN3	696	0.2	1.6	5.5	7.5	9.5	11.6	12.4	7.4	2.5
MYJ	696	0.5	2.1	6.0	7.6	9.1	11.9	12.4	7.5	2.3
SHG	696	2.0	2.3	5.7	7.5	9.4	12.6	13.4	7.6	2.5
YSU	696	1.2	2.3	5.9	7.6	9.5	12.6	13.4	7.6	2.5

Temperatures in March 2016 at Fossalon di Grado										
	# samples	min	1st perc	25th perc	median	75th perc	99th perc	max	mean	STD
mea	744	2.3	3.3	8.1	10.2	12.4	16.8	17.3	10.3	3.0
ACM	744	1.9	2.9	5.2	7.8	9.9	14.0	15.5	7.7	2.9
BLC	744	2.2	3.1	6.9	9.0	11.1	15.1	16.4	8.9	2.8
GBM	744	1.9	2.4	6.0	7.9	10.4	15.2	16.6	8.2	3.0
MN3	744	1.3	2.9	6.1	8.1	10.2	13.6	14.2	8.1	2.7
MYJ	744	-0.1	1.0	5.6	8.1	10.5	14.8	15.8	8.1	3.3
SHG	744	1.6	2.6	6.1	8.3	10.6	15.1	15.9	8.3	3.0
YSU	744	2.4	2.8	5.9	7.9	10.3	13.9	14.2	8.1	2.7

Temperatures in April 2016 at Fossalon di Grado										
	# samples	min	1st perc	25th perc	median	75th perc	99th perc	max	mean	STD
mea	720	5.8	6.7	12.3	14.1	17.1	20.7	21.4	14.4	3.3
ACM	720	5.5	6.3	10.7	12.3	14.5	19.1	20.8	12.6	2.8
BLC	720	5.2	6.0	12.3	13.9	15.7	20.8	21.9	13.9	3.0
GBM	720	5.5	6.9	12.2	14.1	15.9	21.3	21.8	13.9	3.0
MN3	720	5.2	7.1	11.4	12.7	14.4	18.2	19.0	12.7	2.4
MYJ	720	4.7	6.8	11.8	13.4	15.4	21.4	22.7	13.5	2.9
SHG	720	5.3	6.3	11.9	13.6	15.3	20.6	21.5	13.4	2.9
YSU	720	6.0	6.8	11.8	13.7	15.5	21.7	22.6	13.7	3.0

Temperatures in May 2016 at Fossalon di Grado										
	# samples	min	1st perc	25th perc	median	75th perc	99th perc	max	mean	STD
mea	744	8.3	10.0	14.6	17.1	20.1	25.9	26.3	17.4	3.8
ACM	744	6.8	7.7	12.5	15.2	18.4	22.1	22.8	15.3	3.6
BLC	744	8.2	9.7	15.1	17.2	19.3	24.1	24.8	17.1	3.3
GBM	744	6.1	8.6	14.6	16.9	19.1	24.0	25.0	16.8	3.4
MN3	744	5.6	7.4	13.5	16.0	17.9	21.3	22.0	15.5	3.2
MYJ	744	7.3	8.5	14.1	16.7	18.7	24.5	26.0	16.6	3.4
SHG	744	6.2	8.7	13.9	16.7	19.0	23.8	24.4	16.4	3.6
YSU	744	6.0	8.9	13.9	16.8	18.9	23.6	24.1	16.5	3.5

Temperatures in June 2016 at Fossalon di Grado										
	# samples	min	1st perc	25th perc	median	75th perc	99th perc	max	mean	STD
mea	720	13.7	14.7	18.6	21.8	24.8	33.3	33.8	22.1	4.3
ACM	720	13.0	13.5	18.0	20.9	22.7	29.6	30.3	20.8	3.6
BLC	720	16.1	16.5	19.8	22.4	23.9	31.5	32.7	22.4	3.3
GBM	720	14.7	16.1	19.4	21.6	23.3	31.3	32.9	21.8	3.5
MN3	720	13.9	15.4	18.8	20.6	22.4	27.1	29.3	20.7	2.7
MYJ	720	10.8	14.2	19.3	21.6	23.3	30.1	31.3	21.6	3.5
SHG	720	14.1	16.2	19.5	21.8	23.1	30.0	31.4	21.8	3.1
YSU	720	14.8	15.9	19.6	21.8	23.3	29.4	31.1	21.8	3.1

Temperatures in July 2016 at Fossalon di Grado										
	# samples	min	1st perc	25th perc	median	75th perc	99th perc	max	mean	STD
mea	744	12.9	15.7	21.7	25.0	29.1	32.9	33.6	25.2	4.3
ACM	744	14.2	15.4	21.5	24.1	26.3	30.8	31.8	23.9	3.2
BLC	744	13.2	16.3	23.1	25.0	27.6	32.5	34.8	25.2	3.3
GBM	744	13.0	15.8	22.2	24.4	26.3	29.7	32.7	24.1	3.0
MN3	744	14.0	15.7	21.4	23.0	24.6	29.0	31.0	22.8	2.8
MYJ	744	12.5	14.8	22.5	24.8	26.8	31.2	33.9	24.5	3.3
SHG	744	13.2	14.7	21.9	24.4	26.4	30.1	32.9	24.0	3.1
YSU	744	11.9	14.6	22.3	24.9	26.7	29.0	31.7	24.4	3.0

Temperatures in August 2016 at Fossalon di Grado										
	# samples	min	1st perc	25th perc	median	75th perc	99th perc	max	mean	STD
mea	744	12.8	14.5	20.4	23.8	27.7	31.4	32.3	23.9	4.3
ACM	744	19.3	19.9	21.9	24.5	27.3	31.6	32.4	24.7	3.1
BLC	744	13.8	17.1	22.2	24.6	27.2	33.3	34.9	24.7	3.6
GBM	744	16.4	17.4	21.1	23.9	26.2	31.0	32.5	23.8	3.2
MN3	744	15.5	16.8	20.4	22.1	24.0	27.5	28.3	22.2	2.5
MYJ	744	15.5	17.3	21.9	24.0	27.1	31.1	32.5	24.3	3.3
SHG	744	14.0	17.5	21.0	23.6	26.0	31.4	32.7	23.6	3.2
YSU	744	14.4	17.0	20.8	23.6	26.0	30.0	30.8	23.5	3.2

Temperatures in September 2016 at Fossalon di Grado										
	# samples	min	1st perc	25th perc	median	75th perc	99th perc	max	mean	STD
mea	720	10.6	12.7	18.5	21.0	24.4	31.9	33.1	21.7	4.6
ACM	720	15.8	16.5	19.1	21.6	24.3	31.1	32.7	22.0	3.7
BLC	720	12.1	14.8	19.2	21.8	23.9	31.3	32.2	21.9	3.7
GBM	720	12.0	14.5	18.4	21.0	23.5	30.4	30.9	21.1	3.6
MN3	720	11.9	12.9	17.4	19.5	21.5	26.4	26.9	19.4	3.1
MYJ	720	12.0	13.8	18.2	21.2	23.4	30.2	31.5	21.3	3.8
SHG	720	11.9	14.9	17.9	20.3	23.5	30.0	30.9	20.8	3.7
YSU	720	11.5	14.1	18.0	20.6	23.4	30.5	31.5	20.9	3.8

Temperatures in October 2016 at Fossalon di Grado										
	# samples	min	1st perc	25th perc	median	75th perc	99th perc	max	mean	STD
mea	744	3.9	6.1	11.6	14.2	16.5	22.5	23.8	14.2	3.7
ACM	744	9.3	9.8	12.8	15.0	17.2	21.5	22.1	15.2	3.0
BLC	744	6.4	9.6	13.2	15.7	17.9	23.9	24.5	15.8	3.3
GBM	744	7.2	7.7	13.2	15.9	18.5	22.8	24.2	15.9	3.5
MN3	744	7.3	8.7	12.2	15.0	17.0	22.2	22.7	14.8	3.2
MYJ	744	6.8	9.1	12.9	15.8	17.9	22.7	23.8	15.6	3.2
SHG	744	3.7	7.1	12.9	15.2	17.5	22.0	22.4	15.2	3.4
YSU	744	5.7	7.1	12.0	14.8	17.1	22.1	23.2	14.7	3.4

Temperatures in November 2016 at Fossalon di Grado										
	# samples	min	1st perc	25th perc	median	75th perc	99th perc	max	mean	STD
mea	720	-2.4	-0.9	7.8	10.9	13.4	17.6	20.2	10.4	4.1
ACM	720	2.7	3.0	8.9	11.2	13.5	17.9	19.0	11.1	3.4
BLC	720	2.0	2.8	7.8	11.3	14.5	18.8	20.4	11.1	4.0
GBM	720	0.5	0.8	7.1	10.3	13.3	18.6	19.8	10.1	4.3
MN3	720	0.2	1.1	6.8	10.4	13.1	17.5	18.6	9.9	3.9
MYJ	720	-0.8	0.4	7.3	10.6	13.6	17.7	18.9	10.3	4.1
SHG	720	-0.6	0.5	6.6	9.4	13.0	18.4	19.3	9.8	4.2
YSU	720	-0.6	0.2	7.0	9.9	13.2	18.3	19.1	10.0	4.2

Temperatures in December 2016 at Fossalon di Grado										
	# samples	min	1st perc	25th perc	median	75th perc	99th perc	max	mean	STD
mea	744	-3.2	-2.5	2.0	5.3	7.7	13.9	17.3	5.2	3.9
ACM	744	1.1	1.2	4.6	6.3	8.2	12.2	13.6	6.4	2.5
BLC	744	1.9	2.4	5.3	6.8	8.6	12.9	14.7	7.0	2.4
GBM	744	0.0	0.7	4.5	6.0	7.8	12.6	14.5	6.2	2.7
MN3	744	0.3	0.7	4.2	6.1	7.7	11.6	12.6	5.9	2.5
MYJ	744	1.7	2.0	5.2	6.7	8.3	12.4	13.4	6.8	2.4
SHG	744	0.4	1.0	4.1	5.9	7.4	11.9	14.2	5.9	2.6
YSU	744	0.3	0.7	4.3	6.4	7.9	12.5	13.7	6.2	2.7

Temperatures in February 2016 at the Paloma buoy										
	# samples	min	1st perc	25th perc	median	75th perc	99th perc	max	mean	STD
mea	696	4.7	5.3	7.3	8.3	9.6	12.8	14.1	8.5	1.6
ACM	696	4.9	5.4	7.7	8.9	10.0	11.5	11.8	8.8	1.4
BLC	696	6.0	6.4	8.3	9.3	10.3	11.9	12.0	9.3	1.3
GBM	696	4.6	4.8	7.7	9.1	10.5	12.1	12.3	9.0	1.8
MN3	696	5.0	5.3	7.7	8.8	10.0	11.3	11.8	8.7	1.5
MYJ	696	4.8	5.1	7.9	8.7	9.8	11.2	11.4	8.7	1.4
SHG	696	3.5	4.0	7.3	8.8	10.1	11.9	12.2	8.6	1.9
YSU	696	3.9	4.3	7.5	8.9	10.3	12.0	12.3	8.8	1.8

Temperatures in March 2016 at the Paloma buoy										
	# samples	min	1st perc	25th perc	median	75th perc	99th perc	max	mean	STD
mea	744	5.0	5.9	8.8	10.2	11.3	13.7	14.0	10.1	1.8
ACM	744	5.2	5.8	7.7	9.1	10.2	12.7	13.1	9.0	1.7
BLC	744	6.2	6.8	8.5	9.4	10.8	13.5	14.7	9.6	1.6
GBM	744	4.2	4.5	7.0	8.7	10.5	13.6	14.1	8.8	2.2
MN3	744	5.7	6.2	8.1	9.0	10.2	12.1	12.5	9.1	1.5
MYJ	744	4.2	4.9	7.4	9.1	10.5	12.6	13.3	9.0	2.0
SHG	744	3.9	4.1	7.7	9.0	10.9	13.0	13.5	9.1	2.2
YSU	744	4.2	4.6	7.6	8.8	10.2	13.0	13.8	8.9	2.0

Temperatures in April 2016 at the Paloma buoy										
	# samples	min	1st perc	25th perc	median	75th perc	99th perc	max	mean	STD
mea	720	7.6	8.2	12.6	13.8	15.0	17.8	18.8	13.7	2.0
ACM	720	8.5	10.0	12.3	13.3	14.1	16.6	17.1	13.3	1.3
BLC	720	8.8	9.9	13.0	14.0	14.9	17.3	17.7	13.9	1.4
GBM	720	7.8	8.8	12.9	13.8	15.2	17.4	17.8	13.9	1.7
MN3	720	9.1	9.9	12.1	12.8	14.1	16.0	16.5	13.0	1.3
MYJ	720	9.1	10.1	12.5	13.5	14.6	17.3	18.3	13.6	1.5
SHG	720	7.6	8.3	12.4	13.5	14.9	17.4	17.9	13.6	1.7
YSU	720	7.7	8.3	12.6	13.5	15.0	17.6	17.9	13.7	1.7

Temperatures in May 2016 at the Paloma buoy										
	# samples	min	1st perc	25th perc	median	75th perc	99th perc	max	mean	STD
mea	744	11.6	12.9	15.3	16.6	18.1	21.8	22.1	16.8	2.1
ACM	744	9.1	11.8	14.8	16.5	18.3	21.2	22.2	16.6	2.2
BLC	744	11.6	12.3	16.0	17.2	18.5	21.9	22.7	17.4	2.0
GBM	744	9.7	11.0	15.9	17.3	18.7	22.4	23.5	17.3	2.3
MN3	744	10.3	12.0	14.9	16.5	17.7	20.5	21.0	16.4	1.9
MYJ	744	10.4	12.1	15.7	16.9	18.3	21.6	23.1	17.0	2.1
SHG	744	8.8	11.0	15.7	17.1	18.6	22.4	23.2	17.1	2.4
YSU	744	10.8	11.4	15.7	17.1	18.5	22.3	23.6	17.1	2.4

Temperatures in June 2016 at the Paloma buoy										
	# samples	min	1st perc	25th perc	median	75th perc	99th perc	max	mean	STD
mea	720	16.4	16.9	19.4	21.3	23.5	28.0	29.5	21.6	2.8
ACM	720	17.5	17.7	20.0	21.2	23.5	26.3	27.8	21.7	2.1
BLC	720	19.0	19.6	20.8	21.8	23.7	27.4	28.1	22.3	1.9
GBM	720	17.8	18.5	20.3	21.5	24.3	27.1	27.5	22.1	2.3
MN3	720	18.3	18.5	20.1	21.2	22.6	25.6	26.4	21.4	1.7
MYJ	720	17.4	18.3	20.3	21.4	23.9	26.4	27.8	21.9	2.1
SHG	720	18.1	18.9	20.6	21.9	23.4	26.6	27.2	22.2	2.0
YSU	720	17.0	17.5	20.7	21.9	23.6	26.5	27.4	22.2	2.0

Temperatures in July 2016 at the Paloma buoy										
	# samples	min	1st perc	25th perc	median	75th perc	99th perc	max	mean	STD
mea	744	18.3	20.1	23.8	25.1	26.2	28.6	29.7	24.9	1.9
ACM	744	19.3	20.7	24.1	25.0	25.7	27.4	28.0	24.8	1.4
BLC	744	20.0	22.1	24.6	25.5	26.3	28.0	30.0	25.4	1.3
GBM	744	18.0	21.2	24.1	25.1	26.0	27.8	28.9	25.0	1.5
MN3	744	19.2	20.7	22.9	24.1	24.9	26.7	27.4	23.9	1.4
MYJ	744	19.6	21.2	24.2	25.2	26.0	27.7	29.3	25.0	1.4
SHG	744	18.2	20.9	24.4	25.3	26.1	28.0	28.9	25.0	1.6
YSU	744	17.8	20.9	24.7	25.5	26.2	28.0	28.4	25.3	1.4

Temperatures in August 2016 at the Paloma buoy										
	# samples	min	1st perc	25th perc	median	75th perc	99th perc	max	mean	STD
mea	744	17.8	18.7	22.6	24.0	25.0	27.2	27.6	23.7	1.9
ACM	744	20.9	21.2	24.0	24.6	25.1	27.4	28.2	24.6	1.2
BLC	744	20.7	20.9	23.9	24.6	25.4	27.8	28.2	24.7	1.3
GBM	744	19.8	20.3	23.9	24.7	25.3	27.5	28.4	24.5	1.4
MN3	744	19.4	20.1	22.9	23.5	24.3	26.2	26.9	23.5	1.2
MYJ	744	20.8	21.0	23.9	24.6	25.2	27.3	27.8	24.5	1.2
SHG	744	17.9	20.2	23.8	24.7	25.5	27.6	27.9	24.5	1.5
YSU	744	19.4	20.1	23.9	24.7	25.4	27.5	27.8	24.5	1.5

Temperatures in September 2016 at the Paloma buoy										
	# samples	min	1st perc	25th perc	median	75th perc	99th perc	max	mean	STD
mea	720	17.0	17.6	20.4	22.0	24.3	27.4	28.5	22.3	2.4
ACM	720	17.8	18.2	20.8	22.9	24.1	26.3	27.8	22.5	1.9
BLC	720	18.3	19.1	21.1	22.9	24.0	25.8	26.5	22.6	1.7
GBM	720	15.7	16.6	20.6	22.8	24.1	26.0	26.5	22.3	2.2
MN3	720	15.2	16.0	19.7	21.3	22.8	24.5	24.6	21.1	1.9
MYJ	720	17.0	18.1	20.8	22.6	23.9	25.5	26.3	22.3	1.9
SHG	720	16.1	16.9	20.5	22.7	24.1	26.3	26.6	22.3	2.2
YSU	720	16.0	16.9	20.6	22.5	24.1	26.3	26.8	22.4	2.1

Temperatures in October 2016 at the Paloma buoy										
	# samples	min	1st perc	25th perc	median	75th perc	99th perc	max	mean	STD
mea	744	10.9	11.2	14.1	15.1	16.5	21.0	21.3	15.3	2.1
ACM	744	12.3	13.0	15.7	16.6	18.1	22.1	22.4	16.9	2.0
BLC	744	11.6	12.1	16.6	17.2	18.6	22.4	22.8	17.5	2.0
GBM	744	11.4	12.1	15.9	17.3	18.5	22.6	23.2	17.3	2.3
MN3	744	11.8	12.6	15.8	17.1	18.1	21.6	22.2	17.0	1.8
MYJ	744	13.1	13.7	16.2	17.2	18.4	21.9	23.0	17.4	1.8
SHG	744	11.1	11.6	15.4	16.8	18.2	22.1	22.6	16.9	2.4
YSU	744	10.4	10.8	15.4	16.5	17.9	22.2	23.0	16.6	2.3

Temperatures in November 2016 at the Paloma buoy										
	# samples	min	1st perc	25th perc	median	75th perc	99th perc	max	mean	STD
mea	521	5.5	5.8	9.9	11.7	13.5	17.1	19.2	11.7	2.6
ACM	521	8.7	9.1	12.0	13.7	15.6	18.3	18.4	13.8	2.3
BLC	521	7.4	8.5	12.2	14.0	15.8	18.6	19.1	13.9	2.4
GBM	521	3.6	3.8	10.1	12.7	15.2	18.8	19.4	12.4	3.7
MN3	521	6.1	6.9	11.6	13.1	14.7	17.7	17.8	12.9	2.5
MYJ	521	6.8	7.1	12.1	13.4	15.1	17.8	18.2	13.3	2.6
SHG	521	5.4	5.6	9.7	12.9	15.1	18.5	18.8	12.3	3.5
YSU	521	4.6	5.0	10.5	12.9	15.3	18.4	18.6	12.6	3.3

Temperatures in January 2016 at Enemonzo										
	# samples	min	1st perc	25th perc	median	75th perc	99th perc	max	mean	STD
mea	744	-9.0	-7.9	-2.5	0.1	3.7	9.1	9.7	0.5	4.1
ACM	744	-8.6	-6.9	-2.2	0.5	3.3	9.0	10.8	0.6	3.8
BLC	744	-5.5	-5.3	1.7	3.7	5.9	10.3	12.1	3.5	3.4
GBM	744	-6.8	-5.9	0.2	2.3	4.4	9.4	11.3	2.1	3.3
MN3	744	-6.2	-5.8	0.6	3.1	4.6	8.6	9.7	2.5	3.3
MYJ	744	-5.7	-5.4	1.0	3.3	5.1	9.8	12.0	3.0	3.4
SHG	744	-7.0	-5.7	-0.1	2.0	4.0	9.4	11.5	1.9	3.3
YSU	744	-7.6	-6.8	0.0	1.9	4.0	9.2	11.3	1.7	3.4

Temperatures in February 2016 at Enemonzo										
	# samples	min	1st perc	25th perc	median	75th perc	99th perc	max	mean	STD
mea	696	-2.9	-2.3	0.9	3.0	5.7	10.4	11.6	3.4	3.0
ACM	696	-3.8	-3.5	0.6	2.9	5.0	9.5	11.2	2.8	3.1
BLC	696	-0.2	0.9	3.8	5.8	7.5	12.6	14.6	5.7	2.6
GBM	696	-0.1	0.2	2.9	4.8	6.9	12.1	13.9	4.9	2.7
MN3	696	-0.5	-0.2	2.4	4.4	6.3	11.3	12.7	4.5	2.6
MYJ	696	-0.1	0.4	2.9	4.8	6.7	11.0	11.8	4.9	2.4
SHG	696	-1.1	-0.0	2.4	4.2	6.3	11.0	11.8	4.4	2.6
YSU	696	-0.9	0.0	2.3	4.2	6.3	11.3	11.9	4.4	2.6

Temperatures in March 2016 at Enemonzo										
	# samples	min	1st perc	25th perc	median	75th perc	99th perc	max	mean	STD
mea	744	-2.0	-1.5	1.2	4.8	9.6	15.7	16.8	5.7	4.8
ACM	744	-3.9	-3.4	-0.1	3.2	6.8	12.0	12.1	3.4	4.1
BLC	744	0.2	0.4	3.7	6.1	9.5	15.2	16.9	6.7	3.8
GBM	744	-0.8	-0.3	2.9	5.0	8.3	14.4	15.5	5.7	3.7
MN3	744	-0.7	0.1	3.1	5.0	8.2	13.1	14.0	5.6	3.3
MYJ	744	-1.9	-0.9	2.7	5.9	9.0	14.7	16.1	6.2	4.1
SHG	744	-1.5	-1.0	2.2	4.6	8.3	14.7	15.4	5.5	4.1
YSU	744	-1.0	-0.5	2.6	4.7	7.9	13.9	14.8	5.4	3.6

Temperatures in April 2016 at Enemonzo										
	# samples	min	1st perc	25th perc	median	75th perc	99th perc	max	mean	STD
mea	720	-0.7	0.2	8.2	10.8	14.4	20.1	20.8	11.0	4.6
ACM	720	-0.6	1.1	5.1	7.6	10.7	16.0	16.5	7.9	3.8
BLC	720	3.2	3.5	10.0	12.1	14.9	19.7	20.9	12.2	3.8
GBM	720	1.5	2.4	9.1	11.4	14.3	19.2	20.4	11.6	3.9
MN3	720	2.0	2.2	8.4	10.3	12.3	17.3	17.9	10.2	3.4
MYJ	720	3.0	3.3	9.9	11.7	14.5	19.5	19.9	11.9	3.8
SHG	720	1.0	1.8	8.7	11.2	13.9	18.8	19.4	11.2	3.9
YSU	720	0.9	2.1	8.9	11.2	14.1	19.2	19.7	11.3	4.0

Temperatures in May 2016 at Enemonzo										
	# samples	min	1st perc	25th perc	median	75th perc	99th perc	max	mean	STD
mea	744	2.6	4.7	10.1	13.1	16.8	24.2	25.7	13.8	4.8
ACM	744	3.1	3.5	8.2	11.4	14.9	20.8	21.4	11.6	4.5
BLC	744	7.8	9.0	12.2	15.4	18.2	25.5	26.9	15.6	4.1
GBM	744	5.4	6.8	11.5	14.5	17.7	24.3	25.2	14.8	4.2
MN3	744	5.1	6.3	10.8	12.9	15.4	20.0	21.6	13.0	3.4
MYJ	744	5.1	7.1	11.7	14.8	17.6	24.2	25.6	14.9	4.0
SHG	744	3.9	5.6	11.0	13.9	17.5	24.7	26.3	14.4	4.6
YSU	744	4.6	6.0	10.9	14.1	17.6	24.5	26.7	14.4	4.6

Temperatures in June 2016 at Enemonzo										
	# samples	min	1st perc	25th perc	median	75th perc	99th perc	max	mean	STD
mea	720	9.1	9.8	14.4	17.1	21.0	32.1	33.4	18.1	5.0
ACM	720	8.3	9.4	13.8	17.2	20.8	26.0	26.5	17.4	4.5
BLC	720	13.5	14.1	17.1	20.0	22.9	29.7	30.8	20.3	3.8
GBM	720	10.6	11.8	15.9	19.1	22.1	30.0	30.5	19.5	4.4
MN3	720	12.1	12.6	15.4	17.8	20.2	25.3	25.6	18.0	3.1
MYJ	720	11.7	12.7	15.7	19.2	21.9	28.8	29.2	19.4	4.1
SHG	720	10.6	12.1	15.9	18.7	21.8	28.0	28.4	19.0	3.9
YSU	720	11.4	12.6	16.4	18.9	22.2	27.9	28.7	19.3	3.8

Temperatures in November 2016 at Enemonzo										
	# samples	min	1st perc	25th perc	median	75th perc	99th perc	max	mean	STD
mea	720	-5.4	-4.6	2.8	6.4	9.0	13.0	15.3	5.7	4.3
ACM	720	-2.9	-2.4	3.5	5.9	8.3	13.5	15.0	6.0	3.5
BLC	720	-0.3	0.5	4.3	7.4	10.5	15.2	17.0	7.4	3.6
GBM	720	-2.2	-1.2	3.3	5.9	9.0	15.3	16.2	6.1	3.8
MN3	720	-1.0	-0.5	3.5	6.0	8.5	12.4	14.1	6.0	3.2
MYJ	720	-1.0	-0.8	3.7	6.9	10.0	14.5	16.5	6.8	3.8
SHG	720	-2.8	-2.3	2.7	5.5	8.5	13.7	14.7	5.6	3.8
YSU	720	-2.2	-1.2	3.2	5.8	8.6	13.7	15.6	5.9	3.6

Temperatures in December 2016 at Enemonzo										
	# samples	min	1st perc	25th perc	median	75th perc	99th perc	max	mean	STD
mea	744	-5.1	-4.7	-1.9	-0.3	2.7	11.1	14.4	0.7	3.7
ACM	744	-3.8	-3.3	-0.9	1.7	6.0	10.4	11.0	2.5	3.9
BLC	744	1.3	1.8	4.7	6.1	7.8	12.3	13.7	6.3	2.3
GBM	744	0.1	0.3	2.7	3.8	5.7	10.4	11.0	4.3	2.2
MN3	744	0.6	0.8	4.0	5.0	6.3	9.8	10.5	5.1	1.9
MYJ	744	1.0	1.4	4.7	6.0	7.2	10.4	11.9	6.0	1.8
SHG	744	-0.4	0.0	2.6	3.6	5.4	10.2	11.7	4.1	2.2
YSU	744	-0.2	0.5	2.6	3.8	5.6	10.2	11.4	4.2	2.2

B.2 Winds

All values are expressed in m/s.

Wind speed in February 2016 at Udine										
	# samples	min	1st perc	25th perc	median	75th perc	99th perc	max	mean	STD
mea	696	0.0	0.1	1.0	1.8	3.0	8.1	8.8	2.3	1.7
ACM2	696	0.0	0.1	1.9	2.5	3.2	10.2	13.0	2.9	1.9
BLC	696	0.0	0.4	1.9	2.7	4.9	12.4	14.5	3.9	2.9
GBM	696	0.0	0.2	1.8	2.6	4.0	9.8	12.4	3.3	2.2
MN3	696	0.0	0.4	1.8	2.6	3.9	9.9	14.1	3.3	2.1
MYJ	696	0.2	0.5	2.0	2.6	4.4	12.0	15.4	3.6	2.6
SHG	696	0.1	0.5	1.8	2.6	3.8	11.3	15.3	3.3	2.3
YSU	696	0.3	0.6	1.9	2.6	3.7	11.3	15.3	3.2	2.2

Wind speed in March 2016 at Udine										
	# samples	min	1st perc	25th perc	median	75th perc	99th perc	max	mean	STD
mea	744	0.0	0.1	1.0	1.7	2.9	7.2	8.4	2.2	1.6
ACM2	744	0.0	0.2	1.6	2.3	3.5	8.6	9.5	2.8	1.8
BLC	744	0.0	0.5	2.1	2.8	4.5	12.0	15.0	3.8	2.7
GBM	744	0.1	0.3	1.7	2.5	4.5	9.7	10.9	3.4	2.4
MN3	744	0.0	0.2	1.5	2.4	3.5	9.9	11.2	2.8	1.9
MYJ	744	0.2	0.4	1.9	2.6	4.3	13.2	16.0	3.6	2.7
SHG	744	0.3	0.4	1.7	2.5	3.5	9.9	14.8	2.9	2.0
YSU	744	0.1	0.3	1.7	2.4	3.8	11.1	13.1	3.2	2.4

Wind speed in April 2016 at Udine										
	# samples	min	1st perc	25th perc	median	75th perc	99th perc	max	mean	STD
mea	720	0.0	0.1	0.9	1.6	2.8	6.2	10.4	2.0	1.5
ACM2	720	0.0	0.1	1.6	2.4	3.2	6.2	7.0	2.5	1.3
BLC	720	0.0	0.3	1.8	2.5	3.6	7.4	9.6	2.8	1.6
GBM	720	0.1	0.2	1.5	2.4	3.4	7.0	9.0	2.6	1.5
MN3	720	0.0	0.3	1.5	2.1	3.3	7.8	10.1	2.5	1.6
MYJ	720	0.1	0.4	1.8	2.6	3.8	7.7	10.0	2.9	1.6
SHG	720	0.1	0.3	1.6	2.3	3.3	6.9	8.3	2.6	1.4
YSU	720	0.0	0.4	1.6	2.3	3.3	6.1	7.9	2.5	1.3

Wind speed in May 2016 at Udine										
	# samples	min	1st perc	25th perc	median	75th perc	99th perc	max	mean	STD
mea	744	0.0	0.1	1.0	1.6	2.3	5.0	8.0	1.8	1.1
ACM2	744	0.1	0.2	1.8	2.4	3.2	6.8	8.1	2.6	1.4
BLC	744	0.0	0.3	1.8	2.7	4.1	10.5	15.6	3.2	2.1
GBM	744	0.1	0.3	1.9	2.8	3.8	8.0	9.1	3.1	1.7
MN3	744	0.0	0.4	1.7	2.4	3.5	8.6	10.7	2.8	1.7
MYJ	744	0.1	0.6	2.0	2.9	4.3	9.0	13.1	3.3	1.9
SHG	744	0.3	0.4	1.7	2.6	3.8	10.1	13.8	3.0	1.9
YSU	744	0.1	0.3	1.7	2.6	3.7	8.1	10.0	2.9	1.7

Wind speed in June 2016 at Udine										
	# samples	min	1st perc	25th perc	median	75th perc	99th perc	max	mean	STD
mea	720	0.0	0.0	1.0	1.7	2.5	6.3	7.4	1.9	1.3
ACM2	720	0.0	0.1	1.5	2.3	3.0	6.4	8.0	2.4	1.3
BLC	720	0.0	0.3	1.8	2.4	3.7	8.6	11.2	2.9	1.7
GBM	720	0.1	0.3	1.4	2.1	2.9	7.3	9.6	2.3	1.4
MN3	720	0.0	0.1	1.3	2.0	2.8	7.1	9.5	2.2	1.3
MYJ	720	0.1	0.5	1.9	2.5	3.8	8.5	9.3	2.9	1.6
SHG	720	0.1	0.5	1.6	2.4	3.3	7.2	8.9	2.6	1.4
YSU	720	0.1	0.3	1.5	2.3	3.3	7.3	8.4	2.6	1.5

Wind speed in July 2016 at Udine										
	# samples	min	1st perc	25th perc	median	75th perc	99th perc	max	mean	STD
mea	744	0.0	0.1	1.0	1.7	2.4	5.4	10.5	1.8	1.2
ACM2	744	0.1	0.4	1.5	2.0	2.8	6.8	8.9	2.3	1.2
BLC	744	0.0	0.1	1.5	2.2	3.4	7.7	23.5	2.6	1.8
GBM	744	0.0	0.3	1.5	2.1	3.2	7.5	10.7	2.5	1.5
MN3	744	0.0	0.1	1.3	1.9	2.7	6.5	11.4	2.1	1.3
MYJ	744	0.1	0.4	1.7	2.4	3.5	7.4	12.3	2.7	1.5
SHG	744	0.2	0.5	1.6	2.2	3.1	7.3	9.3	2.5	1.4
YSU	744	0.2	0.4	1.5	2.2	3.1	7.2	13.5	2.5	1.4

Wind speed in August 2016 at Udine										
	# samples	min	1st perc	25th perc	median	75th perc	99th perc	max	mean	STD
mea	744	0.0	0.1	1.0	1.5	2.2	5.4	7.8	1.7	1.1
ACM2	744	0.0	0.2	1.5	2.0	2.6	6.4	8.4	2.2	1.2
BLC	744	0.0	0.2	1.6	2.4	3.7	8.2	11.1	2.8	1.8
GBM	744	0.1	0.3	1.5	2.3	3.2	7.3	10.0	2.5	1.4
MN3	744	0.0	0.2	1.2	1.8	2.4	5.2	6.3	2.0	1.1
MYJ	744	0.2	0.4	1.8	2.5	3.4	7.7	10.4	2.8	1.5
SHG	744	0.1	0.4	1.6	2.1	2.9	6.3	9.1	2.3	1.2
YSU	744	0.0	0.3	1.4	2.2	3.0	6.6	9.4	2.4	1.3

Wind speed in September 2016 at Udine										
	# samples	min	1st perc	25th perc	median	75th perc	99th perc	max	mean	STD
mea	720	0.0	0.1	0.9	1.4	2.0	4.8	6.1	1.6	0.9
ACM2	720	0.0	0.2	1.7	2.3	2.9	7.6	10.0	2.5	1.5
BLC	720	0.0	0.3	1.6	2.3	3.3	9.2	11.1	2.7	1.8
GBM	720	0.0	0.3	1.4	2.2	3.2	7.0	8.8	2.5	1.4
MN3	720	0.0	0.1	1.2	1.9	2.5	6.2	9.2	2.0	1.3
MYJ	720	0.2	0.6	1.9	2.4	3.4	9.8	12.2	2.9	1.7
SHG	720	0.1	0.4	1.6	2.3	3.1	7.7	9.4	2.5	1.4
YSU	720	0.1	0.4	1.5	2.3	3.3	7.8	9.9	2.6	1.5

Wind speed in October 2016 at Udine										
	# samples	min	1st perc	25th perc	median	75th perc	99th perc	max	mean	STD
mea	744	0.0	0.1	0.9	1.4	2.3	5.4	7.3	1.7	1.2
ACM2	744	0.0	0.2	1.6	2.3	3.2	9.4	10.5	2.8	1.9
BLC	744	0.0	0.2	1.6	2.3	4.0	10.4	11.7	3.2	2.5
GBM	744	0.1	0.3	1.4	2.1	3.2	8.0	9.9	2.5	1.6
MN3	744	0.0	0.1	1.5	2.2	3.1	8.9	10.8	2.6	1.8
MYJ	744	0.1	0.3	1.6	2.4	3.6	8.6	9.4	2.8	1.8
SHG	744	0.1	0.4	1.5	2.4	3.3	7.6	9.9	2.6	1.6
YSU	744	0.0	0.5	1.6	2.3	3.5	9.2	10.8	2.9	1.9

Wind speed in November 2016 at Udine										
	# samples	min	1st perc	25th perc	median	75th perc	99th perc	max	mean	STD
mea	720	0.0	0.0	0.7	1.1	2.0	6.5	7.9	1.6	1.4
ACM2	720	0.0	0.2	1.6	2.3	3.2	6.9	8.2	2.6	1.5
BLC	720	0.0	0.3	1.8	2.5	4.9	11.6	14.1	3.6	2.7
GBM	720	0.0	0.2	1.6	2.4	3.6	10.4	12.6	3.0	2.2
MN3	720	0.1	0.3	1.6	2.3	3.4	8.5	11.9	2.8	1.9
MYJ	720	0.2	0.4	1.9	2.6	4.0	12.8	13.8	3.4	2.5
SHG	720	0.1	0.4	1.5	2.4	3.6	10.9	12.4	3.0	2.4
YSU	720	0.2	0.3	1.4	2.3	3.4	10.6	12.0	2.8	2.1

Wind speed in December 2016 at Udine										
	# samples	min	1st perc	25th perc	median	75th perc	99th perc	max	mean	STD
mea	744	0.0	0.0	0.7	1.1	1.8	5.1	8.1	1.4	1.1
ACM2	744	0.0	0.0	1.1	1.9	3.0	7.5	8.0	2.3	1.7
BLC	744	0.1	0.3	1.5	2.1	2.6	9.0	11.9	2.4	1.6
GBM	744	0.0	0.1	1.3	1.9	3.1	5.5	7.0	2.2	1.3
MN3	744	0.0	0.2	1.3	2.0	2.7	6.6	7.5	2.3	1.5
MYJ	744	0.1	0.3	1.6	2.1	2.6	6.2	9.4	2.3	1.2
SHG	744	0.1	0.4	1.3	2.0	3.1	5.5	6.4	2.3	1.2
YSU	744	0.1	0.4	1.4	2.0	3.0	5.7	7.2	2.3	1.2

Wind speed in 2016 at Cividale del Friuli										
	# samples	min	1st perc	25th perc	median	75th perc	99th perc	max	mean	STD
mea	8373	0.0	0.3	2.1	3.6	5.1	9.1	14.1	3.7	2.1
ACM2	8373	0.0	0.0	1.5	2.6	3.8	11.6	14.7	3.1	2.4
BLC	8373	0.0	0.3	1.8	2.9	4.5	13.4	18.3	3.6	2.7
GBM	8373	0.0	0.2	1.5	2.6	4.0	11.8	16.3	3.1	2.4
MN3	8373	0.0	0.2	1.4	2.3	3.8	11.4	17.0	2.9	2.2
MYJ	8373	0.0	0.4	1.8	2.9	4.5	14.8	19.7	3.6	2.8
SHG	8373	0.0	0.3	1.5	2.6	3.9	12.6	22.8	3.2	2.5
YSU	8373	0.0	0.3	1.5	2.5	3.9	13.2	16.9	3.1	2.5

Wind speed in January 2016 at Cividale del Friuli										
	# samples	min	1st perc	25th perc	median	75th perc	99th perc	max	mean	STD
mea	744	0.0	0.0	1.8	3.7	5.3	10.1	12.6	3.7	2.3
ACM2	744	0.0	0.0	0.9	2.0	3.1	6.9	10.1	2.2	1.6
BLC	744	0.0	0.3	1.3	2.2	3.5	10.9	13.0	2.8	2.2
GBM	744	0.0	0.1	1.0	1.8	3.3	8.8	13.0	2.4	2.1
MN3	744	0.1	0.2	1.3	2.3	3.5	8.7	9.9	2.7	2.0
MYJ	744	0.1	0.2	1.2	2.2	3.4	8.9	10.7	2.6	2.0
SHG	744	0.1	0.2	1.1	1.9	3.1	7.5	9.3	2.4	1.7
YSU	744	0.0	0.2	1.1	1.9	3.1	7.9	9.1	2.3	1.7

Wind speed in February 2016 at Cividale del Friuli										
	# samples	min	1st perc	25th perc	median	75th perc	99th perc	max	mean	STD
mea	510	0.0	0.0	1.6	3.4	5.2	11.7	14.1	3.7	2.6
ACM2	510	0.1	0.3	2.1	3.0	3.9	13.7	14.7	3.8	3.0
BLC	510	0.3	0.8	2.3	3.1	4.9	16.1	18.3	4.4	3.4
GBM	510	0.5	0.7	1.9	2.9	4.4	13.1	16.3	4.0	3.1
MN3	510	0.3	0.5	2.1	3.0	4.6	14.5	17.0	4.1	3.3
MYJ	510	0.2	0.6	2.2	3.1	4.6	15.5	18.9	4.5	3.7
SHG	510	0.1	0.5	2.1	2.9	4.1	13.6	16.0	4.1	3.3
YSU	510	0.1	0.4	2.1	2.9	4.0	13.6	16.3	4.0	3.2

Wind speed in March 2016 at Cividale del Friuli										
	# samples	min	1st perc	25th perc	median	75th perc	99th perc	max	mean	STD
mea	744	0.0	0.2	2.0	3.3	4.9	10.3	13.9	3.6	2.2
ACM2	744	0.0	0.1	1.8	3.0	6.5	12.1	12.9	4.2	3.3
BLC	744	0.1	0.5	2.1	3.3	6.3	15.0	17.2	4.7	3.7
GBM	744	0.0	0.2	1.8	3.0	6.8	13.9	15.4	4.5	3.5
MN3	744	0.0	0.2	1.5	2.5	5.3	12.1	14.5	3.6	2.8
MYJ	744	0.1	0.4	1.9	3.2	6.4	17.3	19.7	4.9	4.2
SHG	744	0.1	0.3	1.8	3.1	5.5	18.1	20.0	4.3	3.7
YSU	744	0.0	0.4	1.7	2.9	5.3	15.6	16.6	4.3	3.8

Wind speed in April 2016 at Cividale del Friuli										
	# samples	min	1st perc	25th perc	median	75th perc	99th perc	max	mean	STD
mea	720	0.0	0.4	2.1	3.3	4.6	10.3	12.3	3.6	2.1
ACM2	720	0.0	0.1	1.8	2.8	4.0	8.3	10.2	3.0	1.7
BLC	720	0.1	0.2	1.9	2.9	4.1	8.7	9.9	3.1	1.8
GBM	720	0.0	0.2	1.7	2.7	3.9	8.1	9.8	3.0	1.7
MN3	720	0.0	0.3	1.6	2.5	4.0	8.6	12.1	2.9	1.8
MYJ	720	0.2	0.4	1.8	2.9	4.2	8.6	11.0	3.3	1.9
SHG	720	0.1	0.3	1.6	2.6	3.7	8.0	9.1	2.8	1.7
YSU	720	0.1	0.3	1.7	2.5	3.8	9.2	11.7	2.9	1.8

Wind speed in May 2016 at Cividale del Friuli										
	# samples	min	1st perc	25th perc	median	75th perc	99th perc	max	mean	STD
mea	744	0.0	0.3	2.1	3.2	4.6	6.9	8.2	3.4	1.6
ACM2	744	0.0	0.0	1.7	2.8	4.3	10.6	13.4	3.3	2.3
BLC	744	0.2	0.4	1.9	2.9	4.7	13.5	16.8	3.8	2.7
GBM	744	0.0	0.4	1.9	3.1	4.5	10.3	13.0	3.5	2.3
MN3	744	0.0	0.3	1.7	2.7	4.1	10.5	13.8	3.2	2.1
MYJ	744	0.1	0.5	2.2	3.3	4.7	15.2	16.9	4.0	2.9
SHG	744	0.1	0.3	1.7	2.8	4.1	19.7	22.8	3.4	3.0
YSU	744	0.1	0.3	1.6	2.6	3.9	9.9	11.5	3.0	2.0

Wind speed in June 2016 at Cividale del Friuli										
	# samples	min	1st perc	25th perc	median	75th perc	99th perc	max	mean	STD
mea	720	0.0	0.5	2.3	3.6	5.0	7.8	8.4	3.7	1.8
ACM2	720	0.0	0.2	1.7	2.6	3.8	7.2	8.3	2.8	1.6
BLC	720	0.0	0.3	1.9	2.9	4.4	9.7	11.1	3.3	2.1
GBM	720	0.1	0.3	1.5	2.4	3.5	7.9	9.0	2.7	1.6
MN3	720	0.0	0.2	1.3	2.0	3.1	8.2	9.4	2.4	1.6
MYJ	720	0.3	0.6	2.0	3.0	4.4	9.7	12.2	3.4	1.9
SHG	720	0.2	0.4	1.7	2.7	3.8	8.5	9.2	3.0	1.6
YSU	720	0.1	0.3	1.6	2.6	4.0	8.0	9.4	2.9	1.7

Wind speed in July 2016 at Cividale del Friuli										
	# samples	min	1st perc	25th perc	median	75th perc	99th perc	max	mean	STD
mea	744	0.1	0.5	2.2	3.5	5.1	7.9	10.0	3.7	1.9
ACM2	744	0.0	0.2	1.3	2.0	3.3	7.8	12.8	2.4	1.7
BLC	744	0.0	0.3	1.6	2.6	3.9	8.0	10.9	2.9	1.7
GBM	744	0.1	0.3	1.4	2.2	3.6	8.1	10.5	2.6	1.7
MN3	744	0.0	0.1	1.1	1.8	3.2	7.6	8.6	2.3	1.7
MYJ	744	0.0	0.4	1.7	2.5	3.7	9.2	13.9	2.9	1.8
SHG	744	0.1	0.3	1.5	2.2	3.4	8.2	12.5	2.6	1.6
YSU	744	0.0	0.3	1.4	2.2	3.5	7.7	13.2	2.6	1.7

Wind speed in August 2016 at Cividale del Friuli										
	# samples	min	1st perc	25th perc	median	75th perc	99th perc	max	mean	STD
mea	744	0.4	0.5	2.2	3.4	5.0	7.7	9.1	3.6	1.8
ACM2	744	0.0	0.1	1.4	2.4	3.5	7.2	9.6	2.6	1.6
BLC	744	0.0	0.3	2.0	3.2	4.7	10.1	10.8	3.6	2.3
GBM	744	0.1	0.3	1.7	2.7	3.9	7.6	8.8	3.0	1.7
MN3	744	0.0	0.2	1.2	1.9	3.4	8.4	12.7	2.5	1.8
MYJ	744	0.2	0.6	2.2	3.3	4.6	10.1	11.8	3.7	2.0
SHG	744	0.2	0.4	1.8	2.7	3.6	7.5	12.4	2.9	1.5
YSU	744	0.1	0.3	1.6	2.6	3.7	7.8	10.9	2.8	1.7

Wind speed in September 2016 at Cividale del Friuli										
	# samples	min	1st perc	25th perc	median	75th perc	99th perc	max	mean	STD
mea	720	0.0	0.6	2.1	3.8	5.1	7.0	8.5	3.7	1.8
ACM2	720	0.0	0.2	1.8	2.8	3.8	10.6	13.8	3.1	2.1
BLC	720	0.0	0.2	1.7	3.0	4.2	11.3	14.5	3.5	2.5
GBM	720	0.0	0.3	1.5	2.4	3.7	7.9	11.0	2.8	1.6
MN3	720	0.0	0.1	1.3	2.2	3.5	7.0	9.4	2.5	1.6
MYJ	720	0.3	0.6	2.0	3.0	4.3	11.0	12.6	3.4	2.1
SHG	720	0.1	0.3	1.6	2.6	3.6	10.1	12.0	3.0	1.9
YSU	720	0.2	0.3	1.6	2.6	3.7	10.1	12.1	3.0	1.9

Wind speed in October 2016 at Cividale del Friuli										
	# samples	min	1st perc	25th perc	median	75th perc	99th perc	max	mean	STD
mea	744	0.1	0.5	2.5	4.0	5.3	8.4	9.5	4.0	1.9
ACM2	744	0.0	0.1	1.6	2.8	4.4	12.9	14.4	3.6	3.0
BLC	744	0.1	0.3	1.7	3.1	5.2	14.1	15.0	4.1	3.3
GBM	744	0.0	0.1	1.3	2.4	3.9	9.2	10.0	2.9	2.1
MN3	744	0.0	0.2	1.3	2.5	4.1	10.1	11.1	3.0	2.2
MYJ	744	0.1	0.4	1.5	3.0	4.7	12.6	13.6	3.6	2.8
SHG	744	0.1	0.3	1.5	2.6	4.0	10.9	11.7	3.1	2.3
YSU	744	0.1	0.4	1.5	2.8	4.5	12.6	13.5	3.6	3.0

Wind speed in November 2016 at Cividale del Friuli										
	# samples	min	1st perc	25th perc	median	75th perc	99th perc	max	mean	STD
mea	720	0.0	0.3	1.5	3.1	4.9	9.1	10.5	3.4	2.2
ACM2	720	0.0	0.0	1.4	2.6	3.9	13.1	13.6	3.3	2.8
BLC	720	0.0	0.4	2.0	3.2	5.6	14.8	15.4	4.2	3.3
GBM	720	0.0	0.2	1.7	2.8	4.4	15.3	16.0	3.8	3.4
MN3	720	0.1	0.2	1.8	2.8	4.5	13.9	14.9	3.7	3.0
MYJ	720	0.1	0.5	2.1	3.5	5.6	16.7	17.5	4.5	3.6
SHG	720	0.1	0.3	1.6	2.8	4.7	15.2	16.4	3.9	3.4
YSU	720	0.1	0.3	1.5	2.7	4.2	15.7	16.9	3.6	3.2

Wind speed in December 2016 at Cividale del Friuli										
	# samples	min	1st perc	25th perc	median	75th perc	99th perc	max	mean	STD
mea	519.0	0.0	0.3	3.4	5.1	6.3	9.1	10.5	4.8	2.2
ACM2	519.0	0.0	0.0	0.6	1.9	4.2	9.2	10.6	2.6	2.4
BLC	519.0	0.0	0.3	1.2	2.2	4.3	9.1	12.4	2.9	2.2
GBM	519.0	0.0	0.0	1.0	2.2	4.1	6.5	7.5	2.6	1.8
MN3	519.0	0.1	0.2	1.0	1.9	3.7	7.7	8.0	2.6	2.0
MYJ	519.0	0.2	0.3	1.1	1.9	3.9	8.4	9.0	2.7	2.1
SHG	519.0	0.0	0.2	1.1	2.0	3.9	7.2	7.9	2.6	1.9
YSU	519.0	0.2	0.3	1.1	2.0	4.1	7.6	9.5	2.7	2.1

Wind speed in 2016 at Fagagna										
	# samples	min	1st perc	25th perc	median	75th perc	99th perc	max	mean	STD
mea	8781.0	0.0	0.3	1.8	2.9	4.5	8.2	15.0	3.2	1.8
ACM2	8781.0	0.0	0.1	1.6	2.4	3.3	9.1	12.5	2.7	1.8
BLC	8781.0	0.0	0.3	1.9	2.8	3.8	10.8	16.1	3.2	2.1
GBM	8781.0	0.0	0.2	1.6	2.4	3.5	9.8	16.1	2.8	1.9
MN3	8781.0	0.0	0.2	1.5	2.3	3.4	9.8	14.3	2.7	1.9
MYJ	8781.0	0.0	0.4	1.9	2.8	3.8	11.2	17.3	3.2	2.1
SHG	8781.0	0.0	0.4	1.7	2.4	3.5	10.6	17.7	2.9	2.0
YSU	8781.0	0.0	0.3	1.6	2.4	3.5	10.3	14.5	2.9	2.0

Wind speed in January 2016 at Fagagna										
	# samples	min	1st perc	25th perc	median	75th perc	99th perc	max	mean	STD
mea	744	0.0	0.2	1.7	2.9	4.8	6.6	7.8	3.2	1.8
ACM2	744	0.0	0.0	1.2	2.1	2.7	7.0	11.7	2.2	1.5
BLC	744	0.2	0.3	1.4	2.1	3.2	9.7	12.7	2.5	1.7
GBM	744	0.1	0.2	1.1	1.8	2.8	7.0	10.7	2.1	1.5
MN3	744	0.0	0.1	1.3	2.2	3.2	7.3	10.8	2.5	1.6
MYJ	744	0.1	0.2	1.5	2.1	3.2	7.8	9.1	2.5	1.5
SHG	744	0.1	0.3	1.3	1.9	2.8	6.1	7.3	2.2	1.3
YSU	744	0.1	0.2	1.3	1.9	2.9	7.2	9.5	2.3	1.4

Wind speed in February 2016 at Fagagna										
	# samples	min	1st perc	25th perc	median	75th perc	99th perc	max	mean	STD
mea	693.0	0.0	0.2	1.9	3.4	5.5	9.7	12.9	3.8	2.3
ACM2	693.0	0.0	0.1	2.2	2.9	3.8	10.5	12.5	3.4	2.1
BLC	693.0	0.2	0.5	2.3	3.2	5.0	11.8	14.8	4.0	2.6
GBM	693.0	0.1	0.3	2.0	3.0	4.4	10.7	13.6	3.6	2.3
MN3	693.0	0.1	0.5	2.1	3.0	4.3	11.4	12.9	3.6	2.3
MYJ	693.0	0.1	0.6	2.2	3.1	4.8	11.8	17.3	3.9	2.6
SHG	693.0	0.2	0.5	2.1	2.9	4.5	11.2	12.5	3.8	2.5
YSU	693.0	0.2	0.5	2.1	3.0	4.9	11.8	13.7	3.8	2.6

Wind speed in March 2016 at Fagagna										
	# samples	min	1st perc	25th perc	median	75th perc	99th perc	max	mean	STD
mea	744	0.3	0.4	1.8	3.0	4.5	10.5	12.4	3.4	2.0
ACM2	744	0.0	0.1	1.8	2.5	3.8	11.3	12.4	3.2	2.3
BLC	744	0.1	0.4	2.3	3.2	4.4	13.3	16.1	3.7	2.4
GBM	744	0.1	0.3	1.8	2.8	4.7	14.8	16.1	3.9	3.0
MN3	744	0.1	0.4	1.6	2.7	4.4	10.8	13.8	3.5	2.4
MYJ	744	0.2	0.4	2.1	3.0	5.0	12.8	13.8	4.0	2.9
SHG	744	0.3	0.6	1.9	2.8	4.5	15.2	17.7	3.8	3.1
YSU	744	0.1	0.4	1.9	2.8	4.9	13.8	14.5	3.9	3.0

Wind speed in April 2016 at Fagagna										
	# samples	min	1st perc	25th perc	median	75th perc	99th perc	max	mean	STD
mea	720	0.0	0.5	1.7	2.6	3.8	7.4	15.0	2.9	1.7
ACM2	720	0.0	0.2	1.9	2.7	3.8	7.2	8.2	3.0	1.5
BLC	720	0.1	0.3	2.2	3.0	3.8	8.9	10.3	3.2	1.6
GBM	720	0.1	0.2	1.9	2.7	3.7	9.4	12.1	3.0	1.7
MN3	720	0.1	0.2	1.6	2.3	3.4	8.7	10.7	2.7	1.7
MYJ	720	0.1	0.4	2.1	2.9	4.1	8.4	10.1	3.2	1.7
SHG	720	0.1	0.2	1.8	2.6	3.6	7.4	9.2	2.8	1.5
YSU	720	0.1	0.3	1.7	2.5	3.5	7.0	9.7	2.8	1.5

Wind speed in May 2016 at Fagagna										
	# samples	min	1st perc	25th perc	median	75th perc	99th perc	max	mean	STD
mea	744	0.1	0.4	1.8	2.8	4.0	6.9	9.2	3.0	1.6
ACM2	744	0.0	0.1	2.0	2.9	3.9	8.9	10.5	3.2	1.8
BLC	744	0.2	0.5	2.1	3.2	4.6	12.6	15.3	3.7	2.4
GBM	744	0.2	0.4	1.9	3.0	4.3	8.9	11.4	3.4	1.9
MN3	744	0.0	0.3	1.9	2.7	3.9	10.9	13.3	3.3	2.2
MYJ	744	0.4	0.6	2.4	3.3	5.0	12.3	15.5	4.1	2.5
SHG	744	0.4	0.6	1.9	3.0	4.3	14.3	17.0	3.6	2.6
YSU	744	0.2	0.4	1.8	2.9	4.2	10.1	12.9	3.3	2.1

Wind speed in June 2016 at Fagagna										
	# samples	min	1st perc	25th perc	median	75th perc	99th perc	max	mean	STD
mea	720	0.2	0.4	1.9	3.0	4.2	8.5	11.3	3.2	1.7
ACM2	720	0.0	0.0	1.6	2.5	3.4	7.9	8.9	2.7	1.6
BLC	720	0.1	0.5	1.9	2.7	3.6	8.0	12.6	2.9	1.6
GBM	720	0.1	0.4	1.5	2.2	3.1	6.5	14.4	2.5	1.4
MN3	720	0.0	0.2	1.4	2.2	3.1	7.3	10.7	2.5	1.5
MYJ	720	0.1	0.4	2.0	2.9	3.9	7.9	11.3	3.2	1.7
SHG	720	0.1	0.6	1.9	2.6	3.8	7.2	10.3	2.9	1.6
YSU	720	0.0	0.4	1.5	2.3	3.7	7.6	10.5	2.8	1.7

Wind speed in July 2016 at Fagagna										
	# samples	min	1st perc	25th perc	median	75th perc	99th perc	max	mean	STD
mea	744	0.0	0.3	2.1	3.2	4.6	7.6	9.0	3.4	1.7
ACM2	744	0.0	0.0	1.6	2.2	2.9	7.6	9.6	2.4	1.4
BLC	744	0.1	0.4	1.9	2.6	3.5	8.5	11.2	2.9	1.6
GBM	744	0.2	0.4	1.6	2.3	3.2	8.1	11.8	2.6	1.5
MN3	744	0.0	0.2	1.3	2.0	2.8	7.1	12.3	2.3	1.5
MYJ	744	0.0	0.6	2.0	2.6	3.4	8.5	13.6	2.9	1.5
SHG	744	0.1	0.4	1.7	2.3	3.0	8.0	10.0	2.6	1.5
YSU	744	0.1	0.4	1.7	2.4	3.2	7.3	11.9	2.6	1.4

Wind speed in August 2016 at Fagagna										
	# samples	min	1st perc	25th perc	median	75th perc	99th perc	max	mean	STD
mea	744	0.0	0.4	1.9	3.1	4.5	8.1	9.3	3.3	1.7
ACM2	744	0.0	0.2	1.5	2.1	2.8	7.8	11.2	2.4	1.5
BLC	744	0.1	0.3	1.7	2.7	3.7	10.3	12.8	3.1	2.0
GBM	744	0.0	0.3	1.6	2.4	3.3	7.8	10.2	2.6	1.5
MN3	744	0.0	0.1	1.2	1.9	2.6	7.0	8.5	2.1	1.4
MYJ	744	0.1	0.4	1.7	2.6	3.4	9.5	10.9	2.9	1.8
SHG	744	0.1	0.4	1.7	2.3	3.2	7.1	10.0	2.6	1.4
YSU	744	0.0	0.4	1.6	2.2	3.0	7.5	9.3	2.5	1.4

Wind speed in September 2016 at Fagagna										
	# samples	min	1st perc	25th perc	median	75th perc	99th perc	max	mean	STD
mea	720	0.1	0.4	1.8	2.8	4.2	6.9	9.1	3.0	1.6
ACM2	720	0.0	0.3	1.8	2.5	3.3	10.8	11.9	2.9	1.9
BLC	720	0.0	0.2	1.8	2.7	3.6	11.0	13.5	3.0	1.9
GBM	720	0.1	0.5	1.7	2.4	3.4	6.7	9.7	2.7	1.4
MN3	720	0.0	0.2	1.4	2.1	2.9	7.5	8.7	2.3	1.5
MYJ	720	0.2	0.5	2.0	2.7	3.7	11.8	14.7	3.2	2.0
SHG	720	0.2	0.6	1.7	2.4	3.3	7.4	10.2	2.7	1.5
YSU	720	0.0	0.5	1.6	2.4	3.3	8.3	11.0	2.7	1.6

Wind speed in October 2016 at Fagagna										
	# samples	min	1st perc	25th perc	median	75th perc	99th perc	max	mean	STD
mea	744	0.2	0.3	1.6	2.6	4.2	6.8	8.5	2.9	1.6
ACM2	744	0.0	0.0	1.5	2.3	3.4	9.2	11.0	2.8	2.0
BLC	744	0.1	0.3	1.6	2.6	4.0	10.0	12.2	3.2	2.2
GBM	744	0.1	0.2	1.3	2.1	3.2	9.5	11.7	2.5	1.8
MN3	744	0.0	0.2	1.4	2.3	3.5	9.1	14.3	2.7	2.0
MYJ	744	0.1	0.3	1.6	2.6	3.8	8.0	10.0	2.9	1.7
SHG	744	0.1	0.4	1.5	2.3	3.4	8.4	10.8	2.7	1.7
YSU	744	0.1	0.3	1.5	2.3	3.7	10.0	11.5	2.9	2.0

Wind speed in November 2016 at Fagagna										
	# samples	min	1st perc	25th perc	median	75th perc	99th perc	max	mean	STD
mea	720	0.1	0.3	1.5	2.7	4.2	8.3	10.2	3.0	1.9
ACM2	720	0.0	0.1	1.9	2.5	3.3	8.1	10.1	2.9	1.7
BLC	720	0.1	0.3	2.2	3.0	4.3	10.9	15.4	3.6	2.3
GBM	720	0.1	0.3	1.7	2.6	3.5	10.0	11.5	3.0	1.9
MN3	720	0.1	0.4	1.8	2.9	3.9	10.1	14.2	3.2	2.0
MYJ	720	0.2	0.5	2.1	3.1	4.3	11.3	14.7	3.7	2.4
SHG	720	0.2	0.4	1.7	2.6	3.8	10.6	12.1	3.2	2.2
YSU	720	0.1	0.4	1.6	2.6	3.6	10.6	12.3	3.1	2.2

Wind speed in December 2016 at Fagagna										
	# samples	min	1st perc	25th perc	median	75th perc	99th perc	max	mean	STD
mea	744	0.0	0.3	1.9	3.8	5.5	7.4	8.0	3.8	2.0
ACM2	744	0.0	0.0	0.8	1.6	2.7	6.7	8.7	1.9	1.5
BLC	744	0.1	0.2	1.4	2.2	3.0	8.6	13.0	2.4	1.6
GBM	744	0.0	0.2	1.1	1.7	2.4	7.0	10.4	1.9	1.3
MN3	744	0.1	0.3	1.1	1.9	2.7	5.9	9.7	2.0	1.2
MYJ	744	0.1	0.2	1.4	2.1	2.9	5.3	10.3	2.2	1.1
SHG	744	0.0	0.3	1.2	1.9	2.5	7.0	8.7	2.0	1.3
YSU	744	0.1	0.3	1.2	1.9	2.5	6.2	7.4	2.0	1.2

Wind speed in 2016 at Fossalon di Grado										
	# samples	min	1st perc	25th perc	median	75th perc	99th perc	max	mean	STD
mea	8784.0	0.0	0.3	1.4	2.2	3.8	9.8	18.9	2.9	2.1
ACM2	8784.0	0.0	0.1	1.9	2.8	4.5	12.7	15.8	3.6	2.8
BLC	8784.0	0.0	0.5	2.3	3.4	5.5	15.3	18.9	4.5	3.2
GBM	8784.0	0.0	0.4	2.0	3.1	5.0	13.6	18.1	3.9	2.9
MN3	8784.0	0.0	0.4	1.9	2.9	5.0	14.6	21.5	3.9	3.1
MYJ	8784.0	0.1	0.6	2.4	3.4	5.6	16.2	22.7	4.5	3.4
SHG	8784.0	0.1	0.4	1.9	3.0	5.0	14.1	19.1	3.9	3.0
YSU	8784.0	0.0	0.5	1.9	3.0	4.9	14.8	20.5	3.9	3.1

Wind speed in January 2016 at Fossalon di Grado										
	# samples	min	1st perc	25th perc	median	75th perc	99th perc	max	mean	STD
mea	744	0.0	0.1	1.0	1.5	2.4	10.3	13.1	2.1	2.0
ACM2	744	0.0	0.0	1.4	2.2	3.3	11.0	11.9	2.8	2.3
BLC	744	0.0	0.3	1.6	2.5	3.7	13.2	17.7	3.3	2.7
GBM	744	0.1	0.3	1.5	2.3	4.3	12.0	13.6	3.3	2.7
MN3	744	0.0	0.3	1.7	2.6	4.5	12.6	15.2	3.7	2.9
MYJ	744	0.3	0.5	1.8	2.8	4.5	14.1	15.1	3.8	3.0
SHG	744	0.1	0.4	1.6	2.3	3.7	13.1	13.5	3.3	2.8
YSU	744	0.1	0.4	1.6	2.4	3.8	12.9	14.1	3.4	2.8

Wind speed in February 2016 at Fossalon di Grado										
	# samples	min	1st perc	25th perc	median	75th perc	99th perc	max	mean	STD
mea	696	0.0	0.1	1.4	2.5	4.5	12.9	18.9	3.3	2.8
ACM2	696	0.0	0.0	1.8	2.8	5.4	13.5	15.8	4.1	3.4
BLC	696	0.3	0.4	2.5	3.9	9.6	17.5	18.9	5.9	4.5
GBM	696	0.1	0.4	2.1	3.5	8.5	14.9	15.9	5.2	4.0
MN3	696	0.2	0.4	2.3	3.5	7.9	16.2	18.4	5.3	4.2
MYJ	696	0.2	0.7	2.4	3.8	9.2	17.8	18.5	5.8	4.6
SHG	696	0.1	0.5	2.0	3.3	8.3	15.9	17.7	5.1	4.2
YSU	696	0.1	0.5	2.0	3.3	8.3	16.7	18.8	5.2	4.3

Wind speed in March 2016 at Fossalon di Grado										
	# samples	min	1st perc	25th perc	median	75th perc	99th perc	max	mean	STD
mea	744	0.0	0.3	1.8	3.2	5.6	11.4	13.6	3.9	2.7
ACM2	744	0.0	0.3	2.2	3.3	7.9	13.3	15.7	5.0	3.7
BLC	744	0.3	0.6	2.7	4.2	8.7	17.0	18.1	6.0	4.3
GBM	744	0.2	0.6	2.6	4.5	9.2	14.8	16.5	5.8	4.0
MN3	744	0.1	0.2	2.0	3.4	7.0	15.0	15.9	4.8	3.8
MYJ	744	0.2	0.6	2.6	3.9	8.7	21.8	22.7	6.1	5.0
SHG	744	0.2	0.6	2.3	3.7	7.2	14.6	18.6	5.0	3.5
YSU	744	0.2	0.6	2.3	3.6	7.7	17.0	20.5	5.4	4.4

Wind speed in April 2016 at Fossalon di Grado										
	# samples	min	1st perc	25th perc	median	75th perc	99th perc	max	mean	STD
mea	720	0.1	0.3	1.6	2.5	4.3	9.5	12.3	3.2	2.2
ACM2	720	0.0	0.2	2.3	3.2	4.9	9.6	10.2	3.8	2.2
BLC	720	0.2	0.4	2.4	3.5	5.1	9.9	11.4	3.9	2.1
GBM	720	0.1	0.3	1.9	3.2	4.8	8.7	9.3	3.5	2.0
MN3	720	0.2	0.4	1.8	2.9	5.2	11.4	12.7	3.7	2.5
MYJ	720	0.1	0.5	2.1	3.3	5.1	10.5	11.7	3.9	2.4
SHG	720	0.1	0.4	1.8	2.8	4.6	8.8	9.7	3.4	2.1
YSU	720	0.1	0.4	2.0	3.1	4.8	8.7	9.7	3.5	2.0

Wind speed in May 2016 at Fossalon di Grado										
	# samples	min	1st perc	25th perc	median	75th perc	99th perc	max	mean	STD
mea	744	0.0	0.4	1.6	2.4	3.7	8.0	12.6	2.9	1.8
ACM2	744	0.0	0.1	2.0	3.0	4.2	9.7	11.0	3.4	2.2
BLC	744	0.2	0.7	2.4	3.5	5.2	10.9	12.0	4.1	2.4
GBM	744	0.0	0.4	2.0	3.1	4.7	10.0	11.2	3.6	2.1
MN3	744	0.0	0.3	2.1	3.4	5.3	11.6	17.5	4.0	2.6
MYJ	744	0.1	0.5	2.4	3.5	5.5	11.9	16.2	4.2	2.6
SHG	744	0.1	0.3	1.9	2.8	4.3	9.9	12.0	3.4	2.1
YSU	744	0.1	0.4	1.8	2.8	4.4	9.9	11.5	3.3	2.2

Wind speed in June 2016 at Fossalon di Grado										
	# samples	min	1st perc	25th perc	median	75th perc	99th perc	max	mean	STD
mea	720	0.1	0.4	1.5	2.3	3.6	7.4	9.2	2.7	1.6
ACM2	720	0.0	0.1	2.0	2.9	4.3	9.9	12.1	3.4	2.1
BLC	720	0.2	0.7	2.3	3.4	5.5	11.4	12.9	4.2	2.6
GBM	720	0.1	0.4	1.9	2.9	4.3	9.0	10.3	3.3	1.9
MN3	720	0.1	0.3	1.8	2.7	4.0	11.2	14.9	3.3	2.3
MYJ	720	0.3	0.8	2.5	3.7	5.8	12.2	13.2	4.4	2.5
SHG	720	0.1	0.5	2.1	3.3	5.1	9.4	11.3	3.8	2.2
YSU	720	0.1	0.5	1.9	3.0	4.6	9.6	11.4	3.5	2.1

Wind speed in July 2016 at Fossalon di Grado										
	# samples	min	1st perc	25th perc	median	75th perc	99th perc	max	mean	STD
mea	744	0.1	0.3	1.5	2.2	3.4	8.0	9.7	2.7	1.7
ACM2	744	0.0	0.1	1.8	2.5	3.4	7.8	8.4	2.8	1.7
BLC	744	0.2	0.5	2.3	3.1	4.7	9.9	12.8	3.7	2.1
GBM	744	0.2	0.4	1.8	2.7	4.2	8.2	10.2	3.2	1.9
MN3	744	0.1	0.5	1.8	2.6	3.9	10.4	13.1	3.2	2.2
MYJ	744	0.1	0.5	2.3	3.2	4.9	10.9	11.8	3.8	2.2
SHG	744	0.1	0.4	1.8	2.7	4.0	9.0	11.7	3.2	1.9
YSU	744	0.2	0.5	1.8	2.6	4.0	9.5	12.4	3.2	1.9

Wind speed in August 2016 at Fossalon di Grado										
	# samples	min	1st perc	25th perc	median	75th perc	99th perc	max	mean	STD
mea	744	0.0	0.5	1.6	2.5	4.2	8.2	9.6	3.1	1.8
ACM2	744	0.0	0.1	1.8	2.8	4.2	10.0	13.0	3.3	2.1
BLC	744	0.3	1.0	2.8	4.0	6.2	11.5	13.6	4.7	2.7
GBM	744	0.2	0.5	2.2	3.5	5.2	9.3	10.1	3.9	2.2
MN3	744	0.1	0.5	2.0	2.7	4.2	10.4	11.6	3.3	2.1
MYJ	744	0.2	1.2	2.6	3.6	6.0	11.3	12.8	4.5	2.5
SHG	744	0.3	0.6	2.2	3.4	4.9	9.7	10.9	3.8	2.0
YSU	744	0.2	0.5	2.1	3.3	4.9	10.1	11.6	3.8	2.3

Wind speed in September 2016 at Fossalon di Grado										
	# samples	min	1st perc	25th perc	median	75th perc	99th perc	max	mean	STD
mea	720	0.1	0.4	1.5	2.2	3.5	7.3	9.5	2.6	1.5
ACM2	720	0.0	0.1	2.2	2.9	3.9	9.0	10.5	3.3	1.8
BLC	720	0.3	0.6	2.5	3.3	4.8	11.0	12.9	3.9	2.2
GBM	720	0.2	0.6	2.1	3.0	4.3	8.1	9.5	3.3	1.8
MN3	720	0.0	0.3	1.8	2.7	3.8	10.3	11.6	3.2	2.1
MYJ	720	0.3	0.9	2.7	3.4	5.0	11.6	15.4	4.0	2.1
SHG	720	0.2	0.6	2.2	2.9	4.1	8.9	11.3	3.4	1.8
YSU	720	0.3	0.6	2.2	3.0	4.1	9.5	11.5	3.4	1.8

Wind speed in October 2016 at Fossalon di Grado										
	# samples	min	1st perc	25th perc	median	75th perc	99th perc	max	mean	STD
mea	744	0.0	0.2	1.6	2.5	4.1	8.2	9.7	3.0	1.8
ACM2	744	0.0	0.0	1.8	3.0	5.4	13.6	15.4	4.1	3.3
BLC	744	0.3	0.7	2.3	3.4	6.0	15.4	16.1	4.9	3.9
GBM	744	0.0	0.4	1.9	3.1	4.8	12.5	13.8	3.8	2.8
MN3	744	0.0	0.3	1.6	2.7	5.4	15.1	17.2	4.0	3.5
MYJ	744	0.1	0.5	2.1	3.4	5.8	15.2	15.8	4.5	3.3
SHG	744	0.2	0.4	2.0	3.1	5.4	14.3	17.7	4.2	3.3
YSU	744	0.0	0.5	1.8	2.9	5.8	14.4	15.1	4.3	3.5

Wind speed in November 2016 at Fossalon di Grado										
	# samples	min	1st perc	25th perc	median	75th perc	99th perc	max	mean	STD
mea	720	0.0	0.2	1.2	1.8	3.8	10.9	14.3	2.9	2.6
ACM2	720	0.0	0.1	1.9	2.9	5.9	14.3	15.1	4.3	3.5
BLC	720	0.2	0.7	2.7	4.0	8.1	16.0	16.3	5.7	4.1
GBM	720	0.2	0.5	2.1	3.5	7.6	17.5	18.1	5.1	4.1
MN3	720	0.2	0.5	2.1	3.2	6.8	19.5	21.5	5.0	4.3
MYJ	720	0.4	0.7	2.7	4.0	8.0	19.9	21.0	5.7	4.5
SHG	720	0.1	0.5	2.0	3.2	7.7	18.7	19.1	5.2	4.5
YSU	720	0.3	0.4	2.0	3.3	6.6	19.2	19.9	4.9	4.1

Wind speed in December 2016 at Fossalon di Grado										
	# samples	min	1st perc	25th perc	median	75th perc	99th perc	max	mean	STD
mea	744	0.0	0.2	1.3	1.9	3.1	7.3	10.2	2.4	1.6
ACM2	744	0.0	0.0	1.5	2.3	4.4	12.4	13.0	3.5	3.0
BLC	744	0.2	0.5	2.1	2.8	4.0	9.8	11.5	3.3	1.9
GBM	744	0.0	0.2	1.8	2.6	4.1	10.2	10.7	3.3	2.2
MN3	744	0.1	0.6	2.1	2.8	4.8	11.3	12.4	3.7	2.6
MYJ	744	0.1	0.5	2.1	3.0	4.2	11.2	13.4	3.6	2.3
SHG	744	0.2	0.4	1.8	2.5	4.5	11.6	12.2	3.6	2.6
YSU	744	0.2	0.4	1.8	2.5	4.6	11.0	12.0	3.6	2.6

Wind speed in January 2016 at the Paloma buoy										
	# samples	min	1st perc	25th perc	median	75th perc	99th perc	max	mean	STD
mea	175	0.0	0.0	0.7	1.9	4.8	16.8	17.4	3.6	4.6
ACM2	175	0.4	0.5	1.9	2.9	4.6	14.1	14.9	3.7	2.9
BLC	175	0.3	0.6	1.8	3.5	4.7	15.3	15.9	4.1	3.3
GBM	175	0.1	0.3	1.8	3.0	4.7	14.4	15.7	3.9	3.4
MN3	175	0.1	0.3	1.1	2.5	4.4	14.0	14.6	3.5	3.3
MYJ	175	0.2	0.5	1.8	3.3	5.0	14.6	15.0	4.0	3.1
SHG	175	0.4	0.4	1.8	3.2	5.0	15.0	16.1	4.2	3.5
YSU	175	0.2	0.5	1.8	3.3	5.4	15.9	16.9	4.3	3.6

Wind speed in February 2016 at the Paloma buoy										
	# samples	min	1st perc	25th perc	median	75th perc	99th perc	max	mean	STD
mea	695	0.0	0.0	2.2	4.2	7.2	16.5	18.4	5.1	3.8
ACM2	695	0.0	0.5	2.6	4.3	8.8	15.7	17.5	5.7	4.1
BLC	695	0.1	0.5	2.7	4.9	9.7	19.1	20.0	6.4	4.6
GBM	695	0.3	0.7	3.0	5.2	10.0	18.1	19.2	6.6	4.5
MN3	695	0.1	0.8	2.6	4.9	8.7	15.8	17.7	5.9	4.0
MYJ	695	0.1	0.5	2.7	4.9	10.1	17.5	18.7	6.6	4.7
SHG	695	0.3	0.5	2.8	5.0	10.4	18.0	20.0	6.7	4.8
YSU	695	0.1	0.5	2.7	5.1	9.9	20.1	21.2	6.7	4.9

Wind speed in March 2016 at the Paloma buoy										
	# samples	min	1st perc	25th perc	median	75th perc	99th perc	max	mean	STD
mea	744	0.0	0.0	2.6	4.8	8.3	15.5	17.0	5.6	3.9
ACM2	744	0.1	0.6	2.7	5.8	11.1	17.9	18.8	7.1	4.9
BLC	744	0.0	0.4	2.7	5.0	10.0	17.4	18.8	6.5	4.6
GBM	744	0.1	0.6	3.0	5.6	11.5	19.0	21.9	7.3	5.1
MN3	744	0.0	0.2	2.1	4.4	8.6	19.0	19.5	5.7	4.5
MYJ	744	0.2	0.5	2.5	5.1	10.6	21.6	22.6	6.9	5.5
SHG	744	0.1	0.4	2.6	5.2	9.7	20.4	24.6	6.6	5.0
YSU	744	0.0	0.4	2.6	5.5	11.0	23.4	25.1	7.3	5.9

Wind speed in April 2016 at the Paloma buoy										
	# samples	min	1st perc	25th perc	median	75th perc	99th perc	max	mean	STD
mea	720	0.0	0.0	2.1	3.7	5.7	13.2	16.3	4.4	3.2
ACM2	720	0.0	0.4	2.7	4.4	7.2	12.6	14.0	5.0	2.9
BLC	720	0.1	0.3	2.2	3.9	6.0	11.9	13.7	4.3	2.6
GBM	720	0.1	0.4	2.1	3.8	6.0	11.1	14.0	4.2	2.5
MN3	720	0.0	0.4	1.8	3.2	5.8	12.1	12.9	4.0	2.8
MYJ	720	0.1	0.3	2.0	3.5	6.0	12.2	14.2	4.2	2.8
SHG	720	0.1	0.3	1.7	3.1	5.8	13.5	15.0	4.0	2.9
YSU	720	0.1	0.3	1.9	3.6	6.0	12.1	14.6	4.2	2.8

Wind speed in May 2016 at the Paloma buoy										
	# samples	min	1st perc	25th perc	median	75th perc	99th perc	max	mean	STD
mea	744	0.0	0.0	1.8	3.4	5.7	10.7	13.1	3.9	2.7
ACM2	744	0.1	0.4	2.6	4.2	5.9	14.7	18.1	4.7	3.0
BLC	744	0.2	0.3	2.1	3.9	6.4	12.4	13.9	4.4	3.0
GBM	744	0.2	0.5	2.2	3.8	6.2	12.6	14.5	4.4	2.8
MN3	744	0.1	0.5	2.2	4.1	6.7	15.7	19.1	4.8	3.3
MYJ	744	0.0	0.3	2.2	3.7	6.4	13.8	18.2	4.5	3.1
SHG	744	0.2	0.4	1.8	3.5	5.7	13.5	15.8	4.1	2.9
YSU	744	0.2	0.3	1.9	3.5	5.9	14.1	18.9	4.3	3.1

Wind speed in June 2016 at the Paloma buoy										
	# samples	min	1st perc	25th perc	median	75th perc	99th perc	max	mean	STD
mea	720	0.0	0.0	1.9	3.3	5.5	9.9	12.5	3.8	2.5
ACM2	720	0.1	0.3	2.4	4.3	6.2	11.9	14.9	4.6	2.8
BLC	720	0.0	0.4	2.2	3.8	6.2	12.9	15.5	4.5	3.0
GBM	720	0.2	0.4	2.2	3.6	4.9	11.1	13.0	4.0	2.5
MN3	720	0.1	0.3	1.9	3.1	5.4	11.8	13.8	3.8	2.6
MYJ	720	0.2	0.5	2.8	4.2	6.3	12.9	13.9	4.8	2.7
SHG	720	0.1	0.4	2.5	4.4	6.6	13.1	14.6	4.8	2.9
YSU	720	0.1	0.5	2.2	3.8	6.5	13.0	15.5	4.5	3.0

Wind speed in July 2016 at the Paloma buoy										
	# samples	min	1st perc	25th perc	median	75th perc	99th perc	max	mean	STD
mea	744	0.0	0.0	1.4	2.6	4.5	11.9	13.5	3.4	2.7
ACM2	744	0.2	0.5	2.1	3.3	5.0	10.6	15.8	3.8	2.3
BLC	744	0.2	0.4	2.0	3.2	5.3	10.8	12.6	3.9	2.5
GBM	744	0.1	0.5	2.0	3.4	5.7	11.2	12.0	4.1	2.7
MN3	744	0.0	0.3	1.5	2.7	4.5	11.8	14.4	3.4	2.5
MYJ	744	0.2	0.3	1.8	3.1	5.0	12.7	17.1	3.8	2.7
SHG	744	0.1	0.3	1.9	3.5	5.3	11.9	13.7	4.0	2.7
YSU	744	0.0	0.4	1.9	3.2	5.3	12.6	15.4	3.9	2.7

Wind speed in August 2016 at the Paloma buoy										
	# samples	min	1st perc	25th perc	median	75th perc	99th perc	max	mean	STD
mea	744	0.0	0.0	1.8	3.5	5.6	12.5	14.3	3.9	2.7
ACM2	744	0.1	0.4	2.0	3.5	5.6	13.5	15.3	4.4	3.2
BLC	744	0.2	0.6	2.8	4.5	7.7	13.6	15.7	5.4	3.4
GBM	744	0.1	0.5	2.5	4.5	6.5	13.0	14.3	5.0	3.1
MN3	744	0.1	0.3	2.1	3.5	6.0	12.4	14.1	4.3	2.9
MYJ	744	0.1	0.5	2.4	4.2	6.6	14.0	18.0	5.0	3.3
SHG	744	0.3	0.6	2.6	4.5	6.8	13.8	15.3	5.1	3.2
YSU	744	0.0	0.5	2.7	4.7	7.2	13.6	15.4	5.3	3.4

Wind speed in September 2016 at the Paloma buoy										
	# samples	min	1st perc	25th perc	median	75th perc	99th perc	max	mean	STD
mea	720	0.0	0.2	1.7	2.9	4.4	9.7	10.9	3.3	2.1
ACM2	720	0.0	0.5	2.5	3.8	5.7	13.7	14.6	4.5	2.9
BLC	720	0.0	0.3	2.2	3.7	5.7	13.6	16.7	4.3	2.9
GBM	720	0.1	0.4	2.3	3.9	5.9	12.2	14.1	4.4	2.8
MN3	720	0.1	0.3	2.1	3.5	5.4	12.2	13.4	4.2	2.8
MYJ	720	0.1	0.4	2.3	3.8	5.7	13.2	17.1	4.4	3.0
SHG	720	0.0	0.4	2.4	4.0	6.2	13.5	14.7	4.6	3.0
YSU	720	0.1	0.3	2.4	4.0	5.9	13.3	15.4	4.5	2.9

Wind speed in October 2016 at the Paloma buoy										
	# samples	min	1st perc	25th perc	median	75th perc	99th perc	max	mean	STD
mea	744	0.0	0.1	2.2	4.1	7.3	12.7	14.2	4.9	3.3
ACM2	744	0.2	0.4	2.3	4.2	8.7	16.7	18.3	5.7	4.4
BLC	744	0.1	0.3	2.0	4.4	7.3	16.7	17.4	5.4	4.2
GBM	744	0.1	0.2	2.3	4.0	6.6	16.4	16.9	5.0	3.7
MN3	744	0.1	0.2	1.6	3.1	7.1	15.8	17.4	4.6	3.8
MYJ	744	0.1	0.4	2.1	4.6	7.6	15.1	16.5	5.3	3.9
SHG	744	0.1	0.3	2.6	4.5	8.1	16.3	20.4	5.7	4.1
YSU	744	0.1	0.4	2.3	4.4	8.7	16.9	17.8	5.8	4.5

Wind speed in November 2016 at the Paloma buoy										
	# samples	min	1st perc	25th perc	median	75th perc	99th perc	max	mean	STD
mea	521	0.0	0.1	2.1	3.8	8.8	13.7	14.9	5.2	3.8
ACM2	521	0.2	0.5	2.9	5.0	8.3	16.7	17.1	5.9	3.9
BLC	521	0.2	0.4	3.6	6.1	9.2	16.8	17.4	6.8	4.2
GBM	521	0.4	0.7	3.9	6.0	9.8	20.0	20.3	7.4	4.9
MN3	521	0.2	0.3	2.7	4.9	8.2	18.5	18.9	5.9	4.3
MYJ	521	0.2	0.5	3.2	5.4	7.7	19.8	20.4	6.3	4.5
SHG	521	0.4	0.7	3.4	5.5	9.6	19.8	21.0	7.0	4.7
YSU	521	0.1	0.7	3.4	5.8	9.2	21.2	22.2	6.9	4.7

Wind speed in 2016 at Enemonzo										
	# samples	min	1st perc	25th perc	median	75th perc	99th perc	max	mean	STD
mea	8748	0.0	0.1	0.6	0.9	1.4	4.6	6.8	1.2	0.9
ACM2	8748	0.0	0.0	0.2	0.8	1.8	6.1	11.5	1.2	1.3
BLC	8748	0.0	0.1	0.7	1.3	2.2	10.4	16.0	1.9	2.0
GBM	8748	0.0	0.1	0.5	1.1	2.1	6.3	10.3	1.5	1.4
MN3	8748	0.0	0.0	0.6	1.1	2.3	6.5	10.5	1.7	1.5
MYJ	8748	0.0	0.1	0.7	1.3	2.4	7.8	14.7	1.9	1.7
SHG	8748	0.0	0.1	0.6	1.2	2.2	6.2	10.4	1.6	1.3
YSU	8748	0.0	0.1	0.6	1.2	2.2	6.1	10.1	1.6	1.3

Wind speed in January 2016 at Enemonzo										
	# samples	min	1st perc	25th perc	median	75th perc	99th perc	max	mean	STD
mea	725	0.0	0.0	0.6	0.9	1.2	2.8	4.5	1.0	0.6
ACM2	725	0.0	0.0	0.1	0.7	2.1	7.6	10.1	1.3	1.6
BLC	725	0.1	0.1	0.6	1.1	2.0	12.3	15.6	1.8	2.3
GBM	725	0.0	0.1	0.5	1.1	2.3	6.8	10.2	1.6	1.5
MN3	725	0.0	0.1	0.6	1.2	2.2	8.8	10.5	1.8	1.7
MYJ	725	0.0	0.1	0.7	1.1	2.2	9.8	13.4	1.7	1.7
SHG	725	0.0	0.1	0.7	1.4	2.5	5.1	8.1	1.6	1.2
YSU	725	0.1	0.1	0.6	1.4	2.4	6.3	10.1	1.7	1.4

Wind speed in February 2016 at Enemonzo										
	# samples	min	1st perc	25th perc	median	75th perc	99th perc	max	mean	STD
mea	696	0.0	0.0	0.4	0.7	1.1	3.4	5.0	0.9	0.7
ACM2	696	0.0	0.0	0.4	1.4	2.5	6.0	7.3	1.6	1.4
BLC	696	0.0	0.1	0.9	1.5	2.9	10.3	13.6	2.2	2.0
GBM	696	0.0	0.2	0.8	1.4	2.6	5.8	8.5	1.8	1.4
MN3	696	0.0	0.1	0.9	1.5	2.9	6.4	9.0	2.0	1.5
MYJ	696	0.1	0.2	0.9	1.7	2.9	6.5	9.0	2.1	1.5
SHG	696	0.1	0.1	0.9	1.7	2.7	5.1	5.8	1.9	1.2
YSU	696	0.0	0.2	0.9	1.7	2.6	5.2	7.0	1.9	1.2

Wind speed in March 2016 at Enemonzo										
	# samples	min	1st perc	25th perc	median	75th perc	99th perc	max	mean	STD
mea	727	0.0	0.1	0.6	1.0	1.6	5.2	6.5	1.3	1.1
ACM2	727	0.0	0.0	0.3	1.1	2.4	6.3	11.5	1.6	1.6
BLC	727	0.0	0.1	0.7	1.2	2.0	11.1	13.5	2.0	2.3
GBM	727	0.0	0.1	0.7	1.3	2.2	7.9	9.5	1.6	1.4
MN3	727	0.0	0.1	0.7	1.4	2.6	6.3	9.8	1.8	1.5
MYJ	727	0.1	0.1	0.9	1.5	2.3	5.9	7.6	1.8	1.3
SHG	727	0.1	0.1	0.7	1.3	2.1	4.6	6.5	1.5	1.0
YSU	727	0.1	0.2	0.9	1.5	2.4	5.7	7.1	1.8	1.2

Wind speed in April 2016 at Enemonzo										
	# samples	min	1st perc	25th perc	median	75th perc	99th perc	max	mean	STD
mea	720	0.0	0.1	0.7	1.1	1.8	5.5	6.8	1.5	1.2
ACM2	720	0.0	0.0	0.4	1.2	2.1	4.9	6.2	1.4	1.2
BLC	720	0.0	0.2	0.9	1.5	2.5	8.5	11.5	2.1	1.8
GBM	720	0.0	0.1	0.6	1.2	2.1	6.6	7.9	1.6	1.4
MN3	720	0.0	0.0	0.7	1.3	2.6	6.4	8.7	1.8	1.5
MYJ	720	0.0	0.2	0.8	1.5	2.7	7.9	8.8	2.0	1.7
SHG	720	0.0	0.1	0.7	1.4	2.3	6.0	6.9	1.7	1.2
YSU	720	0.0	0.1	0.7	1.3	2.2	6.1	7.2	1.6	1.2

Wind speed in May 2016 at Enemonzo										
	# samples	min	1st perc	25th perc	median	75th perc	99th perc	max	mean	STD
mea	744	0.0	0.1	0.6	1.0	1.6	5.2	6.5	1.3	1.0
ACM2	744	0.0	0.0	0.4	1.3	2.3	6.9	10.4	1.6	1.5
BLC	744	0.1	0.1	1.0	1.8	3.5	12.0	14.7	2.8	2.7
GBM	744	0.0	0.1	0.8	1.6	2.9	8.5	9.6	2.1	1.7
MN3	744	0.0	0.1	0.8	1.6	3.2	7.1	8.0	2.1	1.7
MYJ	744	0.1	0.2	1.0	1.8	3.8	13.2	14.7	2.8	2.6
SHG	744	0.1	0.1	0.9	1.7	3.0	9.4	10.4	2.3	2.0
YSU	744	0.0	0.1	0.8	1.5	2.5	8.1	9.5	1.9	1.6

Wind speed in June 2016 at Enemonzo										
	# samples	min	1st perc	25th perc	median	75th perc	99th perc	max	mean	STD
mea	720	0.0	0.1	0.6	1.0	1.6	4.6	5.9	1.3	1.0
ACM2	720	0.0	0.0	0.3	0.9	1.7	4.8	7.0	1.2	1.1
BLC	720	0.1	0.1	0.9	1.4	2.3	7.8	10.3	1.9	1.7
GBM	720	0.0	0.1	0.6	1.1	2.1	5.3	6.6	1.5	1.2
MN3	720	0.0	0.0	0.5	1.1	2.2	5.5	7.9	1.6	1.4
MYJ	720	0.1	0.1	0.8	1.4	2.7	7.5	9.9	2.0	1.6
SHG	720	0.0	0.1	0.7	1.2	2.1	6.3	7.1	1.6	1.2
YSU	720	0.1	0.1	0.7	1.2	2.1	5.4	7.4	1.6	1.2

Wind speed in July 2016 at Enemonzo										
	# samples	min	1st perc	25th perc	median	75th perc	99th perc	max	mean	STD
mea	744	0.0	0.2	0.7	1.1	1.7	4.4	5.3	1.3	0.9
ACM2	744	0.0	0.0	0.2	0.8	1.6	7.9	9.8	1.2	1.4
BLC	744	0.0	0.1	0.8	1.4	2.3	9.3	10.4	1.9	1.8
GBM	744	0.0	0.1	0.5	1.1	2.2	8.0	8.8	1.6	1.5
MN3	744	0.0	0.0	0.6	1.3	3.0	6.4	7.2	1.9	1.6
MYJ	744	0.0	0.2	0.8	1.5	2.9	8.1	10.2	2.1	1.8
SHG	744	0.0	0.1	0.6	1.2	2.2	5.3	7.1	1.6	1.3
YSU	744	0.0	0.1	0.6	1.2	2.1	6.7	8.7	1.6	1.4

Wind speed in August 2016 at Enemonzo										
	# samples	min	1st perc	25th perc	median	75th perc	99th perc	max	mean	STD
mea	744	0.0	0.1	0.7	1.1	1.8	4.3	5.3	1.4	1.0
ACM2	744	0.0	0.0	0.1	0.5	1.2	3.4	6.2	0.8	0.9
BLC	744	0.0	0.1	0.7	1.2	2.2	8.0	9.4	1.7	1.5
GBM	744	0.0	0.1	0.5	1.0	1.9	4.9	6.8	1.3	1.1
MN3	744	0.0	0.0	0.5	0.9	2.3	5.1	5.4	1.5	1.4
MYJ	744	0.1	0.2	0.7	1.3	2.3	5.4	9.2	1.7	1.3
SHG	744	0.1	0.1	0.6	1.1	2.0	4.2	6.4	1.4	1.0
YSU	744	0.0	0.1	0.6	1.1	1.9	4.8	9.3	1.4	1.0

Wind speed in September 2016 at Enemonzo										
	# samples	min	1st perc	25th perc	median	75th perc	99th perc	max	mean	STD
mea	720	0.0	0.1	0.7	1.0	1.4	4.0	5.0	1.2	0.8
ACM2	720	0.0	0.0	0.2	0.7	1.6	7.9	9.4	1.1	1.5
BLC	720	0.0	0.0	0.7	1.2	2.0	8.2	12.1	1.7	1.6
GBM	720	0.0	0.1	0.5	0.9	1.7	6.8	10.3	1.3	1.3
MN3	720	0.0	0.0	0.5	1.0	2.3	5.2	9.4	1.5	1.4
MYJ	720	0.0	0.1	0.7	1.2	2.3	8.8	11.7	1.8	1.7
SHG	720	0.0	0.1	0.6	1.0	1.8	6.3	8.9	1.4	1.2
YSU	720	0.0	0.1	0.6	1.0	1.7	6.0	8.7	1.3	1.1

Wind speed in October 2016 at Enemonzo										
	# samples	min	1st perc	25th perc	median	75th perc	99th perc	max	mean	STD
mea	744	0.0	0.0	0.5	0.8	1.2	3.5	4.6	0.9	0.7
ACM2	744	0.0	0.0	0.1	0.6	1.5	5.2	7.7	1.0	1.2
BLC	744	0.0	0.2	0.7	1.1	1.9	8.7	11.2	1.6	1.6
GBM	744	0.0	0.1	0.5	0.9	2.1	4.4	5.7	1.3	1.1
MN3	744	0.0	0.0	0.5	0.9	2.1	6.6	7.6	1.6	1.6
MYJ	744	0.0	0.2	0.7	1.2	2.1	6.5	7.7	1.7	1.5
SHG	744	0.0	0.1	0.6	1.2	2.3	5.5	8.3	1.6	1.2
YSU	744	0.0	0.1	0.6	1.1	2.3	5.0	5.9	1.5	1.2

Wind speed in November 2016 at Enemonzo										
	# samples	min	1st perc	25th perc	median	75th perc	99th perc	max	mean	STD
mea	720	0.0	0.0	0.4	0.7	1.0	3.8	4.9	0.8	0.7
ACM2	720	0.0	0.0	0.1	0.6	1.8	5.3	7.4	1.1	1.2
BLC	720	0.0	0.1	0.6	1.1	1.8	11.7	16.0	1.8	2.1
GBM	720	0.0	0.1	0.5	1.0	2.0	5.4	8.0	1.4	1.2
MN3	720	0.0	0.0	0.6	1.0	1.5	5.6	8.1	1.3	1.2
MYJ	720	0.0	0.1	0.7	1.1	2.0	5.4	6.9	1.5	1.2
SHG	720	0.0	0.1	0.6	1.1	2.1	5.0	7.0	1.5	1.1
YSU	720	0.0	0.1	0.5	1.0	2.0	6.5	7.2	1.4	1.2

Wind speed in December 2016 at Enemonzo										
	# samples	min	1st perc	25th perc	median	75th perc	99th perc	max	mean	STD
mea	744	0.0	0.1	0.7	1.0	1.2	2.9	4.1	1.0	0.5
ACM2	744	0.0	0.0	0.0	0.2	0.9	4.2	5.2	0.7	1.1
BLC	744	0.0	0.1	0.5	0.7	1.4	11.2	13.9	1.5	2.3
GBM	744	0.0	0.0	0.3	0.5	1.2	4.0	7.2	0.9	1.0
MN3	744	0.0	0.1	0.5	0.7	1.2	7.0	10.1	1.1	1.2
MYJ	744	0.0	0.1	0.5	0.8	1.2	4.5	6.2	1.1	0.9
SHG	744	0.0	0.1	0.4	0.6	1.5	5.1	8.7	1.1	1.2
YSU	744	0.0	0.1	0.4	0.6	1.4	6.0	9.2	1.1	1.2

B.3 Precipitations

The tables show the statistical values of the hourly precipitations after null values were excluded. Measurements are not available at the Paloma buoy, therefore no table is shown for that location. All values are expressed in mm/h.

Precipitations in 2016 at Udine										
	# samples	min	1st perc	25th perc	median	75th perc	99th perc	max	mean	STD
mea	871	0.1	0.1	0.2	0.8	2.2	16.1	24.1	1.8	2.9
ACM2	742	0.1	0.1	0.1	0.4	1.4	11.6	27.0	1.3	2.3
BLC	713	0.1	0.1	0.1	0.4	1.2	10.4	24.3	1.1	2.1
GBM	566	0.1	0.1	0.1	0.3	1.0	8.7	21.5	1.0	1.8
MN3	1732	0.1	0.1	0.1	0.4	1.3	14.9	26.8	1.3	2.6
MYJ	602	0.1	0.1	0.1	0.3	1.1	13.7	31.6	1.1	2.6
ShG	718	0.1	0.1	0.1	0.3	1.0	12.2	27.1	1.1	2.3
YSU	602	0.1	0.1	0.1	0.4	1.2	9.9	44.8	1.2	2.9

Precipitations in January 2016 at Udine										
	# samples	min	1st perc	25th perc	median	75th perc	99th perc	max	mean	STD
mea	70	0.1	0.1	0.2	0.7	1.4	5.3	7.7	1.0	1.2
ACM2	70	0.1	0.1	0.2	0.5	1.1	3.5	4.0	0.8	0.9
BLC	79	0.1	0.1	0.1	0.3	1.5	4.8	6.0	0.9	1.2
GBM	64	0.1	0.1	0.2	0.6	1.0	2.3	2.4	0.8	0.7
MN3	78	0.1	0.1	0.1	0.3	0.7	2.5	2.5	0.5	0.6
MYJ	68	0.1	0.1	0.1	0.4	0.9	4.0	4.7	0.8	1.0
ShG	83	0.1	0.1	0.1	0.3	0.9	2.5	2.7	0.6	0.6
YSU	79	0.1	0.1	0.1	0.3	0.7	2.8	2.9	0.6	0.7

Precipitations in February 2016 at Udine										
	# samples	min	1st perc	25th perc	median	75th perc	99th perc	max	mean	STD
mea	172	0.1	0.1	0.3	1.2	3.1	7.7	7.8	1.9	2.0
ACM2	124	0.1	0.1	0.1	0.4	1.3	3.5	3.6	0.8	0.9
BLC	92	0.1	0.1	0.2	0.9	1.4	6.0	6.9	1.2	1.4
GBM	104	0.1	0.1	0.2	0.5	1.3	3.7	6.3	0.9	1.1
MN3	108	0.1	0.1	0.2	0.4	1.3	3.7	3.8	0.8	0.9
MYJ	97	0.1	0.1	0.1	0.3	1.3	3.6	4.1	0.8	0.9
ShG	115	0.1	0.1	0.2	0.4	1.3	3.6	4.7	0.8	0.9
YSU	111	0.1	0.1	0.2	0.5	1.2	3.6	5.0	0.9	1.0

Precipitations in March 2016 at Udine										
	# samples	min	1st perc	25th perc	median	75th perc	99th perc	max	mean	STD
mea	72	0.1	0.1	0.2	0.7	1.8	11.0	12.6	1.5	2.2
ACM2	66	0.1	0.1	0.1	0.4	1.3	4.7	5.2	0.9	1.1
BLC	63	0.1	0.1	0.1	0.4	1.3	8.4	12.6	1.2	2.0
GBM	40	0.1	0.1	0.1	0.2	0.7	4.0	4.3	0.7	1.1
MN3	53	0.1	0.1	0.1	0.2	0.8	2.5	2.5	0.6	0.7
MYJ	43	0.1	0.1	0.1	0.5	0.9	2.8	2.8	0.7	0.8
ShG	38	0.1	0.1	0.1	0.7	1.4	4.0	4.3	1.0	1.1
YSU	37	0.1	0.1	0.2	0.7	1.6	7.1	9.0	1.2	1.6

Precipitations in April 2016 at Udine										
	# samples	min	1st perc	25th perc	median	75th perc	99th perc	max	mean	STD
mea	67	0.1	0.1	0.1	0.6	1.2	5.0	6.3	1.0	1.2
ACM2	84	0.1	0.1	0.2	0.4	1.6	7.2	12.7	1.2	1.8
BLC	64	0.1	0.1	0.3	0.6	1.7	7.3	10.6	1.3	1.8
GBM	54	0.1	0.1	0.1	0.3	0.6	4.3	4.5	0.7	1.1
MN3	83	0.1	0.1	0.1	0.3	1.0	4.2	4.5	0.7	0.9
MYJ	62	0.1	0.1	0.1	0.3	0.5	3.2	3.2	0.6	0.7
ShG	43	0.1	0.1	0.1	0.2	0.5	7.1	9.8	0.8	1.6
YSU	56	0.1	0.1	0.1	0.3	1.1	6.2	7.8	0.9	1.4

Precipitations in May 2016 at Udine										
	# samples	min	1st perc	25th perc	median	75th perc	99th perc	max	mean	STD
mea	100	0.1	0.1	0.4	1.0	2.6	20.2	21.6	2.4	3.8
ACM2	88	0.1	0.1	0.3	0.9	2.2	8.7	10.8	1.8	2.2
BLC	74	0.1	0.1	0.2	0.8	1.5	7.3	9.0	1.2	1.6
GBM	60	0.1	0.1	0.1	0.3	1.1	6.3	7.9	1.0	1.6
MN3	122	0.1	0.1	0.2	1.0	2.7	14.3	26.8	2.1	3.3
MYJ	70	0.1	0.1	0.2	0.6	1.6	22.5	31.6	1.8	4.4
ShG	70	0.1	0.1	0.1	0.3	1.1	10.9	10.9	1.1	2.1
YSU	76	0.1	0.1	0.2	0.6	1.2	10.5	11.3	1.4	2.3

Precipitations in June 2016 at Udine										
	# samples	min	1st perc	25th perc	median	75th perc	99th perc	max	mean	STD
mea	75	0.1	0.1	0.1	0.5	1.6	14.5	18.9	1.6	3.1
ACM2	74	0.1	0.1	0.2	0.7	2.4	14.9	19.9	2.1	3.5
BLC	63	0.1	0.1	0.1	0.3	0.7	12.9	18.8	1.0	2.7
GBM	59	0.1	0.1	0.1	0.3	1.0	7.9	11.4	1.1	1.9
MN3	105	0.1	0.1	0.1	0.4	1.1	13.6	22.1	1.3	2.9
MYJ	48	0.1	0.1	0.1	0.6	2.4	18.0	19.5	2.6	4.6
ShG	78	0.1	0.1	0.1	0.4	1.0	10.4	15.8	1.4	2.6
YSU	68	0.1	0.1	0.2	0.4	1.1	6.7	9.9	1.0	1.5

Precipitations in July 2016 at Udine										
	# samples	min	1st perc	25th perc	median	75th perc	99th perc	max	mean	STD
mea	33	0.1	0.1	0.1	0.2	1.6	22.0	23.2	2.8	5.8
ACM2	31	0.1	0.1	0.1	0.5	2.2	11.6	11.6	2.1	3.4
BLC	42	0.1	0.1	0.2	0.4	1.2	20.2	24.3	1.9	4.4
GBM	27	0.1	0.1	0.2	0.7	2.8	10.6	10.9	1.9	2.8
MN3	93	0.1	0.1	0.1	0.4	1.7	15.0	15.0	2.1	3.6
MYJ	31	0.1	0.1	0.2	0.6	1.8	9.8	11.3	1.8	2.6
ShG	51	0.1	0.1	0.1	0.3	1.2	24.4	27.1	2.2	5.2
YSU	23	0.1	0.1	0.1	0.5	1.7	40.7	44.8	4.3	10.5

Precipitations in August 2016 at Udine										
	# samples	min	1st perc	25th perc	median	75th perc	99th perc	max	mean	STD
mea	41	0.1	0.1	0.2	1.1	2.0	10.5	12.1	1.7	2.4
ACM2	15	0.1	0.1	0.2	0.4	3.0	9.3	9.3	2.4	3.3
BLC	32	0.1	0.1	0.2	0.3	1.7	5.4	6.1	1.1	1.3
GBM	27	0.1	0.1	0.1	0.3	0.9	12.3	13.4	1.5	3.1
MN3	41	0.1	0.1	0.2	0.6	1.6	14.6	16.2	1.9	3.4
MYJ	15	0.1	0.1	0.1	0.3	0.6	3.4	3.5	0.7	1.0
ShG	27	0.1	0.1	0.1	0.3	0.9	9.6	10.7	1.3	2.4
YSU	18	0.1	0.1	0.2	0.7	2.8	8.3	8.5	1.9	2.5

Precipitations in September 2016 at Udine										
	# samples	min	1st perc	25th perc	median	75th perc	99th perc	max	mean	STD
mea	34	0.1	0.1	0.3	1.1	2.8	19.4	19.5	3.3	5.4
ACM2	29	0.1	0.1	0.1	0.2	0.5	5.7	6.0	0.9	1.5
BLC	19	0.1	0.1	0.1	0.2	0.9	18.0	18.9	2.1	5.1
GBM	20	0.1	0.1	0.2	0.2	0.3	18.7	21.5	1.6	4.9
MN3	24	0.1	0.1	0.1	0.9	4.1	18.7	19.6	3.6	5.5
MYJ	21	0.1	0.1	0.1	0.5	0.9	4.3	4.6	0.9	1.2
ShG	20	0.1	0.1	0.1	0.2	0.7	18.3	19.9	2.2	4.9
YSU	19	0.1	0.1	0.1	0.3	0.6	6.5	6.8	1.2	2.0

Precipitations in October 2016 at Udine										
	# samples	min	1st perc	25th perc	median	75th perc	99th perc	max	mean	STD
mea	111	0.1	0.1	0.2	0.4	1.6	5.3	8.1	1.1	1.4
ACM2	76	0.1	0.1	0.2	0.4	0.9	16.8	27.0	1.5	3.9
BLC	101	0.1	0.1	0.1	0.3	0.8	7.5	13.8	0.8	1.7
GBM	64	0.1	0.1	0.1	0.3	0.6	6.7	8.4	0.8	1.5
MN3	74	0.1	0.1	0.1	0.4	1.1	10.8	20.9	1.1	2.7
MYJ	75	0.1	0.1	0.1	0.3	0.8	13.0	28.1	1.2	3.4
ShG	98	0.1	0.1	0.1	0.4	1.5	7.3	13.0	1.2	1.8
YSU	79	0.1	0.1	0.1	0.4	1.1	18.8	32.3	1.5	4.1

Precipitations in November 2016 at Udine										
	# samples	min	1st perc	25th perc	median	75th perc	99th perc	max	mean	STD
mea	96	0.1	0.1	0.2	1.1	4.0	14.2	24.1	2.6	3.8
ACM2	80	0.1	0.1	0.1	0.3	1.1	11.2	11.5	1.3	2.3
BLC	83	0.1	0.1	0.1	0.2	0.9	5.9	7.0	0.7	1.2
GBM	30	0.1	0.1	0.1	0.2	0.6	7.2	8.4	0.8	1.7
MN3	62	0.1	0.1	0.1	0.2	1.0	4.4	5.1	0.8	1.1
MYJ	59	0.1	0.1	0.1	0.2	0.6	7.0	7.5	0.8	1.5
ShG	95	0.1	0.1	0.1	0.2	0.5	7.2	16.3	0.7	1.9
YSU	36	0.1	0.1	0.1	0.1	0.7	3.0	3.4	0.5	0.8

Precipitations in December 2016 at Udine										
	# samples	min	1st perc	25th perc	median	75th perc	99th perc	max	mean	STD
mea	0	0.0	0.0	0.0	0.0	0.0	0.0	0.0	0.0	0.0
ACM2	0	0.0	0.0	0.0	0.0	0.0	0.0	0.0	0.0	0.0
BLC	0	0.0	0.0	0.0	0.0	0.0	0.0	0.0	0.0	0.0
GBM	0	0.0	0.0	0.0	0.0	0.0	0.0	0.0	0.0	0.0
MN3	0	0.0	0.0	0.0	0.0	0.0	0.0	0.0	0.0	0.0
MYJ	0	0.0	0.0	0.0	0.0	0.0	0.0	0.0	0.0	0.0
ShG	0	0.0	0.0	0.0	0.0	0.0	0.0	0.0	0.0	0.0
YSU	0	0.0	0.0	0.0	0.0	0.0	0.0	0.0	0.0	0.0

Precipitations in 2016 at Cividale del Friuli										
	# samples	min	1st perc	25th perc	median	75th perc	99th perc	max	mean	STD
mea	959	0.1	0.1	0.2	0.6	1.9	11.9	28.1	1.6	2.6
ACM2	798	0.1	0.1	0.1	0.4	1.5	14.8	22.8	1.4	2.6
BLC	740	0.1	0.1	0.1	0.4	1.2	14.6	29.4	1.4	2.8
GBM	650	0.1	0.1	0.1	0.4	1.1	12.2	26.5	1.1	2.4
MN3	2036	0.1	0.1	0.1	0.4	1.3	15.6	40.1	1.4	3.1
MYJ	721	0.1	0.1	0.1	0.3	1.1	12.9	23.0	1.1	2.3
ShG	765	0.1	0.1	0.1	0.3	1.2	10.6	22.6	1.2	2.3
YSU	669	0.1	0.1	0.1	0.4	1.2	14.6	45.8	1.3	3.6

Precipitations in January 2016 at Cividale del Friuli										
	# samples	min	1st perc	25th perc	median	75th perc	99th perc	max	mean	STD
mea	94	0.1	0.1	0.1	0.6	1.4	5.7	7.2	1.0	1.2
ACM2	94	0.1	0.1	0.1	0.3	1.1	5.2	5.7	0.8	1.2
BLC	87	0.1	0.1	0.1	0.2	0.9	6.7	8.1	0.8	1.4
GBM	77	0.1	0.1	0.2	0.4	1.3	3.5	4.0	0.8	0.9
MN3	97	0.1	0.1	0.1	0.3	0.6	3.2	3.5	0.6	0.7
MYJ	94	0.1	0.1	0.1	0.2	0.9	5.9	6.7	0.8	1.4
ShG	96	0.1	0.1	0.1	0.2	0.8	3.7	4.0	0.7	0.9
YSU	92	0.1	0.1	0.1	0.2	0.7	4.2	4.3	0.6	0.9

Precipitations in February 2016 at Cividale del Friuli										
	# samples	min	1st perc	25th perc	median	75th perc	99th perc	max	mean	STD
mea	196	0.1	0.1	0.2	0.7	2.0	7.9	9.8	1.5	1.8
ACM2	137	0.1	0.1	0.1	0.4	1.3	4.4	4.5	0.9	1.0
BLC	103	0.1	0.1	0.1	0.4	1.3	6.5	7.4	1.0	1.5
GBM	107	0.1	0.1	0.1	0.4	1.4	4.1	4.1	1.0	1.1
MN3	127	0.1	0.1	0.1	0.4	1.0	4.2	10.2	0.9	1.3
MYJ	111	0.1	0.1	0.1	0.3	1.1	3.8	3.9	0.8	1.0
ShG	121	0.1	0.1	0.2	0.5	1.2	4.0	4.4	0.9	1.1
YSU	114	0.1	0.1	0.1	0.4	1.0	4.0	4.2	0.8	1.1

Precipitations in March 2016 at Cividale del Friuli										
	# samples	min	1st perc	25th perc	median	75th perc	99th perc	max	mean	STD
mea	72	0.1	0.1	0.2	0.4	1.3	4.9	6.5	0.9	1.1
ACM2	76	0.1	0.1	0.1	0.4	1.0	5.8	9.6	0.9	1.4
BLC	60	0.1	0.1	0.1	0.6	1.5	9.3	10.8	1.5	2.3
GBM	45	0.1	0.1	0.1	0.4	1.4	5.5	6.5	1.0	1.3
MN3	49	0.1	0.1	0.1	0.5	1.2	2.7	2.9	0.8	0.8
MYJ	59	0.1	0.1	0.2	0.4	1.1	6.7	8.5	1.0	1.4
ShG	42	0.1	0.1	0.1	0.5	1.7	4.5	5.3	1.1	1.2
YSU	41	0.1	0.1	0.1	0.6	1.7	5.4	6.4	1.1	1.3

Precipitations in April 2016 at Cividale del Friuli										
	# samples	min	1st perc	25th perc	median	75th perc	99th perc	max	mean	STD
mea	64	0.1	0.1	0.1	0.4	1.0	6.4	8.3	0.9	1.5
ACM2	93	0.1	0.1	0.1	0.3	1.1	4.7	9.4	1.0	1.4
BLC	60	0.1	0.1	0.2	0.6	1.4	3.8	4.0	1.0	1.0
GBM	56	0.1	0.1	0.2	0.6	1.0	3.8	4.3	0.8	0.9
MN3	100	0.1	0.1	0.1	0.3	1.0	14.8	15.5	1.0	2.2
MYJ	74	0.1	0.1	0.2	0.3	0.7	6.1	14.1	0.8	1.7
ShG	51	0.1	0.1	0.1	0.2	0.6	4.8	4.9	0.7	1.1
YSU	70	0.1	0.1	0.1	0.4	1.0	3.9	4.7	0.8	1.0

Precipitations in May 2016 at Cividale del Friuli										
	# samples	min	1st perc	25th perc	median	75th perc	99th perc	max	mean	STD
mea	119	0.1	0.1	0.2	0.8	1.9	10.1	11.3	1.7	2.3
ACM2	79	0.1	0.1	0.2	0.8	2.1	11.4	20.1	1.9	2.9
BLC	90	0.1	0.1	0.1	0.3	1.3	13.4	13.6	1.1	2.2
GBM	62	0.1	0.1	0.1	0.3	1.0	9.0	11.8	1.2	2.1
MN3	113	0.1	0.1	0.2	0.7	2.2	28.1	40.1	2.1	4.9
MYJ	84	0.1	0.1	0.1	0.3	1.0	10.1	10.4	1.2	1.9
ShG	66	0.1	0.1	0.2	0.3	1.4	11.1	12.0	1.3	2.4
YSU	69	0.1	0.1	0.2	0.5	1.3	6.5	6.6	1.2	1.6

Precipitations in June 2016 at Cividale del Friuli										
	# samples	min	1st perc	25th perc	median	75th perc	99th perc	max	mean	STD
mea	80	0.1	0.1	0.1	0.4	1.5	20.6	28.1	1.8	4.0
ACM2	89	0.1	0.1	0.2	0.6	2.2	10.5	17.2	1.8	2.7
BLC	55	0.1	0.1	0.2	0.4	1.2	11.4	14.8	1.2	2.4
GBM	71	0.1	0.1	0.2	0.3	0.9	6.1	8.8	0.9	1.5
MN3	126	0.1	0.1	0.2	0.5	1.4	16.8	26.7	1.6	3.5
MYJ	49	0.1	0.1	0.2	0.6	1.8	18.5	23.0	2.3	4.4
ShG	71	0.1	0.1	0.2	0.4	1.1	18.0	22.6	1.5	3.5
YSU	72	0.1	0.1	0.2	0.6	1.3	15.8	27.0	1.6	3.7

Precipitations in July 2016 at Cividale del Friuli										
	# samples	min	1st perc	25th perc	median	75th perc	99th perc	max	mean	STD
mea	34	0.1	0.1	0.4	0.9	2.5	19.2	21.9	3.2	5.1
ACM2	38	0.1	0.1	0.2	1.0	4.3	20.9	22.8	3.8	5.8
BLC	49	0.1	0.1	0.1	0.5	1.5	29.2	29.4	2.9	6.5
GBM	35	0.1	0.1	0.2	0.4	1.5	16.6	19.9	1.8	3.8
MN3	125	0.1	0.1	0.2	0.4	1.5	13.4	25.5	1.7	3.2
MYJ	39	0.1	0.1	0.1	0.4	1.9	12.3	13.7	1.6	2.9
ShG	49	0.1	0.1	0.1	0.4	2.3	19.7	21.6	2.5	4.6
YSU	26	0.1	0.1	0.1	0.4	2.6	42.3	44.5	4.5	10.9

Precipitations in August 2016 at Cividale del Friuli										
	# samples	min	1st perc	25th perc	median	75th perc	99th perc	max	mean	STD
mea	41	0.1	0.1	0.3	0.7	4.6	12.1	12.7	2.6	3.7
ACM2	13	0.1	0.1	0.5	0.8	3.4	8.1	8.4	2.1	2.6
BLC	34	0.1	0.1	0.2	0.6	1.4	13.5	15.9	1.9	3.3
GBM	30	0.1	0.1	0.2	0.5	1.5	3.9	4.0	1.1	1.2
MN3	69	0.1	0.1	0.1	1.2	3.9	23.2	28.8	3.1	5.1
MYJ	21	0.1	0.1	0.1	1.1	2.0	4.4	4.6	1.3	1.4
ShG	25	0.1	0.1	0.1	0.4	1.2	6.9	7.0	1.4	2.1
YSU	19	0.1	0.1	0.1	0.4	1.3	14.2	16.0	1.8	3.8

Precipitations in September 2016 at Cividale del Friuli										
	# samples	min	1st perc	25th perc	median	75th perc	99th perc	max	mean	STD
mea	34	0.1	0.1	0.3	1.4	2.7	6.1	6.5	1.8	1.7
ACM2	26	0.1	0.1	0.1	0.3	0.6	3.5	3.8	0.6	0.9
BLC	27	0.1	0.1	0.1	0.3	1.2	14.2	15.3	1.9	3.7
GBM	24	0.1	0.1	0.1	0.2	0.3	18.6	22.5	1.5	4.6
MN3	34	0.1	0.1	0.1	0.4	1.1	9.9	10.0	1.5	2.5
MYJ	19	0.1	0.1	0.2	0.5	1.3	3.6	3.8	1.0	1.0
ShG	28	0.1	0.1	0.1	0.3	1.1	9.1	10.3	1.2	2.2
YSU	20	0.1	0.1	0.3	0.6	2.0	8.5	8.8	2.0	2.7

Precipitations in October 2016 at Cividale del Friuli										
	# samples	min	1st perc	25th perc	median	75th perc	99th perc	max	mean	STD
mea	108	0.1	0.1	0.2	0.5	1.6	10.7	18.8	1.3	2.3
ACM2	66	0.1	0.1	0.2	0.6	1.3	17.1	17.2	1.6	3.3
BLC	84	0.1	0.1	0.2	0.6	1.0	15.8	21.4	1.7	3.5
GBM	86	0.1	0.1	0.1	0.3	0.7	23.3	26.5	1.7	4.5
MN3	91	0.1	0.1	0.2	0.4	1.0	14.3	16.7	1.1	2.5
MYJ	83	0.1	0.1	0.1	0.4	1.2	16.3	22.2	1.5	3.4
ShG	113	0.1	0.1	0.1	0.4	1.4	9.2	9.8	1.4	2.1
YSU	100	0.1	0.1	0.2	0.4	1.2	26.1	45.8	1.9	5.6

Precipitations in November 2016 at Cividale del Friuli										
	# samples	min	1st perc	25th perc	median	75th perc	99th perc	max	mean	STD
mea	116	0.1	0.1	0.2	0.9	3.4	17.8	18.1	2.4	3.4
ACM2	83	0.1	0.1	0.2	0.3	1.5	15.6	18.7	2.1	3.8
BLC	90	0.1	0.1	0.1	0.4	1.2	7.9	9.4	1.1	1.8
GBM	40	0.1	0.1	0.1	0.3	1.0	5.3	5.3	0.8	1.2
MN3	70	0.1	0.1	0.1	0.4	1.2	10.7	15.9	1.3	2.4
MYJ	79	0.1	0.1	0.1	0.2	0.8	8.2	20.2	0.9	2.4
ShG	103	0.1	0.1	0.2	0.3	1.0	14.0	21.2	1.2	2.7
YSU	40	0.1	0.1	0.3	0.5	1.0	8.8	9.9	1.3	2.1

Precipitations in December 2016 at Cividale del Friuli										
	# samples	min	1st perc	25th perc	median	75th perc	99th perc	max	mean	STD
mea	1	0.1	0.1	0.1	0.1	0.1	0.1	0.1	0.1	0.0
ACM2	4	0.1	0.1	0.1	0.1	0.1	0.2	0.2	0.1	0.1
BLC	1	0.1	0.1	0.1	0.1	0.1	0.1	0.1	0.1	0.0
GBM	17	0.1	0.1	0.1	0.1	0.2	0.5	0.5	0.2	0.1
MN3	17	0.1	0.1	0.1	0.1	0.3	0.5	0.5	0.2	0.2
MYJ	9	0.1	0.1	0.1	0.1	0.1	0.4	0.4	0.1	0.1
ShG	0	0.0	0.0	0.0	0.0	0.0	0.0	0.0	0.0	0.0
YSU	6	0.1	0.1	0.1	0.1	0.1	0.1	0.1	0.1	0.0

Precipitations in 2016 at Fagagna										
	# samples	min	1st perc	25th perc	median	75th perc	99th perc	max	mean	STD
mea	936	0.1	0.1	0.2	0.8	2.2	12.5	21.2	1.8	2.6
ACM2	773	0.1	0.1	0.2	0.6	1.5	13.0	28.3	1.5	2.6
BLC	750	0.1	0.1	0.2	0.5	1.3	12.8	22.8	1.3	2.4
GBM	607	0.1	0.1	0.1	0.3	1.0	12.0	28.7	1.0	2.3
MN3	925	0.1	0.1	0.1	0.4	1.2	15.8	38.7	1.3	3.1
MYJ	669	0.1	0.1	0.1	0.4	1.3	13.6	38.4	1.4	3.2
ShG	733	0.1	0.1	0.1	0.4	1.3	11.2	26.9	1.2	2.2
YSU	667	0.1	0.1	0.1	0.4	1.2	14.6	25.0	1.1	2.4

Precipitations in January 2016 at Fagagna										
	# samples	min	1st perc	25th perc	median	75th perc	99th perc	max	mean	STD
mea	76	0.1	0.1	0.2	0.6	1.5	3.7	4.1	1.0	0.9
ACM2	70	0.1	0.1	0.2	0.6	1.0	2.2	2.5	0.6	0.5
BLC	76	0.1	0.1	0.1	0.4	0.8	3.6	4.9	0.7	0.9
GBM	62	0.1	0.1	0.2	0.6	1.1	2.3	2.5	0.7	0.6
MN3	86	0.1	0.1	0.1	0.3	0.7	1.7	1.9	0.5	0.5
MYJ	68	0.1	0.1	0.1	0.3	0.9	3.2	3.3	0.6	0.8
ShG	74	0.1	0.1	0.2	0.4	1.0	2.1	2.3	0.6	0.6
YSU	71	0.1	0.1	0.2	0.3	0.9	1.8	1.9	0.6	0.5

Precipitations in February 2016 at Fagagna										
	# samples	min	1st perc	25th perc	median	75th perc	99th perc	max	mean	STD
mea	186	0.1	0.1	0.4	1.5	3.4	9.6	11.9	2.2	2.3
ACM2	117	0.1	0.1	0.2	0.5	1.5	4.2	5.2	1.0	1.1
BLC	97	0.1	0.1	0.2	0.6	1.8	9.3	10.5	1.4	1.9
GBM	117	0.1	0.1	0.2	0.6	1.6	4.7	5.3	1.0	1.1
MN3	116	0.1	0.1	0.2	0.4	1.4	4.4	4.9	1.0	1.1
MYJ	105	0.1	0.1	0.1	0.4	1.6	4.7	4.9	1.0	1.2
ShG	127	0.1	0.1	0.2	0.4	1.4	3.6	4.6	0.9	1.0
YSU	121	0.1	0.1	0.1	0.4	1.4	3.9	4.6	0.9	1.1

Precipitations in March 2016 at Fagagna										
	# samples	min	1st perc	25th perc	median	75th perc	99th perc	max	mean	STD
mea	73	0.1	0.1	0.2	0.8	1.8	9.3	9.5	1.7	2.3
ACM2	84	0.1	0.1	0.1	0.4	0.9	2.8	3.3	0.6	0.7
BLC	65	0.1	0.1	0.1	0.4	1.5	7.7	8.3	1.2	1.8
GBM	36	0.1	0.1	0.2	0.4	0.9	3.5	4.1	0.7	0.9
MN3	48	0.1	0.1	0.2	0.4	1.1	2.8	2.9	0.8	0.7
MYJ	45	0.1	0.1	0.2	0.4	0.9	2.5	2.6	0.6	0.6
ShG	35	0.1	0.1	0.2	0.6	1.5	3.5	3.7	1.0	1.0
YSU	34	0.1	0.1	0.2	0.6	1.3	3.5	3.6	0.9	1.0

Precipitations in April 2016 at Fagagna										
	# samples	min	1st perc	25th perc	median	75th perc	99th perc	max	mean	STD
mea	73	0.1	0.1	0.1	0.5	1.2	5.1	5.6	0.9	1.1
ACM2	97	0.1	0.1	0.2	0.4	1.3	9.2	12.8	1.1	1.9
BLC	54	0.1	0.1	0.2	0.9	1.9	5.9	6.3	1.4	1.4
GBM	50	0.1	0.1	0.1	0.3	0.6	5.4	7.5	0.7	1.2
MN3	98	0.1	0.1	0.1	0.4	0.8	11.0	11.1	0.9	1.7
MYJ	53	0.1	0.1	0.1	0.4	1.2	7.0	8.5	1.1	1.8
ShG	38	0.1	0.1	0.1	0.2	0.4	6.5	7.3	0.7	1.4
YSU	56	0.1	0.1	0.1	0.3	0.7	3.0	3.7	0.6	0.8

Precipitations in May 2016 at Fagagna										
	# samples	min	1st perc	25th perc	median	75th perc	99th perc	max	mean	STD
mea	121	0.1	0.1	0.2	0.8	2.4	9.1	21.2	1.8	2.7
ACM2	87	0.1	0.1	0.4	1.0	3.0	9.9	10.2	2.1	2.5
BLC	81	0.1	0.1	0.2	0.6	1.1	18.2	20.3	1.3	3.1
GBM	69	0.1	0.1	0.1	0.4	0.7	10.8	12.0	0.9	2.0
MN3	142	0.1	0.1	0.2	0.5	1.5	12.4	18.3	1.3	2.3
MYJ	70	0.1	0.1	0.1	0.6	1.6	8.7	8.8	1.3	1.7
ShG	68	0.1	0.1	0.1	0.3	1.6	9.9	14.2	1.3	2.3
YSU	81	0.1	0.1	0.2	0.5	1.3	7.6	17.2	1.1	2.1

Precipitations in June 2016 at Fagagna										
	# samples	min	1st perc	25th perc	median	75th perc	99th perc	max	mean	STD
mea	94	0.1	0.1	0.1	0.5	1.4	15.2	17.2	1.6	3.1
ACM2	79	0.1	0.1	0.2	0.9	3.2	14.8	25.5	2.3	3.7
BLC	81	0.1	0.1	0.2	0.4	1.6	11.4	15.2	1.3	2.3
GBM	64	0.1	0.1	0.1	0.4	1.4	11.6	12.6	1.3	2.3
MN3	116	0.1	0.1	0.2	0.5	1.3	19.7	30.3	1.4	3.6
MYJ	60	0.1	0.1	0.2	0.5	2.3	20.2	29.9	2.2	4.5
ShG	87	0.1	0.1	0.2	0.4	1.2	14.2	26.9	1.5	3.4
YSU	89	0.1	0.1	0.2	0.5	1.3	14.6	15.0	1.3	2.4

Precipitations in July 2016 at Fagagna										
	# samples	min	1st perc	25th perc	median	75th perc	99th perc	max	mean	STD
mea	31	0.1	0.1	0.2	0.4	1.9	6.9	7.6	1.3	1.8
ACM2	40	0.1	0.1	0.2	0.6	3.1	20.4	23.8	3.4	5.6
BLC	45	0.1	0.1	0.2	0.7	2.2	14.1	15.5	2.0	3.4
GBM	44	0.1	0.1	0.1	0.3	1.2	14.1	14.4	1.8	3.5
MN3	100	0.1	0.1	0.1	0.3	1.0	16.3	38.7	1.9	5.0
MYJ	54	0.1	0.1	0.1	0.4	3.6	29.1	35.9	3.4	6.6
ShG	59	0.1	0.1	0.2	0.5	2.5	13.2	14.3	2.1	3.2
YSU	32	0.1	0.1	0.1	0.2	1.8	21.8	25.0	2.3	5.2

Precipitations in August 2016 at Fagagna										
	# samples	min	1st perc	25th perc	median	75th perc	99th perc	max	mean	STD
mea	48	0.1	0.1	0.2	0.7	2.5	12.6	17.3	2.1	3.2
ACM2	17	0.1	0.1	0.2	0.7	2.1	6.7	6.7	1.7	2.1
BLC	37	0.1	0.1	0.2	0.7	1.9	14.4	15.8	1.8	3.2
GBM	30	0.1	0.1	0.1	0.3	0.8	17.1	19.9	1.7	4.1
MN3	53	0.1	0.1	0.2	0.8	1.9	18.1	26.0	2.2	4.2
MYJ	19	0.1	0.1	0.3	0.7	1.0	6.8	7.8	1.1	1.7
ShG	31	0.1	0.1	0.2	0.5	2.5	14.2	17.9	1.9	3.4
YSU	28	0.1	0.1	0.1	0.3	1.1	10.8	13.0	1.3	2.6

Precipitations in September 2016 at Fagagna										
	# samples	min	1st perc	25th perc	median	75th perc	99th perc	max	mean	STD
mea	31	0.1	0.1	0.3	0.7	4.3	15.4	16.5	2.9	4.3
ACM2	25	0.1	0.1	0.1	0.5	1.0	3.4	3.8	0.8	0.9
BLC	18	0.1	0.1	0.2	0.4	2.0	20.8	22.8	2.6	5.7
GBM	21	0.1	0.1	0.1	0.2	0.4	23.7	28.7	1.9	6.2
MN3	30	0.1	0.1	0.1	0.2	2.7	28.2	33.1	3.2	6.8
MYJ	17	0.1	0.1	0.2	0.5	2.7	33.3	38.4	3.7	9.1
ShG	23	0.1	0.1	0.2	0.5	1.0	6.8	7.4	1.1	1.7
YSU	15	0.1	0.1	0.1	0.2	0.7	17.5	18.0	2.5	5.7

Precipitations in October 2016 at Fagagna										
	# samples	min	1st perc	25th perc	median	75th perc	99th perc	max	mean	STD
mea	106	0.1	0.1	0.1	0.4	1.7	15.7	20.8	1.5	2.8
ACM2	68	0.1	0.1	0.2	0.5	1.1	13.7	14.9	1.5	2.8
BLC	97	0.1	0.1	0.2	0.4	1.2	9.7	14.7	1.1	2.1
GBM	62	0.1	0.1	0.1	0.3	0.6	6.3	11.4	0.6	1.5
MN3	64	0.1	0.1	0.2	0.3	0.8	15.5	31.1	1.2	4.0
MYJ	83	0.1	0.1	0.1	0.4	1.0	11.0	11.8	1.2	2.2
ShG	100	0.1	0.1	0.2	0.6	1.7	10.1	15.1	1.6	2.5
YSU	92	0.1	0.1	0.2	0.3	1.0	16.3	23.9	1.4	3.3

Precipitations in November 2016 at Fagagna										
	# samples	min	1st perc	25th perc	median	75th perc	99th perc	max	mean	STD
mea	97	0.1	0.1	0.3	1.1	3.0	14.1	17.3	2.2	3.0
ACM2	86	0.1	0.1	0.1	0.6	1.7	12.6	28.3	1.7	3.5
BLC	98	0.1	0.1	0.1	0.2	1.0	9.6	13.3	1.0	2.1
GBM	37	0.1	0.1	0.1	0.2	1.1	11.0	12.7	1.4	2.7
MN3	56	0.1	0.1	0.1	0.4	1.5	5.7	6.0	1.1	1.4
MYJ	78	0.1	0.1	0.1	0.2	0.6	14.5	16.0	1.2	2.8
ShG	90	0.1	0.1	0.1	0.2	0.7	8.5	11.4	0.9	1.7
YSU	41	0.1	0.1	0.1	0.3	0.9	11.5	13.0	1.2	2.6

Precipitations in December 2016 at Fagagna										
	# samples	min	1st perc	25th perc	median	75th perc	99th perc	max	mean	STD
mea	0	0.0	0.0	0.0	0.0	0.0	0.0	0.0	0.0	0.0
ACM2	0	0.0	0.0	0.0	0.0	0.0	0.0	0.0	0.0	0.0
BLC	0	0.0	0.0	0.0	0.0	0.0	0.0	0.0	0.0	0.0
GBM	0	0.0	0.0	0.0	0.0	0.0	0.0	0.0	0.0	0.0
MN3	0	0.0	0.0	0.0	0.0	0.0	0.0	0.0	0.0	0.0
MYJ	0	0.0	0.0	0.0	0.0	0.0	0.0	0.0	0.0	0.0
ShG	0	0.0	0.0	0.0	0.0	0.0	0.0	0.0	0.0	0.0
YSU	0	0.0	0.0	0.0	0.0	0.0	0.0	0.0	0.0	0.0

Precipitations in 2016 at Fossalon di Grado										
	# samples	min	1st perc	25th perc	median	75th perc	99th perc	max	mean	STD
mea	781	0.1	0.1	0.2	0.5	1.4	12.9	23.0	1.4	2.6
ACM2	669	0.1	0.1	0.1	0.4	1.0	12.9	25.0	1.2	2.4
BLC	495	0.1	0.1	0.2	0.4	1.0	9.1	18.0	1.0	1.7
GBM	456	0.1	0.1	0.1	0.4	1.0	7.4	22.3	0.9	1.8
MN3	1152	0.1	0.1	0.1	0.3	1.1	18.4	29.7	1.2	2.8
MYJ	465	0.1	0.1	0.1	0.4	1.0	7.8	21.4	0.9	1.7
ShG	574	0.1	0.1	0.1	0.3	1.0	7.4	35.2	0.9	2.1
YSU	513	0.1	0.1	0.1	0.4	1.1	8.0	26.3	1.0	2.1

Precipitations in January 2016 at Fossalon di Grado										
	# samples	min	1st perc	25th perc	median	75th perc	99th perc	max	mean	STD
mea	105	0.1	0.1	0.1	0.4	0.8	3.0	3.7	0.6	0.7
ACM2	81	0.1	0.1	0.1	0.2	0.8	2.3	2.3	0.6	0.7
BLC	72	0.1	0.1	0.1	0.4	0.8	2.6	3.3	0.5	0.6
GBM	70	0.1	0.1	0.2	0.5	1.1	3.5	4.2	0.8	0.9
MN3	89	0.1	0.1	0.1	0.5	1.2	2.6	2.9	0.7	0.7
MYJ	63	0.1	0.1	0.2	0.5	0.9	2.9	3.0	0.7	0.7
ShG	84	0.1	0.1	0.1	0.3	0.9	4.0	5.0	0.7	0.9
YSU	87	0.1	0.1	0.1	0.4	1.0	5.5	15.5	0.8	1.8

Precipitations in February 2016 at Fossalon di Grado										
	# samples	min	1st perc	25th perc	median	75th perc	99th perc	max	mean	STD
mea	169	0.1	0.1	0.2	0.5	1.7	6.5	9.2	1.2	1.5
ACM2	115	0.1	0.1	0.2	0.5	0.9	3.6	4.8	0.8	0.9
BLC	92	0.1	0.1	0.2	0.4	1.3	4.5	10.7	0.9	1.4
GBM	86	0.1	0.1	0.2	0.5	1.2	3.7	3.7	0.9	0.9
MN3	90	0.1	0.1	0.2	0.4	1.0	3.5	3.7	0.7	0.7
MYJ	73	0.1	0.1	0.1	0.4	1.0	3.1	3.8	0.7	0.7
ShG	101	0.1	0.1	0.1	0.4	1.1	4.3	4.6	0.7	0.8
YSU	88	0.1	0.1	0.2	0.4	0.9	3.2	3.5	0.7	0.8

Precipitations in March 2016 at Fossalon di Grado										
	# samples	min	1st perc	25th perc	median	75th perc	99th perc	max	mean	STD
mea	57	0.1	0.1	0.1	0.4	1.1	8.1	11.2	1.2	1.9
ACM2	59	0.1	0.1	0.2	0.3	1.0	4.3	5.9	0.8	1.0
BLC	53	0.1	0.1	0.2	0.3	0.6	8.0	9.7	1.0	1.9
GBM	27	0.1	0.1	0.1	0.6	2.3	5.3	5.4	1.4	1.7
MN3	29	0.1	0.1	0.1	0.2	0.7	1.6	1.7	0.5	0.5
MYJ	39	0.1	0.1	0.1	0.3	0.6	2.1	2.3	0.5	0.5
ShG	30	0.1	0.1	0.3	0.4	1.4	6.5	7.3	1.2	1.6
YSU	31	0.1	0.1	0.2	0.5	1.1	4.0	4.1	1.0	1.1

Precipitations in April 2016 at Fossalon di Grado										
	# samples	min	1st perc	25th perc	median	75th perc	99th perc	max	mean	STD
mea	58	0.1	0.1	0.1	0.3	1.1	13.1	18.9	1.4	3.0
ACM2	66	0.1	0.1	0.2	0.5	1.0	5.3	6.1	1.0	1.3
BLC	49	0.1	0.1	0.4	1.1	2.6	9.7	10.3	2.0	2.3
GBM	65	0.1	0.1	0.2	0.4	0.8	2.9	3.9	0.6	0.7
MN3	59	0.1	0.1	0.2	0.4	1.2	11.1	19.2	1.3	2.7
MYJ	63	0.1	0.1	0.2	0.5	1.4	4.5	4.9	1.0	1.1
ShG	49	0.1	0.1	0.2	0.4	1.1	3.1	3.1	0.7	0.8
YSU	54	0.1	0.1	0.1	0.2	0.9	4.2	5.0	0.7	1.0

Precipitations in May 2016 at Fossalon di Grado										
	# samples	min	1st perc	25th perc	median	75th perc	99th perc	max	mean	STD
mea	64	0.1	0.1	0.2	0.5	1.5	12.0	12.4	1.7	2.8
ACM2	85	0.1	0.1	0.3	0.8	1.9	14.7	15.7	1.8	2.9
BLC	61	0.1	0.1	0.2	0.4	1.0	2.4	2.5	0.7	0.7
GBM	57	0.1	0.1	0.2	0.4	0.8	11.1	14.9	1.2	2.4
MN3	64	0.1	0.1	0.2	0.6	2.0	26.0	29.7	2.8	5.7
MYJ	59	0.1	0.1	0.2	0.4	1.5	7.3	8.6	1.3	1.8
ShG	52	0.1	0.1	0.1	0.3	1.8	7.9	8.4	1.2	1.8
YSU	68	0.1	0.1	0.2	0.4	1.1	7.2	10.9	1.0	1.6

Precipitations in June 2016 at Fossalon di Grado										
	# samples	min	1st perc	25th perc	median	75th perc	99th perc	max	mean	STD
mea	68	0.1	0.1	0.2	0.6	1.6	21.1	23.0	2.0	4.3
ACM2	82	0.1	0.1	0.2	0.4	1.0	8.9	12.5	1.1	1.9
BLC	30	0.1	0.1	0.1	0.8	1.5	8.5	9.5	1.3	2.0
GBM	48	0.1	0.1	0.1	0.2	0.7	11.6	15.1	1.0	2.5
MN3	47	0.1	0.1	0.1	0.3	0.9	7.2	7.5	0.8	1.5
MYJ	26	0.1	0.1	0.2	0.6	1.5	18.1	21.4	2.0	4.3
ShG	41	0.1	0.1	0.1	0.3	1.0	26.3	35.2	1.8	5.8
YSU	41	0.1	0.1	0.3	0.7	2.1	20.7	26.3	2.2	4.5

Precipitations in July 2016 at Fossalon di Grado										
	# samples	min	1st perc	25th perc	median	75th perc	99th perc	max	mean	STD
mea	17	0.1	0.1	0.1	0.2	0.4	9.0	9.9	1.1	2.5
ACM2	11	0.1	0.1	0.2	0.4	0.9	6.1	6.5	1.2	1.9
BLC	6	0.1	0.1	0.2	0.3	0.8	3.4	3.5	0.9	1.3
GBM	14	0.1	0.1	0.1	0.1	0.3	2.9	3.2	0.4	0.8
MN3	53	0.1	0.1	0.1	0.4	1.9	18.5	19.2	1.9	3.8
MYJ	11	0.1	0.1	0.6	2.4	5.9	10.6	11.0	3.4	3.6
ShG	22	0.1	0.1	0.1	0.3	1.0	6.4	6.6	1.4	2.0
YSU	4	0.4	0.4	0.6	3.3	6.4	7.9	8.0	3.8	3.8

Precipitations in August 2016 at Fossalon di Grado										
	# samples	min	1st perc	25th perc	median	75th perc	99th perc	max	mean	STD
mea	25	0.1	0.1	0.2	0.5	1.4	9.2	9.6	1.3	2.4
ACM2	10	0.1	0.1	0.2	0.6	2.6	14.4	15.4	2.6	4.7
BLC	9	0.1	0.1	0.1	0.3	0.6	5.0	5.1	1.2	2.0
GBM	10	0.1	0.1	0.1	0.3	1.1	6.7	7.2	1.2	2.2
MN3	29	0.1	0.1	0.1	0.5	1.6	17.7	19.1	2.6	4.9
MYJ	10	0.1	0.1	0.3	0.6	0.7	1.9	2.0	0.7	0.6
ShG	15	0.1	0.1	0.1	0.5	1.8	7.0	7.4	1.4	2.1
YSU	15	0.1	0.1	0.2	0.4	1.1	6.6	7.4	1.1	1.8

Precipitations in September 2016 at Fossalon di Grado										
	# samples	min	1st perc	25th perc	median	75th perc	99th perc	max	mean	STD
mea	35	0.1	0.1	0.3	1.4	3.2	13.6	16.5	2.4	3.2
ACM2	16	0.1	0.1	0.1	0.3	4.6	22.7	24.7	3.6	6.7
BLC	13	0.1	0.1	0.1	0.4	1.7	5.0	5.2	1.1	1.6
GBM	17	0.1	0.1	0.1	0.2	1.5	5.6	5.8	1.1	1.7
MN3	22	0.1	0.1	0.1	0.2	0.7	2.2	2.3	0.5	0.6
MYJ	17	0.1	0.1	0.2	0.7	4.0	9.3	9.6	2.2	2.8
ShG	19	0.1	0.1	0.2	0.4	1.5	13.0	14.3	1.9	3.5
YSU	8	0.2	0.2	0.2	1.3	3.6	19.4	20.5	3.9	6.9

Precipitations in October 2016 at Fossalon di Grado										
	# samples	min	1st perc	25th perc	median	75th perc	99th perc	max	mean	STD
mea	88	0.1	0.1	0.2	0.5	1.6	13.4	21.7	1.6	3.1
ACM2	73	0.1	0.1	0.1	0.4	0.8	14.0	25.0	1.3	3.4
BLC	53	0.1	0.1	0.1	0.3	0.7	13.1	18.0	1.1	2.8
GBM	36	0.1	0.1	0.1	0.2	0.7	3.2	3.9	0.5	0.8
MN3	38	0.1	0.1	0.1	0.2	0.3	6.2	9.3	0.5	1.5
MYJ	46	0.1	0.1	0.1	0.2	0.4	2.5	3.0	0.4	0.6
ShG	79	0.1	0.1	0.1	0.3	1.0	8.6	14.2	0.9	1.9
YSU	77	0.1	0.1	0.1	0.3	0.9	6.3	7.8	0.9	1.4

Precipitations in November 2016 at Fossalon di Grado										
	# samples	min	1st perc	25th perc	median	75th perc	99th perc	max	mean	STD
mea	91	0.1	0.1	0.2	0.8	1.8	15.2	16.0	1.6	2.6
ACM2	64	0.1	0.1	0.1	0.3	0.5	14.0	15.3	1.3	3.2
BLC	57	0.1	0.1	0.2	0.3	0.5	5.4	5.8	0.8	1.3
GBM	25	0.1	0.1	0.1	0.4	1.1	18.4	22.3	2.0	4.6
MN3	43	0.1	0.1	0.2	0.4	1.4	5.5	6.7	1.0	1.3
MYJ	52	0.1	0.1	0.1	0.4	0.6	1.6	1.7	0.5	0.5
ShG	81	0.1	0.1	0.2	0.3	0.6	1.8	2.0	0.4	0.4
YSU	39	0.1	0.1	0.1	0.2	0.6	5.4	7.0	0.7	1.2

Precipitations in December 2016 at Fossalon di Grado										
	# samples	min	1st perc	25th perc	median	75th perc	99th perc	max	mean	STD
mea	4	0.1	0.1	0.1	0.1	0.1	0.1	0.1	0.1	0.0
ACM2	7	0.1	0.1	0.1	0.1	0.1	0.2	0.2	0.1	0.0
BLC	0	0.0	0.0	0.0	0.0	0.0	0.0	0.0	0.0	0.0
GBM	1	0.1	0.1	0.1	0.1	0.1	0.1	0.1	0.1	0.0
MN3	13	0.1	0.1	0.1	0.2	0.6	1.2	1.2	0.4	0.4
MYJ	6	0.1	0.1	0.1	0.1	0.2	0.3	0.3	0.2	0.1
ShG	1	0.1	0.1	0.1	0.1	0.1	0.1	0.1	0.1	0.0
YSU	1	0.1	0.1	0.1	0.1	0.1	0.1	0.1	0.1	0.0

Precipitations in 2016 at Enemonzo										
	# samples	min	1st perc	25th perc	median	75th perc	99th perc	max	mean	STD
mea	1177	0.1	0.1	0.2	0.6	1.8	16.9	52.9	1.6	3.4
ACM2	804	0.1	0.1	0.2	0.6	1.7	13.2	24.1	1.4	2.5
BLC	848	0.1	0.1	0.2	0.5	1.4	11.2	23.0	1.3	2.3
GBM	655	0.1	0.1	0.2	0.5	1.5	9.0	15.8	1.3	1.9
MN3	810	0.1	0.1	0.2	0.4	1.2	13.6	27.4	1.3	2.5
MYJ	697	0.1	0.1	0.2	0.5	1.5	8.2	17.3	1.2	1.9
ShG	774	0.1	0.1	0.2	0.6	1.9	10.5	25.9	1.5	2.3
YSU	768	0.1	0.1	0.2	0.5	1.4	12.2	26.1	1.4	2.4

Precipitations in January 2016 at Enemonzo										
	# samples	min	1st perc	25th perc	median	75th perc	99th perc	max	mean	STD
mea	46	0.1	0.1	0.4	0.9	1.9	5.8	6.0	1.5	1.5
ACM2	61	0.1	0.1	0.1	0.2	0.7	1.7	1.8	0.5	0.4
BLC	55	0.1	0.1	0.1	0.3	0.6	1.7	2.0	0.5	0.4
GBM	48	0.1	0.1	0.2	0.4	0.8	1.4	1.5	0.5	0.4
MN3	66	0.1	0.1	0.1	0.3	0.6	1.0	1.1	0.4	0.3
MYJ	50	0.1	0.1	0.2	0.4	0.7	1.3	1.5	0.4	0.3
ShG	56	0.1	0.1	0.2	0.4	0.7	1.8	1.9	0.6	0.4
YSU	53	0.1	0.1	0.2	0.5	0.8	1.4	1.5	0.5	0.4

Precipitations in February 2016 at Enemonzo										
	# samples	min	1st perc	25th perc	median	75th perc	99th perc	max	mean	STD
mea	188	0.1	0.1	0.3	0.9	2.5	7.2	7.6	1.6	1.7
ACM2	117	0.1	0.1	0.2	0.7	2.8	5.0	5.5	1.6	1.7
BLC	125	0.1	0.1	0.2	0.7	2.7	5.1	6.3	1.5	1.5
GBM	105	0.1	0.1	0.3	1.0	3.3	7.9	9.0	2.0	2.1
MN3	124	0.1	0.1	0.2	0.7	2.7	6.7	7.3	1.6	1.8
MYJ	93	0.1	0.1	0.2	1.1	3.6	7.6	8.2	2.1	2.1
ShG	110	0.1	0.1	0.2	0.9	3.8	7.3	7.8	2.0	2.1
YSU	115	0.1	0.1	0.2	0.7	3.5	7.1	7.1	1.9	2.1

Precipitations in March 2016 at Enemonzo										
	# samples	min	1st perc	25th perc	median	75th perc	99th perc	max	mean	STD
mea	82	0.1	0.1	0.4	1.0	2.7	4.7	5.2	1.5	1.4
ACM2	71	0.1	0.1	0.3	0.6	0.9	3.8	3.9	0.8	0.9
BLC	75	0.1	0.1	0.1	0.5	1.3	11.3	13.4	1.4	2.5
GBM	28	0.1	0.1	0.3	0.9	1.3	7.5	8.5	1.4	1.8
MN3	39	0.1	0.1	0.2	0.3	0.6	3.6	3.7	0.7	0.9
MYJ	52	0.1	0.1	0.2	0.7	1.2	3.5	3.7	0.9	1.0
ShG	31	0.1	0.1	0.4	1.4	2.3	4.9	5.0	1.6	1.5
YSU	35	0.1	0.1	0.1	0.7	1.8	5.7	6.1	1.5	1.7

Precipitations in April 2016 at Enemonzo										
	# samples	min	1st perc	25th perc	median	75th perc	99th perc	max	mean	STD
mea	90	0.1	0.1	0.2	0.8	1.8	7.8	8.0	1.4	1.8
ACM2	95	0.1	0.1	0.1	0.4	1.3	8.7	9.8	1.0	1.6
BLC	62	0.1	0.1	0.1	0.2	0.9	3.5	3.6	0.7	0.8
GBM	51	0.1	0.1	0.1	0.3	0.8	5.4	6.4	0.7	1.1
MN3	66	0.1	0.1	0.1	0.2	0.6	2.7	3.3	0.5	0.7
MYJ	44	0.1	0.1	0.1	0.2	0.7	4.0	4.6	0.6	0.9
ShG	42	0.1	0.1	0.1	0.2	1.0	4.4	4.6	0.8	1.1
YSU	46	0.1	0.1	0.1	0.2	0.5	4.1	5.4	0.5	1.0

Precipitations in May 2016 at Enemonzo										
	# samples	min	1st perc	25th perc	median	75th perc	99th perc	max	mean	STD
mea	128	0.1	0.1	0.1	0.5	1.6	9.6	12.8	1.3	2.0
ACM2	114	0.1	0.1	0.2	1.0	2.3	18.5	19.0	2.0	3.4
BLC	92	0.1	0.1	0.2	0.5	1.4	6.2	6.7	1.1	1.4
GBM	78	0.1	0.1	0.3	0.8	2.0	4.6	4.7	1.3	1.3
MN3	105	0.1	0.1	0.2	0.6	1.5	12.9	15.5	1.5	2.7
MYJ	77	0.1	0.1	0.2	0.7	1.9	5.2	7.8	1.2	1.3
ShG	60	0.1	0.1	0.1	0.4	1.5	6.6	7.1	1.2	1.6
YSU	86	0.1	0.1	0.2	0.6	1.6	7.8	8.4	1.3	1.6

Precipitations in June 2016 at Enemonzo										
	# samples	min	1st perc	25th perc	median	75th perc	99th perc	max	mean	STD
mea	130	0.1	0.1	0.1	0.3	1.5	14.4	29.4	1.8	3.7
ACM2	114	0.1	0.1	0.2	0.8	2.0	9.6	11.4	1.6	2.2
BLC	95	0.1	0.1	0.1	0.4	1.0	11.2	19.5	1.3	2.7
GBM	75	0.1	0.1	0.1	0.2	0.8	10.8	15.8	1.0	2.4
MN3	148	0.1	0.1	0.2	0.4	1.0	13.8	14.2	1.1	2.2
MYJ	94	0.1	0.1	0.1	0.3	0.9	8.4	9.5	0.9	1.7
ShG	135	0.1	0.1	0.3	1.0	2.0	14.2	25.9	1.8	3.0
YSU	124	0.1	0.1	0.2	0.5	1.2	10.9	16.4	1.3	2.2

Precipitations in July 2016 at Enemonzo										
	# samples	min	1st perc	25th perc	median	75th perc	99th perc	max	mean	STD
mea	84	0.1	0.1	0.1	0.4	1.7	33.3	34.5	3.2	7.2
ACM2	46	0.1	0.1	0.1	0.3	2.1	21.9	24.1	2.4	5.0
BLC	61	0.1	0.1	0.2	0.8	3.1	16.3	23.0	2.3	3.9
GBM	68	0.1	0.1	0.2	0.8	2.4	12.5	15.8	2.0	2.9
MN3	38	0.1	0.1	0.2	0.4	1.6	12.8	14.3	1.7	3.1
MYJ	77	0.1	0.1	0.2	0.4	1.5	13.3	16.8	1.6	2.8
ShG	59	0.1	0.1	0.1	0.5	1.9	16.3	19.4	1.8	3.4
YSU	66	0.1	0.1	0.1	0.6	1.8	19.5	21.3	2.1	4.1

Precipitations in August 2016 at Enemonzo										
	# samples	min	1st perc	25th perc	median	75th perc	99th perc	max	mean	STD
mea	91	0.1	0.1	0.1	0.2	1.4	18.7	27.8	1.6	3.9
ACM2	23	0.1	0.1	0.2	0.4	0.8	3.3	3.4	0.7	0.9
BLC	50	0.1	0.1	0.1	0.4	1.4	8.4	8.8	1.4	2.1
GBM	47	0.1	0.1	0.1	0.4	1.2	5.1	5.4	0.9	1.2
MN3	35	0.1	0.1	0.2	0.4	1.5	9.2	10.9	1.2	2.1
MYJ	38	0.1	0.1	0.3	0.6	1.8	7.8	9.8	1.4	1.9
ShG	47	0.1	0.1	0.2	0.5	3.2	10.0	12.6	1.9	2.6
YSU	64	0.1	0.1	0.2	0.4	1.4	11.1	12.9	1.3	2.4

Precipitations in September 2016 at Enemonzo										
	# samples	min	1st perc	25th perc	median	75th perc	99th perc	max	mean	STD
mea	69	0.1	0.1	0.1	0.3	1.4	29.9	52.9	2.3	7.0
ACM2	43	0.1	0.1	0.2	0.4	1.1	4.6	5.4	0.9	1.1
BLC	32	0.1	0.1	0.2	0.3	0.9	7.4	7.8	1.2	2.0
GBM	26	0.1	0.1	0.1	0.2	2.4	9.1	9.1	1.8	2.8
MN3	21	0.1	0.1	0.1	0.2	0.7	6.0	6.4	1.1	1.8
MYJ	24	0.1	0.1	0.2	0.4	2.2	6.2	6.4	1.4	1.7
ShG	46	0.1	0.1	0.2	0.8	2.1	7.9	9.3	1.6	1.9
YSU	31	0.1	0.1	0.2	0.8	4.8	22.6	26.1	3.2	5.4

Precipitations in October 2016 at Enemonzo										
	# samples	min	1st perc	25th perc	median	75th perc	99th perc	max	mean	STD
mea	133	0.1	0.1	0.1	0.5	1.1	5.6	8.9	1.0	1.5
ACM2	62	0.1	0.1	0.2	0.8	2.2	16.7	18.6	2.3	3.8
BLC	93	0.1	0.1	0.2	0.5	1.4	10.9	11.0	1.3	2.2
GBM	92	0.1	0.1	0.1	0.3	1.0	5.4	8.9	0.9	1.4
MN3	94	0.1	0.1	0.4	0.9	1.5	23.8	27.4	2.4	4.9
MYJ	73	0.1	0.1	0.2	0.5	1.1	11.6	17.3	1.4	2.7
ShG	102	0.1	0.1	0.3	1.0	2.5	11.0	13.0	1.9	2.4
YSU	85	0.1	0.1	0.3	0.6	1.4	4.7	5.6	1.1	1.1

Precipitations in November 2016 at Enemonzo										
	# samples	min	1st perc	25th perc	median	75th perc	99th perc	max	mean	STD
mea	136	0.1	0.1	0.2	0.5	1.5	7.2	7.8	1.1	1.5
ACM2	58	0.1	0.1	0.3	0.9	1.6	4.1	5.0	1.1	1.1
BLC	108	0.1	0.1	0.2	0.6	1.6	18.5	20.4	1.5	3.1
GBM	37	0.1	0.1	0.2	0.7	1.8	4.9	5.3	1.1	1.2
MN3	74	0.1	0.1	0.1	0.4	1.2	5.9	8.6	1.1	1.5
MYJ	75	0.1	0.1	0.1	0.4	1.0	5.8	6.0	1.0	1.4
ShG	86	0.1	0.1	0.2	0.5	0.9	6.9	8.9	1.0	1.5
YSU	63	0.1	0.1	0.1	0.3	1.1	8.4	13.8	1.1	2.1

Precipitations in December 2016 at Enemonzo										
	# samples	min	1st perc	25th perc	median	75th perc	99th perc	max	mean	STD
mea	0	0.0	0.0	0.0	0.0	0.0	0.0	0.0	0.0	0.0
ACM2	0	0.0	0.0	0.0	0.0	0.0	0.0	0.0	0.0	0.0
BLC	0	0.0	0.0	0.0	0.0	0.0	0.0	0.0	0.0	0.0
GBM	0	0.0	0.0	0.0	0.0	0.0	0.0	0.0	0.0	0.0
MN3	0	0.0	0.0	0.0	0.0	0.0	0.0	0.0	0.0	0.0
MYJ	0	0.0	0.0	0.0	0.0	0.0	0.0	0.0	0.0	0.0
ShG	0	0.0	0.0	0.0	0.0	0.0	0.0	0.0	0.0	0.0
YSU	0	0.0	0.0	0.0	0.0	0.0	0.0	0.0	0.0	0.0

Appendix C

WRF namelist

Here is reported an example of a namelist of the WRF. Quantities between two '%' symbols are to be changed at every run to specify the period of time that has to be simulated. As a matter of fact many runs were realized one after the other changing such parameters with bash commands from the terminal.

&time_control
run_days = %DAYS_PER_RUN%,
run_hours = 0,
run_minutes = 0,
run_seconds = 0,
start_year = %SYYYY%, %SYYYY%, %SYYYY%,
start_month = %SMM%, %SMM%, %SMM%,
start_day = %SDD%, %SDD%, %SDD%,
start_hour = 00, 00, 00,
start_minute = 00, 00, 00,
start_second = 00, 00, 00,
end_year = %EYYYY%, %EYYYY%, %EYYYY%,
end_month = %EMM%, %EMM%, %EMM%,
end_day = %EDD%, %EDD%, %EDD%,
end_hour = 00, 00, 00,
end_minute = 00, 00, 00,
end_second = 00, 00, 00,

interval_seconds = 21600

input_from_file = .true.,.true.,.true.,

history_interval = 360, 180, 60,

frames_per_outfile = 4, 8, 6,

adjust_output_times = .true.,

restart = %RESTART%,

restart_interval = 1440,

io_form_history = 2

io_form_restart = 2

io_form_input = 2

io_form_boundary = 2

debug_level = 100

write_hist_at_0h_rst = %RESTARTda0%

auxinput4_inname = “wrflowinp_d<domain>",

auxinput4_interval = 360, 360, 360,

io_form_auxinput4 = 2,

/

&domains

time_step = 200,

time_step_fract_num = 0,

time_step_fract_den = 1,

max_dom = 3,

e_we = 96, 136, 91,

e_sn = 96, 156, 91,

e_vert = 31, 31, 31,

num_metgrid_levels = %NUM_METGRID_LEVELS%,

num_metgrid_soil_levels = 4,

p_top_requested = 5000,

dx = 50000, 10000, 2000,

dy = 50000, 10000, 2000,

grid_id = 1, 2, 3,

```
parent_id = 0, 1, 2,
i_parent_start = 1, 36, 68,
j_parent_start = 1, 27, 112,
parent_grid_ratio = 1, 5, 5,
parent_time_step_ratio = 1, 5, 5,
use_adaptive_time_step = .false.,
step_to_output_time = .true.,
min_time_step = 100, 20, 4,
max_time_step = 400, 80, 16,
target_cfl = 1.2, 1.2, 1.2,
max_step_increase_pct = 5, 51, 51,
starting_time_step = 100, 20, 4,
nproc_x = %NPROC_X%,
nproc_y = %NPROC_Y%,
feedback = 1,
smooth_option = 0
/
nproc_x = 6,
nproc_y = 16,
numtiles = 8,



 &physics
mp_physics = 8, 8, 8,
ra_lw_physics = 1, 1, 1,
ra_sw_physics = 1, 1, 1,
radt = 50, 50, 50,
sf_sfclay_physics = 2, 2, 2,
sf_surface_physics = 2, 2, 2,
bl_pbl_physics = 2, 2, 2,
bldt = 0, 0, 0,
cu_physics = 1, 1, 0,
```

```
cudt = 5, 5, 0,
isfflx = 1,
ifsnow = 0,
icloud = 1,
surface_input_source = 1,
num_soil_layers = 4,
sf_urban_physics = 0,
maxiens = 1,
maxens = 3,
maxens2 = 3,
maxens3 = 16,
ensdim = 144,
bucket_mm = -1,
bucket_J = -1,
prec_acc_dt = 360, 180, 60,
sst_update = 1,
num_land_cat = 24
/
 &fdda


/
 &dynamics


w_damping = 1,
diff_opt = 1,
km_opt = 4,
diff_6th_opt = 0, 0, 0,
diff_6th_factor = 0.12, 0.12, 0.12,
base_temp = 290.
damp_opt = 0,
zdamp = 5000., 5000., 5000.,
dampcoef = 0.2, 0.2, 0.2
```

```
khdif = 0, 0, 0,
kvdif = 0, 0, 0,
non_hydrostatic = .true., .true., .true.,
moist_adv_opt = 1, 1, 1,
scalar_adv_opt = 1, 1, 1,
/
 &bdy_control

spec_bdy_width = 5,
spec_zone = 1,
relax_zone = 4,
specified = .true., .false.,.false.,
nested = .false., .true., .true.,
/
 &grib2

/
 &namelist_quilt

nio_tasks_per_group = 0,
nio_groups = 1,
/
```

Acronyms

ABL Atmospheric Boundary Layer.

ACM2 Improved Asymmetric Convective Model parameterization.

ARW Advanced Research WRF.

BLC Boulac parameterization.

CDO Climate Data Operators.

CI Capping Inversion.

EZ Entrainment zone.

FA Free Atmosphere.

FVG Friuli Venezia Giulia.

GBM Grenier-Bretherton-McCaa parameterization.

HPC High Performance Computing.

LES Large Eddy Simulations.

LLJ Low Level Jet.

ML Mixed Layer.

MN3 MYNN3 (Mellor-Yamada-Nakanishi-Niino level 3) parameterization.

MYJ Mellor-Yamada parameterization.

NL Nocturnal Layer.

RMS Root Mean Square.

SHG Shin-Hong parameterization.

SL Surface Layer.

SST Sea Surface Temperature.

SWDR Shortwave Downward radiation.

TKE Turbulent Kinetic Energy.

WPS WRF pre-processing unit.

WRF Weather Research and Forecasting model.

YSU Yonsei University parameterization.

Bibliography

R. Banks and J. Baldasano. Impact of wrf model pbl schemes on air quality simulations over catalonia, spain. 572:98–113, 12 2016.

R. F. Banks, J. Tiana-Alsina, J. M. Baldasano, F. Rocadenbosch, A. Papayannis, S. Solomos, and C. G. Tzanis. Sensitivity of boundary-layer variables to pbl schemes in the wrf model based on surface meteorological observations, lidar, and radiosondes during the hygra-cd campaign. *Atmospheric Research*, 176-177(Supplement C):185 – 201, 2016. ISSN 0169-8095. doi: https://doi.org/10.1016/j.atmosres.2016.02.024. URL `http://www.sciencedirect.com/science/article/pii/S0169809516300412`.

G. Barenblatt. *Scaling*. Cambridge Texts in Applied Mathematics. Cambridge University Press, 2003. ISBN 9780521533942. URL `https://books.google.it/books?id=05zBYET6tR0C`.

G. Batchelor. *An Introduction to Fluid Dynamics*. Cambridge Mathematical Library. Cambridge University Press, 2000. ISBN 9780521663960. URL `https://books.google.it/books?id=Rla7OihRvUgC`.

A. K. Betts. A new convective adjustment scheme. part i: Observational and theoretical basis. *Quarterly Journal of the Royal Meteorological Society*, 112(473):677–691, 1986. ISSN 1477-870X. doi: 10.1002/qj.49711247307. URL `http://dx.doi.org/10.1002/qj.49711247307`.

A. K. Betts and M. J. Miller. A new convective adjustment scheme. part ii: Single column tests using gate wave, bomex, atex and arctic air-mass data sets. *Quarterly Journal of the Royal Meteorological Society*, 112(473):693–709, 1986. ISSN 1477-870X. doi: 10.1002/qj.49711247308. URL `http://dx.doi.org/10.1002/qj.49711247308`.

R. Boadh, A. Satyanarayana, T. R. Krishna, and S. Madala. Sensitivity of pbl schemes of the wrf-arw model in simulating the boundary layer flow parameters for their application to air pollution dispersion modeling over a tropical station. *Atmósfera*, 29(1):61

– 81, 2016. ISSN 0187-6236. doi: https://doi.org/10.20937/ATM.2016.29.01.05. URL http://www.sciencedirect.com/science/article/pii/S0187623617300176.

C. Bohren and B. Albrecht. *Atmospheric Thermodynamics*. Oxford University Press, 1998. ISBN 9780195099041. URL https://books.google.it/books?id=SSJJ_RWJGe8C.

P. Bougeault and P. Lacarrere. Parameterization of orography-induced turbulence in a mesobeta–scale model. *Monthly Weather Review*, 117(8):1872–1890, 1989. doi: 10.1175/1520-0493(1989)117<1872:POOITI>2.0.CO;2. URL https://doi.org/10.1175/1520-0493(1989)117<1872:POOITI>2.0.CO;2.

C. S. Bretherton, J. R. McCaa, and H. Grenier. A new parameterization for shallow cumulus convection and its application to marine subtropical cloud-topped boundary layers. part i: Description and 1d results. *Monthly Weather Review*, 132(4):864–882, 2004. doi: 10.1175/1520-0493(2004)132<0864:ANPFSC>2.0.CO;2. URL https://doi.org/10.1175/1520-0493(2004)132<0864:ANPFSC>2.0.CO;2.

F. Cavallini and F. Crisciani. *Quasi-Geostrophic Theory of Oceans and Atmosphere: Topics in the Dynamics and Thermodynamics of the Fluid Earth*. Atmospheric and Oceanographic Sciences Library. Springer Netherlands, 2012. ISBN 9789400746916. URL https://books.google.it/books?id=qcTBqfosbxAC.

A. E. Cohen, S. M. Cavallo, M. C. Coniglio, and H. E. Brooks. A review of planetary boundary layer parameterization schemes and their sensitivity in simulating southeastern u.s. cold season severe weather environments. *Weather and Forecasting*, 30(3):591–612, 2015. doi: 10.1175/WAF-D-14-00105.1. URL https://doi.org/10.1175/WAF-D-14-00105.1.

M. C. Coniglio, J. C. Jr., P. T. Marsh, and F. Kong. Verification of convection-allowing wrf model forecasts of the planetary boundary layer using sounding observations. *Weather and Forecasting*, 28(3):842–862, 2013. doi: 10.1175/WAF-D-12-00103.1. URL https://doi.org/10.1175/WAF-D-12-00103.1.

I. V. der Hoven. Power spectrum of horizontal wind speed in the frequency range from 0.0007 to 900 cycles per hour. *Journal of Meteorology*, 14(2):160–164, 1957. doi: 10.1175/1520-0469(1957)014<0160:PSOHWS>2.0.CO;2. URL https://doi.org/10.1175/1520-0469(1957)014<0160:PSOHWS>2.0.CO;2.

J. Dudhia. Numerical study of convection observed during the winter monsoon experiment using a mesoscale two-dimensional model. *Journal of the Atmospheric Sciences*, 46(20): 3077–3107, 1989. doi: 10.1175/1520-0469(1989)046<3077:NSOCOD>2.0.CO;2. URL https://doi.org/10.1175/1520-0469(1989)046<3077:NSOCOD>2.0.CO;2.

T. T. Fujita. Tornadoes and downbursts in the context of generalized planetary scales. *Journal of the Atmospheric Sciences*, 38(8):1511–1534, 1981. doi: 10.1175/1520-0469(1981)038<1511:TADITC>2.0.CO;2. URL https://doi.org/10.1175/1520-0469(1981)038<1511:TADITC>2.0.CO;2.

J. R. Garratt. *The Atmospheric Boundary Layer*. Cambridge Atmospheric and Space Science Series. Cambridge University Press, 1992. ISBN 9780521380522. URL https://books.google.it/books?id=lxJhQgAACAAJ.

H. Grenier and C. S. Bretherton. A moist pbl parameterization for large-scale models and its application to subtropical cloud-topped marine boundary layers. *Monthly Weather Review*, 129(3):357–377, 2001. doi: 10.1175/1520-0493(2001)129<0357:AMPPFL>2.0.CO;2. URL https://doi.org/10.1175/1520-0493(2001)129<0357:AMPPFL>2.0.CO;2.

T. Hey, S. Tansley, and K. Tolle. *The Fourth Paradigm: Data-Intensive Scientific Discovery*. Microsoft Research, October 2009. ISBN 978-0-9825442-0-4. URL https://www.microsoft.com/en-us/research/publication/fourth-paradigm-data-intensive-scientific-discovery/.

J. R. Holton. *An Introduction to Dynamic Meteorology*. An Introduction to Dynamic Meteorology. Academic Press, 1979. ISBN 9780123543608. URL https://books.google.it/books?id=ejZRAAAAMAAJ.

S.-Y. Hong, Y. Noh, and J. Dudhia. A new vertical diffusion package with an explicit treatment of entrainment processes. *Monthly Weather Review*, 134(9):2318–2341, 2006. doi: 10.1175/MWR3199.1. URL https://doi.org/10.1175/MWR3199.1.

X.-M. Hu, J. W. Nielsen-Gammon, and F. Zhang. Evaluation of three planetary boundary layer schemes in the wrf model. *Journal of Applied Meteorology and Climatology*, 49(9):1831–1844, 2010. doi: 10.1175/2010JAMC2432.1. URL https://doi.org/10.1175/2010JAMC2432.1.

Z. I. Janjić. The step-mountain coordinate: Physical package. *Monthly Weather Review*, 118 (7):1429–1443, 1990. doi: 10.1175/1520-0493(1990)118<1429:TSMCPP>2.0.CO;2. URL https://doi.org/10.1175/1520-0493(1990)118<1429:TSMCPP>2.0.CO;2.

Z. I. Janjić. The step-mountain eta coordinate model: Further developments of the convection, viscous sublayer, and turbulence closure schemes. *Monthly Weather Review*, 122(5):927–945, 1994. doi: 10.1175/1520-0493(1994)122<0927:TSMECM>2.0.CO;2. URL https://doi.org/10.1175/1520-0493(1994)122<0927:TSMECM>2.0.CO;2.

P. A. Jiménez and J. Dudhia. Improving the representation of resolved and unresolved topographic effects on surface wind in the wrf model. *Journal of Applied Meteorology and Climatology*, 51(2):300–316, 2012. doi: 10.1175/JAMC-D-11-084.1. URL https://doi.org/10.1175/JAMC-D-11-084.1.

P. Kundu and I. Cohen. *Fluid Mechanics*. Elsevier Science, 2010. ISBN 9780123814005. URL https://books.google.it/books?id=d9B5NElxUKwC.

W. Ledermann and E. Lloyd. *Handbook of Applicable Mathematics, Statistics*. Handbook of Applicable Mathematics. Wiley, 1984. ISBN 9780471902720. URL https://books.google.it/books?id=bHHWAAAAMAAJ.

J. R. McCaa and C. S. Bretherton. A new parameterization for shallow cumulus convection and its application to marine subtropical cloud-topped boundary layers. part ii: Regional simulations of marine boundary layer clouds. *Monthly Weather Review*, 132(4):883–896, 2004. doi: 10.1175/1520-0493(2004)132<0883:ANPFSC>2.0.CO;2. URL https://doi.org/10.1175/1520-0493(2004)132<0883:ANPFSC>2.0.CO;2.

G. L. Mellor and T. Yamada. A hierarchy of turbulence closure models for planetary boundary layers. *Journal of the Atmospheric Sciences*, 31(7):1791–1806, 1974. doi: 10.1175/1520-0469(1974)031<1791:AHOTCM>2.0.CO;2. URL https://doi.org/10.1175/1520-0469(1974)031<1791:AHOTCM>2.0.CO;2.

M. Nakanishi and H. Niino. An improved mellor–yamada level3 model with condensation physics: Its design and verification. 112:1–31, 07 2004.

M. Nakanishi and H. Niino. An improved mellor–yamada level-3 model: Its numerical stability and application to a regional prediction of advection fog. 119:397–407, 05 2006.

W. M. Organization. *Guide to the Global Observing System*. Guide to the Global Observing System. World Meteorological Organization, 2007. URL https://books.google.it/books?id=a2z0SgAACAAJ.

I. Orlanski. A rational subdivision of scales for atmospheric processes. *Bulletin of the American Meteorological Society*, 56:527–530, 1975.

J. E. Pleim. A combined local and nonlocal closure model for the atmospheric boundary layer. part i: Model description and testing. *Journal of Applied Meteorology and Climatology*, 46(9): 1383–1395, 2007a. doi: 10.1175/JAM2539.1. URL https://doi.org/10.1175/JAM2539.1.

J. E. Pleim. A combined local and nonlocal closure model for the atmospheric boundary layer. part ii: Application and evaluation in a mesoscale meteorological model. *Journal of Applied Meteorology and Climatology*, 46(9):1396–1409, 2007b. doi: 10.1175/JAM2534.1. URL https://doi.org/10.1175/JAM2534.1.

S. Pope. *Turbulent Flows*. Cambridge University Press, 2000. ISBN 9780521598866. URL https://books.google.it/books?id=HZsTw9SMx-0C.

R. Rogers and M. Yau. *A short course in cloud physics*. International series in natural philosophy. Pergamon Press, 1989. ISBN 9780080348643. URL https://books.google.it/books?id=dZkRAQAAIAAJ.

U. Schulzweida. *CDO user's guide*. 2006. URL https://code.mpimet.mpg.de/projects/cdo/.

H. H. Shin and S.-Y. Hong. Representation of the subgrid-scale turbulent transport in convective boundary layers at gray-zone resolutions. *Monthly Weather Review*, 143(1):250–271, 2015. doi: 10.1175/MWR-D-14-00116.1. URL https://doi.org/10.1175/MWR-D-14-00116.1.

S. Siegel. *Nonparametric statistics for the behavioral sciences*. McGraw-Hill series in psychology. McGraw-Hill, 1956. URL https://books.google.it/books?id=6t9fAAAAIAAJ.

W. Skamarock, J. Klemp, J. Dudhia, D. Gill, D. Barker, W. Wang, and J. Powers. *A Description of the Advanced Research WRF Version 3*, volume 27. 01 2008. URL https://www.mmm.ucar.edu/weather-research-and-forecasting-model.

R. B. Stull. *An Introduction to Boundary Layer Meteorology*. Atmospheric and Oceanographic Sciences Library. Springer Netherlands, 1988. ISBN 9789027727695. URL https://books.google.it/books?id=eRRz9RNvNOkC.

K. E. Taylor. Summarizing multiple aspects of model performance in a single diagram. *J. Geophys. Res.-Atmos.*, 106(9):7183–7192, 2001.

H. Tennekes, H. Tennekes, and J. Lumley. *A First Course in Turbulence*. MIT Press, 1972. URL https://books.google.it/books?id=_pSyuQAACAAJ.

J. Turner. *Buoyancy Effects in Fluids*. Cambridge Bible Commentary: New English Bible. Cambridge University Press, 1973. URL https://books.google.it/books?id=Su8IAQAAIAAJ.

J. Wallace and P. Hobbs. *Atmospheric Science: An Introductory Survey*. International Geophysics. Elsevier Science, 2006. ISBN 9780080499536. URL https://books.google.it/books?id=HZ2wNtDOU0oC.

D. Wilks. *Statistical Methods in the Atmospheric Sciences*. Academic Press. Academic Press, 2011. ISBN 9780123850225. URL https://books.google.it/books?id=IJuCVtQ0ySIC.

J. C. Wyngaard. Toward numerical modeling in the "terra incognita". *Journal of the Atmospheric Sciences*, 61(14):1816–1826, 2004. doi: 10.1175/1520-0469(2004)061<1816:TNMITT>2.0.CO;2. URL https://doi.org/10.1175/1520-0469(2004)061<1816:TNMITT>2.0.CO;2.